This electronic thesis or dissertation has been downloaded from the King's Research Portal at https://kclpure.kcl.ac.uk/portal/

KING'S College LONDON

Defining and interpreting tolerance and rejection biomarkers in liver transplantation

Bonaccorsi Riani, Eliano

Awarding institution:
King's College London

The copyright of this thesis rests with the author and no quotation from it or information derived from it may be published without proper acknowledgement.

END USER LICENCE AGREEMENT

Unless another licence is stated on the immediately following page this work is licensed

under a Creative Commons Attribution-NonCommercial-NoDerivatives 4.0 International

licence. https://creativecommons.org/licenses/by-nc-nd/4.0/

You are free to copy, distribute and transmit the work

Under the following conditions:

- Attribution: You must attribute the work in the manner specified by the author (but not in any way that suggests that they endorse you or your use of the work).
- Non Commercial: You may not use this work for commercial purposes.
- No Derivative Works - You may not alter, transform, or build upon this work.

Any of these conditions can be waived if you receive permission from the author. Your fair dealings and other rights are in no way affected by the above.

Take down policy

If you believe that this document breaches copyright please contact librarypure@kcl.ac.uk providing details, and we will remove access to the work immediately and investigate your claim.

Download date: 05. May. 2023

"Defining and interpreting tolerance and rejection biomarkers in liver transplantation"

Eliano Bonaccorsi Riani

Register Number 1432234

Thesis presented to obtain the degree of Ph.D.

School of Immunology & Microbial Sciences

Faculty of Life Sciences & Medicine

King's College London

London – United Kingdom

2019

Ó mar salgado, quanto do teu sal
São lágrimas de Portugal!
Por te cruzarmos, quantas mães choraram,
Quantos filhos em vão rezaram!
Quantas noivas ficaram para casar
Para que fosses nosso, ó mar!

Valeu a pena? Tudo vale a pena
Se a alma não é pequena.
Quem quer passar além do Bojador
Tem que passar além da dor.
Deus ao mar o perigo e o abismo deu,
Mas nele é que espelhou o céu

"Mar português"
Fernando Pessoa – Lisboa - 1934

"Eu atravesso as coisas – e no meio da travessia não vejo!
Só estava era entretido na ideia dos lugares de saída e de chegada
Assaz o senhor sabe: a gente quer passar um rio a nado,
e passa; mas vai dar outra banda
e num ponto muito mais embaixo
Bem diverso do em que primeiro se pensou
Viver nem não é muito perigoso?"

Riobaldo in "Grande sertão veredas"
Guimarães Rosa – Rio de Janeiro 1956

This work is dedicated

To my grandfather Bovio (in memoriam) that immigrated to Brazil from Italy

and I made the way back to the old continent

To my father Elio (in memoriam), for making his life an example for us

To my mother Ana Maria, for her endurance and support in every moment

To my sister Luciana and to my brother Albano for their friendship

To my aunts Ione (in memoriam) and Ana Lucia for all their support and encouragement on my journey abroad

To Mrs Nice Ricciardi for her help during the most challenging moments of this project

To Nikki, for her love and understanding during my absence

Abstract

Liver transplantation has become a well-established therapy for end-stage liver diseases over the last decades. Despite the huge progress in perioperative care of liver recipients, which led to an exponential increase on early graft and recipient survival rates, patients are doomed to stay under long-term immunosuppression treatment, being exposed to the consequences of its late side effects. Recently, supported by experimental animal studies and clinical observations, which have endorsed the hepatic tolerogenic trend, attempts to completely wean the patient off immunosuppressive drugs have been made. In a recent published study, 41 (42%) of the 98 enrolled liver recipients could be completely weaned off from immunosuppressive drugs, achieving the operational tolerance status, defined by normal maintenance of clinical graft function without immunological damage in the absence of immunosuppression treatment. On the other hand, eventual rejection episodes were mainly mild and easily treated mostly with reintroduction of the baseline immunosuppression regimen with complete normalization of liver function tests and no graft loss as a consequence of the rejection episode (1). Furthermore, functional analyses performed on baseline liver biopsies suggested that operational tolerance was associated with a differential expression of genes related to iron metabolism (2). In the current study, we checked the influence of iron levels on the immune response using a murine model of ConcanavalinA induced T cell mediate acute liver hepatitis. Iron deficiency significantly blunted the inflammatory liver damage, which was associated with less T cell and NKT cell activation. Aiming to decipher the iron effect on liver tolerance establishment, we set up a fully vascularized rat liver transplant model in the context of iron restriction. Furthermore, taking advantage of the opportunity provided by the sequential liver biopsies and blood samples collected from rejecting recipients in the aforementioned clinical trial, we conducted an extensive molecular analysis trying to identify biomarkers of acute cellular rejection during the immunosuppression withdrawal. Rejection episodes produced distinct blood and liver tissue transcriptional changes independent of HCV status and pharmacological immunosuppression. Gene expression profiles were used to build a blood predictive rejection model in HCV-negative patients. The model identified molecular changes associated with rejection, which were detected 1-2 months before its clinical diagnostic during the clinical trial. Altogether, our results provided insights on the effect that iron has on the tolerance process and in the understanding of molecular rejection biomarkers;

which could improve the patient selection and the safety of the future immunosuppression withdrawal clinical trials.

Table of Contents

Chapter 1 Introduction 21

1.1 Liver Transplantation Background 21

1.2 Long-term Immunosuppression consequences 23

1.2.1 Immunosuppression nephrotoxicity 23

1.2.2 Metabolic consequences of Immunosuppression 24

1.2.3 Cardiovascular events in Immunosuppressed liver recipients 24

1.2.4 Malignancies and infections in liver transplant recipients 24

1.3 Liver allograft rejection 25

1.3.1 Alloantigen recognition 25

1.3.2 T cell activation 26

1.3.3 T cell differentiation, graft cell infiltration, and tissue destruction 26

1.4 Liver transplant tolerance 27

1.4.1 Distinctive immunological hepatic properties 28

1.5 Achievement of Tolerance in Liver Transplant Recipients 29

1.6 Immunosuppression withdrawal trials 31

1.7 Biomarkers of spontaneous operational tolerance and of acute cellular rejection occurring during IS withdrawal from liver transplant recipients 33

1.7.1 Biomarkers of spontaneous operational tolerance in liver transplantation 34

1.7.2 Biomarkers of acute cellular rejection during intentional IS withdrawal protocols 36

1.8 High-throughput gene expression experiments 37

1.8.1 Microarray technique 38

1.8.2 Microarray experiments 38

1.8.3 Microarray experiment design challenges 39

1.8.4 Microarray data analysis 40

1.8.5 Bioinformatics software and microarray public databases 44

1.8.6 Technical validation 44

1.8.7 Transcriptome analysis using next-generation sequencing 45

1.9 Iron homeostasis 46

1.9.1 Iron Uptake and trafficking 46

1.9.2 Iron homeostasis and hepcidin 50

1.9.3 Iron immune system modulation 53

1.9.4 Iron and liver transplantation 57

Chapter 2 : Hypothesis and aims 58

2.1 Hypothesis 58

2.1.1 Operational tolerance in liver transplant recipients is influenced by the axis iron/hepcidn. 58

2.1.2 Molecular biomarkers identified during immunosuppression withdrawal clinical trials forecast ACR episodes before their clinical, biochemistry and histological manifestation. 58

2.2 Aims 59

2.2.1 Effect of iron in the intra-hepatic lymphocyte response 59

2.2.2 Effect of iron deficiency in the establishment of tolerance in liver transplantation 59

2.2.3 Molecular characterization of acute cellular rejection biomarkers during intentional immunosuppression withdrawal in human liver transplantation 60

Chapter 3 : Effects of Iron in the Intra-hepatic lymphocyte responses 61

3.1 Introduction 61

3.2 Material and Methods 62

3.2.1 Reproduction of the mild iron deficiency status in mice employing iron-modified diets: 62

3.2.2 ConA immune-mediated acute liver failure model in mice under iron-modified regimens 62

3.2.3 Hepcidin and iron chelators administration 62

3.2.4 Modulation of mice gut microbiota 63
3.2.5 Biological samples collection 63
3.2.6 Samples manipulation, serum biochemistry and hematologic measurements, cytokine analysis and intra-hepatic iron measurement 64
3.2.7 Liver Histology 64
3.2.8 Isolation of non-parenchymal liver cells, splenic and lymph node leukocytes 65
3.2.9 In vitro naïve $CD4^+$ T cell stimulation 65
3.2.10 Cell phenotyping - Flow cytometry 66
3.2.11 RNA extraction and gene expression experiments 66
3.2.12 Statistical analyses 67
3.3 Results 68
3.3.1 Induction of mild iron deficiency employing iron-modified diets 68
3.3.2 Mild iron deficiency does not modify the steady state immune cell repertoire and systemic cytokine levels 69
3.3.3 Mild iron deficiency significantly reduces inflammatory liver damage following ConA administration 72
3.3.4 Decreased iron availability blunts lymphocyte proliferation and activation 74
3.3.5 Iron deficiency influences intra-hepatic inflammatory responses independently from gut microbiota modulation 77
3.3.6 Intra-hepatic inflammatory responses are influenced by iron but not by baseline hepcidin level. 77
Chapter 4 : Impact of iron changes on the spontaneous tolerance development in a rat liver transplant model 79
4.1 Introduction: 79
4.2 Material and methods: 81
4.2.1 Rat liver transplantation model 81
4.2.2 Different strain combination 84

4.2.3 Induction of Iron Deficiency employing iron-modified diets 85
4.2.4 Recombinant human Interleukin 2 administration..... 85
4.2.5 Statistical analyses 86
4.3 Results 87
4.3.1 Survival curves between the different rat strain combinations 87
4.3.2 Induction of mild iron deficiency in rats 88
4.3.3 Survival curve between the different rat strain combinations under iron-modified diets 89
4.3.4 RhIL-2 administration induces clinical deterioration and liver function impairment associated with more cytokine production in Iron deficient animals..... 91
4.3.5 RhIL-2 challenge does not seem to affect IrDef spontaneous tolerant long-term survivors 93
4.3.6 RhIL-2 challenge seems to affect IrDef long-term induced tolerance survivors 94
4.3.7 Post-transplant long-term complications suggests a systemic effect of iron-modified diets 95
Chapter 5 : Molecular characterization of acute cellular rejection occurring during intentional immunosuppression withdrawal in human liver transplantation 96
5.1 Introduction:..... 96
5.2 Material and Methods 97
5.2.1 Immunosuppression withdrawal clinical trials in liver transplantation 97
5.2.2 Rejecting patients population and control groups 100
5.2.3 Biological specimens..... 105
5.2.4 Histological examinations 106
5.2.5 Liver tissue and blood microarray gene expression..... 106
5.2.6 Gene Set Enrichment Analysis 108
5.2.7 Correlation between gene expression profiling and liver histopathology..... 109
5.2.8 Influence of type immunosuppression on gene expression pattern 109

5.2.9 Validation real-time polymerase chain reaction experiments in peripheral blood samples 110

5.2.10 Determination of predictive gene expression signature of rejection 111

5.3 Results 113

5.3.1 Acute cellular rejection presented a very well characterized transcriptional pattern when compared with baseline analysis. 113

5.3.2 Acute cellular rejection was associated with a common transcriptional signature in spite of the presence of underlying liver inflammation 117

5.3.3 Histological features of acute cellular rejection correlate with specific gene expression changes 123

5.3.4 Acute cellular rejection also presented distinct transcription changes in blood samples, although with only partial overlapping with those observed in liver allograft 125

5.3.5 The blood transcriptional patterns of ACR-associated genes at baseline did not predict the success of immunosuppression weaning 128

5.3.6 Immunosuppressive drug regimens presented a minimal effect on ACR-associated gene expression profiles in both blood and liver tissue samples 129

5.3.7 Sequential gene expression profiling in blood samples collected over the immunosuppression withdrawal period predicts the occurrence of rejection 130

Chapter 6 Discussion 134

6.1 Effects of Iron deficiency in the Intra-hepatic lymphocyte responses 134

6.2 Impact of iron changes on the spontaneous tolerance development in a rat liver transplant model 139

6.3 Molecular characterization of acute cellular rejection in liver transplant recipients occurring during intentional immunosuppression withdrawal 142

6.4 Final Conclusions and Future Work 150

Appendix A: Congress presentations and publications 152

Appendix B: Paper: Iron Deficiency Impairs Intra-Hepatic Lymphocyte Mediated Immune Response 154

Appendix C: Paper: Molecular Characterization of Acute Cellular Rejection Occurring During Intentional Immunosuppression Withdrawal in Liver Transplantation. 172

References..... 202

List of figures

Figure 1: Iron uptake and trafficking 49

Figure 2: Regulation of Hamp transcription at the hepatocyte level 52

Figure 3: Iron and haematological parameters in mice fed with iron-manipulated diets 68

Figure 4: Influence of iron levels on the immune-phenotype of intra-hepatic leukocytes 69

Figure 5: Iron deficiency results in attenuated immune-mediated hepatitis following ConA administration 73

Figure 6: ConA-Induced T and NKT lymphocyte activation is reduced in iron deficiency 75

Figure 7: Iron chelation impairs $CD4^+$ T cell activation and proliferation in vitro. 76

Figure 8: The inhibitory effects of iron deficiency in ConA-induced hepatitis are independent from changes in gut microbiome and hepcidin levels. 78

Figure 9: Panels displaying the sequential anastomoses of the liver allograft implantation. ... 83

Figure 10: Post-liver transplantation outcome between the different strain combinations… ... 87

Figure 11: Clinical, biochemistry, iron and haematological parameters in Lewis rats fed with iron-deficient (IrDef) and iron-replete (IrRepl) diets over three weeks. 88

Figure 12: Post-liver transplant outcome between different strain combinations treated with iron-modified diets before (3 weeks for the donors and 1 week for the recipients) and after the procedure. 90

Figure 13: Post-liver transplantation outcome after rhIL-2 challenge 92

Figure 14: Outcome of long-term spontaneous tolerance transplanted survivors (BN – Lew) challenge with rhIL-2 93

Figure 15: Outcome of long-term Tac-induced tolerance transplanted survivors (DA – Lew) challenge with rhIL-2. 94

Figure 16: Clinical complications on long-term survivors transplant rats 95

Figure 17: Flow chart showing immunosuppression withdrawal trial design 99

Figure 18: Differentially expressed genes in liver tissue 115

Figure 19: Transcriptional changes associated with rejection in HCV-neg and HCV-pos recipients 119

Figure 20: Differentially expressed genes across histological compartments 124

Figure 21: Differentially expressed genes in whole blood. 126

Figure 22: Significantly expressed genes in liver tissues and in PBMC of HCV-negative liver recipients. 127
Figure 23: Baseline acute cellular rejection-associated gene expression in rejecting and tolerant liver recipients 128
Figure 24: Prediction of rejection by sequential gene expression in blood samples 133

List of Tables

Table 1: Immunosuppression withdrawal clinical trials on liver transplant recipients 32

Table 2: Gene expression in liver, spleen and mesenteric lymph nodes (mesLN) of immune-related molecules from IrDef and IrRepl mice 71

Table 3: Serum level of cytokines measured by Luminex technology from IrDef and IrRepl mice 71

Table 4: Rat strain combinations 85

Table 5: Post-liver transplant survival rate in a preliminary experiment using the iron-modified diets 89

Table 6: Post liver transplant long-term complications 95

Table 7: Demographic and clinical characteristics of enrolled rejecting patients 101

Table 8: Time distribution of sequential blood samples selection 102

Table 9 : Demographic and clinical characteristics of patients used in the rejection prediction model test 103

Table 10: Demographic and clinical characteristics of Non-tolerant and Tolerant patients from whom previous qPCR data at the baseline were reassessed 104

Table 11: Top 50 differentially expressed genes in liver tissue samples at baseline and at rejection time 116

Table 12: Liver tissue gene expression markers associated with acute cellular rejection 120

Table 13: Functional pathways significantly over represented in liver allograft rejection-associated transcriptional patterns (Hallmark pathways, MSigDB GSEA analysis) 121

Table 14: Pathogenesis-based transcript sets significantly enriched in liver allograft rejection associated transcriptional patterns (GSEA) 122

Table 15: Differential gene expression by histological compartment 124

Table 16: Differential gene expression by baseline immunosuppression 129

Table 17: Significantly differentially expressed genes at baseline versus rejection based on univariate analysis of Fluidigm data 132

Acknowledgements

I would like to thank all the people for their contributions to the accomplishment of this work. I would like to express my special gratitude to Richard Danger and Adam Pennycuick, who helped me directly with the fulfillment of this research. I also would like to thank Roser, Marta and Elisavet for their valuable technical help in this project. For their insights on the conducting of the study, I would like to thank Maria Hernandez-Fuentes and Marc Martínez-Llordella, and Juanjo Lozano for his valuable assistance on the bioinformatic analysis. Finally, I would like to thank the Prof Alberto Sanchez-Fueyo for his support with this study throughout all the challenges that we experienced during the realization of this study in Barcelona and in London. It has been a long and enriching journey.

Abbreviations

7-AAD	7-Aminoactinomycin D
ACR	Acute cellular rejection
ALT	Alanine aminotransferase
ANOVA	Analysis of Variance
AP	Alkaline phosphatase
APC	Antigen-presenting cells
AST	Aspartate aminotransferase
AZA	Azathioprine
BMP	Bone morphogenetic protein
BMPR1	Bone morphogenetic protein receptor type I
BMPR2	Bone morphogenetic protein receptor type II
CBD	Common bile duct
cDNA	Complementary DNA
CFSE	Carboxylfluorescein succinimidyl ester
CNIs	Calcineurin Inhibitors
ConA	Concanavalin A
CS	Corticosteroid
CSA	Cyclosporin A
CV	Cardiovascular
Cy7	Cyanine 7
DC	Dendritic cells
DCYTB	Duodenal cytochrome b
DMT1	Divalent metal transporter 1
DNA	Deoxyribonucleic acid
DNase I	Deoxyribonuease I
DSA	Donor specific antibody
DTH	Delayed-type hypersensitivity
EAE	Experimental autoimmune encephalomyelitis
EDTA	Ethylenediaminetetraacetic acid
ELTR	European Liver Transplant Register
EPO	Erythropoietin
ES	Enrichment Score
FC	Fold change
FDR	False Discovery Rate
Fe2+	Ion ferrous form
Fe3+	Ion ferric form
FITC	Fluoroscein isothiocyanate
FOXP3	Forkhead box protein 3
FPN	Ferroportin
GGT	gamma-glutamyl transpeptidase

GSEA	Gene Set Enrichment Analysis
H&E	Haematoxylin and eosin
HA	Hepatic artery
HAMP	Hepcidin antimicrobial peptide
HCP1	Heme carrier protein 1
HCV	Hepatitis C virus
HFE	Hemochromatosis protein
HH	Hereditary hemochromatosis
HIF	Hypoxic inducible factor
HJV	Hemojuvelin
HLA	Human Leukocyte Antigen
HO-1	Haemooxygenase-1
HPO	Hydroxypyridinone
HRG-1	Heme-responsive gene-1 protein
HSC	Hepatic Stellate Cells
ICP – MS	Inductively Coupled Plasma – Mass spectrometry
IFNγ	Interferon gamma
IHVC	Infra-hepatic vena cava
IL1	Interleukin 1
IL2	Interleukin 2
IL4	Interleukin 4
IL6	Interleukin 6
IL0	Interleukin 10
IL22	Interleukin 22
Ir Def	Iron deficient diet
Ir Repl	Iron Replete diet
IS	Immunosuppression
ITN	Immune Tolerance Network
JAK	Janus kinase
LFTs	Liver function tests
LOOCV	Leave-one-out cross validation
LPS	Lipopolysaccharide
LSEC	Liver sinusoidal endothelial cells
MAPK	Mytogen-activated protein kinase
MBP	Myelin basic protein
MHC	Major histocompatibility complex
MIT	Massachusetts Institute of Technology
MMF	Mycophenolate Mofetil
MSigDB	Molecular Signatures Database
mTOR	Mammalian target of rapamycin
NARMP2	Natural-resistance-associated macrophage protein-2

NES	Normalized enrichment score
NFAT	Nuclear factor of activated T cells
NF-kB	Nuclear factor kappa B
NGS	New generation sequencing
NK	Natural Killer
NKT	Natural Killer T cell
NHE3	Na^+/H^+ exchanger-3 protein
OLETF	Otsuka Long-Evans Tokushima fatty
PBMC	Peripheral blood mononuclear cells
PBS	Phosphate-buffered saline
PCFT	Proton-coupled folate transporter
PCR	Polymerase chain reaction
PDGF-BB	Platelet-derived growth factor BB
PE	Phycoerythrin
PKC	Protein kinase C
PTLD	Post-transplant lymphoproliferative disorders
PIP2	Phosphatidyl inositol-4,5-biphosphate
PV	Portal vein
qPCR	Quantitative polymerase chain reaction
RBC	Red blood cells
REDD1	Regulated in development DNA damage responses 1
RISET	Reprogramming the Immune System for the Establishment of Tolerance Consortium
rhIL-2	Recombinant human Interleukin 2
RNA	Ribonucleic acid
RNase	Ribonuclease
ROS	Reactive oxygen species
RT	Room temperature
SHVC	Supra hepatic vena cava
SMAD	Mothers against decapentaplegic homologs proteins
SOT	Spontaneous Operational Tolerance
STAT	Signal transducers and activators of transcription
STEAP3	Six transmembrane epithelial antigen of prostate-3 reductase
T cell	Lymphocyte T cell
TAC	Tacrolimus
TF	Transferrin
TFR1	Transferrin receptor 1
TFRC	Transferrin receptor CD71
TNFα	Tumour necrosis factor alpha
TGFβ	Transforming growth factor beta
Treg	Regulatory T cell

UNOS	United National Organ Sharing
WBC	White blood cells

Chapter 1 Introduction

1.1 Liver Transplantation Background

Since the pioneering work conducted by Prof Thomas Starzl's group in the 1960s (3), liver transplantation has had a fantastic evolution over the last five decades. Initially considered a procedure only performed in high-level academic centres due to its challenging surgical and clinical characteristics, it has become a "popularized" treatment performed in over 80 countries worldwide (4). Currently, many centres around the world can achieve reasonable results reflected by the one-year and five-year patient survival rates around 90% and 70% respectively as observed by the two most important liver transplant registers: the United Network for Organ Sharing (UNOS) register in the United States of America (USA) and the European Liver Transplant Registry (ELTR) (5, 6).

The consolidation of liver transplantation as a therapy for end-stage liver diseases can be accredited to: a huge improvement in surgical techniques, in anaesthetic protocols, in better patient selection and better perioperative management, establishment of better organ allocation systems, the creation of transplant intensive care units, the extensive use of radiological imaging for monitoring vascular and biliary status, and in the radiological and endoscopic interventional procedures to treat vascular and biliary post-transplant complications (4, 7).

The previous "multidisciplinary approach", which fundamentally contributed to the evolution and success of liver transplantation as therapy, was markedly influenced by the constant development and introduction, throughout the years, of new immunosuppressive drugs and protocols in the clinical practice. The poor initial armamentarium of immunosuppressive drugs constituted by corticosteroids (CS) and azathioprine (AZA) was expanded with the addition of the calcineurin inhibitors (CNI) cyclosporin A (CSA) and tacrolimus (TAC) in the 1980s. Later the introduction of mycophenolate mofetil (MMF) replaced AZA as purine inhibitor of choice, and then the mammalian target of rapamycin (mTor) inhibitor sirolimus (Rapamycin®) and posteriorly everolimus (Certican®) were introduced and used as liver immunosuppressive drugs in cases of nephrotoxicity due to CNIs and due to its protective oncological properties. Mono- or polyclonal antibodies have also been developed and used as induction immunosuppression (IS) strategy or in the treatment of CS-resistant rejection episodes (8).

This constant progress resulted in the observation of very defined eras on the patient immunological outcomes over time. After the introduction of CNIs, acute cellular rejection (ACR) rates decreased to 10% to 40% from approximately 80% before them and the chronic rejection to less than 5% (8-11). The remarkable reduction in the ACR rate in the era of new refined immunosuppression protocols contributed to the decrease of the incidence of opportunistic infections in the early time post liver transplantation, given that less CS pulse-therapy, the commonest treatment for ACR, was administered to the patients (8). As a result of the highlighted progress and advances, one-year patient and graft survival rates improved considerably. Once the major problems affecting outcomes in the initial post-transplant period were overcome, the transplant medical community shifted its attention to improving the long-term patient and graft survival rates, which have been impacted in most cases by three main issues: recurrence of liver diseases, consequences of long-life IS treatment, and failure of the liver allograft caused by chronic rejection. It is worth noting that long-life immunosuppression treatment can be implicated in at least in some degree in all of these issues. Autoimmune liver diseases can easily recur in under-immunosuppressed patients; allograft livers can develop chronic rejection under sub-optimized IS schemes (12-15). In contrast, over-immunosuppression and long-term immunosuppressive therapy are strongly associated with increased morbidity and mortality of liver transplant recipients, mainly due to their consequences on recipients renal function, cardiovascular events, metabolic syndromes, infections and recurrent or *de-novo* malignancies (16-19).

Aiming to reduce the negative effects of long-life IS treatment, many approaches to optimize and/or minimize IS regimens and in addition, to completely withdraw immunosuppressive drugs in well selected patients under strictly controlled clinical conditions have been conducted in recent years. Some IS withdrawal clinical trials reported that around 20% to 40% of selected liver recipients can be completely weaned off IS achieving the Spontaneous Operational Tolerance status (SOT) defined by persistent stable graft function without clinical and immunological damage in absence of immunosuppressive drugs treatment (20, 21). To better evaluate the patient baseline immune status, predict the success of the IS treatment withdrawal and eventually to early diagnose the failure of withdrawal attempt before the rejection episode has been set, liver transplant immunologists have combined a number of strategies to identify and develop predictive biomarkers of tolerance (22). In a recent

prospective multicentre clinical trial of IS withdrawal, the hepatic expression of iron homeostasis genes and serum-iron parameters were associated with the success of immunosuppressive drug withdrawal, pointing for the first time to the role of iron metabolism in the establishment of operational tolerance in liver transplant recipients (1, 2). Further clinical and/or experimental studies are needed to confirm the influence of iron on possible molecular and functional pathways involved in T-lymphocytes mediated immune response and its contribution to the establishment of operational tolerance.

1.2 Long-term Immunosuppression consequences

Nephrotoxicity, cardiovascular (CV) events, diabetes, hyperlipidaemia, obesity, infections and malignancies are associated with long-term IS treatment. These conditions have a huge impact on morbidity and mortality after liver transplantation, being responsible for 50 to 60% of deaths in the late period of liver transplantation (23-26). Although new immunosuppressive agents have been introduced, until now, CNIs remain as the keystone for the early and long-term IS regimens in liver transplantation, therefore they are strongly implicated in the development of such immunosuppression comorbidities and consequences aforementioned (8, 27).

1.2.1 Immunosuppression nephrotoxicity

Twenty per cent of liver transplant recipients developed chronic renal failure at 5 years post transplant and among those surviving more than 13 years, 18% required dialysis or kidney transplantation (16, 28). Pre-transplant renal status, diabetes, hepatitis C virus (HCV) infection, nephrotoxic antimicrobial agents, and per-operatory hemodynamic and volume oscillations are risk factors for renal dysfunction; nevertheless the CNIs have a preponderant role (28-31). CNI-related nephrotoxicity is a continuum process initially reversible characterized by glomerular afferent arterioles vasoconstriction with tubular vacuolization and thrombotic microangiopathy, which reduces the glomerular filtration rate. Over time the lesions become irreversible and are marked by arteriolar hyalinosis, glomerular and tubular ischemia resulting in glomerular sclerosis and interstitial fibrosis. CNIs directly or indirectly activate and trigger many mediators and factors associated with these processes (32, 33).

1.2.2 Metabolic consequences of Immunosuppression

A recent meta-analysis study was not able to identify IS treatment as a major risk factor for the metabolic syndrome due to data scarcity, contradictory results and lack of control groups. However in numerous previously published series, IS drugs have been considered a risk factor for various conditions of metabolic syndrome criteria (34). CS-free protocols in liver transplantation showed lower rate of weight gain, osteoporosis, hypertension, dyslipidaemia and diabetes on patients without CS or on those with early CS withdrawal. (35-37). Among recipients under CNIs therapy, TAC prompts to more diabetes occurrence, whereas CSA to more weight gain, hyperlipidaemia and also arterial hypertension (38, 39). The mTor inhibitors (sirolimus and everolimus) are strongly associated with hyperlipidaemia and hypertriglyceridemia requiring specific therapy in most of the cases (40).

1.2.3 Cardiovascular events in Immunosuppressed liver recipients

CV events are more prevalent in liver transplant recipients than in the general population being responsible for up to 20% of post transplant deaths. (23). CV causes of death include cardiac disease, myocardium infarction, cerebro-vascular accident and sudden death (41). Early post-transplant CV complications are more related with pre-transplant CV conditions whereas late complications are associated with long-life IS treatment. Apart from the CNIs direct effect on the arterial endothelium causing a hypertensive effect, immunosuppressive drugs, as previously cited, are associated with diabetes, nephrotoxicity, hyperlipidaemia and obesity, being in turn risk factors for CV events (15). Patients with elevated high-risk scores for CV events can be benefited by CNIs-free immunosuppression protocols introduction (17, 42, 43).

1.2.4 Malignancies and infections in liver transplant recipients

The incidence rate of de novo malignancies in long-term liver transplant recipients is two to three times higher than in general population (5, 26). Furthermore, in a study with 4483 liver recipients surviving more than 1 year, malignancies were responsible for 30% of deaths (25). Besides the multiple factors associated with malignancies such as viral infections, exposure to sun, alcohol and tobacco consumption, and transplant indication; immunosuppressive drugs play an important role. Mainly the CNIs and AZA are particularly implicated due to their

molecular carcinogenic effects (19, 44, 45). For example, the recurrence rate of hepatocellular carcinoma is around 20%, and strongly associated with CNIs levels in spite of very strict pre-transplant selection criteria (46). Chronic immunosuppressed liver recipients are more vulnerable to opportunistic infection, mainly viral, and some of them are strongly linked to development of specific type of malignancies (Kaposi sarcoma, nasopharyngeal carcinoma, cervical and vulvar cancer) as well immune-related malignancies as post-transplant lymphoproliferative disorders (PTLD), and tumours localized in sun-exposed areas (skin cancers) (19).

All together, the described consequences of long-term IS exposure; raised the attention of medical transplant community to develop new strategies to minimize IS treatment, and with special interest on protocols aiming to completely wean the IS treatment (31, 47, 48).

1.3 Liver allograft rejection

Despite the immunosuppression protocols currently in use in liver transplantation, ACR rates are still around 40-50% (8, 10). If left untreated, ACR can cause graft destruction, which in the end may require a new transplant to save the patient's life. ACR is the result of an uncontrolled immune response orchestrated by T cells against donor allograft cells (49). This phenomenon can be divided into three phases, beginning with the presentation of donor antigens; mainly MHC molecules expressed on the surface of donor cells, by specific APCs to the recipient T cells. This alloantigen recognition leads to the activation of recipient alloreactive T cells with their subsequent clonal expansion. Later, alloreactive T cells infiltrate the allograft and orchestrate an inflammatory reaction through direct cytotoxicity or via pro-inflammatory mediators, mainly against cholangiocytes and hepatic endothelial cells (49, 50).

1.3.1 Alloantigen recognition

Three different pathways of donor alloantigen recognition by recipient T cells have been described (51, 52). In the direct pathway, intact donor MHC molecules are recognised by recipient CD4+ and CD8+ T cells on the surface of donor-specific APCs, which are eventually transferred to the recipient within the liver graft. This pathway is predominant in the early stages after liver transplantation and it is the main allorecognition pathway involved in episodes of ACR that occur in the first weeks after liver transplantation. In the indirect

pathway, recipient APCs traffic through hepatic graft phagocyte soluble extracellular protein complexes that have been eliminated by donor cells by necrosis and/or apoptosis. These donor proteins are processed and presented on recipient MHC class II molecules to allospecific CD4+ T cells. Because of that, the indirect pathway takes longer to occur compared to the direct pathway, however, it becomes the dominant pathway in the long-term as the graft is a continuous source of alloantigens. On the other hand, the direct pathway tends to disappear as the donor APCs population decreases over time. The semi-direct pathway involves both donor and recipient APCs as intact cell surface molecules, including MHC molecules, which are transferred from donor to recipient APCs by direct contact between them or by engulfment of donor APC-derived exosomes (49-51).

1.3.2 T cell activation

As a consequence of alloantigen recognition, recipient T cells receive antigen-specific signals through the T cell receptor CD3. These signals alone are not able to induce a full T cell activation. For that, a second signal provided by the interaction of co-stimulatory molecules and their ligands is required. Co-stimulatory molecules are essentially divided in two main families: the B7 family containing the T cell co-stimulatory molecules CD28, CD152 (CTLA-4) and PD1, among others, which bind to the CD80/CD86 ligands on the APCs; and the TNF/TNFR receptor family, represented by the prototype CD40 and CD154 (CD40L). Following T cell activation, large amounts of IL-2 and other pro-proliferative cytokines are produced and act in autocrine and paracrine fashion providing the third signal necessary for the clonal expansion and differentiation of activated T cells (50, 51, 53).

1.3.3 T cell differentiation, graft cell infiltration, and tissue destruction

The fate of T cell differentiation depends on the microenvironment and the additional signals they receive upon activation. In the presence of TGF-β and in absence of proinflammatory cytokines, CD4+ T cells acquire tissue protective phonotype, which is involved in the regulation of the immune response, the so-called regulatory T cells (Tregs). On the other hand, in the presence of proinflammatory cytokines, CD4+ T cells acquire tissue destructive phenotype such as the Th1 and Th2 cells. These CD4+ and also CD8+ cytotoxic T cells infiltrate the graft causing tissue damage through direct cytotoxicity (49). Graft destruction is

also caused by the classic delayed-type hypersensitivity (DTH) reaction, which is stimulated by alloantigen-specific CD4+ (mainly Th1) and CD8+ T cells that have been activated by the direct and indirect pathway. There is a huge production of many soluble mediators as pro-inflammatory cytokines and chemokines contribute to the graft infiltration by the other cells such as activated leukocytes, mainly monocytes and eosinophils, natural killer cells and macrophages among other cells. A third mechanism of graft injury is mediated by the complement activation or antibody-dependent cytotoxicity; this mechanism is responsible for the antibody mediated acute rejection. ACR is mainly due to CD4+ and CD8+ T cell infiltration and tissue destruction and by the DTH reaction (51, 54). Due to the necessity of specific T cell priming, activation and proliferation, ACR usually does not occur in the first week after liver implantation. The incidence is higher in the first three months post-transplant, but it can also occur months or years after transplantation. The clinical symptoms are nonspecific, usually with late onset in the course of an ACR episode and are characterized by fatigue, fever, abdominal pain and jaundice. Elevated levels of bilirubin, transaminases and alkaline phosphatase reflect liver damage caused by ACR. The diagnosis is confirmed by a liver biopsy that shows characteristic histological findings of portal tract inflammation, bile duct injury and venous inflammation, which is often associated with centrilobular necroinflammation of hepatic venules and surrounding hepatocytes (55-58).

1.4 Liver transplant tolerance

Due to its anatomical, cellular population and functional characteristics, the liver presents a unique immunological capacity. It is able to move from an orchestrated immune response against invasive pathogenic microorganisms towards a still incompletely understood immune hyporesponsiveness and immune tolerance observed in specific conditions such as HCV infection, and in a more intriguing way after liver transplantation (59-61). Indeed, in the solid organ transplantation setting, the liver has been considered more tolerogenic than other transplanted organs. This concept was initially supported by experimental studies showing a liver recipient exhibiting a spontaneous tolerance against donor liver graft in a full donor/recipient major histocompatibility complex (MHC) mismatch pairs in pigs, mice and in some rat strain combinations (62, 63). In addition, some strategies to induce tolerance revealed to be successful in rodents (64). In humans, clinical findings endorse the

aforementioned hepatic trend toward tolerance. Liver transplant recipients need less potent IS regimens, with lower blood through levels of IS drugs than those practiced for other solid transplanted organs and/or preconized by pharmaceutical industry (65). Hyper acute rejection is a rare condition in liver recipients, and episodes of ACR do not impact liver recipient long-term outcome. Chronic rejection is less frequent than in all other solid transplanted organs. Furthermore, there is not a significant benefit from human leucocytes antigens (HLA) matching, and even that positive cross match could be associated with more acute cellular rejection episodes; their correlation with worse outcome is not clearly demonstrated (66-70). Besides that, it has been demonstrated that a small group of liver recipients (non-compliant patients, patients with severe infections or malignancies), who had completely discontinued the IS treatment, were able to keep the liver allograft with normal function and without immunological graft injury for a long period of time, a stated posteriorly so-called spontaneous operational tolerance as described previously (20, 71).

1.4.1 Distinctive immunological hepatic properties

The aforementioned distinctive hepatic immunological properties have been attributed to its anatomical position, cellular population and physiology. Anatomically situated between the gastrointestinal tract and the systemic circulation, the liver has a peculiar dual vascularisation. Approximately 80% of its blood volume is supplied by the portal vein (PV); and while only 20% of the total blood volume reaches the organ via hepatic artery (HA) almost all-hepatic oxygenation is artery dependent. Intestinal, pancreatic and splenic low oxygenated blood outflow is drained to the liver through the portal system bringing all necessary food nutrients but also constantly exposing the hepatic parenchyma to all food-derived antigens, environmental toxins, pathogenic (mainly bacterial) and blood degradation products (59, 60). Inside the liver, venous and arterial blood flows are mixed passing through a unique honeycomb shaped system of sinusoids formed by a specific cellular type named liver sinusoidal endothelial cells (LSECs), arranged in such a way that makes it the only interface between blood flow and hepatocytes due to the lack of a basal membrane supporting the LSECs. At the same time blood pressure drops drastically from the PV and from the HA to the sinusoids resulting in a very slow blood flow into the sinusoids. These two conditions facilitate the contact and interaction between all blood contents with the multiple subsets of

parenchymal and non-parenchymal liver cells, which include LSECs, the professional antigen-presenting cells (APC) dendritic cells (DC), Kuppfer cells (the liver resident macrophages), hepatic stellate cells (HSC), intrahepatic lymphocyte T cells (T cells) and hepatocytes. Also, interactions between those cells are common and sometimes they present overlapping functions. The hepatic chronic exposition to lipopolysaccharide (LPS) and other bacterial-derived products from the gut and the recognition of these molecules by Toll-like receptors results in an anti-inflammatory cytokines production such as interleukin-10 (IL-10) instead of a pro-inflammatory response (72, 73). An additional key aspect of liver immunobiology is the fact that antigens can be presented in the liver microenvironment not only by professional APCs such as DCs, but also by cells such as LSECs, HSC and hepatocytes. Of note, presentation of antigens by these cells may usually result in sub-optimal T cell activation, as a result of the lack of adequate co-stimulation and the abundance of immunosuppressive cytokines. The result of this tends to be the apoptotic deletion of the antigen-specific T cells. In the clinical setting, the use of co-stimulation inhibitors in combination with reduced doses of CNI has been proposed to reduce the side effects associated with CNI. The use of CTLA4-Ig, which inhibits the CD80/CD86 co-stimulation signalling, has been addressed by many studies in kidney transplantation with interesting results (74). In contrast, in the context of liver transplantation, patients treated with CTLA4-Ig had a higher rate of rejection and mortality compared to patients who received CNI-based immunosuppression (75, 76). In addition to the potential bias due to the study design, one of the mechanistic reasons for these discouraging results could be that, in the hepatic environment, different co-stimulation pathways are involved in the activation of T cells. As animal studies show, PD-1 / PDL-1 co-stimulatory signalling is strongly involved in the activation of T cells in liver transplantation (77).

1.5 Achievement of Tolerance in Liver Transplant Recipients

Initial anecdotal clinical observations that some liver recipients can remain completely off IS treatment without immune allograft damage prompted the conduction of many clinical trials aiming to minimise or completely discontinue IS treatment as a strategy to avoid the deleterious effects of long-term IS. Such minimization strategies included conversion to non-CNI IS schemes, early steroid withdrawal or avoidance, and minimizations of CNI protocols usually made on a trial-and-error basis. Another approach tested to decrease specific IS side

effects, such as diabetes and nephrotoxicity, was the combination of IS drugs at reduced doses. Due the wide variety of IS minimisation study designs with variable sample size, non-homogenous patient inclusion criteria and different IS weaning protocols, results have not been consistent. This in turn has hampered the elaboration of evidence-based IS guidelines in order to decrease patients IS associated comorbidities. Therefore, long-term IS minimisation is still considered an empirical clinical practice (78, 79). Attempts to induce tolerance in early time post liver transplantation have been tried by employing T cell depleting therapies, associated or not with simultaneous infusion of donor hematopoietic cells, followed by rapid minimisation of the maintenance IS, generally based on monotherapy immunosuppression. Unfortunately, due to toxic effects of induction therapies, issues due to availability of donor cells, small series and patient selection bias; it has been difficult to interpret the overall results from these studies (80-83). Supported by experimental animal studies, the infusion in the post-transplant period of ex-vivo expanded liver recipient regulatory T cells (Treg) collected at any time before or after the transplant procedure has been advocated as a promising therapy to induce tolerance. Several groups are currently exploring this strategy. Many of the on-going trials are still in the initial phases and various issues have been raised concerning the doses and infusion time of cells (84, 85). In a recent seminal Japanese study, the infusion of Tregs in the earlier time post living donor liver transplantation (day 13 post-transplantation) was employed to induce tolerance. This strategy was associated with a per-operative splenectomy, T cell depleting therapy at day five post-transplantation and an initial triple IS therapy (Steroids, Calcineurin inhibitors and Mycophenolate Mofetil). Steroids and Micophenolate mofeil were withdrawn by the end of the first month and calcineurin inhibitors supposed to be completely withdrawn at the end of the 18^{th} months post transplantation. Using this protocol, the authors were able to induce tolerance in 7 of the 10 enrolled liver recipients. All ACR episodes occurred in patients presenting autoimmune liver diseases. Although the clinical trial was designed to enrol 40 patients, it was suspended early because 3 episodes of ACR occurred during the IS weaning period. It is interesting to highlight that splenectomy, a procedure not often performed in Western countries during the liver transplantation, was a part of their robust induction protocol. Furthermore, the Treg-enriched cell pool was generated from leukapheresis performed few weeks before the transplant and from splenocytes harvested from the spleen specimen resected at the time of the transplant procedure. Cells were not

cultured in good manufacturing practice (GMP) conditions and at the end, a mixture of immune cells with a wide variation of cell subsets between patients were infused, making the reproducibility of their protocol difficult. Also, in western countries, most transplants are performed using cadaveric liver transplants, which makes it more difficult to prepare and infuse the Treg-enriched cell pool at predefined times. For these reasons, the use of such a protocol in western countries would not be appropriate. However, these remarkable results have already been considered as a milestone in liver transplant tolerance research, prompting new studies to search for more accurate protocols using Treg cell infusion (86, 87).

1.6 Immunosuppression withdrawal trials

The complete discontinuation of IS treatment in stable liver recipients is a feasible approach to identify liver transplant recipients who spontaneously became tolerant in the later times post transplantation when realised under controlled conditions. This concept came about after Starzl et al. reported a small series of 6 liver transplant recipients who maintained normal liver function tests (LFTs) after total discontinuation of IS drugs due either to non-compliance or lymphoproliferative disorders. This initial report inspired posterior prospective studies in order to better characterise this phenomenon (20, 71, 88). Prompted by the capacity of those 6 previously mentioned liver recipients to maintain normal LFTs and no histological damage in the absence of IS therapy, Mazariegos et al., from the same group of Prof. Starzl, planned and conducted the first prospective clinical trial of intentional IS withdrawal in patients presenting clinical adverse effects of long-term IS therapy. Out of 95 liver recipients enrolled, 18 were successfully completely weaned off IS therapy (71, 89). From this clinical trial onward, many studies aiming to completely wean the IS treatment have been reported often in small series of liver transplant recipients. These studies employed different criteria for patient selection and for the IS weaning strategies, which could had contributed to a wide range of success going from the lowest 5% successful rate in one study up to a 60% in recent well controlled study with a overall average prevalence of 20% (Table 1) (20, 21). However, from the review of their patient selection criteria and IS weaning protocols, some favourable inclusion clinical criteria for successful IS withdrawal were visible. They were composed of: liver recipients with at least 3 years after transplantation, preference for more than 6 years after transplantation, predilection for non-autoimmune liver disease as an indication of transplantation (due to the

increased risk of recurrence of primary autoimmune liver disease and risk of developing a rejection episode during the weaning protocol), there are no recent ACR episodes and there are no significant histological or LFT abnormalities before the start of the IS weaning protocol. Furthermore, withdrawal protocols are generally performed over a 6 to 9 months period with a progressive IS drugs weaning with usually no more than 25% dose reduction at each 3- to 4-week interval.

Table 1: Immunosuppression withdrawal clinical trials on liver transplant recipients

Study	Year	Centre	Enrolled patients (n)	Tolerant patients % (n)	Rejection Acute/Chronic %	Graft loss % (n)
Mazariegos et al[89]	1997	Pittsburgh – USA	95	19 (18)	26/0	0
Devlin et al[90]	1998	KCL London – UK	18	16.7 (3)	28/5.6	5.6 (1)
Takatsuki et al[91]	2001	Kyoto – Japan	26	23.8 (6)	12/0	0
Pons et al[92]	2003	Murcia – Spain	9	33 (3)	6/0	0
Eason et al[93]	2005	New Orleans – USA	18	5.6 (1)	61/0	0
Tryphnopoulos et al[94]	2005	Miami – USA	104	19 (20)	67/1.9	0.96 (1)
Tisone et al[95]	2006	Rome – Italy	34	23.4 (8)	76.4/0	0
Assy et al[96]	2007	Ontario – Canada	26	8 (2)	58/0	0
Pons et al[97]	2008	Murcia – Spain	12	41.6 (5)	58.3/0	0
Feng et al[98]	2012	American multicentre	20	60 (12)	35/0	0
Benítez et al[1]	2013	European multicentre	102	42 (41)	58/0	0
de la Garza et al[99]	2013	Pamplona – Spain	24	62.5 (15)	33/4.1	0
Bohne et al[100]	2014	Barcelona/Valencia – Spain	34	50 (17)	44/0	0

Due to the importance of this strategy, substantial research grants have been recently allocated to support studies of IS discontinuation in liver transplantation, notably by the Immune Tolerance Network (ITN) in the USA and the Reprogramming the Immune System for the Establishment of Tolerance Consortium (RISET) by the European Union. These programs supported the first two very well controlled multicentre clinical trials; whose results suggested that tolerance could be achieved in higher rates at late time points after transplantation. In the American paediatric study, 60% of the 20 living donor liver recipients enrolled were able to completely discontinue IS drugs, while in the European adult trial, 41 out of 102 enrolled liver recipients achieved the status of spontaneous operational tolerance (1, 98). A second IS withdrawal clinical trial that was conducted by the same European group, was designed to investigate whether the presence of on-going liver infection process could impair the SOT achievement once all enrolled liver recipients were HCV-RNA positive. Employing the same

previously described IS withdrawal protocol, 50% of the 34 enrolled liver recipients were able to achieve the study primary end-point and became SOT (100). In all three clinical trials, rejection episodes in patients who failed the withdrawal were mild and almost all patients were treated by re-introduction of initial IS doses with a short course of CS in a low dosage. No liver recipients lost the allograft due to the IS discontinuation attempt. The clinical characteristics associated with successful IS weaning were older liver recipients, longer time passed from the transplant procedure, and minimal IS treatment before starting the weaning protocol. Being statistically significant in the first European and in the American multicentre clinical trials, the most robust clinical marker associated with SOT development was when more time had elapsed after the liver transplant (1, 98). Unfortunately, none of these clinical parameters could be used as predictor marker of operational tolerance achievement. In that context, the identification of biological markers of tolerance could be very helpful, in order to circumvent the exposition of less tolerogenic liver recipients to unjustifiable risk of rejection episodes (88, 101).

1.7 Biomarkers of spontaneous operational tolerance and of acute cellular rejection occurring during IS withdrawal from liver transplant recipients

Even taking into account the inclusion and/or exclusion clinical criteria already identified in association with successful IS weaning, there is still a considerable risk for rejection occurrence during IS withdrawal protocols. In this scenario, the identification of liver recipients likely to become tolerant or liver recipients bearing tolerance characteristics before the initiation of IS weaning protocols should be a key step in the liver selection process (101, 102). Unfortunately, the two most robust “clinical markers” of successful IS weaning (age and time elapsed from liver transplant procedure) are not able to precisely forecast the result of IS withdrawal protocols; which raises the necessity for identification of more accurate biological predictors of liver spontaneous operational tolerance (88). Biomarkers were defined as “a characteristic that is objectively measured and evaluated as an indicator of normal biological processes, pathogenic processes, or pharmacologic responses to a therapeutic intervention” by Biomarkers Definitions Working Group (103). Tolerance biomarkers can be used to identify those liver recipients prone to become tolerant, thus circumventing the exposition of unlikely

tolerant liver recipients to the ACR development and graft failure risks. Likewise, they are also useful for the immune monitoring of established tolerant liver recipients over time when tolerance status could in theory fails at later time point after its establishment. Furthermore, the identification of biomarkers able to predict ACR episodes before their clinical or histologic manifestation could be used as immune monitoring safety tool in IS withdrawal protocols. As different types of cells, and different subsets of T cells, are involved on the liver allograft tolerance development and on the occurrence of ACR episodes, tolerance and rejection biomarkers will be, by analogy, characterized by allograft cell phenotype and their behaviour. In fact, the already described biomarkers and assays used in this setting aim to 1) characterize the allograft cell populations and subsets, 2) identify and quantify cytokines or other cellular product from defined immune cell population, and/or 3) investigate the immune cell functional status quantifying the degree of activation, proliferation, gene transcription profile, and the production of immune related molecules as pro-inflammatory cytokines by activated T cells (102).

1.7.1 Biomarkers of spontaneous operational tolerance in liver transplantation

Biomarkers of SOT have been researched since the description of the original 6 tolerant liver recipients. Indeed, in the same report, the authors reported an exhaustive series of tissue and blood analyses performed in a series of liver recipients, which included those off IS treatment, aiming to clarify the allograft acceptance phenomenon (61). Subsequent reports, from the same group and others, attempted to differentiate tolerant from non-tolerant liver recipients using flow cytometry cellular immunophenotyping. So, the Pittsburgh group described a higher plasmacytoid DCs/monocytoid DCs cell ratio in SOT or liver recipients undergoing IS withdrawal in comparison to liver recipients under IS therapy or those who had failed IS withdrawal attempt (104, 105). Later on, other cross sectional studies comparing long term SOT liver recipients with age-matched volunteers and/or stable immunosuppressed liver recipients disclosed a higher frequency of regulatory $CD4^+CD25^+$ T cells among SOT recipients in peripheral blood mononuclear cells (PBMC) by flow cytometry in paediatric and adult SOT liver recipients (106, 107). The presence of $FoxP3^+$ T cells was detected in liver biopsies from SOT paediatric living-donor liver recipients, whereas $FoxP3^+$ T cells were absent in liver recipients with clinical characteristics of chronic rejection (108). In a prospective IS

withdrawal clinical trial, $CD4^+CD25^+$ and $CD4^+CD25^{high+}$ T cell populations and *FoxP3* transcripts progressively increased in blood samples sequentially collected throughout the IS weaning protocol and stayed elevated in liver recipients who were able to completely discontinue IS drugs, a phenomenon that was not observed in recipients who failed the protocol, in whom these cell populations remained stable during the entire protocol (97). In a first study employing microarray gene expression profiling, Martinez-Llordella et al. sought to identify gene footprints present in peripheral blood samples capable to differentiate long-term SOT liver recipients from those under IS treatment. Those signatures contained genes encoding for γδ T cells, $CD8^+$ and natural killer (NK) receptors, and many proteins associated with cell proliferation arrest (107). In the following work, with an enlarged cohort of SOT liver recipients, the same authors, using the training and validation set protocol design, reported a group of gene signatures containing up to seven genes capable to accurately discriminate tolerant from non-tolerant liver recipients suggesting that transcriptional gene profile of peripheral blood could be useful in identifying candidates to IS discontinuation (109).

Focusing on the identification of possible mechanisms involved in the tolerance development process and on tolerance biomarkers which could predict the success of the weaning protocol before changes in the IS treatment, Bohne et al. conducted a molecular study analysing sequential biological samples taken at the enrolment time, during the weaning protocol, and in the follow-up after total IS discontinuation or after the rejection episode from patients enrolled in the initially mentioned European multicentre IS withdrawal clinical trial. The molecular analysis of liver biopsies taken before the initiation of IS drug diminution accurately discriminated tolerant from non-tolerant liver recipients. The two groups of patients had differentiated expression of genes involved in iron homeostasis, notably the transferrin receptor (*TFRC*) and the hepcidin antimicrobial peptide (*HAMP*). Differences were also observed in the serum levels of hepcidin (the only iron absorption regulator currently known), ferritin, and in levels of hepatocyte iron deposition. Five genetic classifiers with up to 9 genes transcripts were reported to be able to forecast the result of IS weaning protocol with much sensitivity, specificity, and negative and positive predictive value; with less than 17.5% overall error rate. All of those genetic footprints contained at least two genes involved in iron homeostasis. Altogether, these results highlighted for the first time the influence of iron in the regulation of intra-graft allo-immune responses in liver transplantation pointing to the necessity

of further clinical and experimental studies in order to better understand how iron metabolism could interact with liver allograft acceptance by the recipients (2).

1.7.2 Biomarkers of acute cellular rejection during intentional IS withdrawal protocols

In the context of IS withdrawal monitoring, the identification of molecular biomarkers able to detect ACR in its early phases during the weaning period could be as useful as the finding of predictive tolerance biomarkers prior to starting the withdrawal protocol. Such ACR-associated biomarkers could be used as a fundamental monitoring immunologic tool throughout the IS weaning period. Theoretically, the detection of molecular biomarkers of rejection by non-invasive tests before serum liver tests deterioration alteration and/or liver graft histological alteration in a given patient under IS weaning protocol could trigger some clinical strategies in order to halt the rejection evolution. Some of these measures could be: 1) holding up the weaning protocol, 2) reverting the doses of IS drugs to the previous IS doses, 3) spacing the time between drug reductions and 4) excluding the liver recipient from the weaning protocol.

Blocking the ACR progression in its beginning when only rejection biomarkers are detected and no intense lymphocyte allograft infiltration has yet occurred could in theory, spare future non-tolerant liver recipients from the complete immune system reactivation manifested by clinical, laboratorial and histological ACR image. This strategy could avoid the “rejection priming effect”; which can prevent later attempts of IS withdrawal when those patients will be older and more time will have elapsed from the transplant procedure, these two being the most robust clinical factors associated with successful complete IS withdrawal. It is worth highlighting that normally, candidates for IS withdrawal clinical trials present stable LFTs, no important histological liver allograft damage at enrolment time and no occurrence of ACR episode in the previous 12 months before trial inclusion (1). Furthermore, in liver transplant settings, few studies have addressed the molecular profile and cellular pathways associated with ACR, hampering its own characterization and making difficult the comparison with cellular rejection occurring in other solid organs transplantation, such as in kidney and heart transplantation difficult. This could be related to the fact that the molecular assessment of ACR at the early time post-liver transplantation is strongly influenced by possible confounding factors such as ischemic-reperfusion injury, surgical complications inherent to the procedure

and/or systemic consequences of underlying liver end-stage disease, as well as the high incidence of opportunistic infections. Historically, liver recipient patients with more than 3 years post transplant have higher probability of becoming SOT when compared to liver recipients with less than 3 years after transplantation. Therefore the minimum period of 3 years after liver transplantation is currently accepted as an inclusion criterion in most clinical trials of IS withdrawal. In addition, at this stage, the aforementioned confounding factors that may influence the molecular characterization of ACR are absent and sequential biological specimens (liver tissue, blood samples, urine and stools) can be obtained at precise time points for monitoring purposes. So, it is expected that detected molecular changes will probably be more related to the ACR episode than to another possible event. As such, the clinical setting of IS withdrawal trials appears to provide the appropriate scenario for characterizing ACR biomarkers. In these studies, liver recipients recruited less than 6 years after transplantation were the most at-risk population to fail the IS weaning protocol and to develop an episode of ACR, compared to liver recipients whose transplants were performed more than 6 years before (87% vs. 62%) (1). Thus, the majority of patients included in a prospective study to characterize ACR biomarkers in the context of IS withdrawal should have less than six years of follow-up after liver transplantation.

1.8 High-throughput gene expression experiments

Microarray essays have the property to determine transcription expression levels of thousands of genes at the same time. The study of the all cellular or tissue sets of ribonucleic acid (RNA) transcripts, the transcriptome, can provide a comprehensive dynamic understanding of physio- or pathophysiological processes in a given moment. This so-called gene fingerprint determination is particularly interesting for studies related to the dynamic allograft acceptance or rejection processes in the organ transplant field (110, 111). However, some specific measures should be observed for the correct use of the microarray technology, otherwise data acquisition and analysis can be problematic and lead to spurious conclusions. Such measures include experiment design, array probe selection, samples choice, control of probe hybridization, expression levels image acquisition and transformation, data normalisation and filtering, correct statistic analysis and interpretation (112).

1.8.1 Microarray technique

Basically, the microarray method requires messenger RNA (mRNA) extraction from biological samples, which is reverse-transcribed into complimentary deoxyribonucleic acid (cDNA). The cDNA is labelled with a fluorescent dye and then applied into a slide support, usually a quartz surface sealed inside a plastic cartridge, the microarray gene chip, where dozens of thousands of cDNA probes, each of them characterizing a particular gene, are robotically printed in a defined address in the array support. After a "hybridization" phase, the gene-chip is washed to eliminate probe-unbound cDNA. Finally the gene-chip is laser-scanned for data acquisition by capturing the image of all fluorescent intensities of the dyes labelled to the hybridized cDNAs with posterior transformation into intensity values. When the signal captured at a determined spot is more intense; then the expression profile is more abundant for that gene specifically identified by the probe placed at the exact position in the gene chip (113, 114). Initial gene-chips made with cDNA probes currently have been replaced by gene-chips printed with oligonucleotide probes due to their higher DNA specificity and lower cross-hybridization effects that were frequently detected in first cDNA gene-chip versions (115).

1.8.2 Microarray experiments

Gene profiling experiments using microarray technology have been widely used in transplantation (116). In transplant research, as well in other clinical fields, microarray experiments are usually divided into unsupervised and supervised methods. In the unsupervised methodology, clinical samples are clustered based on gene expression profiling with no previous knowledge of biological and clinical information. The objective here is to identify subgroups presenting specific patterns with possible clinical interest based on gene similarities (117). Applying the hierarchical clustering methodology, Mueller et al. were able to disclose a subgroup of kidney transplant recipients at increased risk for developing delayed graft function based on the analyses of the transcriptome of post-reperfusion kidney biopsies (118). Conversely, the supervised method's objective is to determine differentially expressed genes that fit a predefined clinical pattern. These strategies are subdivided in class comparison and class prediction studies. The former approach aims to differentiate distinct groups based on differentially expressed genes, while the latter strategy's objective is to generate a mathematical algorithm containing differentially expressed genes that could

accurately predict the response to a treatment or to a specific clinical strategy adopted (119). As aforementioned, Martinez-Llordella et al. used a class comparison strategy to analyse PBMC gene expression profile in order to discriminate tolerant liver recipients from immunosuppression-dependent patients. In the following study, the same group applied the class prediction approach to define a gene signature to predict which liver transplant recipients were prone to develop spontaneous operational tolerance (107, 109).

1.8.3 Microarray experiment design challenges

In a representative microarray experiment, expression levels of thousands of genes are produced per sample in the same experiment, which represents an enormous quantity of data to process and analyse. This condition, the "curse of dimensionality" is tightly linked to the restricted number of samples normally available per study group, the "curse of dataset scarcity". The challenge concerning this common situation in transplant studies is to extract the correct clinical interpretation from too much data originated from few tested samples (120). The risk here is to find a highly superior number of gene candidates to constitute a gene classifier from a reduced number of available cases. Such classifier could accurately discriminate a specific data set but with no veritable correlation between the gene profiling and the clinical pattern studied. Experiment designs including internal validation mechanisms try to circumvent the reduced sample's limitation (121). The "split sample validation" strategy has been largely used in studies aiming to determine tolerance gene signatures, particularly in kidney transplantation due to the low availability of tolerant kidney recipients to include, as well in other transplant organs. This methodology uses a "training set" of samples to create the gene classifier, which is posteriorly confirmed in a distinct "validation set" of samples (109, 122-124). The leave-one-out cross validation (LOOCV) method is mainly employed when the creation of two distinct groups is very limited by the scarce number of samples. Here the classifier is repeatedly developed as many times as the number of samples, testing at each time one different sample against the group of remaining samples used in this case as the training set (125). Microarray analysis of cardiac biopsies from heart recipients using the LOOCV method was able to identify two different gene sets to differentially predict ACR from *T cruzi* infection at least 2 weeks before histological diagnostic (126). A similar approach, the leave-one-organ-out analysis, was applied in meta-analysis examining data sets from four

different transplanted organs (kidney, heart, lung and liver) to determine a common rejection gene signature. Due to the unbalanced number of datasets from each organ and in order to determine a gene-set overexpressed independently from the organ origin, Katri et al. removed datasets from each organ one at a time. A common signature containing 11 genes significantly overexpressed was identified across all four transplanted organs during the acute cellular rejection process (127).

1.8.4 Microarray data analysis

The analysis and interpretation of the huge amount of data generated by microarray experiments constitutes an unquestionable challenge for biological researchers. Currently, it is impossible to tackle those tasks without the help provided by Bioinformatics, the umbrella term used to define an interdisciplinary science field that combines biological fundaments, mathematic tools, statistical methods and computational software to analyse and interpret biological data (128).

1.8.4.1 Data normalization

Raw microarray results are inappropriate for a straight statistical analysis and interpretation. Actually there are many causes of systematic variation in a microarray experiment that are not truly related to the biological phenomenon. Sources of variation such as differences in dye labelling efficiency, unequal RNA quantities, background noise, spot overall intensity and probe gene chip position (print-tip variation) are inherent to the microarray method, which can influence the gene expression levels measurement (129). Those systematic variations need to be removed by the data normalization process before any definitive analysis. Data normalization aims to minimize the influence of those variations. As consequence, the true biological differences become more evident, which makes the analysis of gene expression levels within a single gene chip or between more than two gene chips comparable (130, 131). The transformation of raw data in a logarithmic scale is a recommended pre-normalization step due to the fact that fluorescent dye intensity values are highly asymmetric and it is assumed that log scales provide normal distribution data (132-134). Different normalization techniques are available, such as: quantile normalization, variance stabilizing normalization and background subtraction. The choice of the normalization technique will depend on the

type of microarray experiment. As an example, quantile normalization can be used in experiments employing two fluorescent dyes, as it renders the dyes' intensity distribution identically for all arrays and colours. Also, depending on the experiment's configuration there are three possible obtainable situations: i) normalization inside one gene chip, ii) paired gene chips normalization and iii) multiple gene chip normalization. For each situation, a set of genes has to be defined for the normalization. Global normalization uses all the genes in the array for the normalization when it is expected that only a small proportion of genes will be differentially expressed or there is symmetry in the expression levels of down- and up-regulated genes. Another option is the local normalization, when only a small group of genes that presents a constant expression level across different conditions, the so-called housekeeping genes, is used as reference in the normalization process (132, 134).

1.8.4.2 Data Filtering

Usually, a small number of samples generate thousands of gene expression levels in a microarray experiment, which is responsible for a dimensionality issue. Statistically, it is expected that the number of false positive results, the type I error, increases when thousands of gene expressions levels are tested at the same time. However, the strict control of the false positive rate can decrease the sensitivity of the experiment to disclose the real differentially expressed genes (135, 136). Furthermore, many probe sets in a gene chip are associated with non-expressed genes or genes with small expression profile and with no relevant association with the biological condition in question and their expression levels. Removing those genes' expression levels, considered experiment background noise, through a filtering process reduces the dimensionality problem (fewer results to analyse) and increases the experiment's power to discovery the real differentially expressed genes (137). However, as filter strategies and threshold levels are arbitrarily defined, caution should be taken to avoid an over filtering issue, which can exclude the true differentially expressed genes with real interest for the investigated biological condition from the final microarray analysis (134, 138).

1.8.4.3 Controlling multiple hypothesis testing

The greatest advantage of a microarray experiment for determining the expression level of thousands of genes at the same time can also be a risk factor for the data analysis, due to the

fact that there are too many data being analysed simultaneously. This situation characterizes the multiple hypothesis testing, wherein each gene expression level from all the genes from that specific microarray experiment are tested at the same time against the null hypothesis, which on occasion can be defined by not been differentially expressed and no association between the expression level and the studied condition (129, 139, 140). Therefore, traditional t-statistic tests and parameters are not adequate for such analyses. For instance if the historical p-value of 0.05 is used as significance threshold to identify differentially expressed genes in a microarray experiment where the expression levels of 25.000 genes were determined, it is expected that approximately 1250 genes would attain this value merely by chance, even when they are not truly differentially expressed. More appropriate statistical methods to analyse the multiplicity testing effect of microarray data, have been described (129). Probably the simplest and initially extensively used is the Bonferroni correction method. A new significance threshold value (α) value is calculated when the *p*-value (0,05) is divided by the number of *n* separate tests performed. In other words, the α value expresses the probability that at least one gene is considered significantly expressed when it is not. This is known as the family wise error rate (FWER). As FWER is considered too strict for the microarray analysis, a better option is to define the percentage of genes identified by chance in a given microarray experiment, the so-called false discovery rate (FDR). The proportion of truly differentially expressed genes, the true difference distribution, measures of variability, and samples characteristic, influence the FDR calculation (141). FDR is frequently calculated using the significance analysis of microarrays method (SAM) in most of the studies focusing on tolerance or rejection allograft signatures (100, 142-145). SAM employs adapted *t*-test methods for each gene in a dataset. A score for each gene is calculated based on its expression level changes in proportion to the standard deviation of repeated quantifications for that gene. Normally, in a SAM procedure, up to a thousand permutations tests are performed per each gene in order to identify whether the expression level is significantly associated with the condition studied by the experiment. Genes with values above a pre-determined threshold are considered as being significantly differentiated. A smaller or a larger set of identified significant genes depends on adjustments to the threshold level. Normally, most of studies assume a FDR threshold to 5% (146).

The prediction analysis of microarrays (PAM) is another *t*-statistic test modified by the incorporation of a fudge factor in its formula; which is commonly employed in class prediction transplant studies (109, 147). PAM aims to identify significant genes to be included in a prediction gene classifier by the measurement of the difference between the mean expression level of a given gene in a set of genes with the overall mean of expression level of such gene (148). In the transplant field, the PAM methodology has been used to identify gene signatures able to predict tolerance in long-term stable transplanted patients as well as constructing gene classifiers able to predict acute cellular rejection (109, 147).

Furthermore, a possible microarray interpretation pitfall is only to consider the expression level changes from individual genes, which can produce misleading results. A given list of statistically significant genes may have no correlation with the biological condition investigated. Single-gene analysis does not consider the global effect of gene sets in a specific biological pathway. Sometimes a small expression increase of all genes involved in a particular metabolic pathway is more effective to regulate a cell process than an exponential increase in the expression level of a single-gene (149). The gene set enrichment analysis (GSEA) assesses microarray data considering gene-sets, which are defined based on the understanding of previous biological pathways. Liver biopsy GSEA analysis identified IFN I (IFN α/β) as the most transcriptional pathway associated with tolerance in HCV positive liver recipients when compared to publically available transcript gene sets databases, whereas in HCV negative liver recipients, tolerance was more associated with iron ion homeostasis pathway (2, 100). Employing a stepwise mathematical algorithm, GSEA estimates the tendency for members of a gene set to appear on the top or on the bottom of a ranked list of gene expression levels in order to determine the correlation between the gene-set with a specific biological phenotype. GSEA interprets gene expression profiles paying attention to their genic chromosomal location similarities, to their biological function and regulation analogies with the objective of obtaining a thorough understanding of specific biological mechanisms and discovering data clinical implication (149, 150). Further, GSEA allows the possibility of comparing gene datasets originating from independent laboratories, as well as comparing experiments performed using distinct microarray platforms (151).

1.8.5 Bioinformatics software and microarray public databases

All of the aforementioned described complex statistical methods to analyse the huge amount of microarray data required the development of sophisticated software customized to explore thousands of components of biological information and hypotheses at the same time. Bioinformatics package systems, notably the R package, were developed by consortia of renowned universities and kept online for free use (152). Package systems process raw microarray data into normalised expression levels; calculate differential expressions and control false positivity; select significant expression cut-offs levels; and create clusters based on identified gene regulation similarity along with many other functions (153). Additionally, in order to facilitate microarray data sharing, research groups are encouraged to store their data in online public repositories sponsored by referent universities, where free online consultation is allowed for comparison purposes. The result comparison strategy seeks to check data reproducibility and to certify clinical validity of data from different experiments and laboratories increasing the data robustness, sensitivity and biological relevance (154).

1.8.6 Technical validation

Microarray technology is a powerful and widely employed assay to determine gene transcription changes in organ transplantation immunological studies (111). Results are interpreted more correctly due to the development of adjusted statistic tools and sophisticated software. Modern gene expression microarrays are commercially available making microarray experiments easier and more simplified. Meta-analysis studies allow the possibility to disclose gene expression similarities, which can characterise immunological process throughout different transplanted organs (127). However, microarray results can be contaminated by the presence of experimental noise due to inappropriate probe annotation, cross-hybridization due to lower probe specificity, different platform designs, and laboratory and researchers' dependent factors. Also, microarray expression profiling is usually employed to investigate thousands of genes aiming to identify a small set of them with biological and clinical implications (155). Then, in order to exclude the presence of all these experimental noises, it is strongly advised to validate the microarray results for the given genes of interest by employing a different method such as the quantitative polymerase chain reaction (qPCR). This

strategy, not only excludes factors of interference, but also contributes to confirm the future gene classifier for clinical application using a reduced number of genes (156, 157).

1.8.7 Transcriptome analysis using next-generation sequencing

Since its discovery in the 1990s, microarrays have been widely used in many areas of biological science. More specifically in the transplant field, this technique has proven very useful for determining transcriptomes associated with specific immunological phenotypes after organ transplantation (2, 107, 122-124, 158, 159). Accordingly, microarray technique is used in the present study to determine gene signatures associated with acute cellular rejection in the context of immunosuppression withdrawal post liver transplantation (160). However it should be noted that microarray limits, such as probe cross hybridization, background noise, and inaccurate measurements could compromise experiment results and analyses In addition, only genes for which a specific gene-probe is present in the microchip can be detected by a microarray experiment, excluding unknown genes that could be eventually differentiated (112, 113, 129, 134, 137, 161). Conversely, the new platform RNA-seq uses high-throughput sequencing techniques, the so-called next-generation sequencing (NGS) to direct sequence all transcriptome of a specific sample. Briefly, RNA-seq comprises sample RNA extraction and fragmentation with posterior reverse transcription into stable double strand complimentary DNA (ds-cDNA). The ds-cDNA is sequenced by employing high-throughput short read sequence methods. Then, sequences are aligned to a reference genome sequence to determine which genome regions have been transcribed. The acquired data are used to determine gene annotation and relative levels of gene expression. (162, 163) This promising platform could replace microarrays for genome-wide transcriptome profiling studies (164). In the meantime, there are still some challenges ahead. RNA-seq exponentially generates more data than microarrays, which requires special data storage platforms as cloud technology and complex bioinformatics algorithms, for accurate analysis and interpretation. In addition, the RNA-seq popularisation as a technique of choice for large-scale studies of gene expression is still limited by its high cost (162-165).

1.9 Iron homeostasis

Due to its capacities to accept or donate electrons, iron is a vital cellular element, which is an essential component of many molecules implicated in metabolic and synthetic processes, oxygen transport, mitochondrial metabolism and DNA cycling. However, unbalanced iron redox activity can generate toxic and harmful free radicals as reactive oxygen species (ROS) via Fenton/Haber Weiss reactions (166, 167). Elaborate pathways are responsible for maintaining iron homeostasis, avoiding free iron accumulation and delivering the required amount of iron to organs and tissues avoiding the deleterious effects either of iron overload, the pathogenesis of many iron disorders, or iron deficiency which leads to anaemia and its consequences (168). Iron has been also implicated in immune defence mechanisms, once its serum restriction could be considered a protective mechanism against pathogenic microorganisms. Besides its contribution to innate immunity, iron is also important for the immune cell development and physiology participating in this way with the immune system modulation (169).

1.9.1 Iron Uptake and trafficking

The mean concentration of iron in an adult human is around 3-4g. Iron is presented in all tissues, but approximately 60% of all body iron is found in erythrocytes (≈ 2-3g) as component of heme in haemoglobin. Transferrin (TF), the main plasma iron transporter to tissues, is usually 20-40% saturated (≈ 3-7mg) in normal conditions. About 1g of iron is stored within intracellular proteins as ferritin and hemosiderin (167). Daily body iron requests are supplied by recycling iron from aged erythrocytes and by dietary absorption. On the other hand, radiotracer studies estimated quotidian iron losses at 1-2mg per day via cell desquamation or exfoliation, and minimal blood losses in gastrointestinal and urinary systems (170). Even though these losses could be considered a kind of iron excretion mechanism, currently there is no mechanism of iron excretion described; which makes the iron dietary absorption of the sole evolutionary instrument to regulate body iron content (171).

1.9.1.1 Dietary Iron Uptake

Diet contains two principal forms of iron: inorganic or non-heme iron is present in a vast assortment of aliments and is poorly absorbed, and heme iron mainly originates from animal-

protein. Ferric iron (Fe^{3+}), the most abundant form of inorganic iron is taken up in the proximal duodenal portion (172). The presence of acid gastric secretions enhances Fe^{3+} solubility promoting its reduction into Fe^{2+} by the apical membrane reductase duodenal cytochrome b (DCYTB). Fe^{2+} crosses the enterocyte membrane coupled to the divalent metal transporter 1 (DMT1), initially known as natural-resistance-associated macrophage protein-2 (NARMP2), through a proton gradient generated by the Na^{+}/H^{+} exchanger-3 protein (NHE3) (Figure 1) (173). Heme dietary iron, originating from animal proteins, is more effectively absorbed than inorganic iron, however its absorption mechanism is not fully understood. The heme carrier protein 1 (HCP1) and the proton-coupled folate transporter (PCFT) have been proposed as candidates to transport heme from duodenal lumen into enterocytes, where iron is released as Fe^{2+} upon heme haemooxygenase-1 (HO-1) degradation (174-176).

1.9.1.2 Heme iron recycling and heme-oxygenase-1

Senescent erythrocytes are mainly phagocytised by macrophages situated in liver sinusoids and in the splenic red pulp. Whereas the haemoglobin proteolysis occurs inside the phagolysosome, heme compound is exported into the cytosol coupled to the heme-responsive gene-1 (HRG-1) protein to be degraded by the HO-1 with subsequent release of Fe^{2+} for posterior reutilisation (177-179). The degradation of heme is necessary to avoid the consequences of its pro-oxidant effects and to recycle iron for later reuse. Indeed, heme is involved in the production of oxidative radicals that can lead to tissue damage such as lesions on endothelial cells (180, 181). Specific enzymes called heme oxygenases (HO) degrade the heme molecule. Three isoforms of HO have been described: HO-1, HO-2 and HO-3, with OH-1 being the most studied and characterized. HO-1 is mainly expressed in hepatic, endothelial, myeloid, and respiratory epithelial cells (182). In the presence of oxygen and nicotinamide adenine dinucleotide phosphate (NADP), HO-1 cleaves the heme compound giving the antioxidant molecules, biliverdin and carbon monoxide, as well as the pro-oxidant Fe2 + (183). The sequestration of $Fe2^{+}$ by ferritin neutralizes its pro-oxidant effects (181). Finally, CO acts as a co-signal of biliverdin reductase in the reduction of biliverdin to bilirubin. In addition, beyond its enzymatic actions and anti-oxidant cytoprotective effects, other important roles have been attributed to the inactive form of HO-1 as cellular signalling, which includes transcription factor activation, protein binding, phosphorylation, among others (181). New

evidence suggests that HO-1 suppression may be associated to the increased inflammatory status in patients with lupus erythematous and multiple sclerosis (184, 185). HO-1 plays a dual role in the evolution of cancer; the nuclear expression of HO-1 is associated with cancer progression and metastasis in prostate cancer and in malignant head and neck tumors (186, 187), while it seems to play a protective role in breast cancer (188). More specifically, in organ transplantation, the expression of HO-1 has been associated with the modulation of ischemia reperfusion injury and the innate and adaptive immune response (189, 190).

1.9.1.3 Iron export and trafficking

Intracellular Fe^{2+} originating from diet uptake can be sequestered and stored within Ferritin, the main iron-storage protein; or be exported to plasma coupled at Ferroportin (FPN) at the level of duodenocyte basolateral membrane (191-193). Currently, FPN is the unique mammalian iron transmembrane protein exporter described. Then, it also mediates the transfer of iron originated from erythrophagocytosis from macrophages and hepatocytes to the plasma (194, 195). Iron export from macrophages needs the multicopper oxidase ceruloplasmin protein to convert Fe^{2+} into Fe^{3+} before being loaded into the main plasma iron carrier TF, while Fe^{2+} exported from duodenocytes requires a ceruloplasmin homologue, the hephaestin to be oxidised to Fe^{3+} (191). TF deliveries ferric iron to all tissues, however about two thirds of all body iron is required by bone marrow for the erythropoiesis. At the cell surface, TF binds to the Transferrin receptor 1 (TFR-1) being internalised via endocytosis. Endosome pH changes favour iron releasing and reduction into Fe^{2+} by the six-transmembrane epithelial antigen of prostate (STEAP3) reductase (196). The apotransferrin-TFR1 is recycled at the cell membrane with posterior release of apotransferrin into the plasma. Fe^{2+} is transported from the endosome to the cytosol coupled to the DMT1, where it is sequestered and stabilised within Ferritin in its ferrous nonreactive reduced status, precluding the production of noxious free ROS via Fenton/Haber Weiss reactions (197).

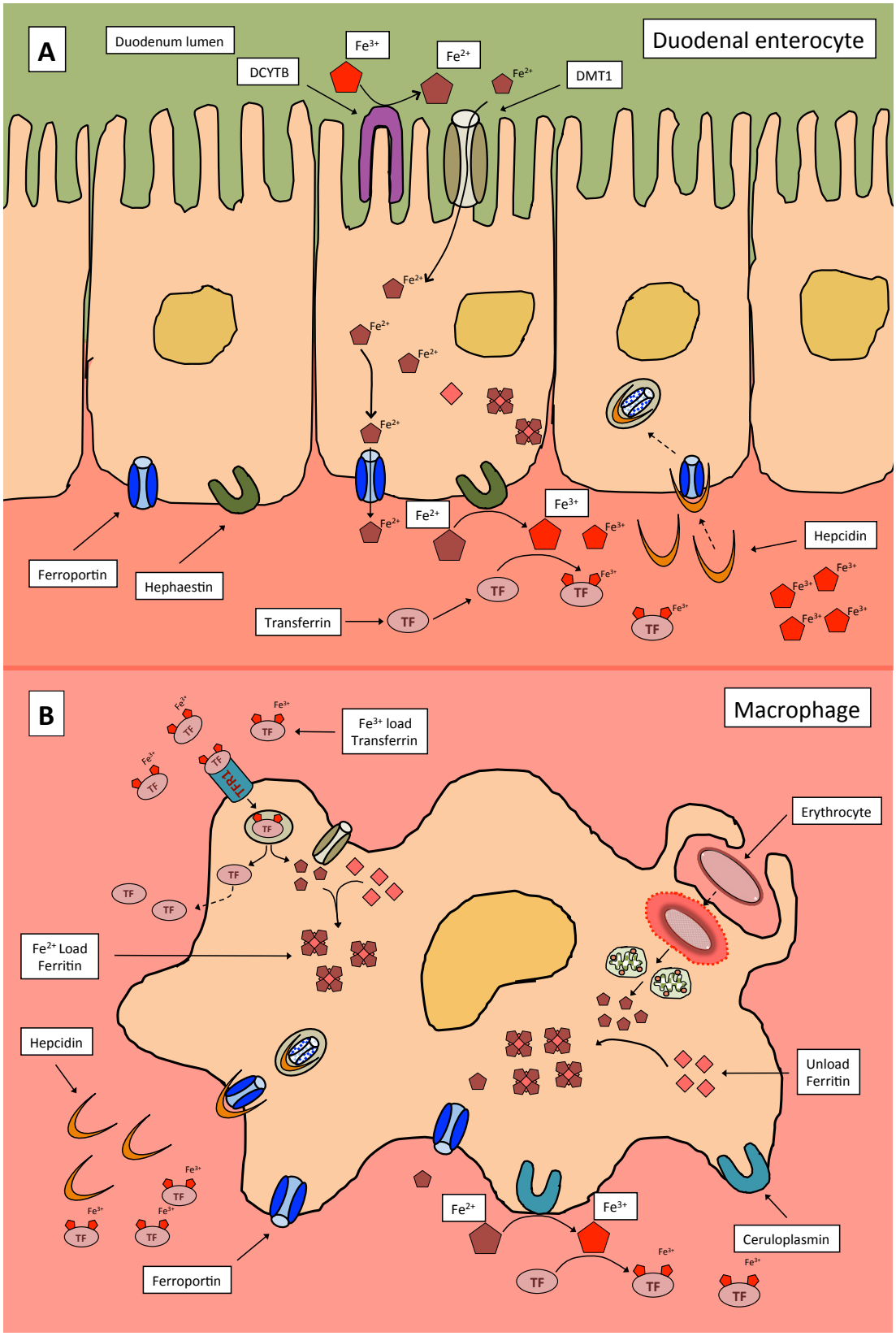

Figure 1: Iron uptake and trafficking: (A) Duodenal cytochrome b (DCYTB) reduces dietary inorganic Fe3+ to Fe2+ at the cellular apical membrane, then Fe2+ crosses the cellular membrane coupled to the divalent metal transporter 1 (DMT1). Ferritin stabilizes and stores Fe2+ avoiding its intracellular oxidation. Ferroportin, situated at the basolateral membrane, exports Fe2+ that is prompted oxidized by Hephaestin to Fe3+ facilitating the Transferrin (TF) uptake. **(B)** At the macrophage membrane, iron-load-TF binds to transferrin receptor 1 (TFR1). Fe3+TF-TRF1 complex enters the cell by endocytosis. Fe3+ is reduced inside the endosome to Fe2+ and transported into the cytosol coupled to DMT1 to be stored by Ferritin; the apotransferrin is recycled and liberated into the plasma. Heme oxigenase 1 (HO-1) catalyses the degradation of heme compounds originated from phagocytized senescent erythrocytes recycling Fe2+ for posterior use. High iron levels induce hepcidin transcription at the hepatocyte level. Hepcidin binds to Ferroportin at the macrophage membrane inducing its internalization and degradation, resulting in intracellular iron accumulation. The author based on the articles mentioned in the text drew the figure.

1.9.2 Iron homeostasis and hepcidin

Iron overload and/or deficiency, inflammation status, erythropoiesis, and hypoxia are identified stimuli that modulate the iron homeostatic machinery. It happens at different levels as uptake, trafficking, utilization and storage (198). Hepcidin, a small protein constituted by 25 amino acids on its active conformation and mainly produced by hepatocytes has a central role on iron regulation (199-201). In physiological conditions, when iron levels are sufficient, hepcidin binds to FPN at the cell membrane of duodenocytes, macrophages and hepatocytes. This interaction triggers FPN endocytosis with subsequent proteolysis at lysosomal level. Reduced availability of FPN at the cell membrane level inhibits iron efflux from duodenocytes. The same occurs with macrophages and hepatocytes, where cellular iron efflux inhibition due to FPN cellular internalisation leads to intracellular iron overload with consequent reduced serum iron levels (202). Hepcidin expression modulation takes place in hepatocytes at transcriptional level in a negative feedback way. Hepcidin synthesis is enhanced by iron overload and its production is down regulated in the presence of iron deficiency. The bone morphogenic proteins and signal mothers against decapentaplegic homologs proteins (BMP/SMAD) pathway is the main regulator of hepcidin expression on physiological conditions. BMPs react to high iron levels and bind to type I and type II BMP receptors at the hepatocyte membrane. Hemojuvelin protein (HJV) acts as a co-receptor of BMP ligands, mainly BMP2 and BMP6, and binds to BMP-BMPR. The complex HJV/BMPR/BMP triggers the phosphorylation of receptor-activated SMAD proteins forming at the end activate transcriptional complexes including the common mediator SMAD4. The SMAD4 complex translocates to the nucleus, where the hepcidin antimicrobial peptide gene *HAMP*, the main hepcidin-coding gene is up regulated (203). Additionally, at high levels of TF-Fe^{2+}, HJV protein enhances the interaction between TF-Fe^{2+} to TFR-2 instead to TFR-1 via modulation of the hemochromatosis protein HFE (a major complex class 1-like protein). Then the complex TF-Fe^{2+}/HFE/TFR-2 probably induces hepcidin expression via SMAD signalling pathway (168, 204, 205). Hepatocytes can sense plasma iron levels through multiple interactions between TRF1, TFR2, HJV, and HFE. High levels of TF-Fe^{2+} promote the interaction between HFE and TFR2 instead of TFR1. Then, the HFE-TFR2 complex activates the ERK/MAPK and BMP/SMAD signalling pathways leading to hepcidin expression (Figure 2: Iron sensing). In the same way, BMP-HJV complex combines with its receptors BMPR1 and BMPR2 at hepatocyte membrane inducing receptor-

activated SAMD phosphorylation (R.SAMD-p). SMAD proteins (1, 2, 3, 5 and 8) undergo a sequential phosphorylation with a final formation of activated hepcidin transcriptional complexes. Finally an activated hepcidin transcriptional factor is formed involving the co-SMAD factor SMAD4. The SMAD4 complex translocate to the nucleus, where the hepcidin antimicrobial peptide gene *HAMP* is up regulated (Figure 2: BMPR complex) (203-205).

1.9.2.1 Iron homeostasis under hypoxia and erythropoiesis

Besides iron levels alterations, hepcidin expression is also modulated by hypoxia, erythropoiesis and infection/inflammation. Stress conditions as hypoxia or bleeding stimulate erythropoiesis in order to enhance oxygen transport to tissues. Erythropoiesis stimulus enlarges the population of erythropoietic precursors increasing iron consumption destined to haemoglobin synthesis. Hypoxia-inducible factors (HIF) are key actors in cellular adaptation to oxygen imbalance. Hypoxemic conditions inhibit the activity of oxygen-dependent prolyl-4-hydroxylases, decreasing the hydroxylation of HIF. Then, stabilized HIF-1 and HIF-2 are translocated to the nucleus to bind to the HIF-1β subunit, resulting in the up-regulation of a variety of genes involved in different pathways, including cell proliferation, energy metabolism, angiogenesis, among many others (206, 207). In mice exposed to hypoxia, HIF is involved in the up-regulation of HO-1 (208), which is involved in heme degradation and iron recycling, as discussed in section 1.8.1.2. Furthermore, hypoxic conditions *per se* inhibit hepcidin expression; volunteers maintained in hypoxic chambers during 6 hours and under physiologic and exercise conditions presented low levels of hepcidin associated to an elevation of the platelet-derived growth factor BB (PDGF-BB) (Figure 2 Iron sensing) (209). In addition HIFs modulate erythropoietin (EPO) hepatic and renal production (210). EPO-induced erythropoiesis supresses *Hamp1* expression in mice leading to the suppression of hepcidin synthesis, with consequent increase on diet iron uptake and cellular iron release (211).

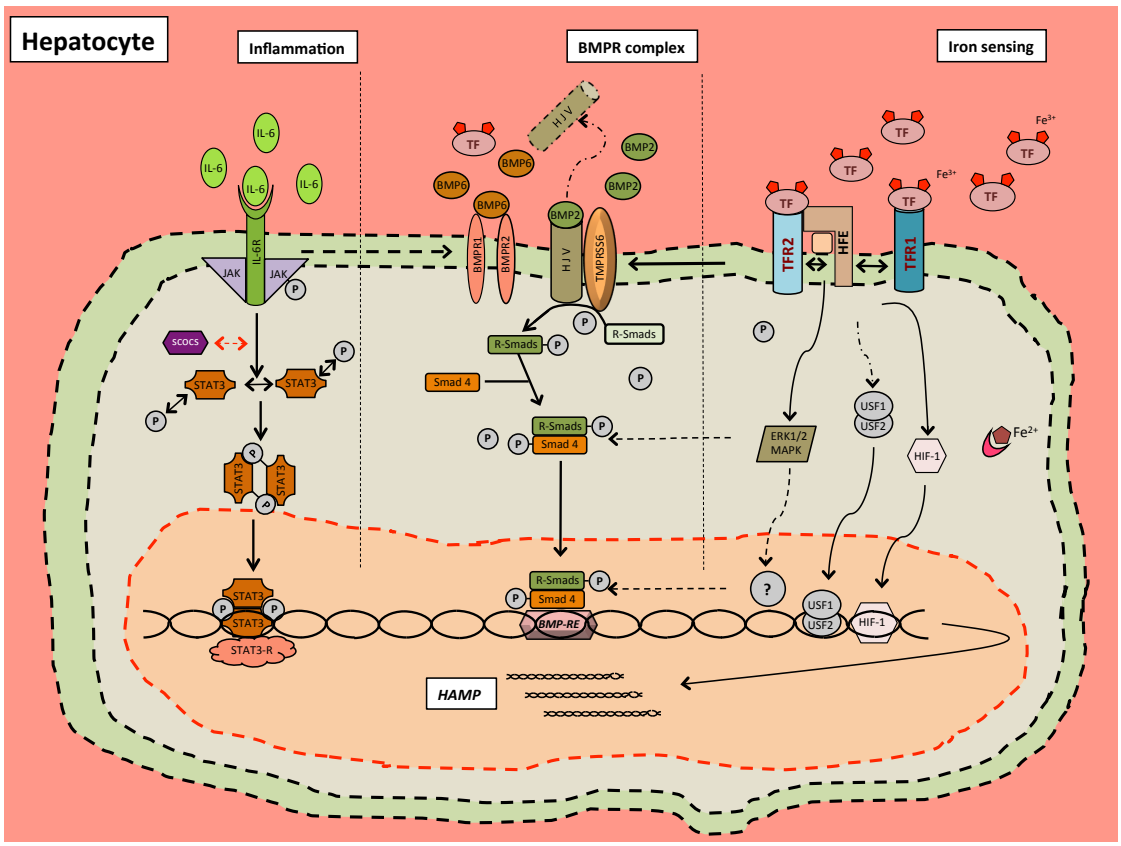

Figure 2: Regulation of Hamp transcription at the hepatocyte level: Inflammation: Pro-inflammatory cytokine, IL6 binds to its receptor (IL-6R) at the cell membrane provoking the phosphorylation of the Janus kinase 1 (JAK1). IL-6-IL-6R-JAK1-p complex induces the phosphorylation of the signal transducer and activation of transcription 3 (STAT3) factor. STAT3 forms homodimers that translocate to the nucleus where they bind to STAT3-R the interferon γ-activation sequences which drives the hepcidin transcription. Suppressors of cytokine signalling (SOCS) factors can inhibit the JAK1-STAT3 pathway of hepcidin transcription**. BMPR complex:** BMP/SMAD pathway is the main described regulator signalling of hepcidin transcription responding to iron-related and inflammatory signals. BMP6 interacts with its receptor BMPR1 and BMPR2 inducing the phosphorylation of receptor-activated SMADs. Phosphorylated R-SMADs make activated transcriptional complexes with phosphorylated SMAD4. P-SMAD4/R-SMAD-P complex enters to the nucleus and stimulated hepcidin transcription. Hemojuvelin (HJV) can inhibit this downstream signalling; TMPRSS6 interacts with HJV provoking its fragmentation. **Iron sensing:** The HFE-TFR2 complex can also trigger hepcidin transcription via the extracellular signal-regulated kinase (ERK1/2) and the mitogen-activated protein kinase. Iron sensing factors as upstream stimulatory factors (USF) compete with hypoxia inducible factor-1 for the binding to hepcidin transcription factors as the enhancer boxes (E-box)**.** The author based on the articles mentioned in the text drew the figure.

1.9.3 Iron immune system modulation

Iron levels interfere not only on the host immune response modulation, but also on the invading microorganisms growth and survival. Besides their influence on the innate immune response, the iron/hepcidin axis participates in T cell activation and proliferation influencing in this way the adaptive immune response (169) (212).

1.9.3.1 Infection/Inflammation and iron modulation

In response to noxious stimuli as infection and inflammation, a coordinated response is initiated by activation of many cell types as monocytes, macrophages, and T cells amongst many others (213). Pro-inflammatory cytokines enhance immune cell recruitment and promote the synthesis and secretion of a high number of other proteins involved in the inflammatory response. In a murine model, *Pseudomonas aeruginosa* intraperitonal challenge enhances hepcidin production via TLR4-dependent pathway and increases iron deposition in splenic macrophages. In the same work, subcutaneous infection of group A *Streptococcus* in mice induced local neutrophil infiltration with increasing hepcidin expression on infected skin biopsies, suggesting a mechanism of local hepcidin production (214). Moreover, Nemeth et al showed in an elegant work that in vitro hepcidin production by human and mice cell cultures requires IL-6 after microbial stimuli (215). Additionally, iron excess contributes to the formation of ROS, which can cause tissue injury via oxidative stress and inflammation. So, iron restriction decreases the oxidative stress and inflammatory tissue injury in models of acute hepatitis, renal interstitial fibrosis, experimental autoimmune encephalomyelitis (EAE), and type II diabetes in rodents (216-220). Specific pro-inflammatory cytokines as IL-1 and IL-6, IL-22 and type I interferon strongly induce hepcidin expression via the Janus kinase 2 and signal transducer and activators of transcription (JAK/STAT) pathway. IL-6, the main inflammatory hepcidin stimulus, binds to its receptor alpha and gp130 on the hepatocyte cell surface. The formed complex activates JAKs with subsequent phosphorylation of STATs, mainly STAT3. Phosphorylated STAT3 translocates to the nucleus leading to the *HAMP* up-regulation with consequent hepcidin expression (Figure 2: Inflammation) (221, 222).

1.9.3.2 Iron levels modulate innate immune response

Infectious and pro-inflammatory stimuli induce hepcidin expression mainly via IL-6 pathway; leading to cellular iron export inhibition with macrophage and hepatocyte intracellular iron overload. This results in plasma iron restriction. In the inflammation/infection scenario, such iron restriction inhibits microbial growth and has been considered an important mechanism of defence in mammals against microbial damage (215, 223). Hepcidin-deficient mice infected with *Vibrio vulnificus* presented increased bacteremia and higher mortality when compared with wild-type mice. Administration of hepcidin agonists leads to hypoferremia, with subsequent diminution in bacterial counting and animal survival improvement (224). Hereditary hemochromatosis (HH) patients, characterized by iron overload and a variable degree of hepcidin deficiency, present an elevated risk for atypical infections including *Vibrio vulnificus*, *Yersinia enterocolitica*, and *Listeria monocytogenes* (167, 225). An experimental model of malaria infection suggests that *Plasmodium beghei* infection induces hepdicin production with iron redistribution from hepatocytes to macrophages, which could impair future iron hepatocyte uptake by Plasmodium reinfections (226). Additionally, clinical data shows that iron supplementation in an endemic malaria African country increased children hospitalization rates and mortality suggesting that anaemia is a defence mechanisms against Plasmodium infection (227). Conversely, macrophages, a key player in the innate immunity, present deficient phagocytic functions and impaired cytokine production under iron surcharge, which undermine their ability to clear intra-cellular infecting microorganisms. In addition, some microorganisms acquire the capacity to utilize intracellular accumulated iron, escaping from innate defence mechanisms (228, 229).

1.9.3.3 Iron and adaptive immune response

Besides iron effect on the innate immune response, the axis iron/hepcidin can influence the adaptive immune response required for immune cell function, activation and proliferation. Iron deficient patients presented impaired lymphocyte activity as reviewed by Dallman in the late 80s (230). A potential reason could be the influence of iron level changes on the activity of ribonuleotide reductase, an iron-dependent enzyme, involved in DNA synthesis and cell division (231). However, other mechanisms could be involved in the influence of the iron homeostasis on the adaptive immune response. In the EAE model, an experimental model of

CD4+ T cell-mediated demyelination, designed to study multiple sclerosis-related human disease, iron-deficient mice did not develop EAE up to 42 days post myelin basic protein (MBP) administration. The authors claimed that activation of CD4+ T cells was hampered by iron restriction. In this way, inactive CD4 + T cells cannot infiltrate the central nervous system and cause the symptomatology of EAE. In addition, the authors hypothesized that iron-deficient mice may have a higher frequency of regulatory T cells, since iron-deficient mouse lymphocytes produced more IL-2 than the control group when they were incubated in the presence of MBP (219). Furthermore, in a model of type 2 diabetes using Otsuka Long-Evans Tokushima Fatty (OLETF) rats, iron restriction improved lipid and glucose levels, and also diminished hepatic and pancreatic iron deposition, with less oxidative stress and lower IL-6 levels. These results could be explained by the reduced production of ROS with consequent less tissue damage (220). In vitro stimulated splenic lymphocytes originating from iron deficient mice presented lower protein kinase C (PKC) activity and inhibited hydrolysis of phosphatidyl inositol-4,5-biphosphate (PIP2) when compared with control or pair fed animals. These results correlated with decreased lymphocyte proliferation rates suggesting that both impaired PKC translocation or activation, and reduced PIP2 hydrolysis are implicated in the reduced lymphocyte proliferation rate in the presence of iron scarcity (232, 233). Conversely, it has been suggested that hepcidin is an important factor for the inflammatory response following LPS challenge, rather than iron deficient *per se*. Administration of hepcidin one hour before LPS challenge in iron deficient mice abrogated the subsequent inflammatory response (234, 235). In fact, basal hepcidin messenger RNA expression reported in human PBMCs was up regulated after lymphocyte activation (236). However, the hepcidin influence on LPS-induced inflammatory response was not confirmed by Wang et al. studies, which suggested that iron levels modulated cytokine expression after LPS challenge in mice (237).

1.9.3.4 Iron and immune response in organ transplantation

In the context of solid organ transplantation, T cell activation is a fundamental condition on the orchestration of the allo-immune response. Iron levels changes or iron transporter and storage proteins availability can modulate all of the signals of the proposed three-signal model for the allo-immune-mediated T cell activation process (238, 239). Allo-antigens presented to T cells by MHC class II molecules express on APC cell surfaces characterises the signal I. The

transferrin receptor CD71 is co-expressed with the T cell receptor CD3. Upon T-lymphocyte activation induced by CD3 antibody, CD71 expression increases on the T cell surface, making the CD71 a marker for T-lymphocyte activation (240). Furthermore, anti-CD71 antibody inhibits foetal T-lymphocytes proliferation in vitro (241). In addition, blockage of CD71 inhibited T cell function, altered cytokines production including IL-2, IL-10 and IFN-y resulting in a prolonged allograft survival in an experimental model of murine heterotopic cardiac transplantation. Based on those studies the use of anti-CD71 monoclonal antibody was proposed as a new potential immunosuppressant (242, 243). On the signal II, CD80 and CD86 expressed on the surface of APCs co-stimulate T cells through their engagement with T cell CD28. This engagement is preceded by an interaction between the CD40 ligand on the APC surface to the CD154 expressed on T cell surface. Even that iron deficiency can alter CD80 and CD86 concentration and function, the reduced T cell proliferation observed in iron deprivation can not be explained by such marker alterations *in vitro* and *in vivo* studies (244). Conversely, CD28 expression is reduced under iron deficiency and might contribute to lower T cell proliferation *in vitro* murine studies (245). The outcome of combined signals I and II is the activation of (i) the calcineurin, (ii) the RAS-mitogen-activated protein kinases (MAPK), and (iii) the nuclear factor kappa B (NF-kB) pathways. Calcineurin, the main target protein of tacrolimus and cyclosporin, is an iron dependent phosphatase, which requires iron to dephosphorylate the nuclear factor of activated T cells (NFAT) (246). Activation of MAPK and NF-kB pathways is iron dependent on cell cultures of hepatic macrophages (247). In fact, iron chelation treatment inhibits the NF-kB pathway and induces cell apoptosis in a lymphoma experimental model (248). Furthermore, iron changes are associated with cell survival in ovarian cancer cells in mitogen-activated protein kinase (MAKP) dependent manner (249). Signal I and II induced the expression of many molecules including IL-2, CD25 and CD154. IL-2 interacts with CD25 on the T cell surface in a paracrine way leading to the activation of the mTOR protein, which constitutes signal III for the initiation of the cell cycle (239). Iron chelation with deferasirox inhibits mTOr signalling in myeloid leukaemia cells through up-regulation of Regulated in development DNA damage responses 1 (*REDD1*) gene, a hypoxia inducible factor-1 target gene, which is crucial for the inhibition of mTOR (250).

Finally, as previously mentioned, the possible role of the iron/hepcidin axis in the adaptive immune response was surprisingly highlighted in an immunosuppression withdrawal

prospective clinical trial in liver transplant recipients. Patients who failed the IS weaning protocol presented lower storage iron parameters as serum ferritin, and serum and intrahepatic hepcidin levels in comparison with patients who were able to completely discontinue immunosuppression treatment (2). Taking in account that the achievement of spontaneous tolerance in rodent models of liver transplantation is marked by a transitory recipient alloreactive T cell activation followed by deletion of intra-hepatic lymphocyte population (60, 251, 252); and the iron changes effect on lymphocyte function and differentiation aforementioned, we could speculate about the potential involvement of the iron/hepcidin axis effect on the establishment of spontaneous tolerance in liver transplantation.

1.9.4 Iron and liver transplantation

The impact of iron levels changes has been also investigated in other phases of the liver transplantation process. In the context of liver cirrhosis, the reduced hepatocyte population presents an abnormal hepcidin expression with increased overload of iron in the remaining hepatocytes (253, 254). In fact, around 30% of patients listed for liver transplantation present hepatic iron overload, regardless the chronic liver disease aetiology (255). Liver recipients with marked iron deposition in the explanted livers present higher risk for infections and heart failure in the post-transplant period (256-258). Ischemia reperfusion injury, the inherent consequence of the cold organ preservation interval is influenced by cellular iron homeostasis as well. In fact the released iron from hepatocytes and Kupffer cells, during the liver cold static storage period enhances the free oxygen species formation intensifying the ischemia-reperfusion tissue damage. Therefore, the use of iron chelators in preservation solutions in rodent experimental models reduced this oxidative process improving graft primary function and viability (259, 260).

Chapter 2 : Hypothesis and aims

2.1 Hypothesis

2.1.1 Operational tolerance in liver transplant recipients is influenced by the axis iron/hepcidn.

2.1.1.1 The axis iron/hepcidin plays an important role in the T cell immune mediated response influencing the achievement of spontaneous tolerance in liver transplant recipients.

2.1.1.2 Iron changes modify intra-hepatic T cell immune mediated response in a murine model of acute liver failure induced by Concanavalin A (ConA), which is driven by macrophages, natural killer T cells, and T cells.

2.1.1.3 Iron changes influences the anti-donor T cell response modulating the development of spontaneous liver transplant tolerance in experimental models of rat liver transplantation.

2.1.2 Molecular biomarkers identified during immunosuppression withdrawal clinical trials forecast ACR episodes before their clinical, biochemistry and histological manifestation.

2.1.2.1 Transcriptional changes in blood samples sequentially collected alongside the weaning process precede the clinical, biochemistry and histological manifestations of ACR in liver transplant patients.

2.2 Aims

To decipher the influence of the axis iron/hepcidin in the tolerance process in liver transplant recipients and to determine ACR-associated molecular biomarkers we aimed to perform the following specific experiments:

2.2.1 Effect of iron in the intra-hepatic lymphocyte response

a) To manipulate iron dietary content in order to induce mild iron deficiency in mice
b) To characterize the phenotype of immune cells in mice in the setting of iron level modulation
c) To set up a murine model of immune mediated liver damage
d) To assess the impact of iron levels manipulation on the lymphocyte population and their functional status
e) To validate the impact of dietary iron levels manipulation on the liver immune-mediated damage by changing other factors that can change iron homeostasis as gut microbiota or metabolic changes

2.2.2 Effect of iron deficiency in the establishment of tolerance in liver transplantation

a) To set up a full vascularized model of rat liver transplantation
b) To check the feasibility of the model in different rat strain combinations as 1) the syngeneic, 2) spontaneous tolerance, and 3) the Tacrolimus-induced tolerance combinations
c) To study the effect of iron dietary modulation at the pre-, per-, and post-transplant outcome in all rat strains combinations described above
d) To study the effect of iron dietary manipulation at the post-transplant outcome of the same strain combinations under inflammatory challenge

2.2.3 Molecular characterization of acute cellular rejection biomarkers during intentional immunosuppression withdrawal in human liver transplantation

a) To define the patient population and to identify the available biological samples for future analysis
b) To define possible control groups for comparison purposes with the rejecting patients from the withdrawal clinical trials
c) To identify liver tissue gene expression markers associated with ACR in liver biopsies collected at the baseline before start IS weaning and at the time of rejection
d) To identify liver gene expression markers associated with ACR in sequential blood samples collected at the baseline before start IS weaning and at the time of rejection
e) To identify ACR-associated transcriptional patterns in tissue and blood samples and to check possible functional pathways associated with ACR employing the Gene Set Enrichment Analysis
f) To correlate the ACR-associated gene expression patterns with liver histopathology analysis
g) To check the influence of immunosuppression regimens on gene expression patterns at the time of rejection
h) To validate microarray results using real-time polymerase chain reaction (q-PCR) on sequential blood samples collected during the weaning IS period
i) To identify possible predictive gene signatures of rejection

Chapter 3 : Effects of Iron in the Intra-hepatic lymphocyte responses

3.1 Introduction

Sub-clinical changes in iron and hepcidin levels have been associated with unsuccessful development of SOT in stable liver transplant recipients in a recent IS withdrawal clinical trial (2). In experimental animal models, SOT required an intra-hepatic lymphocyte infiltration and activation before their subsequent deletion. Besides that, lymphocyte activation is impaired by iron deficiency *in-vitro* studies. On account of these findings, we hypothesized that light alterations in iron levels could be responsible for intra-hepatic lymphocyte activation in vivo which could modulate the intra-hepatic immune responses. To check this hypothesis we first chose a well-proven murine model of sub-lethal immune-mediated hepatitis induced by ConA administration. ConA-induced liver damage is triggered by T cells, Kupffer cells and, NKT cells interaction and activation with the involvement of many pro-inflammatory cytokines (261, 262). To reproduce the small iron level variation observed in the liver recipients enrolled in the IS withdrawal clinical trial, we used an iron-modified diet regimen or a treatment with iron-specific chelators prior mice ConA challenge. We assessed how these induced iron homeostasis alterations influenced immune cell populations, the intra-hepatic lymphocyte activation and viability and its consequences on pro-inflammatory mediators production.

3.2 Material and Methods

3.2.1 Reproduction of the mild iron deficiency status in mice employing iron-modified diets:

Four-week old males C57Bl/6 were purchased from Charles River, France, and bred under specific pathogen-free conditions. A special regimen of an iron deficient diet (<6mg/Kg) or iron replete (iron deficient diet supplemented with 200mg/Kg iron carbonyl) diet (SAFE, Augy - FR), introduced after an acclimatization period of five days, was given for a total of three weeks in order to induce a mild iron deficiency prior to the realization of any experiments. Experiments were realized under isoflurane inhalation anaesthesia and euthanasia performed by exsanguination under anaesthesia or in CO_2 chamber. All procedures were in accordance with the national and institutional guidelines for animal care and use, and had been approved by the Animal Welfare and Ethical Review Body – King's College London (AWERB-KCL) at the Denmark Hill Campus and the Home Office – United Kingdom (UK).

3.2.2 ConA immune-mediated acute liver failure model in mice under iron-modified regimens

To investigate the potential iron-related functional effects in the immune system, we used an immune modulated model of acute hepatitis using a sub-lethal intravenous injection of 15mg/Kg of type IV ConA (Sigma-Aldrich, Saint Louis, MO - USA). In this model, acute liver hepatitis is mediated by the interaction of sinusoid endothelial cells, T cells, macrophages and NKT cells, which mimics the physiopathology of autoimmune hepatitis (261, 262). Following ConA injection mice were anaesthetized with isoflurane (Abbott – UK) and sacrificed at various time points to collect blood, spleen, lymph nodes, and liver tissues. An initial experiment was performed to test the model efficacy using mice fed with normal diet. Otherwise, when not mentioned, the following experiments were performed using the modified iron diets.

3.2.3 Hepcidin and iron chelators administration

Systemic iron levels regulate the hepcidin expression, which controls the subsequent iron absorption in the duodenal mucosa. To verify whether the effects of iron-modified diets on the

immune-meditated hepatitis induced by ConA were dependent of hepcidin levels rather than iron levels, we first performed additional experiments where a single dose of 100µg of exogenous mouse hepcidin (PLP-3773, Peptides International, Louisville, KY, USA) or phosphate-buffered saline (PBS) (control group) was injected via intra-peritoneal two hours before the ConA challenge. In the same way, we realized experiments where a 3 day-course of a hydroxypyridinone iron based chelator administration (HPO CP28, 20nmoles, intra-peritoneal, ip.), which does not modify the hepcidin level (263, 264), was performed before ConA challenge in *vivo experiments*. For *in vitro* experiments using iron chelators, cells were incubated with low doses of either HPO CP182 (5µM) or deferoxamine (DFO) 10µM (Sigma-Aldrich, Saint Louis, MO - USA). At these doses iron chelators had no apparent effects on lymphocytes cell death (Figure S1 - Appendix B).

3.2.4 Modulation of mice gut microbiota

To determine whether the effects of iron deficiency on the liver environment is influenced by the bacterial growth and microbial composition, mice under the 3-weeks IrDef and IrRepl diet regimens received simultaneously a broad spectrum cocktail of 4 antibiotics in order to reduce the faecal microbial populations by around 90%: Ampicillin, 1g/L; vancomycin, 0.5g/L (Laboratorios Normon S.A. Tres Cantos - Spain); metronidazole, 1g/L (BBraun Medical S.A, Barcelona - Spain); and neomycin, 1g/L (Laboratorios Salvat, Barcelona, Spain) were dissolved in drinking water, which was changed every 3 days, and given throughout the entire period of three weeks as previously described (265). Afterwards, mice were challenged with ConA as stated in the section 3.2.2.

3.2.5 Biological samples collection

For biological specimen collection, mice underwent a midline laparotomy under inhaled anaesthesia. Then, a cardiac puncture was performed through the diaphragm to collect blood samples. Immediately after blood harvesting and completion of the euthanasia, the PV was cannulated and the liver perfused with 10ml of PBS to wash all remaining blood volume from the liver. Then liver samples were collected as described. A small slice of liver tissue was immediately conditioned in formalin solution for posterior histological analyses, samples for gene expression studies were conditioned in RNAlater® solution (Ambion, Carlsbad, CA -

USA) kept at 4ºc for 24 hours, and then stored at -80ºc for later analyses. A fresh liver slice was immediately sent for iron measurement when necessary. The remaining liver tissue, reserved for cell isolation, was conditioned in sterile PBS at 4ºC and rapidly processed within next two hours.

3.2.6 Samples manipulation, serum biochemistry and hematologic measurements, cytokine analysis and intra-hepatic iron measurement

Serum was obtained after 10 minutes centrifugation at 8.000g at room temperature (RT) from recent harvested clotted blood samples, and then stored at -20ºC for posterior analyses. The alanine aminotransferase (ALT) plasma activities, which reflect the liver injury intensity, and the serum iron level, were quantified by automated measurements using the ADVIA 2400 Systems kits (Siemens, Erlangen - DE). Hematologic parameters were assessed in fresh blood samples conditioned in appropriate tubes by automated measurements using the ADVIA 2120 System kits (Siemens, Erlangen – DE). Serum cytokine levels were measured with multiplex fluorescent bead-based Luminex Flexmap3D technology according to manufacturer's recommendation (Thermo Scientific, Waltham, MA –USA). A small biopsy of at least a 10 mm slice of fresh liver tissue was used for intra-hepatic iron measurement using the ICP – MS method (Inductively Coupled Plasma – Mass Spectrometry) (NexION 350D – PerkinElmer, Waltham, MA, USA) according to the manufacture's recommendations.

3.2.7 Liver Histology

Formalin-fixed and paraffin embedded liver tissue sections were stained with haematoxylin and eosin (H&E). Then, a senior liver histopathologist Dr Miquel Brugrera (MB), Hospital Clinic, University of Barcelona, Barcelona Spain, who was blinded to the identity of the experimental groups assessed the slices for the presence of hepatocytes ballooning, cellular infiltration, hepatocyte cohesion and necrosis. Liver tissues from mice that were not exposed to ConA were used as controls

3.2.8 Isolation of non-parenchymal liver cells, splenic and lymph node leukocytes

After liver collection following the description in section 3.2.5, samples were digested at 37ºC in the presence of collagenase II 5% (PAA Laboratories, Exton - UK), and 100µg/mL DNase I (Roche, Mannheim -DE) for 30 minutes, as described by Ramachandran (266). Liver tissue was then passed through a 70µm nylon mesh. Hepatocytes were removed following low-speed centrifugation (60xg, 2 minutes, RT), and liver mononuclear cells were isolated using Ficoll-Paque (GE Healthcare, Uppsala – Sweden) separation (800xg, 20 minutes) (RT). Spleens were smashed and passed through a 70µm nylon mesh to obtain single cells suspensions, then red blood cells were removed using 5mL ammonium chloride potassium (ACK) lysing buffer (Life Technologies, Carlsbad CA – USA) for 5 minutes (RT) followed by a second washing in PBS. The same procedure was used to isolate lymphocytes from lymph nodes.

3.2.9 In vitro naïve $CD4^+$ T cell stimulation

Lymphocyte proliferation was investigated using the carboxyfluorescein succinimidyl ester (CFSE) assay. CFSE has the ability to bind covalently to long-live intracellular molecules and to be retained intracellularly for a long time. At each cell division, the fluorescent carboxyfluorescein dye is divided equally into each daughter cell, which has half the fluorescence of the parent cell. $CD4^+$ naïve T cells were isolated from spleen and lymph nodes after preparation described in the previous section using EasySep Mouse Naïve $CD4^+$ T cell stimulation kit (STEMCELL Technologies, Vancouver - CA). Enriched cells were labelled with 2.5 µM CFSE (Carboxylfluorescein succinimidyl ester) (BioLegend, San Diego CA - USA) for 10 minutes. A total of $250x10^3$ cells were incubated for 5 days in 96 well-plate coated with anti CD3 and CD28 antibodies (BioLegend – San Diego, CA – USA) (2µg each, clone 145-2C11 and 37.51, respectively) in RPMI-1640 (Life technologies, Carlsbad, CA - USA) supplemented with 5% Foetal Calf Serum (Sigma-Aldrich, Saint Louis, MO - USA), 1% penicillin-streptomicyn and 2mM L-glutamine AND 50µM β-mercaptoetanol (Life technologies, Carlsbad, CA - USA).

3.2.10 Cell phenotyping - Flow cytometry

Cells aliquots up to $1x10^6$ cells were labelled in staining solution (PBS, Foetal Calf Serum 2%, 2mM EDTA) (Sigma-Aldrich, Saint Louis, MO - USA) using the following antibodies: APC/Cy7 antiCD3e, PE/Cy7 anti CD4, APC anti-CD25, PE anti-CD4, FITC anti-CD62L which were all purchased from BioLegend. In order to quantify cell viability, dead cells were stained either with 7-AAD (BioLegend – San Diego, CA - USA) or Livedead cell viability assay (Life Technologies, Carlsbad, CA - USA). Before cytometer acquisition cells were fixed for 20 minutes using fixation buffer (BioLegend – San Diego, CA - USA) in the dark (RT). To label regulatory T cells, cells aliquots were initially incubated in a FOXP3 Perm/Fix solution for 20 minutes with PE anti-FOXP3 antibody (BioLegend, San Diego, CA - USA) according to manufacturer's instructions. Intracellular IFNγ staining was performed using permeabilization buffer following manufacturer's instructions and FITC and anti-IFNγ antibody and APC anti-IL4 antibody (BioLegend, San Diego, CA - USA). Experiment results were acquired on a BD FACSCanto II flow cytometer (BD Becton, Dickinson and Company, Franklin Lakes, NJ - USA). Analyses were made employing FlowJo software (FLOWJO LLC, Ashland, OR - USA).

3.2.11 RNA extraction and gene expression experiments

Liver or spleen tissue samples were harvested, processed and stored at -80ºC as described in the section 3.2.4. For RNA extraction, samples were initially thawed and homogenised using an RNAse-free pestle in TRizol ® reagent (Invitrogen, Carlsbad, CA - USA), total RNA was extracted according the TRizol manufacturer's protocol. DNA was removed from total RNA preparations using Turbo DNA-free DNAse ® treatment (Ambion – Carlsbad, CA - USA). RNA quality and quantity were assessed with the Agilent 2100 Bioanalizer® (Agilent Technologies, Santa Clara, CA - USA) and Nanodrop ND-1000 (Thermo Scientific, Waltham, MA - USA), respectively. Total RNA was then reverse transcribed into cDNA using the High-Capacity cDNA Reverse Transcription Kit® (Applied Biosystems, Foster City, CA - USA). A pre-amplification of cDNA was performed using pooled TaqMan assays® (final concentration of 0.2x each) and the TaqMan PreAmp Master Mix® (Applied Biosystems, Foster City, CA - USA) using 10 cycles of amplification. qPCR was performed using the 48.48 Dynamic Array® following manufacturer's protocol using a BioMark Instrument (Fluidigm Corporation, South San Francisco, CA - USA). To quantify transcript levels, target gene Ct values were

normalized using Ct values of HPRT1 as reference gene to generate -ΔCt values. Real-time PCR gene expression experiments were performed using liver samples collected at 12 hours post ConA injection.

3.2.12 Statistical analyses

Statistical analyses were performed with GraphPrism software version 5.0. Student T-test was used for comparison between two groups and ANOVA analysis with Tukey's post-hoc correction for pairwise comparisons was used to compare more than 2 groups. Fisher test was used for categorical variables. P-values inferior to 0.05 (two tailed) were considered statistically significant in all analyses.

3.3 Results

3.3.1 Induction of mild iron deficiency employing iron-modified diets

When compared to mice fed with an iron-replete diet (IrRepl), mice fed with an iron-deficient diet (IrDef) presented decreased serum iron and serum transferrin saturation (73.22 ± 56.49 versus 156 ± 36.99 µg/dL; p<0.0001 and 18.80 ± 6.32 versus 56.20 ± 4.53%; p=0.0013 respectively). Additionally, liver tissue analysis exhibited reduced iron stores and hepcidin (*Hamp*) gene expression (p 0.017 and p<0.0001, respectively). When IrRepl samples were compared with samples from mice fed with the regular diet, there were no differences in those iron parameters. IrDef mice also developed mild anaemia (haemoglobin 107.6 ± 46.10 versus 147.9 ± 6.50 g/L; p=0.028) and increased platelet count (145 ± 469.2 versus 769.4 ± 174x10^9 /L; p=0.0004), which is in accordance with the previous description in the literature (234, 267). Animals from both groups presented the same clinical evolution without behavioural changes and with both groups gaining presenting comparable gain weight at the end of 3-weeks under iron-modified diets (Figure 3).

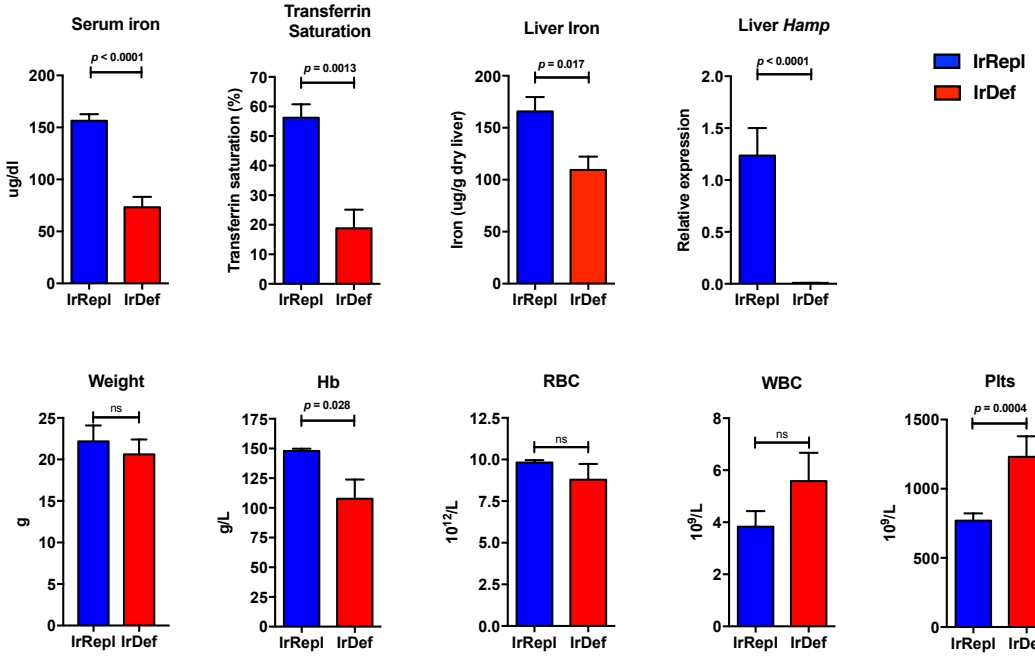

Figure 3: Iron and haematological parameters in mice fed with iron-manipulated diets. Mice were fed for 3 weeks with an iron-deficient diet (IrDef) or iron-replete diet (IrRepl). Bars plots display mean and SEM. Abbreviations: RBC: red blood cells, Hb: haemoglobin, Plts: platelets, WBC: white blood cells. Hamp: Hepcidin antimicrobial peptide, gene responsible for Hepdicin codification. Number of animals IrRepl/IrDef: Serum Iron: 34/33, Transferrin Sat: 5/5, Liver Iron: 5/5, Liver Hamp: 11/10, Weight 34/33, hematologic parameters: 11/8.

3.3.2 Mild iron deficiency does not modify the steady state immune cell repertoire and systemic cytokine levels

To check the influence of mild iron deficiency caused by the iron modified diets on immune parameters; we initially compared liver and spleen immune cell subsets in IrDef and IrRepl mice. Both groups of mice exhibited similar frequencies of intrahepatic NK1.1^{+}CD3^{+}NKT, CD4^{+} and CD8^{+} T cells, FOXP3^{+} T cells, and resident CD45^{+}CD11^{+}F4.80^{+} Kupffer cells (Figure 4A). Likewise, no differences between IrDef and IrRepl splenic T cell subsets were noted (Figure 4B), which can suggest that in the steady state the mild iron deficiency induced by IrDef regimen did not induce major immunological effects.

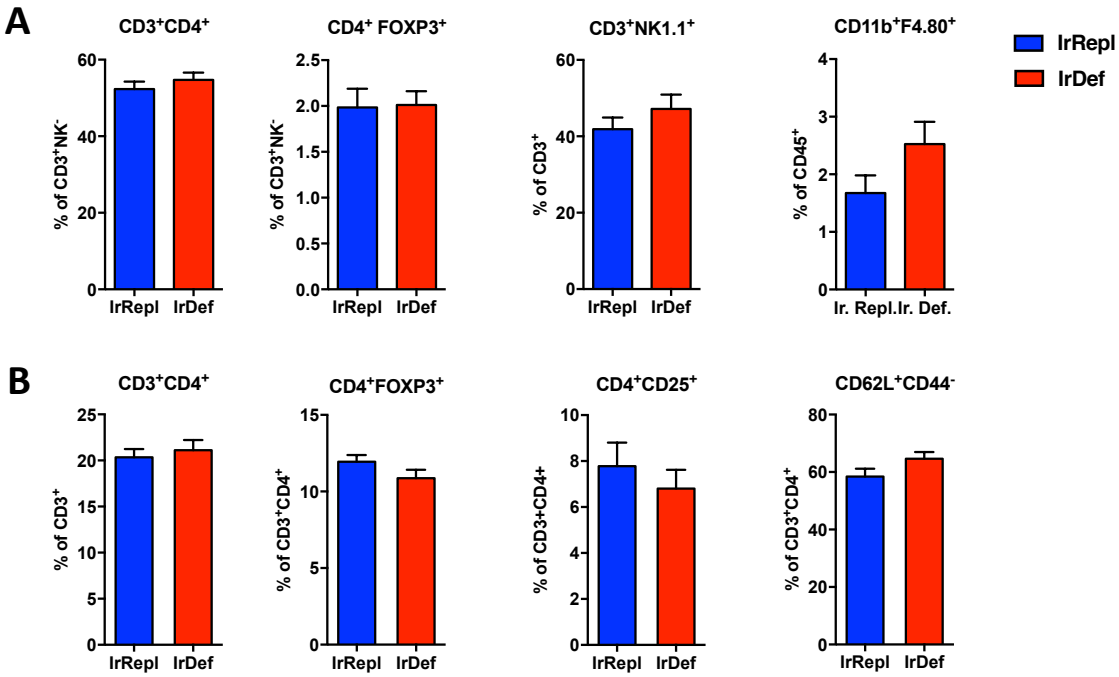

Figure 4: Influence of iron levels on the immune-phenotype of intra-hepatic leukocytes (A) and spleen (B) leukocytes. Mice were fed for 3 weeks with an iron-deficient diet (IrDef) or iron-replete diet (IrRepl). Bar plots show the frequency (mean and SEM) of specific leukocytes subsets in the liver (A) and in the spleen (B), as assessed by flow cytometry after excluding dead cells. Number of animals IrRepl/IrDef: Liver: CD3+CD4+: 8/8, CD3+FOXP3+: 8/8, CD3+NK1.1+: 13/13, CD11b+F4.80+: 10/10; Spleen: CD3+CD4+: 14/14, CD3+FOXP3+: 14/14, CD4+CD25+: 11/11, CD62CD44+: 4/4.

In the next experiment, we explored the effects of iron deficiency on pro-inflammatory and immunoregulatory genes by measuring the expressions of interleukins *Il2, Il4, Il6, Il10, Il15*, tumor necrosis factor α (*Tnf)*, transforming growth factor β (*Tgfb1*), interferon γ (*Ifng*), *Cd86*, forkhead box P3 (*Foxp3*), and *Cd274* in whole livers, spleens and mesenteric lymph nodes from IrDef and IrRepl mice. Only small decreases were observed on the *Tnf* expression (Fold change [FC] =-0.36, p=0.032) and *IFNG* (FC=-0.72, p=0.044) in the liver and spleen of IrDef mice, respectively (Table 2). Again, no significant changes were observed on the production of serum cytokine between IrDef and IrRepl mice measured by the Luminex technique following the manufacturer instructions (Table 3).

Table 2: Gene expression in liver, spleen and mesenteric lymph nodes (mesLN) of immune-related molecules from IrDef and IrRepl mice

Symbol	Name	Liver		Spleen		mesLN	
		FC	p.value	FC	p.value	FC	p.value
Il2	Interleukin 2	0.75	0.090	-0.49	0.20	-0.26	0.28
Il4	Interleukin 4	0.32	0.14	-0.038	0.90	0.24	0.50
Il6	Interleukin 6	-0.20	0.39	-0.094	0.70	-0.48	0.15
Il10	Interleukin 10	-0.15	0.48	-0.11	0.74	0.060	0.83
Il15	Interleukin 15	0.098	0.68	-0.38	0.18	0.36	0.13
Ifng	Interferon gamma	0.31	0.26	**-0.72**	**0.044**	0.40	0.54
Tnf	Tumor necrosis factor	**-0.36**	**0.032**	-0.29	0.38	0.024	0.94
Tgfb1	Transforming growth factor, beta 1	0.17	0.14	-0.26	0.14	-0.12	0.53
Foxp3	Forkhead box P3	-0.046	0.88	-0.32	0.34	0.052	0.85
Cd86	CD86 antigen	0.003	0.97	-0.41	0.083	-0.24	0.26
Cd274	CD274 antigen	0.10	0.38	-0.40	0.10	0.020	0.95

Fold change is exhibited as Log_2 of IrDef/IrRepl values. Genes with significant differential expression are highlighted in bold.

Table 3: Serum level of cytokines measured by Luminex technology from IrDef and IrRepl mice

Symbol	Name	FC	p.value
IFNy	Interferon gamma	0.85	0.59
IL-1α	Interleukin 1alpha	-0.73	0.57
IL-2	Interleukin 2	-3.35	0.20
IL-4	Interleukin 4	0.90	0.48
IL-6	Interleukin 6	-0.48	0.68
IL-10	Interleukin 10	-1.11	0.26
IL-15	Interleukin 15	1.47	0.10
IL-17	Interleukin 17	-1.69	0.15
CXCL10	chemokine (C-X-C motif) ligand 10 (IP-10)	0.008	0.96
CXCL9	chemokine (C-X-C motif) ligand 9 (MIG)	0.41	0.61
TNF α	Tumor necrosis factor alpha	-0.27	0.51

Fold change is exhibited as Log_2 of IrDef/IrRepl values.

3.3.3 Mild iron deficiency significantly reduces inflammatory liver damage following ConA administration

As described in section 3.2.2, we used the ConA-induced immune mediated hepatitis model to check the functional effect of mild iron deficiency on intra-hepatic lymphocyte responses. IrDef mice presented a significantly lower increase of alanine aminotransferases (ALT) than the IrRepl mice (p=0.0028 and 0.0035 at 6 and 12 hours after ConA administration, respectively) (Figure 5A). Likewise, IrDef mice showed reduced serum levels of the pro-inflammatory cytokines IFNy, IL-6 and TNFα, which reached statistical significance at 6 hours after ConA challenge (p=0.0037, 0.0013 and 0.0021, respectively) (Figure 5C). Similar changes were observed in the intra-hepatic expression of *Il4* and *Tnfa,* whose transcript levels significantly decreased in IrDef mice 12 hours after ConA injection (p=0.0053 and p=0.021 respectively) (Figure 5D). These results were in agreement with the liver histopathology analysis, which demonstrated decreased hepatocyte necrosis and inflammatory infiltration in IrDef as compared to IrRepl mice (p=0.0082 and 0.0020 respectively) (Figure 5B).

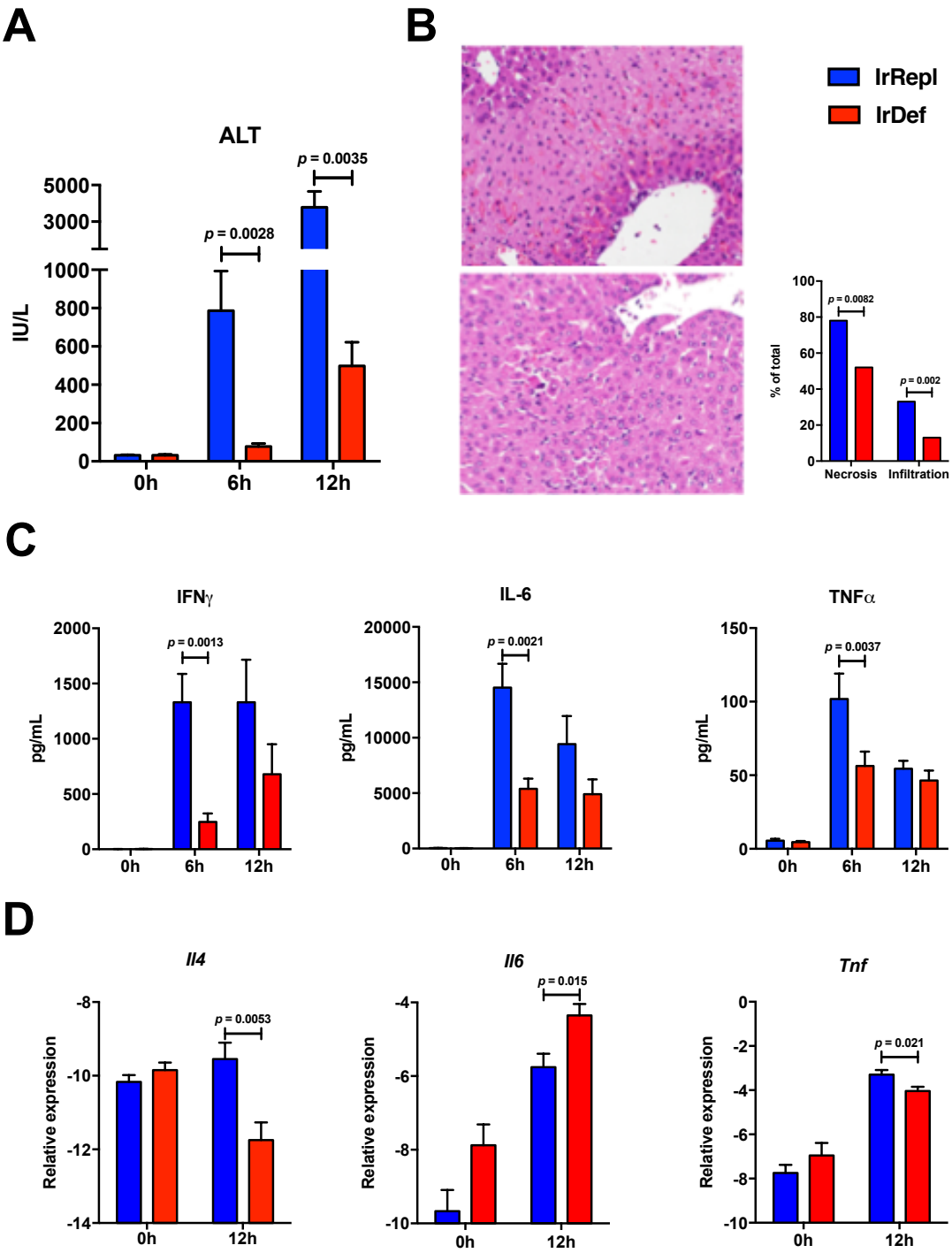

Figure 5: Iron deficiency results in attenuated immune-mediated hepatitis following ConA administration: (A) Serum levels of alanine alanine aminotransferase (ALT; IU/ml) before 6 hours and 12 hours after administration of ConA in mice fed for 3 weeks with IrDef or IrRepl diets. **(B)** Representative liver histology (H&E, 200x) at 12 hours after the administration of ConA in a IrRepl mouse (upper picture) and in an IrDef mouse (lower picture) and histologic evaluation of necrosis and infiltration (lateral graphic). **(C)** Cytokine levels in serum samples collected before, 6 hours and 12 hours after the administration of ConA. **(D)** Transcript levels of *Il4, Il6*, and Tnf in liver tissue samples collected before and 12 hours after the administration of ConA. Number of animals (IrRepl/IrDef) (A) 0h: 32/31, 6h: 23/20, 12h: 28/19; (B) 0h: 8/8, 6h: 4/6, 12h: 10/10; (C) 0h: 4/4, 12h: 7/8; (D) 23/15.

3.3.4 Decreased iron availability blunts lymphocyte proliferation and activation

ConA administration initiates an inflammatory cascade, which requires activation of T and NKT lymphocytes and macrophages; at the end these events lead to liver tissue damage (261, 262). Being activated by ConA administration, lymphocytes produce IFNy, which is directly implicated in the pathogenesis of ConA-induced hepatitis (262, 268, 269). Additionally, NKT cells down-regulate NK1.1 and CD3 surface markers, whose expression is inversely correlated to the degree of NKT activation (270). To investigate that the iron deficiency effects were mediated by inadequate lymphocyte activation, we assessed the phenotypic and functional properties of splenic and intra-hepatic lymphocytes isolated at different time points after ConA administration. IrDef mice presented significantly less accumulation of liver-infiltrating $CD3^+$ lymphocytes when compared to IrRepl mice ($p=0.048$ at 6 hours) (Figure 6A). This was associated with a less prominent decrease in the expression of NK1.1 in CD3 cells (a NKT cell activation marker) both at 3 and 6 hours after ConA injection ($p=0.0056$ and 0.029 respectively) (Figure 6A). Additionally, intra-hepatic NKT and T lymphocytes from IrDef mice exhibited lower intra-cellular IFNy levels at 3 hours after ConA injection when compared to IrRepl mice ($p=0.034$ and 0.081 respectively) (Figure 6B). It is worth noting that contrary to the significant differences detected in the liver compartment, IFNy-producing splenic lymphocytes presented comparable frequencies in IrDef and IrRepl mice (Figure 6C).

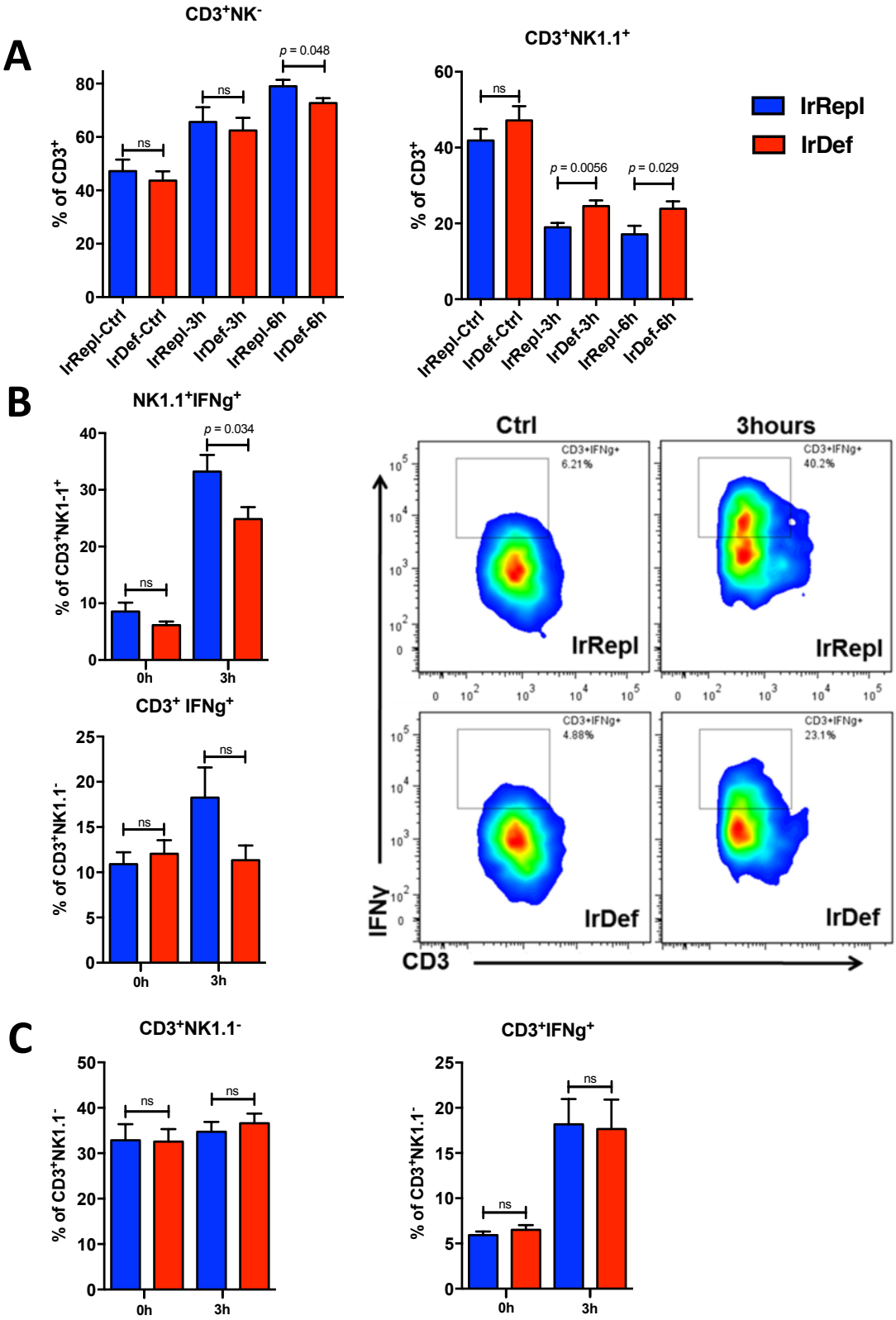

Figure 6: ConA-Induced T and NKT lymphocyte activation is reduced in iron deficiency. (A) Intra-hepatic frequency of CD3+ expressing NK1.1 and CD3+ NK1.1- at baseline, 3 hours and 6 hours after ConA injection. **(B)** Intra-hepatic frequency of IFNy production by NKT cells and T cells, defined as CD3+ NK1.1+ and CD3+ NK1.1-, respectively, (left panel) and representative staining of IFNy production by NKT cells (right panel). **(C)** Frequency of splenic CD3+ NK1.1- T cells and the percentage of these ones producing IFNy. Number of animals (IrRepl/IrDef) (A) CD3+ 0h: 13/13, 3h: 16/16, 6h: 12/11; NK1.1+ 0h: 11/11, 3h: 14/14, 6h: 11/12; (B) 0h: 12/12, 3h: 9/9; (C) 0h: 9/9, 3h 9/9

To corroborate the influence of iron deficiency on T cells activation and proliferation, we incubated splenocytes *in vitro* in presence of ConA (0.1mg/ml) and low doses of a specific hydroxypyridinone iron chelator (HPO CP182; 5 µM) or desferoxamine (DFO; 10µM) (263, 264). Iron chelation provoked an impaired $CD3^+$ $CD4^+$ T cell proliferation ($p<0.0001$). Additionally, the presence of iron chelator also hampered the activation of isolated $CD4^+$ naïve T cells, which after stimulation within anti CD3/CD28 plate-bound, showed decrease CD25 expression and cell proliferation (Figure 7).

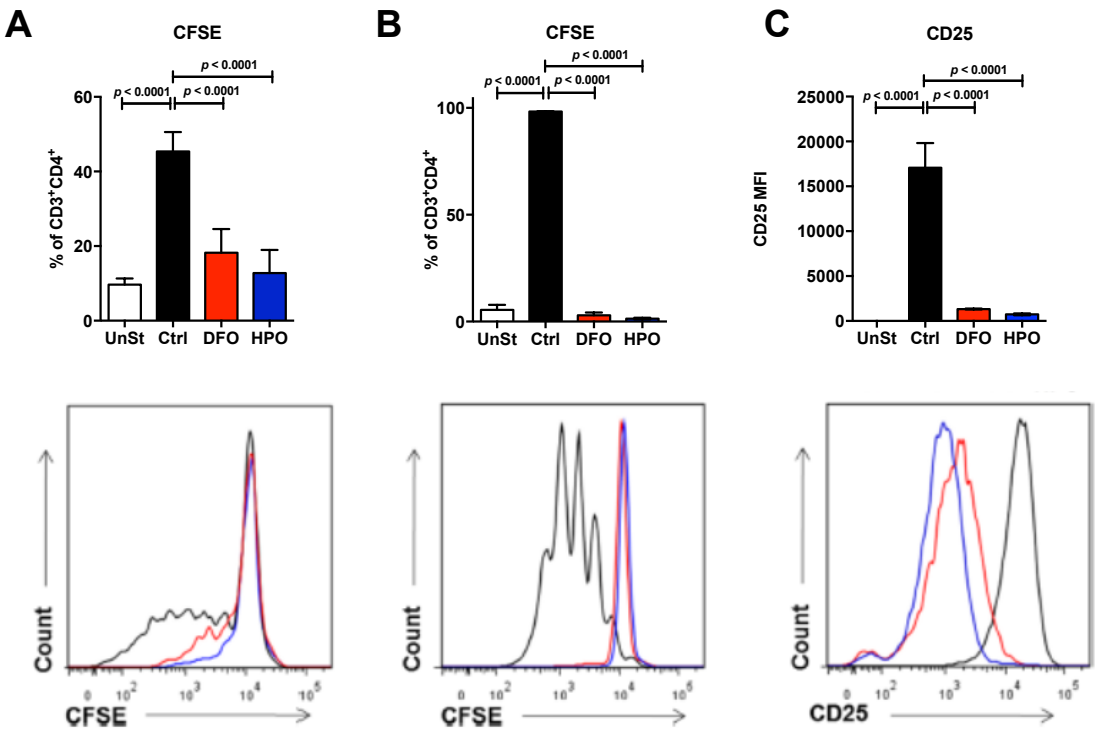

Figure 7: Iron chelation impairs $CD4^+$ T cell activation and proliferation in vitro: (A) The graphic on the top represents the percentage of CD4+CD3+cells from splenocytes undergoing at least one division, which is detected by the CFSE assay as shown in the representative fluorescent histogram on the lower part of the panel. Splenocytes were incubated 96 hours in presence of: ConA (0.1mg/mL), CFSE, and in presence of low doses of iron chelator (HPO CP182, 5µM or DFO, 10µM). Data were acquired on a BD FACSCanto II flow cytometer **(B)** Graphic showing the percentages of CD4+CD3+cells from isolated naïve CD4+ cells undergoing at least once division as represented on the histogram at the bottom of the panel, and **(C)** Graphic at the top of panel represents the CD25 MFI detected on the fluorescent histogram in the lower part. Isolated CD4+ naïve T cells incubated 5 days in presence of anti-CD3/CD28 plate-bound antibody (2µg each). Un means un-stimulated cells. Number of animals: (UnSt/Ctrl/DFO/HPO) (A) 2/6/6/5; (B) 3/4/4/4; (C) 3/4/4/4.

3.3.5 Iron deficiency influences intra-hepatic inflammatory responses independently from gut microbiota modulation

Taking in account the impact of gut microbiota on the liver environment (271) and the well-described modulator effect of iron changes on bacterial growth and intestinal microbial composition (272), we checked if the blunted immune-mediated hepatitis observed in IrDef mice could be influenced by changes in gut bacteria population. Mice under the 3-week IrDef and IrRepl diet protocol received simultaneously and for the same period a broad spectrum cocktail containing 4 antibiotics in order to decrease more than 90% of gastrointestinal microbiota before ConA administration at the end of 3-week period (265). IrDef mice receiving antibiotics presented comparable results to experiments realized in IrDef mice without antibiotic treatment, with significantly reduced levels of ALT in IrDef mice in comparison with IrRepl mice (Figure 8A).

3.3.6 Intra-hepatic inflammatory responses are influenced by iron but not by baseline hepcidin level.

Low iron availability leads to a reduced hepcidin expression, which can have a direct impact on the regulation of immune responses as demonstrated in some experimental models (234). We sought to determine whether the influence of an iron deficient diet on an immune-mediated hepatitis model might be related to differences in hepcidin levels rather than to alterations in iron levels. To do this, we performed a first experiment employing mice fed with standard diet (normal iron concentration) and receiving a 3-day course treatment of HPO CP28 iron chelator (263, 264). Before the ConA challenge, we checked whether the iron chelation treatment had an influence on the expression of intrahepatic hepcidin. The iron chelator-treated group had similar levels of intra-hepatic *HAMP* (the hepcidin gene coding) expression compared to a control group ($p=0.48$) (Figure 8B). Subsequently, following ConA challenge, mice treated with HPO CP28 exhibited a significantly blunted hepatitis compared to controls, similar to that observed with an iron deficient diet ($p=0.041$) (Figure 8C). In a second experiment aimed at determining whether hepcidin levels could restore the IrRepl ConA-induced hepatitis phenotype to IrDef mice, IrDef received a single dose of exogenous hepcidin two hours prior to ConA challenge (234). Hepcidin-treated IrDef mice had ALT levels similar to those of placebo-treated IrDef mice, suggesting that exogenous hepcidin treatment failure to restore

the IrRepl phenotype of ConA-induced hepatitis to IrDef mice (p=0.84) (Figure 8D). Altogether, these results suggested that iron restriction inhibits lymphocyte activation and ConA-induced hepatitis independent from its effects on hepcidin secretion.

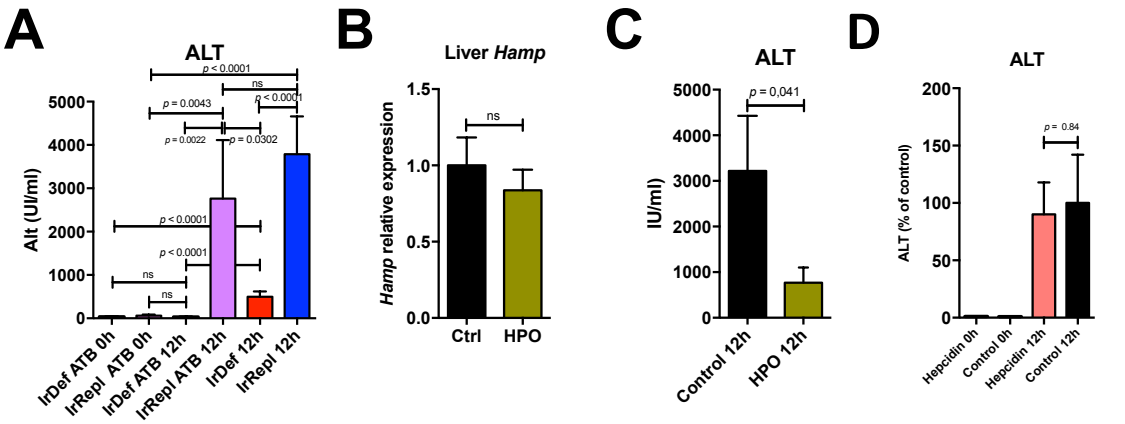

Figure 8: The inhibitory effects of iron deficiency in ConA-induced hepatitis are independent from changes in gut microbiome and hepcidin levels. (A) ALT serum levels (IU/ml) before, and 12 hours after the administration of ConA to mice fed for 3 weeks with iron deficient (IrDef) or iron-replete (IrRepl) diet, in the presence or absence of a 4-antibiotic (Atb) cocktail. **(B)** Relative expression of *Hamp* in liver tissue samples from mice fed with standard diet (normal iron concentration) receiving a 3-day course of HPO CP28 (20nmoles, daily) compared to control mice receiving PBS (p=0.48). **(C)** ALT serum levels 12 hours after ConA challenge in mice fed with standard diet (normal iron concentration) treated with HPO CP28 or with PBS (p=0.041). **(D)** ALT serum levels 12 hours after ConA challenge in mice fed with IrDef diet pre-treated with a single intraperitoneal injection of 100µg of mouse hepcidin or sterile PBS two hours before ConA challenge (p=0.84). Bar plots display mean and SEM. Number of animals: (A) (IrRepl/IrDef): 0h: 8/8, 12h: 7/7; (B) (Ctrl/HPO): 6/7; (C) (Crtl/HPO): 10/10; (D) (Ctrl/Hep) 6/10.

Chapter 4 : Impact of iron changes on the spontaneous tolerance development in a rat liver transplant model

4.1 Introduction:

Based on clinical observations that alterations on iron and hepcidin levels were associated with the outcome of IS withdrawal in stable liver transplant recipients (2), we hypothesized that iron stores and/or hepcidin levels influence the intensity of the intra-hepatic non-specific inflammatory reactions and the anti-donor T cell mediated responses. Using a well-known immune-mediated hepatitis model induced by ConA, we previously tested the influence of iron and/or hepcidin levels on the magnitude of the intra-hepatic non-specific T cell response. Here, our aim was to set-up a rodent liver transplant model to check our hypothesis that iron and/or hepcidin changes impact the anti-donor T cell mediated response, which can influence the establishment of spontaneous tolerance across different rat strain combinations. In the rat liver transplant model, allograft liver tolerance spontaneously develops in some donor/recipient rat strain combinations in spite of the presence a full MHC mismatch. This phenomenon may prevent complete replication of the clinical setting in which long-term liver recipients can be weaned off immunosuppression therapy. However, spontaneous tolerance in the rat liver transplant model is associated with a transient immune response. In this model an allograft T cell infiltration was observed in the early phase post-liver transplantation. This was followed by subsequent T cell deletion some weeks later resulting in a clinical long-term allograft acceptance. The same pattern was observed in transaminase levels after transplantation, with an increase at the beginning of the post-transplant period, followed by normalization over time (273). At the same time, a percentage of SOT liver recipients present a transient worsening in the LFTs during the IS weaning protocol. Furthermore, in tolerant liver recipients, portal lymphocyte infiltration increases at 1 year post IS withdrawal and decreases at the 3 years follow-up biopsy (1, 274). Given the immunological similarities described above, the rodent liver transplant model provides the best conditions for closely replicating the human clinical context of spontaneous operational tolerance. To do that, we aimed to establish a fully-vascularised rat liver transplant model including the HA anastomosis, which is considered a challenging step in rodent liver transplant models. The rationale to arterialize the liver allograft was based on the fact that hypoxia can modulate the iron/hepcidin axis (209). Furthermore, it

has been shown that arterialisation of the liver allograft decreases the rejection rate in a rejecting donor/recipient strain combinations (275). As soon as we achieved more than an 80% long-term survival rate, we started our experiments by transplanting animals that were kept on iron-modified regimens in the same way as in our murine model of immune-mediated acute hepatitis. Conversely to the clinical setting, the rodent model of liver spontaneous tolerance does not require long term IS treatment, so we administered high doses of recombinant human IL-2 (rhIL-2) in order to challenge the immune system during the early phase post-transplant aiming to check the influence of the iron-deficiency on the spontaneous tolerance establishment (276, 277). To quantify the impact of the iron deficiency and the rhIL-2 inflammatory challenge, we assessed the post-transplant survival rate under such conditions in addition to the clinical, biochemistry, histological evolution, T cell population and cytokines production.

4.2 Material and methods:

4.2.1 Rat liver transplantation model

All procedures were in accordance with the national and institutional guidelines for animal care and use and were approved by the Animal Welfare and Ethical Review Body – King's College London (AWERB-KCL) at the Denmark Hill Campus and the Home Office – UK. Lewis and Dark Agouti male rats were purchased from Harlam (UK), whereas Brown Norway male rats were purchased from Charles River (UK). The purchases were planned so that the animals presented a weight of approximately 180 to 220g at the time of the transplant procedure. The rat liver transplant technique described by Kamada et al. was employed in our first experiments (278). This technique, considered somewhat easier to perform, employs small plastic cuffs on realization of the termino-terminal PV anastomosis and on the termino-terminal infra hepatic vena cava anastomosis (IHVC). However, this technique does not contemplate the arterialisation of the liver graft (279). We were trying to completely replicate the clinical scenario of human liver transplantation, and take into account that axis iron/hepcidin is influenced by hypoxia; the non-arterialisation of the liver graft which could influence our results. Furthermore, circulatory and hemodynamic changes such as portal hypertension and increased cardiac index observed in the post-transplant follow-up have been attributed to the fixation of the PV and IVHC diameters caused by the plastic cuffs (280, 281). Based on that, we moved to the fully-vascularized technique of rat liver transplantation initially described by Lee et al. in 1973 and modified by Ariyakhagorn et al. in 2009 wherein venous anastomoses were performed by running suture and re-arterialization of the liver allograft was achieved by the HA anastomosis employing small plastic stent (282, 283). The donor and recipient procedures are described in the following sections. All procedures were performed in sterile conditions.

4.2.1.1 Rat liver transplantation – Donor procedure

Initially the animal was put in the induction chamber, where induction was achieved by employing isoflurane at 5% (Forane®. Abbott, IL - USA). After induction the animal was placed and attached using plastic adhesives on a wood pad previously and continuously warmed using an appropriate warming device placed under the wood pad. General anaesthesia was

maintained with vaporization of isoflurane at 2% with oxygen flow at 2l/min. Antiseptic measures were taken: the abdominal region was shaved; a povidone-iodine base antiseptic solution (Iso-Betadine ®, Meda – UK) was applied and sterile surgical drapes were positioned. Painkillers were used following the AWERB-KCL recommendations. Then a cruciform laparotomy was made, the liver was dissected from its attachments, the supra coeliac aorta, the infra renal aorta, the supra hepatic vena cava (SHVC), the IHVC, the PV, the common bile duct (CBD) and the HA were identified and dissected. The infra-renal aorta was catheterized in order to perfuse the liver with 20ml of Celsior ® (Institute Georges Lopez - Lion, France) preservation solution. The supra coeliac aorta was cross-clamped and the perfusion was started. The SHVC was sectioned for exsanguination. After finishing the liver perfusion, the total hepatectomy was completed. Two corner stiches of a 7/0 polypropylene (Prolene® - Ethicon - OH – USA) were placed on the SHVC stump and one corner stich of 8/0 polypropylene was place on the left corner of the PV stump. Afterwards, the graft was kept in a small bowl, immersed in cold preservation solution at 4ºC until the time of implantation in the recipient.

4.2.1.2 Rat liver transplantation – Recipient procedure

The animal was anesthetized following the same protocol as described for the donor in the previous section, once appropriately installed and with sterile surgical drapes in place, a median laparotomy was made; the native liver was mobilised from its attachments, the SHVC, the IHVC, the PV, the CBD and HA were identified, dissected and freed. The PV, the IHVC, the SHVC, and the HA were clamped and divided. Then the native liver was taken out finishing the recipient hepatectomy. At this time isoflurane concentration was decreased to 0.5% and the oxygen flow rate increased to 4l/min. The donor liver implantation was started by the SHVC anastomosis performed by a running suture using the corner stiches placed during the donor hepatectomy, followed by the PV anastomosis performed by a running suture using the 8-0 Prolene® stich previously placed. The PV and the SHVC clamps were released with the consequent reperfusion of the liver allograft. Then, anaesthetic parameters returned to initial concentrations and flows. The next step was the IHVC anastomosis, which was performed by a running suture using the 8-0 Prolene ®, at the end the IHVC clamps were released re-establishing the normal circulation. Finally the HA and the CBD anastomoses

were performed using an internal plastic stent secured with two 7/0 silk ligatures. The haemostasis was secured and the abdominal wall was closed, the anaesthetics were stopped and the animal was awakened (Figure 9).

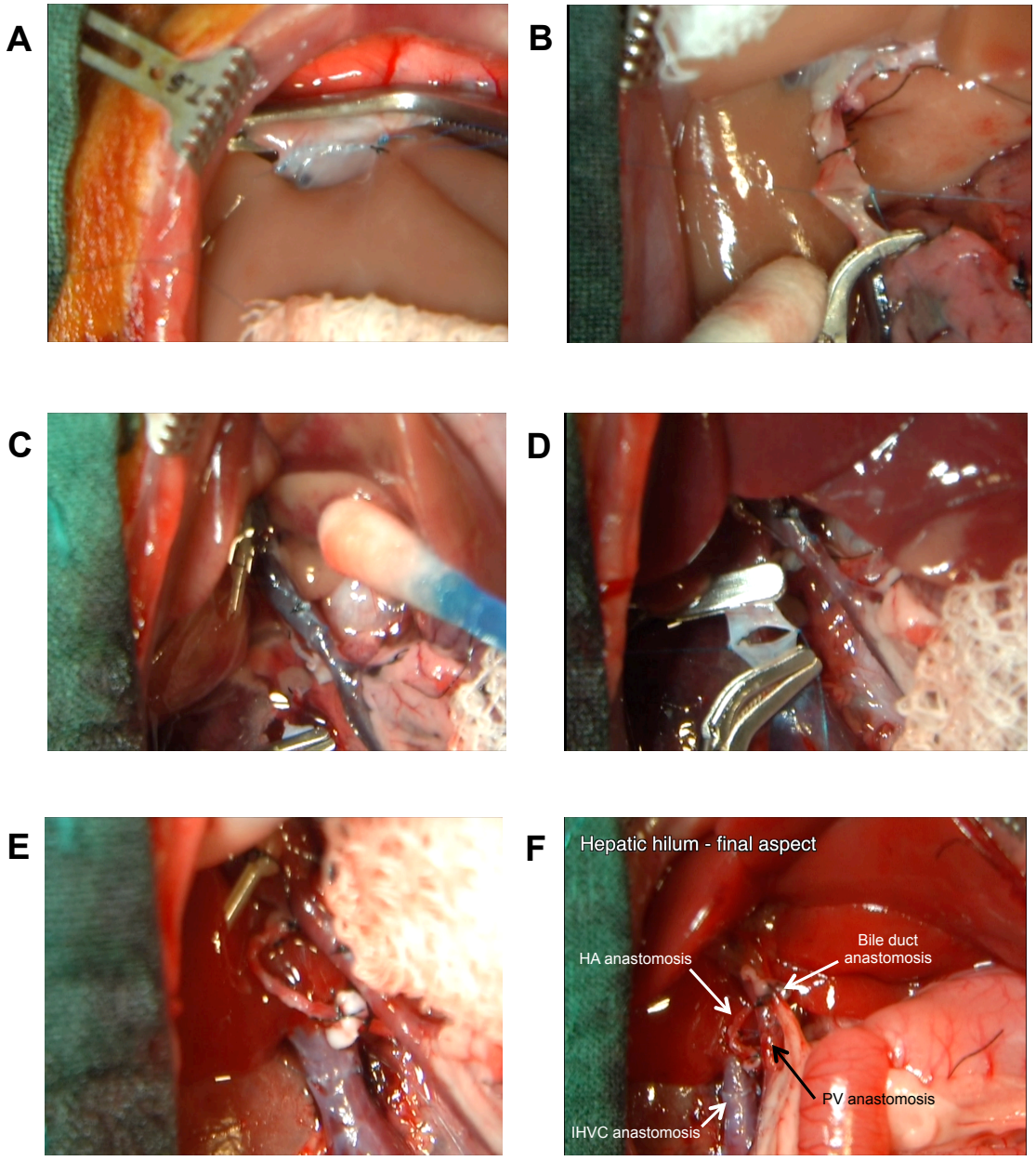

Figure 9: Panels displaying the sequential anastomoses of the liver allograft implantation. (A) Supra hepatic vena cava (SHVC anastomosis). **(B)** Portal vein (PV) anastomosis. **(C)** Few seconds after liver reperfusion, note the partial recoloration of the liver graft. **(D)** Infra hepatic vena cava (IHVC) anastomosis construction. **(E)** Hepatic artery (HA) anastomosis. **(F)** Final aspect of hepatic hilum, note the liver allograft homogenously reperfused.

4.2.2 Different strain combination

Two different agglutinins (*a* and *m*) and their respective agglutinogens can be detected in the blood of the *Rattus norvergicus* species, which allows the identification of four different blood types. However, agglutination is a very rare event that occurs only in very few combinations of strains. Normally, there is no agglutination between most of the rat strains currently used in laboratory experiments. For this reason, the blood group is not taken into account in the rat liver transplant model (284). Conversely, the antigens of the major histocompatibility complex, which in rats is named the RT1 barrier, are more relevant in transplantation research. Laboratory rats present a limited number of standard and derivative RT1 haplotypes, with *a*, *av1*, *l*, *n* and *u* being present in the most common strains used for transplantation research (285). Skin grafts performed against the RT1 barrier are rapidly rejected, with the same happening in the rat kidney transplantation. However, indefinite tolerance can be spontaneously achieved in the rat liver transplant model between animals with complete MHC mismatch depending on which strain combination is used; for example, livers from Brown Norway ($RT1^{n}$) donors are accepted by Lewis ($RT1^{l}$) recipients, whereas, livers from Dark Agouti ($RT1^{av1}$) donors are rejected up to two weeks post-transplant by Lewis ($RT1^{l}$) recipients. This tolerance phenomenon is not a passive event since there is a clear rejection type process evidenced by the allograft lymphocytic infiltration associated with abnormal LFTs in the first two weeks post-transplant. Some weeks later, the LFTs progressively and spontaneously normalise and the lymphocytic infiltrate similarly disappears (273). For our experiments, we decided to only work with one rat strain as recipient and change the donor strains to have the following different phenotypes: 1) syngeneic, 2) spontaneous tolerance, 3) rejection (no treatment), and 4) Tolerance induced by tacrolimus strain combinations (286). In the spontaneous or induced tolerance combinations, transplanted rats surviving more than 100 days are considered tolerant (287). The strain combinations used in our experiments are shown in Table 4.

Table 4: Rat strain combinations

	Donor	Recipient	Phenotype
1	Lewis ($RT1^l$)	Lewis ($RT1^l$)	Syngeneic combination
2	Brown Norway ($RT1^n$)	Lewis ($RT1^l$)	Spontaneous tolerant combination
3	Dark Agouti ($RT1^{av1}$)	Lewis ($RT1^l$)	Rejection combination (no treatment)
4	Dark Agouti ($RT1^{av1}$)	Lewis ($RT1^l$)	Tacrolimus-induced tolerant combination*

*Tacrolimus (1mg/Kg) IM during 10 days post transplant. RT1: rat related MHC locus.

4.2.3 Induction of Iron Deficiency employing iron-modified diets

Inbred rats weighting around 120 to 140g were used as donors, they were fed with either iron-deficient (<6mg/Kg iron) or iron-replete (iron deficient diet supplemented with 200mg/Kg iron carbonyl) diets (SAFE, France) for a total of 3 weeks; rats weighting around 160 to 180g were used as recipients and fed for 1 week prior to the liver transplant procedure. After three weeks of iron-modified diets the donor rats weighed around 180 to 220g, and the recipients after one week of the iron-modified diets achieved the same weight ranges, which were considered the ideal weights to perform the liver transplant procedure. Rats with less than 180g have very delicate vascular structures and rats weighting more than 300g present increased abdominal fat tissues making the procedure both more difficult and longer.

4.2.4 Recombinant human Interleukin 2 administration

The establishment of tolerance in similar experimental rat models of spontaneous tolerance strain combinations was abrogated by a course of high doses of rhIL-2 (276, 277). We replicated this strategy in our model of spontaneous tolerance in order to question if iron level changes can interfere with the rhIL-2 effect in the tolerance establishment. An injection of 200.000IU of rhIL-2 was performed every day by intra-peritoneal via during 21 days. Blood samples were collected at day 0, 3, 7, 10, 14, 17 and at day 21 by tail puncture for biochemistry analyses. Animals were sacrificed at day 21 and blood and tissue samples were collected for further analysis. Two additional experiments were realized on long-term transplant survivors following the same protocol, with only an adjustment on the rhIL-2 doses to 400.000IU per day proportional to the animal weight gain overtime.

4.2.5 Statistical analyses

Statistical analyses were performed with GraphPrism software version 5.0. The Mann-Whitney U test was used for comparison between two groups, whereas the two-way ANOVA analysis with Tukey's post-hoc correction for pairwise was used to compare more than 2 groups. The Fisher test was used for categorical variables. Survival rates were calculated using Kaplan-Meier estimation. P-values inferior to 0.05 (two tailed) were considered statistically significant in all analyses.

4.3 Results

4.3.1 Survival curves between the different rat strain combinations

Our first results using the Kamada technique were discouraging with no long-term survival after 76 transplant essays using Wistar rats as donors and recipients. At this point I had only 15 animals had survived few hours after the procedure, two animals had survived more than 24 hours and only one more than 48 hours. So we decided to move to the fully vascularized method due to the aforementioned reasons, and in order to be fully trained on this technique I attended a one-week training course at the Charité University Hospital in Berlin. From that week onward and after changed the rat strain used from Wistar to the Lewis as donor and recipient, which is more appropriate for the liver transplant procedure, our survival rate improved up to 80% in the syngeneic strain combination and in the spontaneous tolerant strain combination where the Brown Norway strain was used as donor. The tacrolimus induced-tolerance strain combination presented the worst survival rate, around 50% (Figure 10A). All long-term survival strain combinations presented similar clinical and biochemistry post-operative outcomes - gaining weight in the same proportion and with prompt normalization of the liver transaminases (Figure 10B and C). These results allowed us to start the experiments to check the influence of induced iron-deficiency on the anti-donor T cell mediated response.

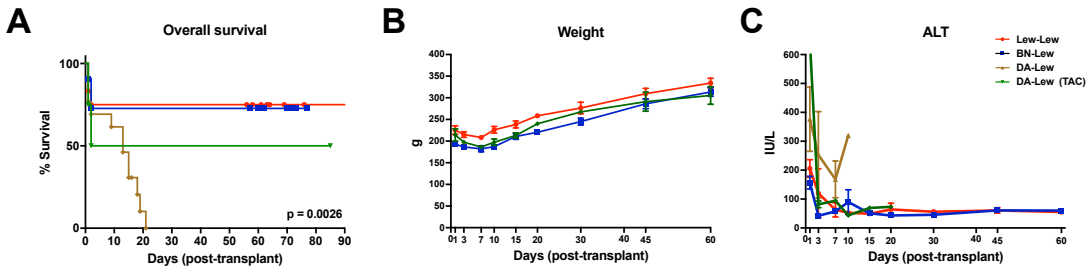

Figure 10: Post-liver transplantation outcome between the different strain combinations. (A) Overall survival rate post-liver transplantation including all transplants performed with animals under normal diet. **(B)** Rats weight evolution on the post-transplant period reflecting the clinical evolution between the three different strain combinations. **(C)** Alanine aminotransferase (ALT) kinetics on the post-transplant period: Number of animals: Lew-Lew: 12, BN-Lew: 11, DA-Lew: 11, DA-Lew (TAC): 8.

4.3.2 Induction of mild iron deficiency in rats

Once we had set up our rat liver transplant model with an overall survival rate of 80 to 90%, we tried to induce mild iron deficiency by modifying the iron levels in the animal diets as we had done in our work with mice. Rats were fed for three weeks with an iron deficient diet (IrDef) and the control group with an iron-replete diet (IrRepl). When compared with IrRepl, IrDef rats presented a decreased serum iron from the first week under the special regimen, which achieved statistical differences at three weeks (mean 16.87±2.77 versus 36.63±0.73μg/dL; p<0.0001). Additionally, intra-hepatic iron measurement revealed reduced iron stores at day 21 (131.0±7.04 versus 321.0±12.5μg/g of dried tissue, p=0.0002). IrDef rats presented no significant decrease in the haemoglobin serum levels in comparison to IrRepl rats (mean 130.7±4.33 versus 141.7±1.g/L; p=0.07), a slightly significant difference in RBC (8.41±0.09 versus 8.80±0.9x10^{12}/L, p=0.048), and in WBC (5.77±0.94 versus 6.72±0.52x10^{9}/L, p=0.42) and increased platelets (624.7±43.77 versus 462.7±115.0x10^{9}/L, p=0.25). Otherwise, IrDef rats remained clinically healthy and gained weight at the same rate as IrRepl rats with no differences in evolution of ALT levels over the post-transplant time (Figure 11).

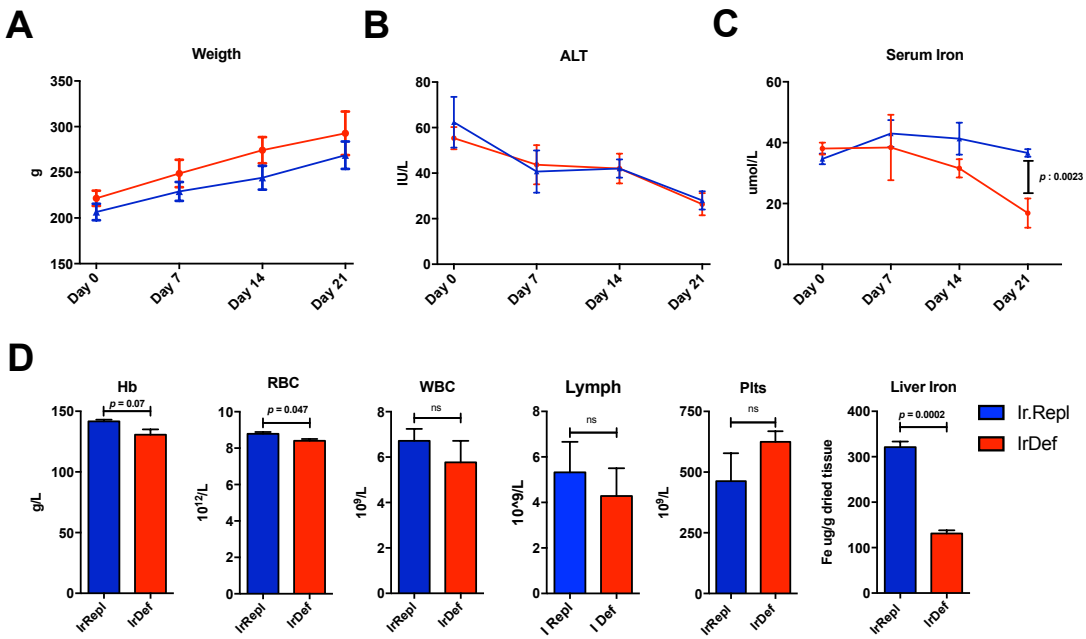

Figure 11: Clinical, biochemistry, iron and haematological parameters in Lewis rats fed with iron-deficient (IrDef) and iron-replete (IrRepl) diets over three weeks. (A) Rats weight evolution over the three weeks of iron-modified diets regimen. **(B)** Serum alanine aminotransferase (ALT) kinetics at the same period. **(C)** Serum iron evolution at the same period. **(D)** Haematological parameters and liver iron concentration evolution at the day 21 under iron-modified diets regimen. Bar plots display mean and SEM. Abbreviations: ALT: alanine aminotransferase, Hb: haemoglobin, RBC: red blood cells, WBC: white blood cells, Plts: platelets. Number of animals: (IrRepl/IrDef) 3/3.

4.3.3 Survival curve between the different rat strain combinations under iron-modified diets

For these experiments, donor and recipient rats were fed with iron deficient or iron-replete diets for a 3-week period. In a preliminary experiment, IrDef recipient rats presented a 50% per-operatory mortality rate, and all rats died within 3 days post-transplant. IrDef recipients presented an important colonic dilatation with liquid accumulation. They exhibited a high sensibility to anaesthesia and some of them became very unstable, even with a small amount of blood loss (Table 5).

Table 5: Post-liver transplant survival rate in a preliminary experiment using the iron-modified diets

	IrDef (n)	IrRepl (n)
Per-operative deaths	2	0
Deaths < 3days	2	2
Survivals > 100 days	0	2
Survival rate at 100 days	0%	50%

In this experiment both donor and recipient rats were fed with iron-modified diets during 3 weeks

Therefore, we decided to feed the donors during three weeks and the recipients for only one week before the transplant procedure. Using this protocol the survival rate for the three strain combinations used under iron-modified was similar to the transplanted rats for the same strain combinations under normal commercial diets. In the iron-modified diet experiment, all of the three strain combinations performed, the IrDef recipients presented similar clinical and biochemistry outcomes when compared with IrRepl recipients (Fig12 A and B).

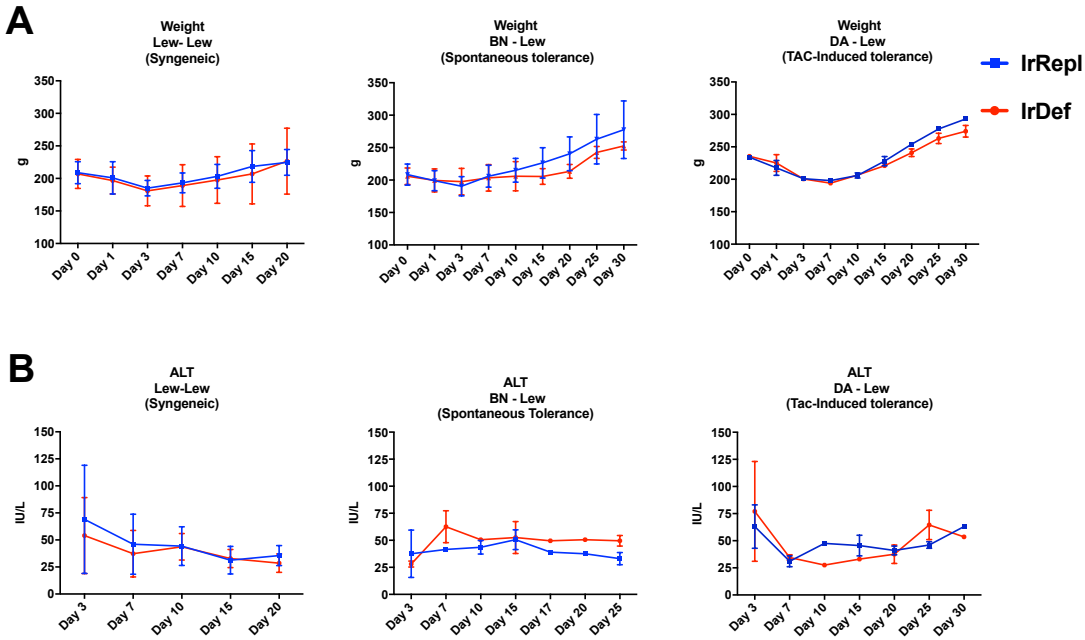

Figure 12: Post-liver transplant outcome between different strain combinations treated with iron-modified diets before (3 weeks for the donors and 1 week for the recipients) and after the procedure. (A) Animals weight evolution on the post-transplant period reflecting the clinical evolution between the three different strain combinations under iron-deficient diet (IrDef) and iron-replete diet (IrRepl). **(B)** ALT kinetics on the post transplant period reflecting similar liver function in both groups IrDef and IrRepl in all of the three strain combinations. Number of animals (IrRepl/IrDef): Lew-Lew: 2/2, BN-Lew: 2/2, DA-Lew: 2/2.

4.3.4 RhIL-2 administration induces clinical deterioration and liver function impairment associated with more cytokine production in Iron deficient animals

In the previous experiment, we had demonstrated that the induction of a slight iron deficiency could not hinder spontaneous tolerance. We then administered a potent immune-stimulatory treatment, such as high doses of rhIL-2 for three weeks, to amplify a possible subtle effect of iron deficiency on the establishment of tolerance. For these experiments, four groups of grafted liver rats were used: 1) spontaneous tolerance IrDef, 2) spontaneous tolerance IrRepl, 3) IrDef Syngeneic and 4) Syngeneic IrRepl, where the last two groups were considered as control groups. IrDef transplant rats presented a clinical deterioration reflected by the significant decrease in body weight in comparison with IrRepl animals (177.0±10.39 vs. 217.8±13.36g at day 21, $p<0.0001$). Furthermore, IrDef were apathetic and presenting piloerection, which are signs of animal illness (288). The LFTs presented an earlier worsening and a more accentuated deterioration in the IrDef group. Serum level of bilirubin was increased in IrDef animals at day 21 (94.60±21.15 vs. 63.40±18.98umol/L $p=0.02$) and ALT remained increased in IrDef animals in comparison with the IrRepl group during the 21 days of rhIL-2 administration. Upon euthanasia, IrDef transplant rats presented more intra-hepatic CD4+ T cells and less CD8+ T cells and more cytokine production. Interestingly, both syngeneic groups did not present the clinical deterioration or the LFTs impairment observed on the Spontaneous Tolerance IrDef group. Furthermore, the Syngeneic IrRepl did not present the late deterioration of the LFTs presented by the Spontaneous Tolerance IrRepl group. Altogether, these results suggest that the use of a potent immune inflammatory stimulus has been able to detect differences in post-transplant immune outcomes between groups with different levels of iron stores. These differences appear to occur only in the case of allograft lymphocyte infiltration in combinations of strains exhibiting complete MHC mismatch. This was the case with the Spontaneous Tolerance strain combination of Brown Norway / Lewis rats employed in such experiments (Figure 13).

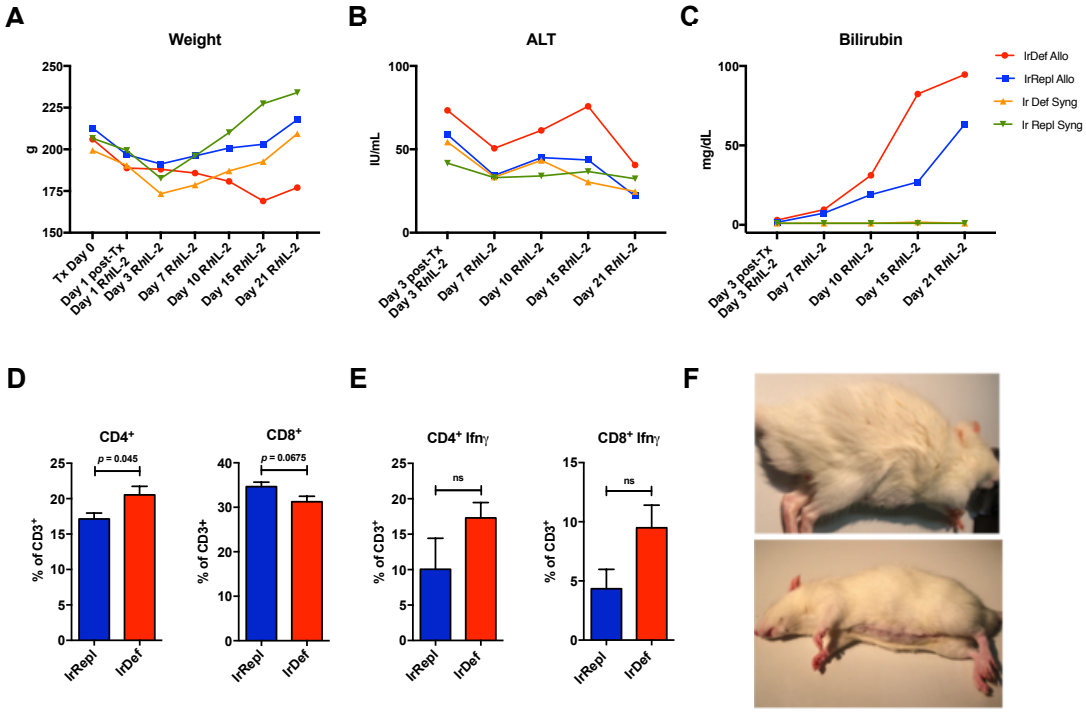

Figure 13: Post-liver transplantation outcome after rhIL-2 challenge. (A) Animals weight evolution on the post-transplant period reflecting the clinical evolution between the syngeneic and spontaneous tolerant IrDef and IrRepl groups. **(B and C)** Graphics showing the post-transplant ALT and bilirubin evolution. **(D)** Frequency of intra-hepatic CD4+ and CD8+ T cells in the two groups of spontaneous tolerant IrDef and IrRepl at day 21 post transplant and post RhIL-2 administration. **(E)** Intra-hepatic frequency of Interferon Gamma production by CD4+ and CD8+ T cells in a second identical experiment in where the animals were euthanized at day 14 post-transplant and post rhIL-2 administration. **(F)** Pictures showing one IrDef transplant rat (upper panel) and one IrRepl animal (lower panel) aspect after 21 days under rhIL-2 challenge (Spontaneous tolerant strain combination). The IrDef transplanted rat present piloerection, peripheral vasoconstriction and signs of losing weight. Number of animals: Syngeneic (IrRepl/IrDef): 3/3, Spontaneous tolerant (IrRepl/IrDef): 5/5.

4.3.5 RhIL-2 challenge does not seem to affect IrDef spontaneous tolerant long-term survivors

In order to check the influence of the transitory lymphocyte liver allograft infiltration in early time post liver transplantation, we replicate the rhIL-2 protocol in some spare spontaneous tolerant long-term survivors that had been kept under the same iron-modified diet protocol over all post-transplant period. For this experiment two IrDef spontaneous tolerant and only one IrRepl spontaneous tolerant animals were available. Mean serum iron level on the IrDef animals was 13,2 ug/dl while the IrRepl animal presented 41ug/dl of serum iron levels. Animals were challenged with 400.000IU of rhIL-2 (adjusted for their body weights) for 21 days in the same way as in the previous experiments. There were no modifications in animal weights or behaviours. Also no differences and/or alterations were observed in the ALT and bilirubin levels throughout the entire experiment (figure 14).

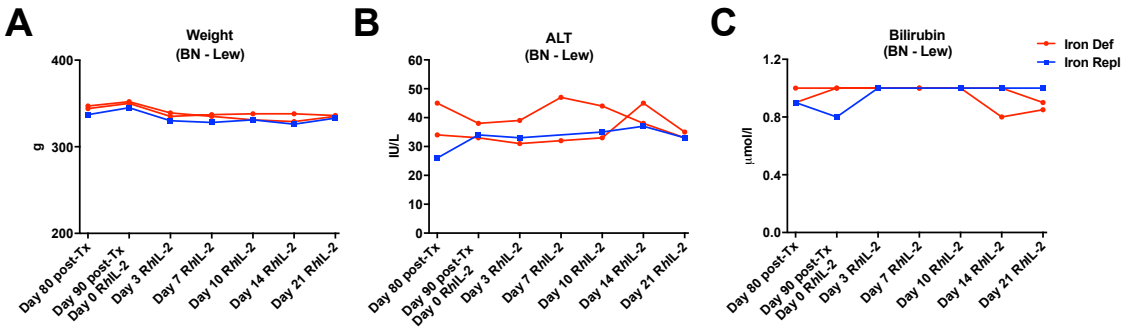

Figure 14: Outcome of long-term spontaneous tolerance transplanted survivors (BN – Lew) challenge with rhIL-2. (A) Animal weight evolution on rhIL-2 challenge period showing the similar clinical evolution between the spontaneous tolerance IrDef and IrRepl groups. **(B and C)** ALT and bilirubin kinetics during rhIL-2 challenge in the same groups. Number of animals (IrRepl/IrDef): 1/2.

4.3.6 RhIL-2 challenge seems to affect IrDef long-term induced tolerance survivors

RhIL-2 challenge caused a clinical and laboratorial effect in early spontaneous tolerant transplant rats, but not in early syngeneic transplant rats. Also this initial effect was abolished on long-term spontaneous tolerant transplant survivor rats. Then, we questioned what could be the effect of the rhIL-2 challenge on the induced tolerant strain combination. We aimed to replicate the same experiment on the aforementioned strain combination (DA-Lew). Unfortunately again, only two IrDef induced tolerant transplant and one IrRepl induced tolerant transplant rats were available for the experiment. In spite of that, one IrDef induced tolerant rat showed clear LFTs deterioration during the rhIL-2 challenge while one IrDef transplant rat did not present alterations. Likewise, the IrRepl animal did not show alterations in its weight and LFTs (Figure 15).

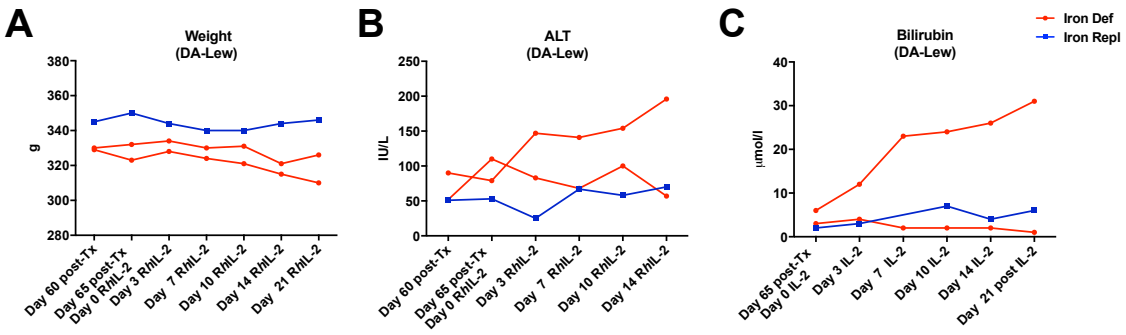

Figure 15: Outcome of long-term Tac-induced tolerance transplanted survivors (DA – Lew) challenge with rhIL-2. (A) Animal weight evolution on the post-transplant period showing no apparent clinical changes between the Tac-induced tolerance (DA-Lew) IrRepl and the two IrDef transplant rats during the rhIL-2 challenge. **(B and C)** ALT and bilirubin kinetics during the rhIL-2 challenge from the same animals. Number of animals (IrRepl/IrDef): 1/2.

4.3.7 Post-transplant long-term complications suggests a systemic effect of iron-modified diets

We initially checked the iron-modified diets' impact on the growth rate and on the hematologic and biochemical parameters before starting our transplants in rats previously fed with those diets. Three weeks of the special diet protocol did not alter the weight gain between the two groups. Likewise, we did not detect important differences in hematologic parameters or in LFTs. Those observations allowed us to proceed with the transplant on animals under the special diet protocol. However, we aimed to interrogate whether the use of the special iron-modified diets for a long period was detrimental for the clinical evolution after transplantation. For that, we checked our clinical evolution records for long-term transplant survivor rats kept for more than 4 months under the iron-deficient and/or iron-replete regimens and we compared them with a large group of spontaneous tolerant transplant rats kept under normal chow diet. Transplant rats under special iron diets (iron deficient and iron-replete) showed a higher rate of complications (p=0.0001). They developed more abdominal wall abscesses, incisional hernias and biliary obstructions with hepatic abscesses and cirrhosis than the group fed with normal chow diet (Table 6 and Figure 16).

Table 6: Post liver transplant long-term complications

Diet	N	Mean Survival (days)	Incisional hernia	Abdominal wall abscess	Biliary obstruction Hepatic abscess Cirrhosis	Total	Total %
Normal	36	168.78	0	0	3	3*	8.3
Iron-modified	27	137.14	5	4	10	19*	70.4
Iron deficient	14	135.28	4	2	5	11	78.5
Iron replete	13	139	1	2	5	8	61.5

* p=0.0001

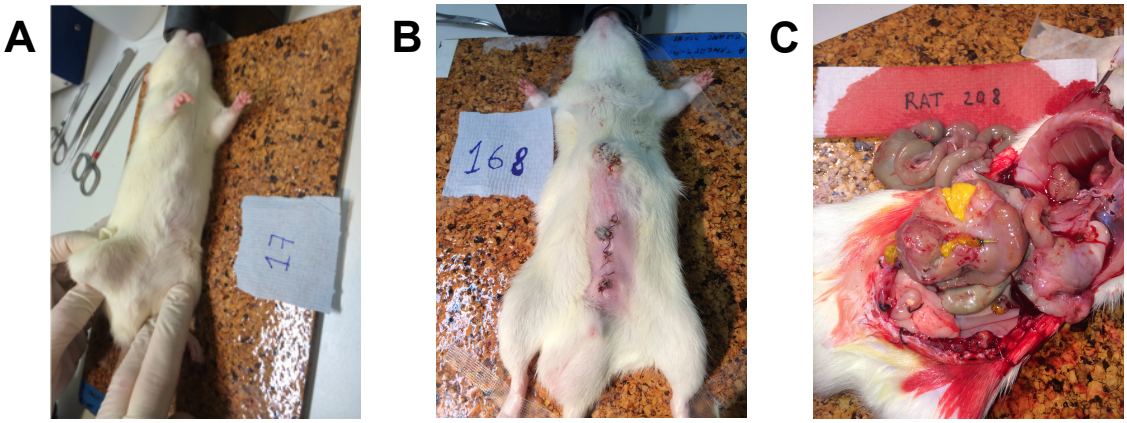

Figure 16: Clinical complications on long-term survivors transplant rats: (A) Picture showing an incisional abdominal wall hernia on an IrDef transplant rat. **(B)** Picture showing abdominal wall abscesses alongside the surgical incision on an Ir Repl transplant rat. **(C)** Picture showing an intra-hepatic abscess with a cirrhotic liver in an Ir Def transplanted rat.

Chapter 5 : Molecular characterization of acute cellular rejection occurring during intentional immunosuppression withdrawal in human liver transplantation

5.1 Introduction:

Spontaneous operational tolerance was initially observed in non compliant or in liver transplant recipients that interrupted IS treatment due to uncontrolled infectious episodes or by the presence of malignancies such as PTLD. These observations instigated the realisation of intentional IS withdrawal on stable liver recipients. On average, around 20 to 40% of the enrolled liver recipients could be completely weaned from the IS treatment in such studies. On the other hand, eventual ACR episodes are mild and mainly treated by reintroduction of initial IS treatment. Since recruited liver recipients have been transplanted for more than three years, we can expect that such ACR episodes are not influenced by the ischaemic-reperfusion injury, surgical complications and/or by the consequences of the underlying liver disease that are very intense in the first weeks post liver transplantation. In agreement with that, we hypothesized that molecular profiling analysis of sequential biological samples collected from rejecting liver recipients during the IS weaning protocol could be used to decipher ACR pathways and to discovery rejection biomarkers without the interference of such mentioned confounders. In the present study, we analysed liver tissue and blood samples collected before starting the weaning protocol and at the ACR time, in addition to sequential blood samples taken across the weaning process. We conducted a gene expression profiling employing whole-genome microarrays and real-time PCR technologies. Results were correlated with the type of immunosuppression and with the histological damage intensity. Furthermore, we compared our gene molecular dataset with public gene set databases. Finally, we analysed the gene transcriptional profile from the sequential blood samples collected during the weaning process, trying to define a gene signature that could diagnose ACR before its clinical or histological manifestation in that specific set of IS withdrawal.

5.2 Material and Methods

5.2.1 Immunosuppression withdrawal clinical trials in liver transplantation

From April 2006 to December 2009, one hundred and thirty-six stable liver transplant recipients were enrolled in two prospective multicentre clinical trials of IS withdrawal. The first trial (ClinicalTrials.gov NCT00647283) was designed to study the development of operational tolerance in a very selected liver transplant recipient population that met the following inclusion criteria: more than 3 years of follow-up since the liver transplantation; no history of autoimmune liver disease; absence of graft rejection in the last 12 months, aspartate aminotransferase (AST) and alanine aminotransferase (ALT) levels less than 2-fold and alkaline phosphatase (AP) less than 1.5-fold the local laboratory superior normal limit; presence of comorbidities associated to immunosuppressive regimens (arterial hypertension, diabetes, renal dysfunction), and risk of malignancy occurrence (previous history of extra hepatic cancer, history of smoking or alcohol consumption, older than 60years-old). From 341 patients initially screened with more than 3 years since the liver transplantation, 102 patients were enrolled in the trial, 24 of whom were transplanted for HCV related cirrhosis and 12 presented RNA-HCV positive at the time of enrolment (1). The second trial (ClinicalTrials.gov NTC00668369), focused on the investigation of the influence of the inflammatory responses induced by the hepatitis C virus (HCV) on the development of operational tolerance, screened 130 patients and enrolled 34 patients who matched the following inclusion criteria: liver transplantation for HCV-associated liver disease with more than 3 years of follow-up after the transplant, positive HCV RNA at study enrolment, no indication for anti-HCV treatment, no history of autoimmune disease, absence of graft rejection in the last 12 months before enrolment, stability of LFTs, and positive biomarker screening (high blood Vδ1/Vδ2 T cell ratio measured by flow cytometry on whole blood samples and/or elevated *SLAMF7/KLRF1* transcript level expression detected by real-time PCR platform (100). Exclusion criteria were similar in both studies: age inferior to 18 years; pregnancy; alcohol or illicit drug abuse; psychiatric or medical illnesses interpreted as incompatible with safe participation in the study (e.g., cardiac failure; chronic obstructive pulmonary disease; on going malignancy, major depression); altered baseline LFTs; altered baseline liver biopsy with: (1) signs of acute or chronic rejection as stated by Banff criteria (55); (2) portal inflammation more than 50% of

portal tracts unrelated to chronic HCV infection; (3) central perivenulitis in more than 50% of central veins; (4) or fibrosis stage III-IV as stated by Metavir criteria; HIV co-infection or combined liver-kidney transplantation. In both studies, an identical drug withdrawal protocol was employed and has been previously described (Figure 19) (1, 100). Initially, immunosuppressive drug doses were gradually tapered, by reducing 25% to 50% of the dosage at each 3-week interval. Once the minimum possible daily dose was attained, the next step was to space the doses over the weekdays, always respecting the 3 week period for each dose reduction until one dose per week was achieved and then the immunosuppressive treatment was completely discontinued. The weaning process was realized over a 6-9 month period and patients who completely stopped the IS treatment were followed for a minimal period of 12 months. Patients who did not develop rejection were classified as operationally tolerant as long as immunosuppressive drug cessation was maintained for at least 12 months with no laboratorial and no histologic evidence of acute and/or chronic rejection were observed.

5.2.1.1 Liver biopsies protocol

Protocol liver biopsy samples were obtained in all patients at baseline, at 12 months after successful drug withdrawal in patients who did not reject or at the time of rejection in those patients that presented it. Blood samples were taken at enrolment, at every three weeks during the withdrawal period, at the rejection episode and monthly during the 12 months after drug cessation or after the rejection episode resolution. During the weaning process or after complete IS treatment withdrawal; allograft dysfunction was determined by any increase of AST, ALT, or simultaneous increase on gamma-glutamyl transpeptidase (GGT) and AP above the superior normal limits. In patients with initial abnormal LFTs, allograft dysfunction was considered when they presented an increase superior to 2-fold the baseline levels and/or an increase on GGT an AP at the same time superior to 1.5-fold the baseline levels. When LFTs were increased more than 2-fold the baseline levels of AST or ALT, and/or more than 1.5-fold increase of GGT and AP baseline levels, liver biopsy was promptly realised. In case of alterations of LFTs inferior to the previous cut-off described, drug minimization was temporarily interrupted and LFTs were repeated in two weeks time. If the deterioration persisted, a liver biopsy was carried out, and in case of amelioration of blood tests, the weaning protocol was

reassumed. Rejection was diagnosed by the combination of allograft dysfunction and characteristic liver biopsy findings according to BANFF criteria (55).

5.2.1.2 Rejection treatment

Rejection episodes were predominantly mild to moderate and promptly resolved following reinstitution of baseline immunosuppression regimen (29 patients, 21 from the first trial and 8 from the second trial) associated or not with low dose steroids (20mg/day over a period of 4-6 weeks) (35 patients, 30 patients from the first trial and 5 from the second trial) or moderate-dose steroids doses (7 patients, 4 patients from the first and 3 from the second trial**),** only one patient required steroid boluses to treat the rejection episode. No grafts were lost due to the rejection episodes. At the end of both studies, drug withdrawal was successfully achieved in 41 patients while 57 rejected in the first clinical trial; whereas, in the second clinical, complete IS weaning was successful in 17 patients and rejection occurred in 15. In total, from the initial 136 liver transplant recipients enrolled, 58 patients were considered tolerant, 72 patients presented a rejection episode and 6 patients were excluded (Figure 19).

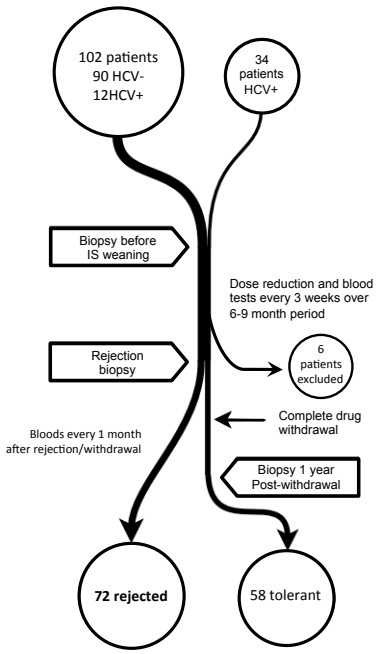

Figure 17: Flow chart showing immunosuppression withdrawal trial design. Data was included from two trials with identical withdrawal protocols (ClinicalTrials.gov NTC00647283 and NTC00668369). A subset of these patients was included in the current study.

5.2.2 Rejecting patients population and control groups

Even though the previous described clinical trials had been designed to study the development of operational tolerance in liver transplant recipients, with all derived recent publications reported mainly focusing on the clinical outcomes of operational tolerant recipients and possible mechanistic pathways involved on the development of operational tolerance (1, 2, 100, 274), these studies also provide an exceptional opportunity to investigate the molecular mechanisms of acute cellular rejection, which still represents an important concern for the liver transplant follow-up. This present worked focused on the rejecting patient population in those trials aiming to identify possible biomarkers associated with acute cellular rejection occurring during intentional immunosuppression withdrawal in liver transplantation.

5.2.2.1 Rejecting patients and samples selection

Out of the total population of 72 liver recipients who developed an episode of ACR during the two previous described clinical trials, 55 patients were included in the current study. Forty-seven patients were enrolled in the first clinical trial, one of them was RNA-HCV positive at the enrolment time (1), and the remaining 8 patients were initially included in the second clinical trial destined to enrolled only RNA-HCV positive liver recipients (100) (Table 7). Patient selection for the present study was based on availability of liver samples for molecular and histologic analyses and blood samples for molecular analyses. Thirty-three patients were identified having 61 liver tissue samples available for analysis, (34 biopsies at baseline and 27 biopsies at rejection time). Sequential blood samples were initially available from 77 patients. Due to the variation in the days of blood sample collection in relation to the day of rejection episode, we defined time intervals in order to uniformly group the samples according to the time before and after the rejection episode for rejecting patients and/or the time before and after complete immunosuppression withdrawal for tolerant recipients used as control groups (Table 8). After processing and control tests, one hundred and ninety-three sequential blood samples from 45 rejecting patients were used in our study.

Table 7: Demographic and clinical characteristics of enrolled rejecting patients

Characteristic	Total cohort (55)
Age at transplant (years)	48.23 ± 11.73
Age at weaning start (years)	55.53 ± 11.83
Gender (% male)	54.5
Caucasian (%)	100
Transplant Indication	
HCV cirrhosis	21
VHC-RNA positive at enrolment	(9)
HBV cirrhosis	9
Alcoholic cirrhosis	9
Amyloidotic polyneuropathy	5
Fulminant hepatitis	3
Other causes	8
Time from transplant to weaning start (years)	6.83 ± 3.55
Time from weaning start to rejection (months)	7.82 ± 4.49
Immunosuppressive therapy at weaning start	
Tacrolimus	25
Cyclosporin A	22
Mycophenolate	11
Rapamicine	2
Cyclosporin A + Mycophenolate	5
CNI-based immunosuppression at weaning start (%)	85
Immunosuppressive drug trough levels at weaning start (ng/mL)	
Tacrolimus	5.2 ± 2.3
Cyclosporin A	57.4 ± 36
Liver function tests at weaning start	
Aspartate aminotransferase (U/L)	33 ± 22
Alanine aminotransferase (U/L)	38 ± 35
Gama-glutamyl transpeptidase (U/L)	40 ± 70
Alkaline phosphatase (U/L)	172 ± 64
Total Bilirubin (mg/dL)	0.75 ± 0.3
Rejection severity	
Indeterminate	19
Mild	23
Moderate	7
Severe	6
Banff Score*	4 (2-9)
Liver function tests at rejection time	
Aspartate aminotransferase (U/L)	150 ± 137
Alanine aminotransferase (U/L)	207 ± 196
Gama-glutamyl transpeptidase (U/L)	188 ± 208
Alkaline phosphatase (U/L)	287 ± 173
Total Bilirubin (mg/dL)	1.55 ± 4.51
Rejection treatment	
Baseline IS	23
Baseline IS + Prednisone 20 mg/day (4-6 weeks)	26
Baseline IS + Prednisone 40-60mg/day (4-6 weeks)	4
Corticosteroids boluses	2

Table 8: Time distribution of sequential blood samples selection

Sample Code	Time interval for samples collection	Blood samples from 45 rejecting patients	Bloods samples from 7 tolerant patients
- 6	> 9 Mo bef.	45	7
- 5	< 9 Mo and > 6 Mo bef.	4	4
- 4	< 6 Mo and > 3 bef.	8	5
- 3	< 3 Mo and > 1 Mo bef.	9	6
- 2	< 1 Mo and > 15 days bef.	6	6
- 1	< 15 days and > 7 days bef.	8	4
0	Rejection episode/ Complete IS stop	45	5
+ 1	< 15 days after	6	4
+ 2	> 15 and < 1 Mo after	11	7
+ 3	> 1 Mo and < 3 Mo after	12	7
+ 4	> 3 Mo and < 6 Mo after	13	7
+5	> 6 Mo and < 12 Mo after	14	7
+6	> 12 Mo after	12	7
Total	Total	193	69

5.2.2.2 Patient control groups

A cohort of 86 stable immunosuppressed liver recipients, from Hospital Clinic in Barcelona – Spain, with no biological evidence of rejection; no previous attempts of drug withdrawal, from whom at least one cryopreserved blood sample was available, was used as control group for the molecular blood samples experiments. All patients in this group were initially enrolled in a previous clinical study designed to investigate the immunologic characteristics of stable liver transplant patients under immunosuppression treatment at determined time. The 86 patients selected as control group for this present study were matched for age, sex and time from transplantation with the group of 22 rejecting patients from whom, sequential blood samples were used to construct predictive models of rejection (Table 9). At least one cryopreserved blood sample in conformity for molecular analyses was available per patient. An additional experiment was performed to check if ACR-associated gene expression was differentially expressed between tolerant and rejecting patients before starting the weaning process. For that, we reanalysed a previously generated gene expression data originated from baseline blood samples of a group of 25 tolerant patients and compared with results of 43 rejecting patients, all of them enrolled in the first clinical trial (ClinicalTrials.gov NCT00647283) (1) (Table 10). Finally, in order to create a positive control group of rejection happening in the early time post-transplant and outside of drug-withdrawal setting, nine early post-transplant rejection biopsies collected originated from clinically stable and without major surgical complications (vascular and biliary events) HCV negative patients within the first 4 weeks

following transplantation were included as a control cohort and used in the tissue molecular experiment.

Table 9 : Demographic and clinical characteristics of patients used in the rejection prediction model test

Characteristics	Non-Tolerant (22)	Tolerant (7)	Stable (86)	*p*- value
Age at transplant (years)	53 ± 9.59	50.49 ± 9.34	51.97 ± 10.16	0.88
Age at weaning start or sample collection (years)	59.71 ± 8.84	60.43 ± 8.69	58.33 ± 9.95	0.80
Gender (% male)	68.2	85,7	69.4	0.45
Transplant Indication				
HCV cirrhosis	8	0	36	
HBV cirrhosis	5	3	8	
Alcoholic cirrhosis	4	4	25	
PAF	2	0	5	
Fulminant hepatitis	-	0	1	
Other causes	3	0	11	
Time from transplant to wean start or sample collection	6.96 ± 2.56	10.08 ± 3.6	6.39 ± 2.15	0.022

Table 10: Demographic and clinical characteristics of Non-tolerant and Tolerant patients from whom previous qPCR data at the baseline were reassessed

Characteristics	Total cohort (68)	Non-Tolerant (43)	Tolerant (25)	*p*- value
Age at transplant (years)	47.75 ± 10.34	46.15 ± 11.53	50.45± 7.40	0.068
Age at weaning start (years)	56.11 ± 10.85	52.62 ± 11.40	61.96 ± 6.70	0.000
Gender (% male)	68.5	60.5	72.0	0.34
Caucasian (%)	100	100	100	
Transplant Indication				
HCV cirrhosis	21	12	9	
HBV cirrhosis	18	11	7	
Alcoholic cirrhosis	12	6	6	
Amyloidotic polyneuropathy	4	4	0	
Fulminant hepatitis	3	3	0	
Other causes	9	6	3	
Time from transplant to weaning start (years)	8.20 ± 3.81	6.50 ± 3.29	11.06 ± 2.80	0.000
Immunosuppressive therapy at weaning start				
Tacrolimus	29	21	8	
Cyclosporin A	25	16	9	
Mycophenolate	17	6	11	
Tacrolimus + Mycophenolate	2	1	1	
Cyclosporin A + Mycophenolate	2	1	1	
Liver function tests at weaning start				
Aspartate aminotransferase (U/L)	23.03 ± 5.3	24 ± 5.67	21.5 ± 4.54	0.18
Alanine aminotransferase (U/L)	21.29 ± 6.84	22.9 ± 6.52	18.75 ± 6.82	0.10
Gama-glutamyl transpeptidase (U/L)	28 ± 33.6	20.89 ± 16.53	39.9 ± 49	0.23
Total Bilirubin	0.73 ± 0.23	0.7 ± 0.33	0.71 ± 0.2	0.41
Alkaline phosphatase (U/L)	153.76 ± 45.9	158.16 ± 49.0	139.83 ± 29.8	0.29

5.2.3 Biological specimens

As previously mentioned, liver biopsy samples were obtained in all patients before the initiation of the immunosuppressive drug weaning protocol (baseline), at the time of rejection if it occurred, and at 12 months after successful drug withdrawal in patients who did not reject. Blood samples were taken at enrolment, at every three weeks during the withdrawal period, at the rejection episode and monthly during the 12 months after drug cessation or after the rejection episode resolution.

5.2.3.1 Liver samples collection and conditioning:

Liver specimens were collected through a percutaneous or a trans-jugular liver puncture under aseptic conditions and local anaesthesia. A 10- to 15mm portion of the biopsy cylinder was immediately formalin-fixed and sent to pathology laboratory to be posteriorly embedded in paraffin, sectioned and stained in haematoxylin-eosin and Masson's trichrome preparations. The remaining liver tissue, usually a minimum of 2- to 3mm portion of the biopsy cylinder, was immediately preserved in RNA*later*® reagent (Ambion – Carlsbad, CA - USA), kept at 4ºC for 24 hours, and then snap frozen in liquid nitrogen after removal of RNA*later*®.

5.2.3.2 Blood samples collection and conditioning:

After venepuncture under aseptic conditions, blood samples were collected, conditioned in specific laboratory tubes and sent for haematological and biochemistry tests. An additional blood volume (2,5ml) were directly collected for immediate stabilisation in Paxgene® tubes (Qiagen – DE), specially designed for RNA preservation, then filled tubes were stabilized for at least two hours in RT and then stored at -80ºC until thawing for posterior analyses.

5.2.3.3 Total RNA extraction from liver tissue and blood samples

For total RNA extraction, frozen liver tissue samples were thawed and homogenized in Trizol® reagent (Invitrogen – Carlsbad, CA - USA) using a pestle and nuclease-free 1.5ml reaction tubes (Ambion – Carlsbad, CA - USA) and then total RNA was extracted following the manufacturer's instructions, posteriorly, RNA extracted quality was checked using Agilent2100 Bioanalizer® (Agilent Thecnologies – Santa Clara, CA - USA).

For total RNA extraction from the frozen whole blood samples, blood samples were thawed in RT for a minimal period of two hours, then samples were processed using the Paxgene Blood RNA kit ® (Quiagen – DE) following the manufacturers instructions, after extraction the RNA quality was assessed using Nanodrop1000 Spectrophotometer (Thermo Scientific – USA).

5.2.4 Histological examinations

The liver biopsy slides stained with H&E and Masson's trichrome stain were systematically analysed by a senior hepatic pathologist (R.M.) who was blind to all clinical and biological data. For histological analysis purposes following criteria were quantitatively measured: 1) lobular inflammation, 2) central vein perivenulitis, 3) central vein endothelitis, 4) portal inflammation, 5) interface hepatitis, 6) bile duct lesions, 7) ductular reaction, 8) ductopenia, 9) portal vein endothelitis, 10) perisinusoidal fibrosis, and 11) portal fibrosis.

5.2.5 Liver tissue and blood microarray gene expression

Several thousands of genes could be differently expressed during biological processes and it is particularly evident during an inflammatory and immunological event as the acute allograft cellular rejection. Depending on which kind of stimulus they receive, genes can be overexpressed, down regulated or not be influenced by the on going stimulus. To simultaneously access the expression profile of several thousands of genes probably associated with the acute cellular rejection phenomenon we employed the microarray technology. This technology, which involves many steps and requires sophisticated software and algorithms to analyse the huge amount of generated data, has its core principle in the hybridization of two complementary strands of nucleic acids using a biochip consisting of a small solid substrate covered in a high density way by thousands of oligonucleotide probes specific for the target genes. Biological samples were processed and analysed employing two microarray platforms in the present study: Illumina® (San Diego, CA – USA) microarray platform for liver tissue experiments and Agilent® (Santa Clara, CA – USA) microarray platform for blood samples analysis as described below:

5.2.5.1 Liver tissue data extraction and normalization

Transcriptional profiling of liver tissue samples was conducted employing Illumina® microarrays. Fifty-eight liver tissue RNA samples (pre-weaning and rejection time points) from 28 patients (21 HCV-negative and 7 HCV positive patients) were processed into cRNA and hybridized onto IlluminaHT 12 Expression BeadChips containing up to 48,771 probes which correspond to 25,000 annotated genes and analysed using BeadArray Reader (Illumina®). Then, microarray expression data was computed using BeadStudio data analysis software (Illumina®) and subsequently processed employing quantiles normalisation using the Lumi bioconductor package (Bioconductor® project – www.bioconductor.org). Next, a conservative probe-filtering step was conducted excluding those probes with a coefficient of variation <4%, which resulted in a list of 20,965 evaluable from the original set of 48,771 probes.

5.2.5.2 Blood sample data acquisition and normalization

RNA extracted from blood samples was analysed on a custom Agilent® complementary DNA (cDNA) microarray containing probes for 5069 preselected immunology-related transcripts (123). Seventy-four paired blood samples (37 pre-weaning and 37 rejecting blood samples) from 37 non-tolerant HCV-negative patients were hybridized on the custom Agilent cDNA microarrays according to the manufacturer's instructions. Array images were acquired with Agilent's microarray scanner G2505C and signal data was collected with dedicated Agilent Feature Extraction software (v9.5.1). Probes with gIsPosAndSignif (Boolean value representing whether the spot's Cy3 signal exceeds significantly background) value of zero in at least 10 samples were disregarded and labeled as "null". Background adjustment and normalization were done using normexp and quantile normalization. Median values were calculated for multiple probes with the same Agilent Probe ID.

5.2.5.3 Statistical microarray analysis

Analysis for differential expression on a probe basis was done by *limma* Bioconductor® software package, which included the correction for multiple testing using the FDR method. We defined statistically significant differences in gene expression as those that showed a FC > 1.2 and a FDR <0.05. When we compared expression data between different microarray

platforms (blood [Agilent] versus liver tissue [Illumina]), a lower threshold of significance was used (FC >1.2 and p-value <0.01).

5.2.6 Gene Set Enrichment Analysis

The huge amount of gene profile data generated by microarray experiments makes the analysis and interpretation a real challenge due to many factors as the massive volume of results by itself, the large number of tested genes, reduced number of samples and the high variability between tested individuals. In complexes biological processes, it is unlikely that a given specific gene, differentially expressed with statistical significance in a microarray experiment, could be determinant for that process where thousands of genes are involved. Furthermore, the same given gene can present different expression profiles across individuals with the same phenotype. Considering these factors, it is more logical to analyse the results for pre-defined sets of genes known to be involved in the functional pathways associated with the biological process in question. To assess the functional pathways associated with ACR in the present study, we used the GSEA application (149, 150). This tool, which compares differently expressed genes with previously identified gene sets, presents three fundamental steps: 1) An Enrichment Score (ES) for each gene set from the complete list of expressed genes is calculated taking in account the position (top or bottom) of each gene from the list of genes to study in a pre-defined gene set and its correlation with the biological phenotype. The score is calculated by a normalized Kolmogorov-Smirnov statistic like sum walking across the list of genes, its value increases when a gene from the list is encountered in the gene set and decreases when the gene is not present in the gene set. The ES corresponds to the maximum deviation from zero in the random walk across the gene set. 2) The statistical significance of each ES (nominal *P* value) is estimated though an empirical class label permutation (1,000 times), which at each time recorded the maximum ES over all gene sets. In this way the alternative hypothesis of association between gene sets and the class phenotype is tested. 3) Once a complete database is evaluated, the ES of each gene set is normalized in regard to the size of the set, which generates a normalized enrichment score (NES), then a FDR correspondent to each NES is calculated in order to estimate the probability that a gene set with a given NES is a false positive result. In the present GSEA analysis, three different gene set databases were employed: 1) *Hallmark* gene sets from the molecular signature data base

(MSigDB) at the Massachusetts Institute of Technology (MIT) Broad Institute (Cambridge, MA – USA) (149), which include 50 gene sets mapped to known biological processes; 2) HaemAtlas gene set database (289), which contains gene sets preferentially expressed by specific peripheral blood subsets (CD4, CD8, CD19, CD14, CD56, CD66B, EB, MK); and 3) Pathogenesis-based transcript gene sets, which have been associated with different sub-types of rejection in both experimental animal models and in human kidney and heart allografts (http://atagc.med.ualberta.ca/Research/GeneLists/Pages/default.aspx) (158, 290). The full list of gene sets used is shown later on the results section (Table 12 and 13). All analyses were performed using the GSEA Pre-ranked tool, based on t-statistic and a weighted scoring scheme with 1,000 permutations.

5.2.7 Correlation between gene expression profiling and liver histopathology

To check which histological compartment on liver biopsies contributed to the transcriptional changes at the moment of rejection, we correlated histopathology data with complete liver tissue microarray data. A total set of 80 biopsy samples with full quantitative histological data for the each of 11 parameters mentioned on the section 5.2.4 could be uniquely mapped to tissue microarray data. Using this criteria, 21 samples taken at the rejection time, 57 biopsies taken before the drug withdrawal and two follow-up biopsies taken 1 year after complete withdrawal of immunosuppressive drugs. A graduation scale from 0 to 3 (0: absent, 1: mild, 2: moderate, 3: severe) was used to quantify all parameters in each sample. For each parameter, differentially expressed genes were identified using the *limma* Biocondutor package. Gene expression was correlated with severity of each parameter using a linear regression model constructed for that purpose.

5.2.8 Influence of type immunosuppression on gene expression pattern

To check whether maintenance immunosuppression regimens (TAC, CSA, MMF, and mTor inhibitors) could influence gene expression profiles in samples collected before starting the weaning protocol, we employed linear regression models constructed employing the *limma* Biocondutor® package to analyse our microarray data originated from 74 blood samples and 33 liver tissue samples at baseline.

5.2.9 Validation real-time polymerase chain reaction experiments in peripheral blood samples

Quantitative real-time polymerase chain reaction (qPCR) gene expression experiments were performed using a Fluidigm Biomark HD® system (Fluidigm, South San Francisco, CA - USA) and following the manufacturer's instructions as described below to validate a set of gene expression profiles generated by microarray experiments performed in blood samples and liver tissue samples at the baseline and at the time of rejection.

5.2.9.1 Genes and samples selections for Fluidigm Biomark HD system *qPCR* experiments

We selected forty genes from the results of liver tissue and blood microarray gene expression profiles based on their FC and FDR classification and, on their overlapping expression between the two compartments. A small group of 5 genes were intentionally added taking in account their involvement in immunological processes (*GZMB*, *PRF1*, *FOXP3*, *TGFB1* and *IL15*). *HPRT1* and *GAPDH* were added as housekeeping genes for the Fluidigm experiments (160)(Table S1 Appendix C). Sequential blood RNA samples from 22 rejecting recipients (14 HCV-negative and 8 HCV-positive) and 7 tolerant recipients were used in these experiments; which includes samples at baseline, during the weaning process, at the rejection time for the rejecting patients, at the time of complete IS stopping for the tolerant recipients, and samples from the follow-up period after rejection episode or after complete IS stopping following the selection criteria described in the section 5.2.2.1 (Table 7). Cryopreserved blood samples, from a cohort of 86 stable immunosuppressed liver recipients (one sample per patient) with no biochemical evidence of rejection, were included for comparative purposes (Table 8).

5.2.9.2 qPCR experiments using Fluidigm Biomark HD system

Total RNA extracted from blood samples following description protocol in section 5.2.3.2 was initially treated with Turbo DNA-free DNAse (Ambion, Carlsbad, CA – USA) in order to remove DNA contamination. RNA purified samples were then reverse transcribed into cDNA using HighCapacity cDNA Reverse Transcription Kit (Applied Biosystems, Foster City, CA - USA). A pre-amplification step was performed as stated by Fluidigm Biomark HD protocol. Then, qPCR transcriptions were run using the Fludigm 96.96 Dynamic Array™ IFC plates following

manufacturer's instructions. To quantify transcript levels target gene Ct values were normalized to the housekeeping genes HPRT1 and GAPDH to generate ΔCt values. The results were then computed as relative expression between cDNA of the target samples and a calibrated sample according to the ΔΔCt method.

5.2.9.3 Additional real-time PCR experiment

At the same time of the Fluidigm analysis, we conducted additional real-time PCR experiments as part of the biomarker portfolio studies determined by the Reprogramming the Immune System for the Establishment of Tolerance (RISET) European consortium. For these experiments, the gene expressions of *CD3, FOXP3, MAN1A1, PRF1,* and *TOAG-1* were quantified in blood samples collected before the initiation of weaning from 43 non-tolerant and 25 tolerant patients (Table 9) using an Applied Biosystem real-time PCR platform.

5.2.10 Determination of predictive gene expression signature of rejection

To determine a gene expression signature predictive of rejection before its clinical and laboratory detection, we performed a multivariate logistic regression analysis to identify gene signatures predictive of rejection among the 45 genes analysed by Fluidigm real-time PCR. Initially, we analysed all gene expression data from 44 paired blood samples (collected at baseline and at time of rejection) from 14 HCV-negative and 8 HCV-positive patients plus the 86 comparative samples from stable immunosuppressed liver recipients. The 28-paired collected at baseline and at the time of rejection from the 14 HCV-negative patients were used as training set. The regression algorithm used to build a gene model to predict rejection was defined in the varSelect method of the MMIX Bioconductor package. Following variable selection, a generalized linear model was generated employing the *glm* method in the R statistical pachage (R Foundation for Statistical Computing, Vienna - AT), using the 28-paired samples to classify a given sample into a rejection or non-rejection sample (baseline) group. Internal cross-validation was performed using the boot R package. Given the small number of samples available the analysis was confined to signatures containing up two genes. The best gene model was used to compute the risk probability of rejection in the blood samples collected from the same HCV-negative patients, but at different intervals of time as described in section 5.2.2.1 and in all available blood samples from the remaining patients (HCV-positive

rejecting recipients and Tolerant recipients). When applied to samples from patients not exhibiting clinically apparent rejection, we defined the model as giving “correct” result if the probability of rejection was < 50% and an “incorrect” result if it predicted rejection with > 50% probability.

5.3 Results

5.3.1 Acute cellular rejection presented a very well characterized transcriptional pattern when compared with baseline analysis.

To determine the gene expression profile associated with ACR in the context of immunosuppression withdrawal clinical trial, we initially conducted an unpaired microarray analysis employing all liver samples available from rejecting patients at the baseline and at the rejection time. For this experiment, (28) pre-weaning liver samples were analysed, while only (20) samples at the time of rejection were available for analysis. Nevertheless, for each rejection sample employed, a baseline liver sample from the same patient was available. Using Illumina microarrays platform, we identified 158 differentially expressed genes with a FDR <5% and a FC >1.32. The Heat map plotting the 50 genes with the highest FC showed a clear differentiation pattern between the baseline and the rejection time. Mainly of these genes were associated with pathways related to inflammatory response, interferon signalling, IL-6/JAK/STAT3 signalling and apoptosis (Figure 18 and Table 11). Some of the differentiated genes such as *CXCL9*, *CXCL10*, *UBD*, *STAT1*, *CCL19*, *GBP1*, *GBP2* and *CCL8* are related to the interferon pathway, which is one of the most important pathways associated with acute cell rejection. The secretion of chemokine (C-X-C motif) ligands 9 and 10 (CXCL9 and CXCL10) by different cell types such as monocytes, endothelial cells, and fibroblasts increases with IFNy stimulation. Through their interaction with the CXCR3 receptor found on the on the surface of monocytes, T cells, NK cells, and dendritic cells, both ligands can act as chemokine promoting immune cells attraction, migration, differentiation and activation (291). Both of them have been associated with ACR (147, 292). Other significant expressed genes are *IL32*, *CD2*, *CD83*, *TAP1* and *HLA-F*. Their corresponding encoded proteins are associated with the innate and adaptive immune response. In the presence of a mitogenic stimulus such as IL-2, expression of the IL-32 gene in human lymphocytes and NK cells is stimulated. Cytokine IL-32 can induce immune cells such as monocytes and macrophages to secrete other inflammatory cytokines, such as TNFa, IL-6 and IL-8. (293, 294). Cluster of differentiation 2 (CD2) is a specific cell marker found on the surface of T cells and NK cells, which is involved on the T cell co-stimulation. The engagement of CD2 with its CD28 and CD58 ligands induces the proliferation and differentiation of various T cell subsets such as

Tregs and CD28-CD8+ T cells (295-297). CD83 is an immunoglobulin that can be expressed in its soluble form (sCD83) and in its membrane form (mCD83). sCD83 expression is increased during autoimmune diseases and hematological malignancies. mCD83 is cell surface activator marker that is found in many immune cells, but primarily in the activated dendritic cells. Its inhibition seems to be related with clinical improvement of graft versus host diseases (GVHD)(298). The transporter-associated protein-1 (TAP1) is involved in the antigen presentation by acting in the translocation of antigenic peptides into the endoplasmic reticulum where they are loaded onto major histocompatibility complex I (MHC I) (299). HLA-F, a non-classical MHC molecule, has recently been associated with antigen presentation. It is overexpressed in pregnancy, viral infection and during cancer processes (300).

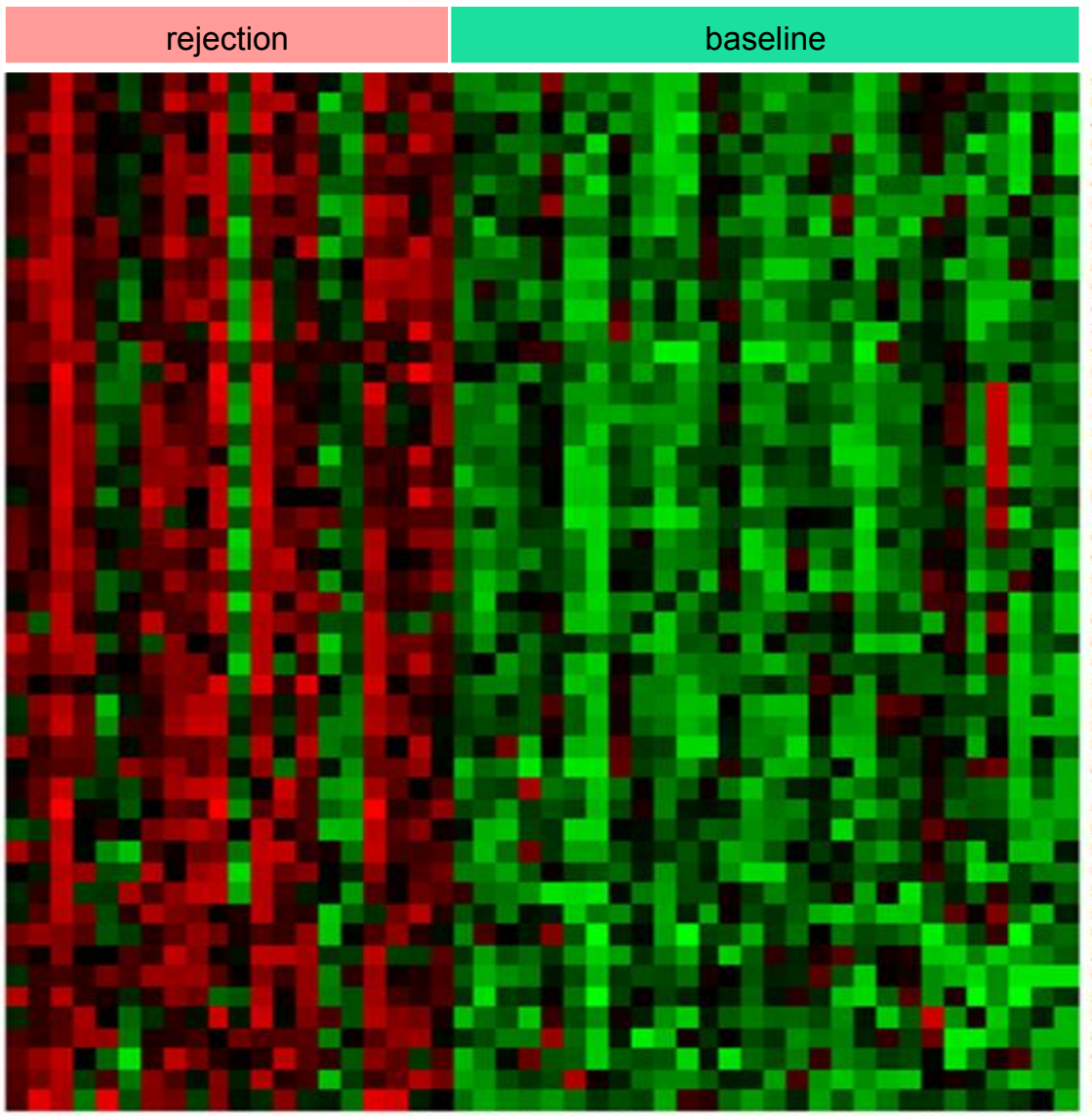

Figure 18: Differentially expressed genes in liver tissue: Heatmap displaying the top 50 genes differentially expressed in liver tissue based on t-statistic comparing unpaired baseline samples (28 samples) with rejection samples (20 samples).

Table 11: Top 50 differentially expressed genes in liver tissue samples at baseline and at rejection time

Gene Symbol	Fold change	Gene Symbol	Fold change
CXCL10	3,32	*HLA-F*	1,57
CXCL9	3,26	*ABCB4*	1,57
UBD	2,68	*CD3D*	1,56
TOP2A	1,97	*UBE2C*	1,56
STAT1	1,95	*MELK*	1,56
GPNMB	1,93	*GBP1*	1,55
STAT1	1,92	*CD2*	1,55
CCL19	1,80	*CXCR4*	1,54
GBP1	1,74	*HLA-H*	1,54
DHRS9	1,72	*BIRC3*	1,54
STAT1	1,70	*NUSAP1*	1,54
TAP1	1,67	*PTTG1*	1,54
LYZ	1,66	*CD83*	1,53
CD8A	1,66	*CCL8*	1,53
IL32	1,65	*HCP5*	1,51
IL18BP	1,63	*IL32*	1,51
IRF1	1,63	*PLA2G7*	1,50
CD52	1,61	*PSMB9*	1,50
CD8A	1,61	*CECR1*	1,50
GPNMB	1,61	*IGSF6*	1,49
HMMR	1,60	*LOC613037*	1,49
APOL3	1,60	*CD3D*	1,49
PLEK	1,60	*CCNB2*	1,49
GBP2	1,59	*CDC20*	1,48
MMP9	1,58	*FCN1*	1,48

5.3.2 Acute cellular rejection was associated with a common transcriptional signature in spite of the presence of underlying liver inflammation

To more accurately identify the transcriptional patterns highly associated with ACR we re-analysed the liver tissue microarray gene expression results employing only the liver tissue paired-samples available for the baseline (pre-weaning) and for the time of rejection. In animal models, concomitant pathogenic infections, particularly viral infections, are associated with the production of pro-inflammatory mediators and / or the direct activation of specific T cell populations (301, 302). In the clinical context, it is difficult to histologically distinguish an episode of ACR from a recurrence of hepatitis C in the post liver transplant period (303). Then, to verify whether a concomitant inflammatory process, hepatitis C in this case, influences the transcriptional rejection profile, liver recipients were grouped according to their HCV RNA status at the time of enrolment in the clinical trials. In this way, 40-paired samples were available from 13 liver recipients RNA HCV-negative and 7 recipients RNA-HCV positive. The influence of rejection was more considerable in HCV-positive recipients, in whom it significantly modified the gene expression profile of 408 genes. In HCV-negative recipients, rejection was associated with statistically significant changes in 34 transcripts. A small set of 19 genes presented an overlapping expression profile being significantly expressed in both groups. (Figure 19 A and B) (Table 12). Most of such genes were already identified as significantly differentiated in the first microarray experiment (Figure 18 and table 11) as *CXCL9*, *CXCL10*, *UBD*, *CD83*, *CD2*, *IL32,* and *TAP1*. In addition, four overlapping genes encode proteins of the major histocompatibility complex: *HLA-DMA*, *HLA-DRA*, *HLA-F*, and *HLA-DQB1*. More recently, the presence of donor specific antibodies (DSA) was associated with the risk of ACR in liver transplantation (11). Unfortunately, we were unable to investigate the possible association between its presence and the rejection episodes observed in the current study, since the measurement of the pre-transplant DSA was not a clinical routine at the time when the patients included in our study were transplanted.

We used the GSEA methodology to explore which functional pathways were more highly associated with ACR episodes. For that, we first compared our liver tissue gene expression profile with the Hallmark gene sets from MSigDB to identify high-level functional pathways. Hallmark pathways are a collection of 50 sets of annotated gene sets, which represent specific biological states or well-defined processes. Differentially expressed genes were involved in a

variety of functional pathways related to, among others, allograft rejection, inflammatory response, interferon signaling, IL-6/JAK/STAT3 signaling, IL2/STAT5 signaling, TNFα signaling, complement and apoptosis. These gene sets had elevated normalized enrichment scores (NSE) and significantly differentiated FDRs according to the GSEA analyses. Hallmark pathways were more over represented in liver tissue transcripts. The GSEA analysis showed that transcripts from liver samples of HCV-pos patients presented a significantly differentiated FDR with 40 of the 50 Hallmark gene sets, while transcripts from liver samples of HCV-neg patients were significantly over represented with 31 Hallmark gene sets. The weakest association was found with the gene expression profile of blood samples, which showed a significant over representation with only 7 gene sets of Hallmark gene sets (Table 13). Next we explored the overrepresentation of our results with pathogenesis-based transcript gene sets, which were previously validated in kidney and heart human allografts (290, 304, 305). Gene expression profiles from liver samples collected at the rejection time showed significant overlap with gene sets associated with T cell-mediated rejection in kidney and heart allografts, with infiltrating macrophages and effector T lymphocytes being the principal cell subsets involved. Although with a weaker signal when compared with T cell-associated transcript gene sets, hepatic ACR also presented enrichment in transcript gene sets related to B cells and donor-specific antibodies (Table 14).

We aimed to confirm the specificity of our rejection gene expression profile results, taking in account the particular characteristics of the ACR episodes analysed in the present study: notable rejection episodes which occurred during intentional immunosuppression withdrawal clinical trials at least three years after the liver transplant, with low Banff scores in the majority of cases, and easily treated with the reintroduction of baseline IS regimens associated or not with a short course of low-moderate doses of corticosteroids. For that, we compared the results from the 13-HCV negative recipients with 9 early post-transplant rejection biopsies all taken from HCV-negative patients within the first 4 weeks after transplantation. The two cohort of recipients differed in the expression of 213 genes, however no differences were noted in the expression of the overlap group of 19 genes, which were associated with rejection over all conditions (Figure 19 C). Furthermore, we applied the GSEA methodology, both groups showed enrichment in similar functional pathways (Table S3 – Appendix C).

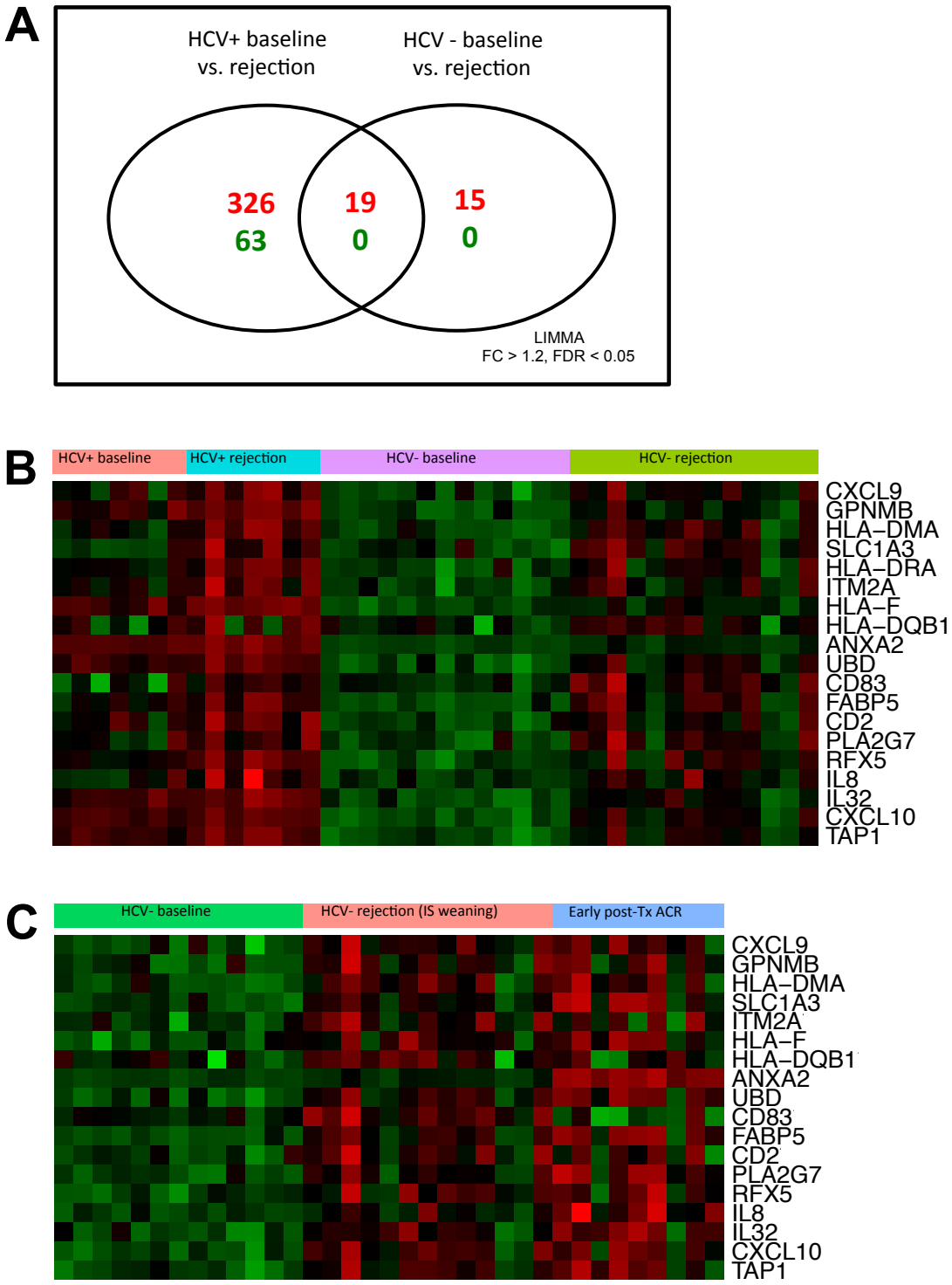

Figure 19: Transcriptional changes associated with rejection in HCV-neg and HCV-pos recipients. (A) Venn diagram displaying the number of up-regulated (red) or down-regulated (green) genes at FDR<5% and FC >1.2 following LIMMA analysis comparing liver tissue samples obtained from HCV (-) and HCV (+) patients at baseline (before IS weaning) and at the time of rejection. **(B)** Heatmap displaying the common set of 19 significantly expressed genes when comparing baseline (pre-weaning) liver tissue samples with those collected at the rejection time in HCV (-) and HCV (+) patients. **(C)** Heatmap showing the 18 genes set in 13 HCV-neg recipients undergoing weaning (at baseline and at rejection time) and in HCV-negative recipients developing rejection shortly after transplantation. HLA-DRA is excluded due to poor data quality in the control group. FC, fold change; FDR, false discovery rate; HCV, hepatitis C virus; IS, immunosuppression.

Table 12: Liver tissue gene expression markers associated with acute cellular rejection

Gene Symbol	Gene Name	Fold-change Rejection versus Pre-wean time HCV-neg. recipients	FDR HCV neg.	Fold-change Rejection versus Pre-wean time HCV-pos. recipients	FDR HCV pos.
CXCL9	Chemokine (C-X-C motif) ligand 9	3.214	0.002	3.241	1.42e-6
GPNMB	Glycoprotein (transmembrane) nmb	1.779	0.006	1.832	0.001
HLA-DMA	Major histocompatibility complex, class II, DM alpha	1.573	0.027	1.764	0.001
SLC1A3	Solute carrier family 1 (glial high affinity glutamate transporter), member 3	1.572	0.027	1.854	0.001
HLA-DRA	Major histocompatibility complex, class II, DR alpha	1.529	0.027	1.734	0.001
ITM2A	Integral membrane protein 2A	1.554	0.027	1.615	0.003
HLA-F	Major histocompatibility complex, class I, F	1.520	0.041	1.605	0.004
HLA-DQB1	Major histocompatibility complex, class II, DQ beta 1	1.615	0.008	1.607	0.005
ANXA2	Annexin A2	1.556	0.032	1.743	0.006
UBD	Ubiquitin D	3.370	0.002	1.678	0.009
CD83	CD83 molecule	1.615	0.008	1.667	0.009
FABP5	Fatty acid binding protein 5 (psoriasis-associated)	2.105	0.002	1.625	0.011
CD2	CD2 molecule	1.480	0.034	1.503	0.013
PLA2G7	Phospholipase A2, group VII	1.631	0.013	1.454	0.022
RFX5	Regulatory factor X, 5 (influences HLA class II expression)	1.419	0.029	1.403	0.026
IL8	Interleukin 8	1.549	0.021	2.194	0.029
IL32	Interleukin 32	1.848	0.006	1.537	0.031
CXCL10	Chemokine (C-X-C motif) ligand 10	3.738	0.002	1.485	0.039
TAP1	Transporter 1, ATP-binding cassette, sub-family B (MDR/TAP)	1.651	0.027	1.363	0.047

Table 11 shows the 19 common differentially expressed genes in HCV-negative and –positive liver recipients when compared liver samples at rejection time with liver samples collected before the start of IS withdrawal. FC > 1.2, FDR <0.05, p<0.001. FC: fold change; FDR: false discovery rate; HCV: hepatitis C virus

Table 13: Functional pathways significantly over represented in liver allograft rejection-associated transcriptional patterns (Hallmark pathways, MSigDB GSEA analysis)

Gene Set	NES[1] HCV-	FDR[2] HCV-	NES HCV+	FDR HCV+	NES Blood	FDR Blood
ALLOGRAFT_REJECTION	2.93	0.00*	2.97	0.00*	1.84	0.02*
INTERFERON_GAMMA_RESPONSE	3.00	0.00*	2.38	0.00*	2.11	0.00*
E2F_TARGETS	2.51	0.00*	2.56	0.00*	1.79	0.02*
INTERFERON_ALPHA_RESPONSE	2.77	0.00*	1.78	0.00*	2.14	0.00*
G2M_CHECKPOINT	2.31	0.00*	2.55	0.00*	1.69	0.03*
IL6_JAK_STAT3_SIGNALING	2.25	0.00*	2.22	0.00*	1.86	0.02*
INFLAMMATORY_RESPONSE	2.49	0.00*	2.24	0.00*	1.56	0.07
TNFA_SIGNALING_VIA_NFKB	2.66	0.00*	2.25	0.00*	1.13	0.39
APOPTOSIS	2.28	0.00*	2.33	0.00*	1.37	0.17
IL2_STAT5_SIGNALING	2.19	0.00*	2.25	0.00*	1.31	0.22
COMPLEMENT	2.08	0.00*	2.09	0.00*	1.26	0.23
EPITHELIAL_MESENCHYMAL_TRANSITION	1.79	0.00*	2.60	0.00*	0.97	0.66
P53_PATHWAY	1.91	0.00*	2.07	0.00*	1.29	0.20
MYC_TARGETS_V1	1.36	0.07	1.62	0.01*	1.75	0.02*
ESTROGEN_RESPONSE_LATE	1.75	0.00*	1.91	0.00*	1.05	0.48
UV_RESPONSE_UP	1.66	0.00*	1.48	0.03*	1.52	0.08
PI3K_AKT_MTOR_SIGNALING	1.60	0.01*	1.66	0.01*	1.30	0.21
APICAL_JUNCTION	1.64	0.01*	1.86	0.00*	0.89	0.73
MTORC1_SIGNALING	1.72	0.00*	1.65	0.01*	0.96	0.66
KRAS_SIGNALING_UP	2.28	0.00*	2.48	0.00*	-0.80	1.00
ADIPOGENESIS	1.21	0.21	1.16	0.23	1.38	0.17
PEROXISOME	1.30	0.11	1.27	0.13	1.08	0.46
DNA_REPAIR	1.12	0.34	1.54	0.02*	0.73	0.91
SPERMATOGENESIS	0.91	0.66	1.31	0.10	1.07	0.48
NOTCH_SIGNALING	0.95	0.62	1.46	0.03*	0.81	0.84
MITOTIC_SPINDLE	1.87	0.00*	2.00	0.00*	-0.83	1.00
TGF_BETA_SIGNALING	0.92	0.66	1.18	0.21	0.93	0.67
MYC_TARGETS_V2	0.88	0.71	1.19	0.21	0.94	0.67
ANGIOGENESIS	1.83	0.00*	2.23	0.00*	-1.26	1.00
HYPOXIA	1.56	0.01*	1.71	0.00*	-0.73	1.00
GLYCOLYSIS	1.60	0.01*	1.80	0.00*	-0.86	1.00
MYOGENESIS	1.69	0.00*	1.41	0.04*	-0.60	0.98
ESTROGEN_RESPONSE_EARLY	1.55	0.01*	1.80	0.00*	-0.88	1.00
HEDGEHOG_SIGNALING	1.50	0.02*	1.45	0.04*	-0.73	1.00
PROTEIN_SECRETION	1.39	0.06	1.64	0.01*	-0.88	1.00
UNFOLDED_PROTEIN_RESPONSE	1.42	0.04*	1.49	0.03*	-0.78	1.00
COAGULATION	1.45	0.03*	1.59	0.01*	-0.98	1.00
ANDROGEN_RESPONSE	1.10	0.36	1.50	0.03*	-0.64	1.00
UV_RESPONSE_DN	1.47	0.03*	1.60	0.01*	-1.12	1.00
REACTIVE_OXIGEN_SPECIES_PATHWAY	1.64	0.01*	0.99	0.50	-0.84	1.00
HEME_METABOLISM	1.48	0.03*	1.19	0.21	-1.19	0.95
WNT_BETA_CATENIN_SIGNALING	1.09	0.37	1.42	0.04*	-1.05	1.00
APICAL_SURFACE	0.97	0.59	1.61	0.01*	-1.23	1.00
PANCREAS_BETA_CELLS	-1.13	0.43	0.83	0.77	1.36	0.17
KRAS_SIGNALING_DN	1.10	0.35	0.90	0.66	-1.33	1.00
CHOLESTEROL_HOMEOSTASIS	1.30	0.11	-1.61	0.04*	0.82	0.84
XENOBIOTIC_METABOLISM	0.81	0.82	-1.55	0.03*	1.22	0.26
OXIDATIVE_PHOSPHORYLATION	-1.04	0.50	-1.25	0.10	1.50	0.08
FATTY_ACID_METABOLISM	-0.83	0.84	-1.41	0.04*	1.25	0.22
BILE_ACID_METABOLISM	-1.31	0.25	-1.50	0.03*	-0.92	1.00

[1] Normalised Enrichment Score, as generated by GSEA software
[2] False Discovery Rate

Table 14: Pathogenesis-based transcript sets significantly enriched in liver allograft rejection associated transcriptional patterns (GSEA)

Symbol	Description	Ref	SIZE[1]	NES[2] HCV-	FDR[3] HCV-	NES HCV+	FDR HCV+
GRIT1	Human orthologs of IFN-gamma dependent, rejection associated transcripts defined in mice. Expressed in TCMR, especially in association with AMAT1.	(306)	19	2.64	0.00*	2.42	0.00*
QCMAT	Macrophage associated transcripts defined in purified cell lines, associated with TCMR in kidney patients.:	(307)	45	2.54	0.00*	2.34	0.00*
QCAT	Transcripts associated with cytotoxic T lymphocytes, defined in purified cell lines. Associated with TCMR in renal transplants, with expression levels correlating with T cell infiltration.	(304)	21	2.48	0.00*	2.44	0.00*
IRITD3	Injury and rejection induced transcripts up regulated day 3 post isograft transplant (humanised results from mouse model).	(308)	173	2.30	0.00*	2.60	0.00*
IRITD5	As for IRITD3, measured on day 5.	(308)	133	2.25	0.00*	2.68	0.00*
CIRIT	Cardiac injury and repair induced transcripts, expressed following heart isograft transplant. Mouse data extrapolated to humans.	(309)	174	2.20	0.00*	2.22	0.00*
IRRAT	Injury-repair response associated transcripts, defined in early renal transplants with *no* rejection, and derived as a model for AKI.	(308)	22	2.05	0.00*	1.67	0.00*
BAT	B-cell associated transcripts, derived from purified B cells. Up regulated in both ABMR and TCMR.	(310)	55	1.97	0.00*	2.15	0.00*
DSAST	DSA Positive specific transcripts derived from comparative analysis of DSA + and – renal biopsies. Observed in both ABMR and TCMR with much higher levels in ABMR.	(311)	15	1.64	0.01*	1.18	0.29
HTS	Heart selective transcripts derived from control mice without inflammation present.	(309)	385	1.54	0.03*	1.59	0.01*
TCB	T cell specific transcripts based on purified cell lines.	(312)	4	1.47	0.04*	1.66	0.00*
ENDAT	Endothelial cell associated transcripts derived from purified cell lines. Increased in ABMR and TCMR with higher levels in ABMR.	(313, 314)	81	1.46	0.04*	2.23	0.00*
NKB	NK cell specific transcripts derived from purified cell lines. Identified in early TCMR and late ABMR in renal patients.	(312)	3	1.43	0.05	1.04	0.43
IGT	Immunoglobulin associated transcripts, observed in both ABMR and TCMR.	(310)	4	1.36	0.08	1.57	0.01*
AMAT1	Alternative Macrophage Associated Transcripts 1. Human orthologs of mouse data. High GRIT1+AMAT1 scores correlate with TCMR.	(307)	6	1.31	0.12	1.73	0.00*
MCAT	Mast cell associated transcripts, associated with scarring and poor survival in renal transplants.	(305)	3	-0.80	0.78	1.13	0.32

ABMR, antibody-mediated rejection; AKI, acute lidney injury; DSA, donor-specific antibody; FDR, false discovery rate; GSEA, gene set enrichment analysis; IFNγ, interferon gamma; NES, normalized enrichment score; TCMR, T cell-mediated rejection. *Significance threshold based on FDR < 0.05 n gamma;

[1] Size is the number of transcripts in gene set.

[2] NES – Normalized Enrichment Score as calculated by GSEA software (http://www.broadinstitute.org/gsea/doc/GSEAUserGuideTEXT.htm#_interpreting_GSEA_results)

5.3.3 Histological features of acute cellular rejection correlate with specific gene expression changes

Liver ACR is characterized by portal and, sometimes, lobular inflammation, portal tract nonsuppurative cholangiolitis and portal and/or central vein sub-endothelial inflammation. To identify the main histological drivers of transcriptional patterns associated with ACR, we correlated liver tissue gene expression profiles with quantified histological data. In the cohort of samples studied, the distribution of histological damage and the number of genes for which expression was significantly differentiated correlated with severity of damage (FC > 1.2, FDR < 0.05) (Table 15). There was a correlation between the magnitude of histological damage in each histological compartment and expression of a set of 423 genes mostly associated with inflammation and rejection. The genes expressed were relatively homogenous across histological compartments; however, the signal was much stronger in acute inflammatory processes such as lobular inflammation, portal inflammation and interface hepatitis (Figure 20) (Table S4 - Appendix C).

We applied the GSEA methodology to check which functional pathways could drive these pathological processes, and, once more, results disclosed homogeneity over histological compartments with inflammatory and rejection-associated pathways being up-regulated across all compartments (with exception of ductopenia, which was a very rare event and thus could not be appropriately accessed) (Table 5S - Appendix C). The overall severity of rejection as defined by the Banff Rejection Activity Index (55) was not associated with significant differential gene expression profiles originated from the 20 biopsies with complete rejection activity index (data not shown).

Table 15: Differential gene expression by histological compartment

Histological compartment	Number of patients by severity level				Gene count
	0	1	2	3	
Lobular inflammation	29	34	15	0	354
Portal inflammation	17	33	21	2	223
Interface hepatitis	44	23	10	0	284
Portal fibrosis	29	24	21	2	31
Bile duct lesions	51	19	3	1	16
Central vein perivenulitis	53	12	4	0	10
Endothelitis portal veins	54	16	3	1	4
Ductopenia	76	3	0	0	4
Endothelitis central vein	70	3	0	0	1
Ductular reaction	50	20	0	0	0
Perisinusoildal fibrosis	52	8	5	0	0

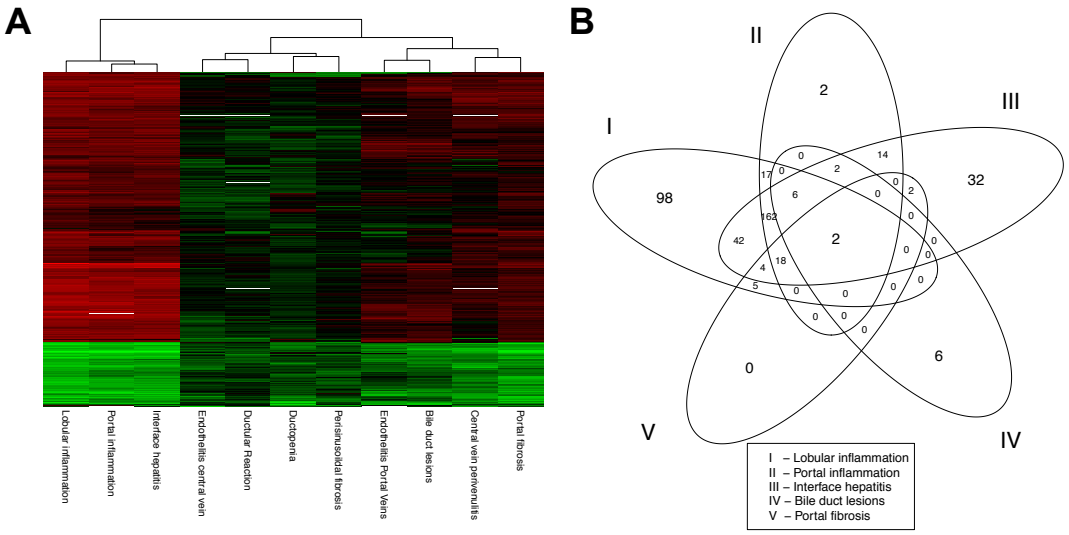

Figure 20: Differentially expressed genes across histological compartments. (A) Clustered heat map demonstrating all genes significantly differentially expressed across histological compartments (fold change > 1.2 and false discovery rate <0.05 in at least one compartment). Analysis performed in *limma* comparing gene expression against quantified severity score for each histological parameter (Red indicates up-regulation and green indicates down regulation). **(B)** Venn diagram representing the number of genes differentially expressed in each histological compartment and demonstrating overlap between compartments1

5.3.4 Acute cellular rejection also presented distinct transcription changes in blood samples, although with only partial overlapping with those observed in liver allograft

To determine ACR-associated transcriptional patterns in whole blood compartment, we employed the same exploratory strategy described for liver tissue experiments. However in this case, analyses were conducted using a custom Agilent microarray to analyse 74 paired baseline/rejection samples from 37 HCV-negative patients. We identified 293 differentiated genes using the same statistical thresholds (FC > 1.2 and FDR < 0.05) employed in the liver tissue experiment (Figure 21).

In functional analysis employing GSEA methodology with the MSigDB Hallmark gene sets displayed comparable up-regulated pathways in blood and liver tissue, however with weaker signals for the blood than liver tissue results (Table 13). Further analyses employing HaemAtlas gene sets (289) unveiled the significant association of ACR with transcripts preferentially expressed by CD14-positive cells (monocytes). In contrast, transcripts associated with CD8 (cytotoxic cells) and CD66B (granulocytes) cells were significantly down regulated at the time of rejection. Within the analysed samples, no other blood cell types showed significant contribution to the rejection-associated transcriptional pattern. When we compared transcriptional patterns across the two compartments, a reduced group of 22 genes, mainly associated to immune response and cell cycle control (e.g. *CXCL9, CXCL10, CNPM, CDC20, CCNB2, and CD74*), were significantly associated with ACR in blood and liver tissue samples This small group of overlapping genes within the two compartments could also be attributed to the fact that there are proportionately less inflammatory cells in a liver biopsy sample than in the blood, which is essentially composed of inflammatory cells, while hepatocytes are the main population cell found in a liver biopsy (Figure 22).

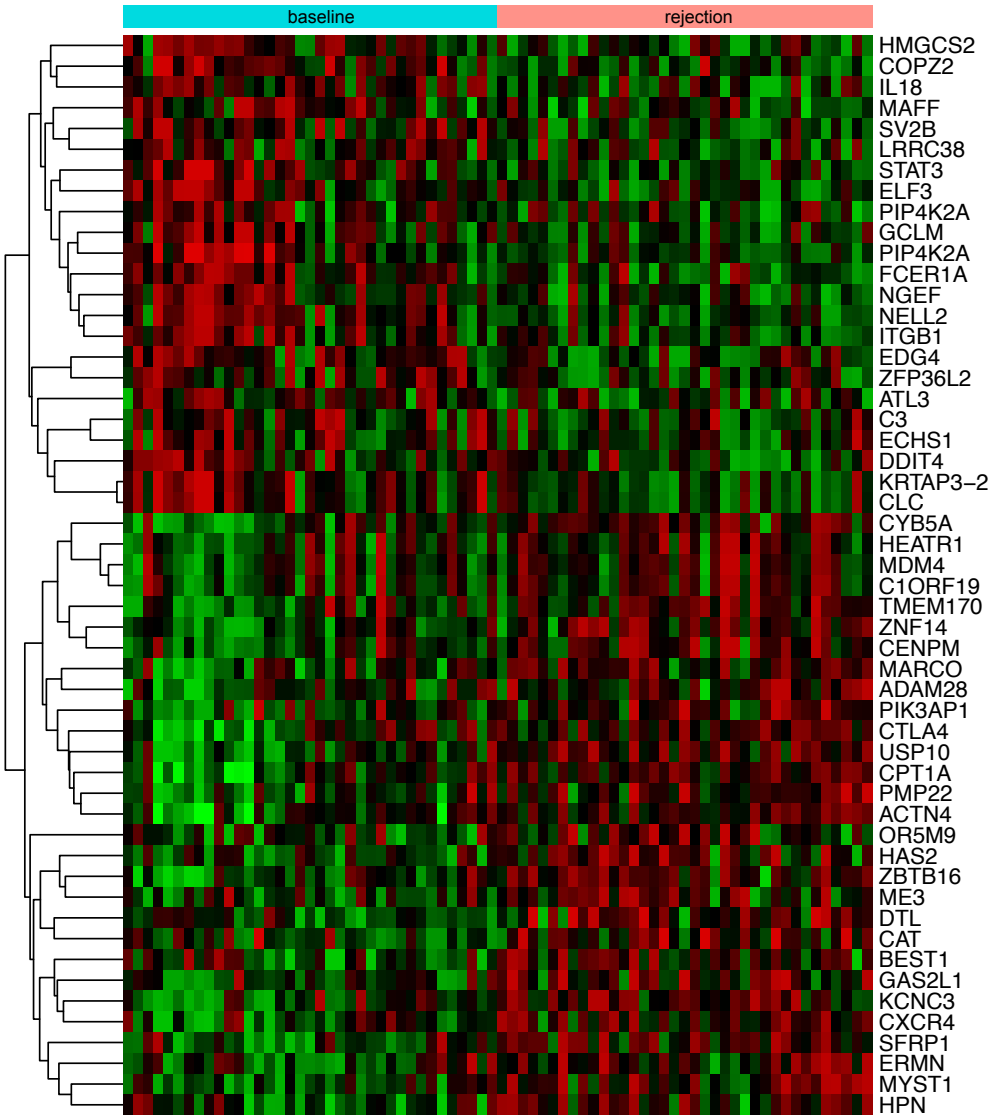

Figure 21: Differentially expressed genes in whole blood. Heat map of top 50. Genes differentially expressed in whole blood based in t-statistic comparing paired baseline (pre-weaning) and rejection samples. All liver samples in this experiment were from HCV-negative liver recipients

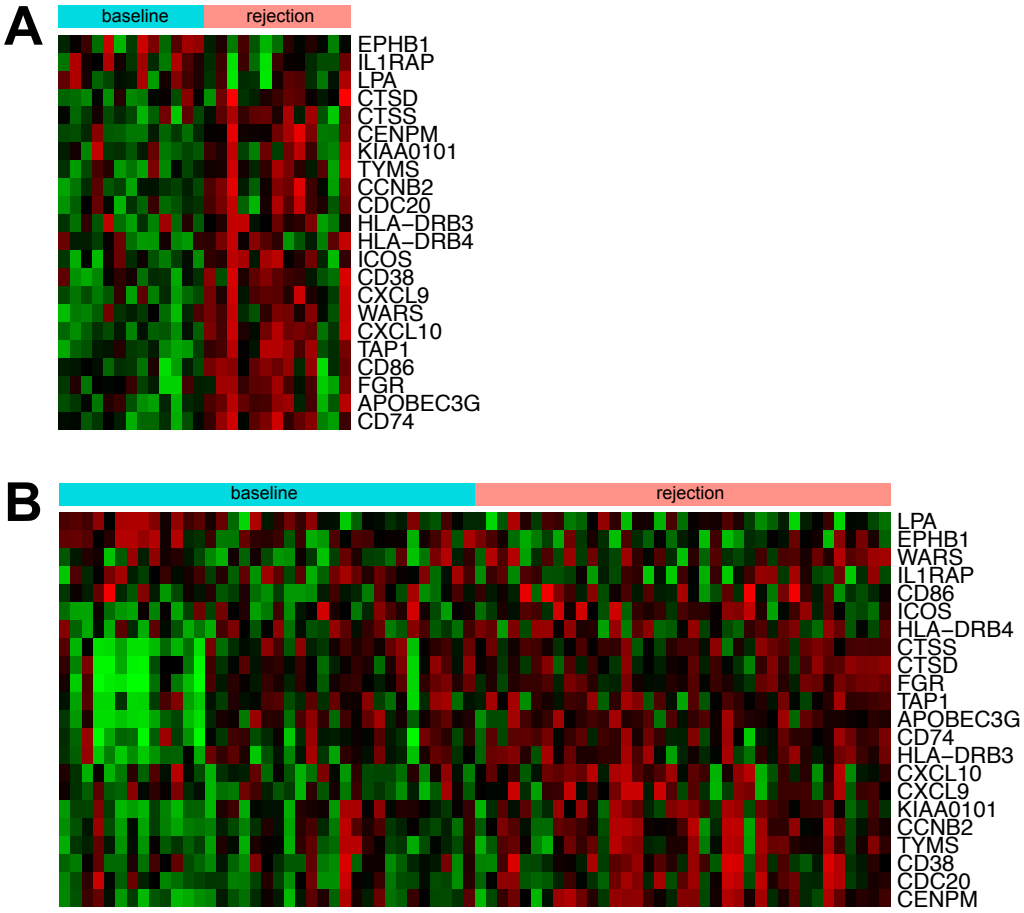

Figure 22: Significantly expressed genes in liver tissues and in PBMC of HCV-negative liver recipients. Heat maps displaying the common set of 22 significantly expressed genes when comparing baseline (pre-weaning) liver tissues samples **(A)** with those collected at the time of rejection in HCV-negative liver recipients, and in PBMC samples **(B)** in the same time points for the same patient group.

5.3.5 The blood transcriptional patterns of ACR-associated genes at baseline did not predict the success of immunosuppression weaning

To interrogate whether ACR-specific genes were differentially expressed between tolerant and rejecting liver recipients before the initiation of IS weaning protocol, we revisited a previously reported Affymetrix® microarray gene expression database generated with blood samples collected at the baseline from 43 rejecting and 25 tolerant liver recipients**.** Before starting the IS discontinuation, none of the ACR-associated gene expression markers showed significant differentiated transcription patterns between recipients who would eventually reject and those who would successfully discontinue IS drugs (data not shown). In addition to this reanalysis, we quantified the expression of *CD3*, *FOXP3*, *MAN1A*, *PRF1*, and *TOAG-1*, which made part of the RISET consortium biomarker portfolio and had been previously evaluated in the setting of kidney transplantation (123, 315). From all genes tested, *FOXP3* expression, which was up regulated in tolerant recipients, was the only marker differentially expressed between tolerant and rejecting liver recipients at baseline blood samples (Figure 23).

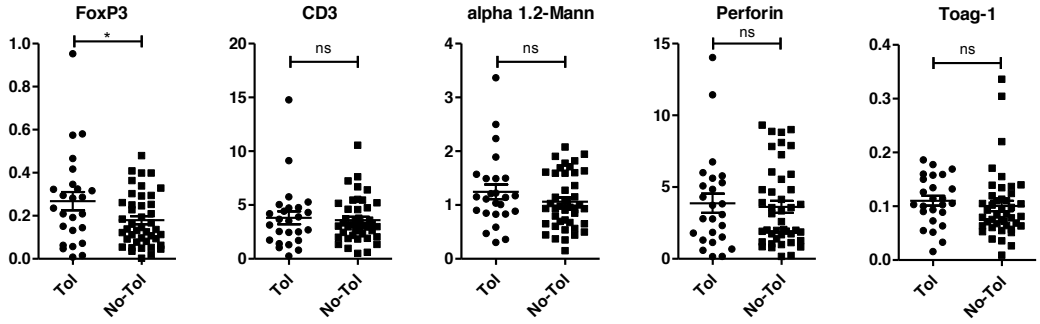

Figure 23: Baseline acute cellular rejection-associated gene expression in rejecting and tolerant liver recipients. Graphics showing the quantitative gene expression in blood samples of five genes included in the Reprogramming the Immune System for the Establishment of Tolerance (RISET) consortium biomarker portfolio performed at baseline (pre-weaning) in 43 tolerant and 25 rejecting liver recipients. Tol, tolerant; Rej, rejecting liver recipients. *p <0.05. Due to the small group of genes analysed, statistics calculation was performed without correction for multiple comparisons.

5.3.6 Immunosuppressive drug regimens presented a minimal effect on ACR-associated gene expression profiles in both blood and liver tissue samples

We interrogated at which level the type of immunosuppression at the time of enrolment could impact the gene expression profiles on liver tissue and blood samples from our rejecting liver recipients. A linear regression model was applied to analyse the gene expression patterns on three microarrays datasets available (microarray liver tissue, microarray blood samples and Fluidigm blood qPCR results). Our results show that the type of immunosuppressive regimen did not impact liver tissue gene expression profiles at baseline. Furthermore, analyses of blood transcriptional profiles disclose no differences between patients on CSA monotherapy against TAC monotherapy. Conversely, a set of 17 genes was differentially expressed between patients on CNI inhibitor monotherapy and patients on MMF (Table 15), but only 8 out from the 17 genes were included in the set 293 genes associated with ACR (*LOC652494*, *ENST00000359488*, *LOC100132941*, *ENST00000377226*, *C13ORF33*, *A_24_P110487*, *ENST00000322032*, and *SPTA1*).

Table 16: Differential gene expression by baseline immunosuppression

	Tissue		Blood (microarray)		Blood (Fluidigm)	
Immunosuppression	**n**	**Genes expressed**	**N**	**Genes expressed**	**n**	**Genes expressed**
TAC	18	0	29	0	12	0
CSA	14		23		11	
CNI monotherapy	32	0	52	17	23	N/A
MMF monotherapy	6		12		0	
CNI monotherapy	32	0	52	1	23	3
CNI + MMF	6		8		6	
mTOR inhibitor	2	13	0	N/A	2	3
Other therapies	44		72		29	

CNI, calcineurin inhibitor; CSA, Cyclosporin A; MMF, mycophenolate mofetil; mTOR, mammalian target of rapamycin, NA, not available; TAC, tacrolimus.

5.3.7 Sequential gene expression profiling in blood samples collected over the immunosuppression withdrawal period predicts the occurrence of rejection

Aiming to identify specific changes in rejection-associated transcriptional markers occurring over the IS weaning period and preceding the clinical and histological diagnosis of the eventual episodes of ACR, which could be used as predictive gene signature of rejection, we quantified the expression of the target set of 45 genes described in section 5.2.9.1 in sequential blood samples collected from 14 HCV-negative and 8 HCV-positive rejecting liver recipients. In average, six sequential blood samples collected before the diagnosis of rejection were available per liver recipient. Initially, univariate analysis of gene expression profiles from samples collected at baseline and at time of rejection unveiled that eight and two genes were significantly up regulated at the time of rejection in HCV-negative and –positive liver recipients (Table 17). Next, a stepwise multivariate logistic regression analysis identified *CXCL10* and *FOXP3* as the best combination of markers, which discriminated rejection and baseline samples in the cohort of HCV-negative liver recipients (cross validated area under de curve [AUC] 0.82). Applying this gene signature in all sequentially collected blood samples showed that the probability of ACR continuously increased over time, with a peak that coincided with the time of the diagnosis of biopsy-proven ACR and showed a rapid decline after reintroduction of immunosuppression treatment (Figure 24A). We used the cohort of 86 liver recipients with stable graft function 3-10 years after transplantation under immunosuppression as a negative control group; *CXCL10* plus *FOXP3* expression correctly predicted the absence of rejection in 81% of the liver recipients. Surprisingly, this model failed to accurately classify 70% of 57 blood samples sequentially collected from 7 tolerant liver recipients who successfully discontinued the immunosuppression in the clinical trials. Taking in account the well-described influence of CNIs on *FOPX3* expression, we excluded the *FOXP3* in second analysis made only with *CXL10* as gene signature (316) (Figure 24B). This strategy proved that *CXCL10* was the most powerful gene signature to predict rejection and non-rejection samples in HCV-negative liver recipients. *CXCL10* alone precisely categorized rejecting samples with a cross-validated AUC of 0.76 and accurately predicted absence of rejection in 79% of stable liver recipients and 67% of samples from tolerant recipients (Figure 24C). The probability of rejection as predicted by expression of *CXCL10* increased 1-2 months before the rejection episode was clinically suspected and a liver biopsy was considered indicated according to the protocol

criteria. However, a detailed analysis of the evolution of the hepatic function tests measured in the same blood samples used for the molecular analyses showed that changes in CXCL10 expression began to increase approximately two weeks before the start of the increase in serum LFT levels in liver receptors that presented an ACR episode approximately two months later (Figure 24D). Opposite to these described findings for HCV-negative liver recipients, an ACR predictive molecular signature with accurate diagnostic interpretation could not be created from the same 45-gene Fluigdim data set in the in the cohort of eight HCV-positive liver recipients (data not shown).

Table 17: Significantly differentially expressed genes at baseline versus rejection based on univariate analysis of Fluidigm data

Gene	p-value (HCV-negative)	p-value (HCV-positive)
ABCB1	0.441	**0.048***
APOL3	0.383	0.942
CCL19	0.570	0.369
CCN2B	0.053	0.799
CD52	0.083	0.144
CD74	0.567	0.742
CD8A	0.587	**0.011***
CDC20	0.777	0.559
CECR1	0.141	0.911
CENPM	0.634	0.505
CXCL10	**0.019***	0.794
CXCL9	**0.010***	0.809
DHRS9	**0.046***	0.933
DOCK11	0.412	0.511
EMILIN2	0.096	0.604
EZH2	0.329	0.263
FOXP3	**0.002***	0.321
GBP1	0.689	0.078
GBP2	0.680	0.610
GPNMB	0.856	0.233
GZMB	0.149	0.234
GZMK	0.518	0.053
HLA.DMA	0.718	0.927
HLA.DMB	0.935	0.624
HMMR	0.935	0.254
IL15	0.335	0.436
IL18BP	0.592	0.761
IL32	0.586	0.136
IRF1	0.084	0.532
LYZ	0.062	0.952
ME2	0.327	0.554
MMP9	0.836	0.366
PARVG	0.353	0.354
PLEKHG1	0.788	0.873
PRF1	0.670	0.068
RFX5	0.604	0.731
STAT1	**0.024***	0.839
TAP1	0.154	0.937
TGFb1	0.166	0.098
TK1	**0.019***	0.608
TLR8	0.978	0.748
TOP2A	0.203	0.572
TYMS	**0.013***	0.720
UBD	**0.002***	0.209
ZWINT	0.144	0.368

HCV, Hepatitis C virus.
*Significant difference between baseline and rejection ($p < 0.05$)

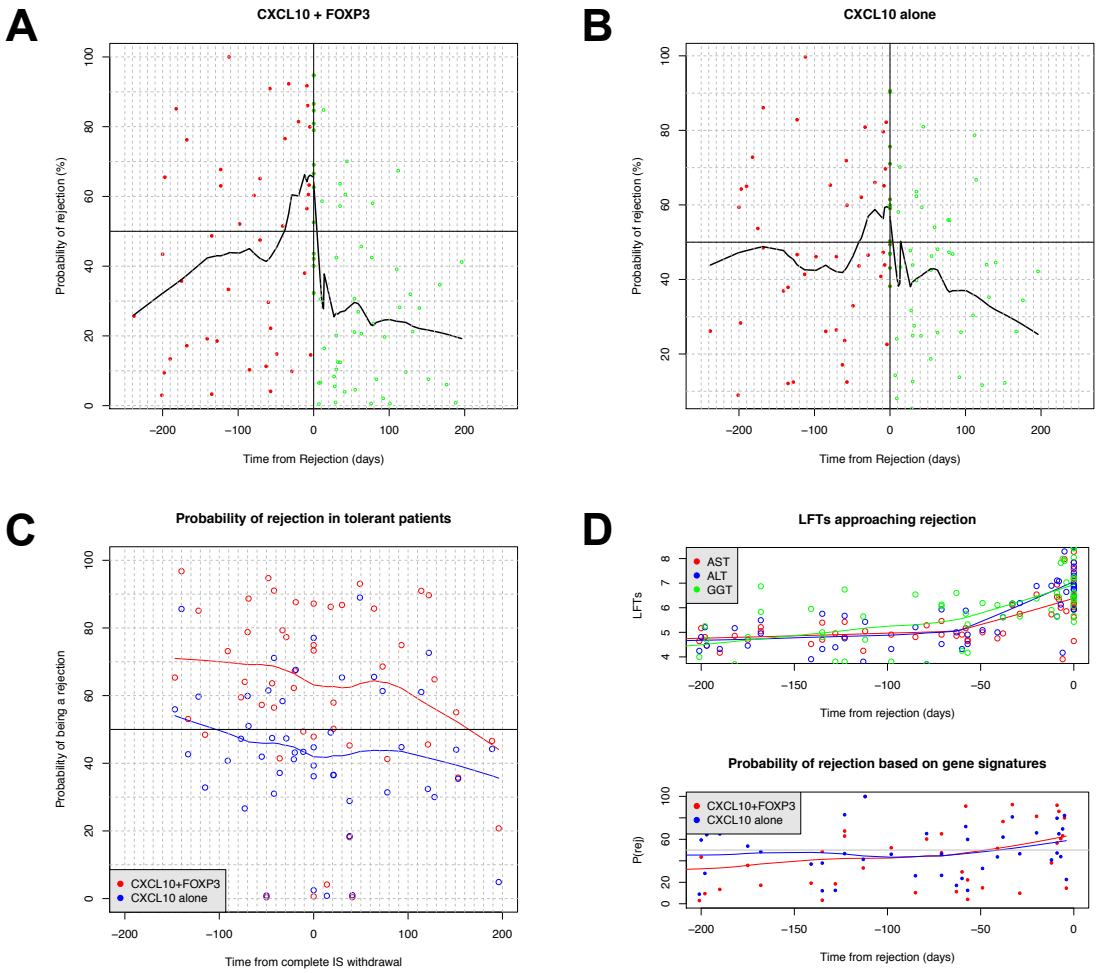

Figure 24: Prediction of rejection by sequential gene expression in blood samples: (A and B) Time evolution of risk probabilities for rejection based on gene signatures for *CXCL10* plus *FOXP3 and CXCL10 a*lone, respectively. Both models show a peak coinciding with acute cellular rejection biopsy-proven diagnosis (time 0), with a rapid reduction following reinstitution of reinforcement of IS. **(C)** Evolution of risk probabilities in operationally tolerant recipients up to and after complete withdrawal of IS (time 0), showing that *CXCL10* plus *FOXP3*, but not *CXCL10* alone, misclassifies as rejecting 70%of blood samples. **(D)** Sequential risk probabilities based on gene signature models alongside conventional LFTs. Risk increases gradually ≈1-2 months before rejection, correlating with a rise in LFTs. IS, immunosuppression; LFT, liver function test. AST, aspartate aminotransferase; ALT, alanine aminotransferase; GGT, gamma-glutamyl transpeptidase.

Chapter 6 Discussion

This research work was triggered by the results of a recently published European multi-centre clinical trial of immunosuppression withdrawal in long-term post-liver transplantation recipients. This study demonstrated that liver recipients who developed a rejection episode during the withdrawal protocol displayed lower iron storage markers (e.g. serum ferritin and serum and intra-hepatic hepcidin) than liver recipients who successfully finished the IS withdrawal becoming operationally tolerant recipients, the primary end-point of the study. These alterations were reproducible and statistically significant even though they were not clinically evident. Furthermore, those rejection episodes occurred at least three years after the transplant procedure; when clinical and biochemistry changes attributed to the baseline liver disease, inflammatory response to the ischemic/reperfusion injury and to the surgical procedure and/or early complications were not present. Rejection episodes were well controlled and unable to provoke a graft loss in any rejecting patient (1, 100). We postulated that this clinical scenario could be an adequate opportunity for the molecular characterisation of the acute cellular rejection process.

Using a very well known immune-mediated experimental model of acute liver failure we checked the influence of small iron changes on the intra-hepatic T cell activation and function. Afterwards, we aimed to check the impact of iron changes on the specific anti-donor T cell response employing a full-vascularized rat experimental liver transplant model. Furthermore, taking advantage of the availability of the sequential blood and liver tissue samples collected during the weaning protocol from rejecting patients, we investigated if progressive transcriptional changes could forecast over time the ACR before clinical, biochemistry, and histological manifestations of the rejection episodes.

6.1 Effects of Iron deficiency in the Intra-hepatic lymphocyte responses

As spontaneous liver tolerance requires an initial activation of recipient alloreactive T cells before lymphocyte deletion (60, 251, 252), we hypothesized that the iron-hepcidin axis could exert an unrecognized place in the regulation of intra-hepatic lymphocyte activation and function. To investigate this concept, we replicated the mild iron homeostasis changes detected in the liver recipients included in the clinical trial by administering iron-modified diets to mice for a short period of three weeks or by the administration of low-dose iron specific chelators. While

it is challenging to define the ideal level of iron deficiency due to the many factors to be controlled, the iron deficiency induced by our iron-modified diet protocol was comparable with other studies addressing the influence of iron levels on the acute inflammatory responses (234). Furthermore, our three-week iron-modified regimens did not significantly affect the animal outcomes, their liver function tests, and the hepatic steady-state immune cell population. In order to challenge the liver immune homeostasis, we employed a well-known experimental model of immune-mediated acute sub lethal hepatitis induced by ConA. A close interaction between Kupffer cells, lymphocytes and cytokine production regulates the ConA model, where the intra-hepatic T/NKT cell activation is necessary to trigger the inflammatory liver injury (261, 262, 269). Then, in our experiments, the intensity of the liver injury provoked by the ConA challenge was significantly reduced in iron deficient fed mice, which was determined by decreased serum ALT levels, hepatic necrosis and intra-hepatic cellular infiltration on histologic evaluation. These findings were associated with reduced serum levels of IL-6, TNFα and IFNγ (pro-inflammatory cytokines) and with an increase in intra-hepatic transcript levels of *Il4* and *Tnfα*, all of which are implicated in ConA immune-mediated acute liver failure (262). Other studies, using different models of acute hepatitis as the thioacetamide-induced toxic hepatitis and Fas-induced fulminant hepatitis also reported a favourable effect of iron restriction induced by diet or iron chelation on liver inflammation (216, 217). The possible beneficial anti-inflammatory effects caused by iron restriction in those studies were credited to a reduced oxidative stress and less Kupffer and hepatic cell activation. Oxidative stress and macrophage activation are manifestly implicated in the amplification of the ConA induced liver injury in our experiments. However, our observations of less T/NKT lymphocyte infiltration in intra-hepatic histologic analyses from iron deficient mice suggest that reduced lymphocyte activation and effector function in this animal group could also influence the outcome of the immune-mediated hepatitis by a direct inhibition of intra-hepatic lymphocyte function. We confirmed this hypothesis performing an *in vitro* experiment in which isolated T cells were challenged with either ConA or anti-CD3/anti-cd28 associated with iron chelation, which resulted in impaired T cell activation and proliferation.

Again, our findings suggesting that lymphocyte activation and proliferation due to iron homeostasis modification can modulate the inflammatory hepatic injury are in agreement with the results observed in an experimental $CD4^+$-driven model of autoimmune encephalomyelitis, where iron deficiency inhibits the neurological damage evolution (219). The possible

mechanisms responsible for this T cell inhibition are not yet completely revealed. Intracellular iron deficiency can decrease the activity of various enzymes implicated in the cell-cycle control such as ribonuclease reductase involved in DNA synthesis during the phase S of cell cycle, cyclin A, and Cdc2 (317, 318). Other proteins essentials for the intracellular signalling cascade triggered by T cell activation can also be inhibited by iron restriction as the hydrolysis of phosphatidyl inositol-4,5-biphosphate and the activity of protein kinase C (232, 233). Furthermore, at least in the central nervous system, CXCL10 release following the engagement of the Toll-like receptor 3 (TLR3) is inhibited by desferrioxamine, which can decrease the tissue infiltration by $CXCR3^+$ T cells (319).

Using a systemic inflammatory model induced by LPS which also induces liver damage, Pagani et al. and Di Domenico et al. were able to demonstrate that hepcidin directly inhibited inflammatory responses after LPS challenge independent from iron levels (234, 235). In this way, we investigated whether low hepcidin levels impact the influence of iron levels on the ConA-mediated immune hepatitis. In agreement with the previous reports, iron limitation led to a decrease in hepatocyte hepcidin expression, and this figure persists after ConA challenge (data not shown). Trying to dissect the role of hepcidin on the ConA immune mediated hepatitis, mice fed with normal iron diet were treated with an iron-specific chelator that does not influence hepatocyte hepcidin expression before the ConA challenge. Iron chelation pre-treatment reproduced the results observed when an iron deficient diet was employed. In the next experiment mice fed with iron-modified diets received one injection of exogenous hepcidin prior to ConA challenge. On the contrary with what was previously reported in the LPS model, exogenous hepcidin did not influence the effect of iron deficiency in our model of immune-mediated hepatitis induced by ConA. Altogether, those series of experiments allow us to conclude that in our model, low iron levels are the main determinant factor for the reduced liver inflammatory injury in iron deficient mice after ConA administration. Taking in account the effector role executed by macrophages in ConA immune mediated hepatitis and the hepatotrophic characteristics of ConA action, our findings seem to be in contrast with observations reported in the two previous mentioned studies, where LPS challenge exacerbated the pro-inflammatory mediators release by iron-deprived macrophages (234, 235). Although those observations need further investigation, as Wang et al found contradictory results using the LPS model (237); they point to a complex immunological regulation elicited by iron deficiency with different outcomes depending on which cell is targeted and which organ is

involved in the inflammatory response. Consequently, we theorized that effective T cell activation is required in the ConA model to induce immune mediated liver damage, different from that which is observed in the systemic inflammation model caused by LPS administration, which could influence the different outcomes demonstrated by the two models in the presence of iron deficiency.

Changes in dietary iron concentrations influence the gut microbiota constitution, which in turn may influence liver metabolism and immunogenicity (271). In order to check the impact of gut microbiota modifications in our model we administered an antibiotic cocktail well known for the reduction of more than 90% of the faecal microbial populations (265). Iron deficient mice treated with the cocktail still presented a significantly reduced immune mediated liver injury after ConA challenge. Furthermore, worth highlighting is the fact that those antibiotic treated mice presented lower transaminase levels following ConA injection when compared to non-treated mice. This result was especially evident in iron deficient mice, in which transaminases elevation was almost completely abolished. These findings are in accordance with a study reported by Chen et al., which showed that depletion of gram-negative gut derived bacteria induced by gentamycin treatment decreased the ConA-induced liver damage. This effect was mediated by intestinal dendritic cell function impairment and by changes in intra-hepatic NKT cells activation (320). While our preliminary results do not allow us to draw deeper conclusions about the influence of the intestinal microbiome on the allograft immune response, it is worth noting that several recent studies have addressed how the intestinal microbiome can influence the efficacy of immunotherapy against malignant tumours (321, 322). In fact, the intestinal microbiome composition can influence the efficacy of the immune checkpoint inhibitors targeting the co-signalling PD1/PDL1 axis to treat cancers (323, 324). Patients having an abnormal gut microbiome composition, as e.g. after having an antibiotic treatment during their cancer immunotherapy, were resistant against PD1/PDL1 inhibitors (325). As for the continuation of our preliminary experiments, additional studies are being carried out in the laboratory of Prof. Sanchez-Fueyo with the aim of verifying the influence of the intestinal microbiome on the liver steady state immune cell repertoire.

Iron deficient mice showed decreased serum IL-6 levels after ConA challenge; on the other hand *Il6* intra-hepatic expression was increased. These findings are consistent with the different kinetic profiles of the expression of IL-6 (cytokine) and the expression of *Il6* (gene) after an acute liver injury previously described by Sass el al. Indeed, serum levels of IL-6 reach a

maximum at 3-4 after the ConA challenge with the subsequent decrease to their lowest levels at 12 and 24 hours. Although the increase in the expression of the Il6 gene is not as intense, it reaches a maximum at 1 or 2 hours after ConA and shows a plateau effect during the next 10 hours, when it has a second peak approximately 12 hours after the challenge ConA (269). The literature usually reported the IL-6 as a pro-inflammatory cytokine, however our clear outcome of transaminases in the ConA model rules out an exacerbation of liver inflammation. Those findings are in agreement with some studies that reported a protective effect made by rIL-6 injection before ConA challenge and a possible IL-6-gp130-STAT3 pathway mechanism involved in the liver protection on the ConA T cell mediated liver injury (326-329). Indeed, the most studied IL-6 hepatic protective mechanism involved the IL-6 induction of MAPK pathway and the induction of STAT3, a key-signalling molecule in intracellular pathways, which blocks apoptosis and induces liver regeneration. Briefly, IL-6 binds to its sIL-6R soluble receptor, then the complex IL-6/sIL-6r binds to the gp130 cell surface receptor that leads to the phosphorylation and activation of JAK into the cytosol. p-JAK can activate MAPK, a transduction signal, which induces nuclear transcription of genes associated with liver regeneration. p-JAK, also induces STAT3 phosphorylation with subsequent activation and translocation to the nucleus, where transcription of anti-apoptotic and anti-necrosis genes is induced, which favours liver regeneration (330, 331). The increase *Il6* expression in the iron deficient group is coherent with a hepatic protection effect demonstrated in our model, however from those findings we are not able to infer that iron deficiency *per se* contributes to *Il6* increased expression or that its expression is hindered by the increased liver necrosis observed in the IrRepl group. The contrast between serum levels of IL-6 and the hepatic expression of *Il6* may display the different immunological outcomes in the liver prompted by the iron deficiency when compared with other compartments. More specifically it could be due to a divergent effect exerted by changes in iron levels on different cell types, as what is observed in hepatocytes and in macrophages. In fact, the decreased hepcidin expression caused by an iron deficient environment could be involved in the increased IL-6 production by intra-hepatic macrophages as previously reported (235).

In conclusion, in this first part of our work, we report that iron restriction dampens intra-hepatic lymphocyte activation and proliferation leading to a favourable effect on the acute T cell and NKT mediated hepatitis induced by ConA. Taking in account the pivotal place of the liver in the iron homeostasis tuning, even as an important iron reservoir or as the main place of hepcidin

synthesis, these findings could be implicated in many inflammatory liver conditions. Future studies are needed to establish the iron restriction effect on different lymphocyte subsets. Additional studies could focus on the iron effect in the lymphocyte function in the situations of chronic antigenic stimulation as observed in the clinical trial of immunosuppression withdrawal of long-term liver transplant recipients. For that, the use of rodent models of liver transplantation appears to be a more indicated model.

6.2 Impact of iron changes on the spontaneous tolerance development in a rat liver transplant model

As previously mentioned, successful IS weaning has been associated with iron and hepcidin levels in a recent IS withdrawal clinical trial in stable long-term liver transplant recipients. Based on that, we hypothesized that iron and/or hepcidin changes impact the anti-donor T cell mediated response influencing the establishment of spontaneous tolerance. To investigate the possible responsible mechanisms involved in such association we set up an experimental model of liver transplantation in which we reproduced the mild iron deficiency in rats. We chose the rat liver transplantation model because of the possibility of having different post-transplant immunological phenotypes depending on the donor/recipient rat strain combination employed (syngeneic, spontaneous tolerant, rejection and IS induced tolerance) (273, 287).

The rat liver transplant model, however, is a challenging surgical model with a high rate of failing procedures. Hori et al described that a minimum of 30 procedures are typically required before completing a successful transplant and recommended performing at least 50 transplants in order to be technically competent to perform the transplants in a standardized way (332). In my case the training phase was even more challenging, as I did not achieve long-term survival in my first 76 transplants. This had to do with the use of Wister rats, which are cheaper than other strains but do not tolerate complex surgery well, and with problems in executing the cuff technique described by Kamada et al. (278). My results gradually improved after switching to Lewis rats and following a stay at Charité Hospital in Berlin, where I was trained in the fully vascularized hand sewn rat liver transplantation technique (283). To reproduce the subclinical iron deficiency conditions observed in the non-tolerant liver recipients in the recent IS withdrawal clinical trial; we employed the same protocol on iron-modified diets set up in our previous murine work. As demonstrated in mice, three weeks on iron deficient diet were

sufficient to induce mild but statistically significant iron deficiency as compared with control group. IrDef rats showed only mild differences in some hematologic parameters such as haemoglobin, white blood cells and platelets levels but no differences were noted on growth of LFTs. This is in contrast to the effects on weight, growth, LFTs and other biological parameters that have been described by other studies (333, 334). These divergent results can be attributed to the fact that in previous studies iron deficient diets were compared to normal commercial animal chow. In our case, both the IrDef diet and IrRepl diets were prepared with the same iron-free ingredients and the only difference was the supplementation with iron carbonyl to reach normal iron ranges in the IrRepl diet (notice from the diet manufacturer SAFE®, Augy - France). Despite the apparently mild effects induced by the iron-deficient diets and described above, rats fed for three weeks with IrDef diet did not tolerate the liver transplant procedure. First, they were shown to be much more sensitive to inhalation anaesthesia and even small blood losses that IrRepl rats. Second, despite appearing healthy, they developed severe colic dilatation with liquid sequestration. Due to these complications, we modified the protocol to induce iron deficiency by feeding the rats with the iron-modified diets for only one week prior to the transplant procedure. This led to acceptable survival rates in both animal groups. Of note, when we compared the long-term results observed with either the IrDef of the IrRepl diets with those observed in rats fed with normal commercial chow, we observed that the use of both IrDef and IrRepl diets was associated with more frequent long-term complications such as abdominal hernias, abscesses and bile duct obstructions with secondary cirrhosis. Prasnicka et al. demonstrated an increase on the bile flow with augmentation of bile acids, glutathione, cholesterol and phospholipids excretion in rats under iron-deficient regimens for long-time (333). Based on the similarly increased morbidity rate induced by both iron-modified diets in comparison with liver recipients kept under normal commercial chow, we hypothesized that the iron carbonyl supplementation does not prevent the occurrence of complications initially attributed to iron deficiency *per se*, including in our case the biliary complications. Consequently, the use of iron-modified regimens could be considered a confounding factor for studies where animals should be kept under such regimens for long time.

As aforementioned, the rat liver transplant model affords the possibility to have different immunological phenotypes depending on which donor/recipient rat strain pair is employed (273, 287). However, what cannot be accurately replicated is the clinical setting in which long-term surviving liver recipients on maintenance IS are gradually wean from IS. In rats, when the

rejecting strain combination is employed, tacrolimus is capable of inducing tolerance after just a 10-day course (286). Furthermore, as described above, the long-term use of iron-modified regimens results in multiple complications. For these reasons, we chose to concentrate for our experiments in the immediate post-transplant period. We first investigated if the induction of mild iron deficiency was capable of breaking spontaneous tolerance, but this what not the case. We then explored whether tolerance was still established in the presence of iron deficiency and a potent immune-stimulant such as high dose of rhIL-2 (276, 277). In comparison with IrRepl liver recipients, IrDef rats developed a clear clinical deterioration during rhIL-2 administration; reflected by piloerection, weight loss, raised LFTs and behaviour changes. At the end of two weeks, IrDef liver recipients showed higher frequency of intra-hepatic CD4+ T cells and less CD8+ T cells. Furthermore, IrDef showed more inflammatory cytokine production by the intra-hepatic CD4+ and CD8+ T cells. No differences were observed in the frequency of macrophages and on regulatory T cells, which are normally involved on the tolerance and rejection phenomena (335, 336). Furthermore, at the end of rhIL-2 treatment, no marked histological differences were observed between two iron-modified groups (data no shown). Differently to the previous two reports that described 100% mortality rate when the one-week rhIL-2 is administered, none of our iron-modified liver recipients died during our three weeks rhIL-2 treatment protocol. The main technical difference between our surgical protocol and the two models referenced is the fact that our protocol, unlike the other two included arterialization of the liver allograft (276, 277). As previously mentioned, we opted for the arterialization technique due to the well-established impact that hypoxia exerts on the iron/hepcidin homeostasis (209). The use of arterial anastomosis in the rat liver transplant model, however, is known to improve the micro vascular liver circulation, prevent biliary damage, improve graft function and reduce the rate of rejection (275, 337-339). We believe that this technical difference contributed to our better survival rates and the weaker effects observed with rhIL-2. Of note, R*h*IL-2 administration did not have any significant harmful effects on rats fed with the two iron-modified diets and transplanted with syngeneic livers. These results suggest that the association of the mild iron deficiency and the lymphocytic allograft infiltration in the early time post-transplant contribute to the effects of the rhIL-2 treatment evidenced on the IrDef spontaneous tolerance transplanted rats. We replicated the same experimental conditions in spontaneously tolerant animals surviving more than two months post-transplant, when no intra-hepatic lymphocytic infiltration can be observed anymore. Differently to the early post-transplant

period, in this setting, IrDef animals were not affected by the rhIL-2 treatment. We had planned to replicate these experiments in a transplant setting (i.e. induction of tolerance by tacrolimus) more immunogenic than the BN to Lewis model. Unfortunately, due to time and funding reasons we were not able to replicate the rhIL-2 protocol on such strain combination at early times post-liver transplantation. We could however perform a limited number of experiments using Lewis rats that had been tolerized to DA livers for several months after having received the short course of tacrolimus. While at this late time the Lewis rats bearing a DA liver are considered fully tolerant (286), we observed that in one of the two animals to which we administered 3 weeks of rhIL-2 and under IrDef diet, the ALT/AST levels significantly increased. We have to acknowledge the very limited number of animals employed (2 IrDef versus 1 IrRepl), but one could hypothesize on the basis of these results that a tacrolimus-induced tolerance model could be a better setting to explore the effects of iron deficiency on liver tolerance than the spontaneous tolerance model.

In conclusion, we were able to set up a fully vascularized rat liver transplant model and to replicate the mild iron condition. Such iron-deficiency was not able to abrogate the spontaneous tolerance establishment. Further, caution should be taken when the diet model is used because the high rate of complication at long term. The tacrolimus-induced tolerance rat strain combination seems to be a more appropriate strain combination to check the impact of iron levels on the tolerance establishment at early time points post liver transplantation

6.3 Molecular characterization of acute cellular rejection in liver transplant recipients occurring during intentional immunosuppression withdrawal

Until now, histologic examination is the backbone on the diagnosis of ACR in the organ transplant setting. Allograft biopsy is an invasive procedure and samples interpretation can be challenging and lead to misdiagnosis (340, 341). Because that, the determination of reproducible non-invasive and/or more accurate surrogate biomarkers of graft rejection is an important research field of in the organ transplantation. Post-transplant molecular profiles have been already exhaustively studied in the kidney transplantation leading to the characterization of subtypes of rejection and other different types of graft injury (159). Data from single- and multicentre studies, mostly using mRNAs as specific biomarkers, can be helpful diagnostic tools (342). Conversely, in liver transplantation; few studies approached the molecular

characterisation of ACR. Most of those studies were addressed in small series of liver transplant recipients, which limits results extrapolation for the general population of liver transplant recipients. By consequence, our comprehension of the predictive accuracy and specificity of molecular biomarkers in different clinical conditions and different biological samples in the liver transplantation setting remains incomplete.

Our microarray experiments performed on liver samples showed a clear transcriptional difference between rejecting and non-rejecting liver allografts, in similitude with what has already been demonstrated in other organ transplanted organs as e.g. kidney and heart transplants. A clear transcriptional read-out was more evident in HCV-positive than in HCV-negative, once that ten times more genes were differentially expressed in the former group when compared with the later group. In spite of that, an overlapping group of 19 genes were significantly expressed in both groups. A control experiment using liver samples taken from rejecting HCV-negative patients who rejected their liver in the first month post transplantation confirmed the rejection specificity of these 19 common expressed genes.

Functional analyses comparing our findings with available public gene expression data sets revealed that many of our identified genes were already clearly associated with rejection occurring in other transplant settings, with many of then corresponding to functional pathways involved with allograft rejection, as nuclear factor-κB, STAT1/interferon-γ, tumour necrosis factor-α, chemokine receptor networks and immune effector networks. More specifically, from the previous mentioned group of 19 genes, 12 genes were already reported (*CXCL9, HLA-DMA, HLA-DRA, ITM2A, HLA-F, HLA-DQB1, UBD, CD2, IL8, IL32, CXCL10, TAP1*), in a meta-analysis published by Spivey et al., which include rejecting samples from liver, kidney, heart and lung transplant recipients (342). Then, 10 genes (*CD2, CXCL10, CXCL9, HLA-DMA, HLA-DQB1, HLA-DRA, HLA-F, IL32, TAP1* and *UBD*) were already demonstrated in rejecting kidney recipients (142, 143, 147, 343, 344); 3 genes (*CXCL10*, *CXCL9* and *HLA-F*) in rejecting cardiac recipients as described by Karason et al., 3 genes (*IL32*, *IL8*, and *ITM2A*) in common with lung rejecting recipients demonstrated by Patil et al. (345, 346). None of the four liver rejection transcriptional studies included in the Spivey et al. meta-analysis disclosed overlapping gene with our list of 19 rejection-associated genes (342). Only seven genes were exclusively recognised by our study (*GPNMB, SLC1A3, ANXA2, CD38, FABP5, PLA2G7, RFX5*). Two liver transcriptional studies addressed the difficulties of rejection diagnostic in the context of HCV-positivity. In Sreekumar et al. report, a rejection gene signature was described in protocol liver

biopsies performed at day 21 post-transplant from a small series of 4 rejecting HCV-positive patients compared with 4 non-rejecting HCV-positive recipients (347). In a larger cohort of HCV-positive patients, Asaoka et al. used the Ingenuity Pathway Analysis methodology to analyse transcriptional profiles from liver biopsies taken in the second month post-transplant. They were also able to describe a differential gene signature in rejecting HCV-recurrent patients from those only with HCV recurrence (348). While there was a similitude between their rejection associated functional networks with those identified by our study, there was no overlapping with our list 19 genes differentially expressed at the rejection time. In the following study from the same group, which included liver recipients also transplanted by other indications than HCV-related cirrhosis, two of their rejection-associated genes (*CD2 and CXCL9*) were also present in our list of differentially expressed genes (349). This reduced overlapping of individual genes among the transcriptional liver studies can be accredited to the issues concerning small series, different population characteristics, differences on biopsies collection time points, the employ of different transcriptional platforms and variation on the genes tested selection. Concerning to the interference of HCV-positivity on the ACR characterization, the higher number of differentially expressed genes in our HCV-positive recipients in comparison with HCV-negative patients, is in agreement with previous findings already reported by Bohne et al. who showed a significant interaction between HCV infection and alloimmune responses at the molecular transcriptional level. Nevertheless, the identification of ACR-specific rejection genes in the context of underlining HCV infection could be an important tool to discriminate ACR from HCV recurrence as previously stated by the previous mentioned studies (347, 348).

Changes on the regulation of specific genes have been associated with acute cellular rejection. The detection of some specific gene polymorphisms genotypes as *NFKBIA* and *TNFA-308 A/A* in peripheral blood samples of liver transplant recipients has been associated repeat ACR episodes (350, 351). However biological conditions used to be a resultant of many factors, including the regulation of complexes genes pathways. Then, analyses of transcriptional changes of individual genes can lead to major misinterpretation of biological processes. We used available bioinformatics tools to explore which functional pathways were more highly associated with ACR, by comparing our data with pathogenesis-based transcripts gene sets already described in kidney and heart human allografts. This analysis disclosed a predominance of T cell associated transcripts differentially expressed at the time of rejection in our samples. The same picture was observed in other transplant organs, mainly kidneys,

suggesting a similar response by the liver allograft to T cell mediated rejection (TCMR) episodes. Furthermore, it is worth to note the presence of a significant association with transcripts containing genes reputed by an overexpression in the occurrence of antibody-mediated rejection (ABMR) in kidney allografts, notably B-cells and NK cells related genes. Here again there is a similitude with what occurs in kidney transplant setting, where ABMR-associated transcripts were also present with a weaker signal in the context of TCMR. These findings are in accord with the concept that transcriptional differences between TCMR and ABMR are more quantitative than qualitative. It is known that ABMR is less frequent in the liver recipients than in the kidney counterparts; however the fact that ABMR-associated transcripts could be differentiated expressed on the TCMR episode should be taken in consideration when liver allograft biopsies exhibit mixed or unclear histological patterns. In those cases, transcriptional analyses would be used to supply complementary diagnostic information.

In addition to the functional liver biopsy analyses, we applied the same functional research algorithm to analyse sequential blood samples in HCV-negative rejecting liver recipients. Even though we found similar pathways associated with ACR, the blood compartment presented a weaker signal in comparison to the tissue compartment. Also, in contrast with the tissue observations, T cell associated transcripts were down regulated in blood at the time of ACR suggesting an allograft "tropism effect" evidenced by the T cells, mainly $CD8^+$ T cells, migration to the transplant organ at the time of allograft rejection (352). In fact in the liver transplant setting, Taubert et al. found an enrichment on regulatory T cells in liver biopsies at the time of rejection and HE et al found a decreased frequency of $CD4^+CD25^{high}$ $FoxP3^+$ on peripheral blood of rejecting liver recipients (353, 354).

We checked if our ACR-related group of genes were already differentially expressed at the baseline blood samples, which could be used as predictor of the IS withdrawal. In contrast with the association of iron-related genes transcriptional patterns in liver biopsies at baseline and the IS withdrawal outcome; none of our genes tested was differentially expressed at the baseline blood samples suggesting that at the moment allograft transcriptional changes are more accurate to predict the outcome of IS withdrawal than the transcript patterns on the peripheral blood compartment.

We attempted to establish a correlation between molecular changes occurring in the liver allograft and in the periphery by comparing our ACR transcriptional data sets found in liver biopsies and in the blood samples, both taken at the time of the rejection episode. However

before doing that, we needed to acknowledge the fact that different microarray platforms were employed in each experiment, which can impair the outlining of definitive conclusions. Taking in consideration this condition and employing a slightly lower significance threshold to compare the two data sets, 22 genes were identified as differentially expressed in both compartments, with most of them known to be associated to the immune response and cell cycle pathways. These findings, in addition with the similar networks identified by functional analyses in both groups of specimens, support the concept of overlapping transcriptional profiles between the two biological compartments at the rejection time.

As previously mentioned, diagnosis of allograft rejection episodes requires histological evaluation. Rejection histologic diagnostic criteria are usually built based on retrospective analyses of historical sets of histologic allograft specimens with correlation to clinical outcome. Worldwide renowned expert panel constantly review and updated the histological Banff rejection score system is in specific periodic meetings (355, 356). In spite of that, histological rejection approach presents some limitations, which can interferer on the final result and series comparisons as arbitrary lesions grading, subjectivity on biopsies readings, variability on site sampling, and the disagreement between pathologists on lesions scoring (340, 357). Studies comparing gene expression profiles on allografts specimens with histological Banff scores have showed a correlation of inflammatory expressed genes with histological rejection classification in the kidney transplant setting(147, 358) (358). Using a very detailed inflammatory classification, which included 11 histological parameters, we were able to demonstrate a clear correlation between the expression of inflammatory and rejection associated genes in liver tissues with the degree of inflammatory lesions disclosed by the histological scoring. Such correlation was relatively uniform over all different histological compartments analysed, however the number of expressed genes were remarkable in lobular and portal inflammation and in interface hepatitis. However, we need to acknowledge that few patients presented severe central vein endothelitis of ductopenia, limiting the detection of transcriptional signatures for more severe forms of ACR in our series. This is probably due the fact that patients achieved biochemical criteria for *per indication* liver biopsy in the early stages of the rejection process when no clinical symptoms were observed and only mild or moderate biological allograft dysfunction was detected by the strict biological monitoring protocol recommended by the clinical trials guidelines and, probably, as a consequence no serious histological damage has been installed yet.

The presence of CNI-based IS regimens at the time of enrolment was associated with the failure of IS weaning protocol in a univariate analysis but not in a multivariate analysis in the original cohort of patients from the IS withdrawal clinical trial reported by Benitez el al. (1). Therefore, we aimed to investigate if the type of IS at the baseline could influence the gene transcripts profile among rejecting liver recipients. In our sub analysis, baseline immunosuppression did not influence gene expression profiles on liver tissue. The same algorithm was employed on blood samples, which disclosed no differences between gene expression patterns between patients taking TAC monotherapy and patients taking CSA monotherapy. There was only a small group of 17 genes deferentially expressed between patients on CNI monotherapy and patients initially on MMF; however only 8 out of the 17 genes were included on the original set of ACR-associated genes. Altogether, these findings suggest that baseline immunosuppression regimens have no influence on the gene expression patterns at the time of enrolment, and it was not a confounding factor for our further analyses. Previous studies aiming to disclose gene signatures of tolerance in the transplant setting, mainly kidney but also in the liver transplant setting, did not pay much attention to the patient initial IS regimens (109, 122-124). Basically they compared patients completely off IS with patients under IS therapy without take in account the tolerant patients previous IS regimens. However, in a recently study, Rebollo-Mesa et al. re-analysed three independent cohorts of patients initially studied in some of such previous reports in addition with a new prospective group of kidney recipients under a corticosteroids weaning protocol. Employing complex bioinformatics statistical models in *training*, *validation* and *proof of concept* stepwise algorithm, they demonstrated that IS had a bias effect on their original tolerance gene signatures, with azathioprine exerting the major negative influence. In addition, they were able to disclose a new tolerance gene signature that remained stable before and after the corticosteroids withdrawal (359). Even that our analysis showed no interference of immunosuppression on the gene expression patterns from samples of our rejecting liver recipients, this mentioned study highlights the need for deeper analyses or re-analyses of rejection and/or tolerance gene signatures on the IS withdrawal in the liver transplant setting.

We investigated if sequential transcriptional changes over the IS weaning period could be used as a gene signature able to forecast ACR episode before its biological, histological and clinical appearance. For that, we studied the kinetics changes on the transcriptional patterns in a well-selected group of 45 ACR-associated genes, most of them identified by our own microarrays

experiments. From that group, using a univariate analysis, we were able to determine a target group of 10 genes differentially expressed in blood samples at the time of rejection in comparison with samples collected at the time of enrolment. Using a stepwise multivariate logistic analysis to construct a predictive model of rejection in the context of IS withdrawal, we identified that the combination of *CXCL10* and *FOXP3* were the most accurate gene combination able to determine rejection in blood samples when compare with baseline samples. The use of this gene signature on blood sequential samples collected across the weaning protocol showed a peak on the gene expression coinciding with the rejection episode and with the peak of serum transaminases. Gene expression levels decrease after that rejection treatment had been started, which was in agreement with transaminases serum levels normalisation. Since that most of rejecting liver recipients were under CNI-based IS regimens, and taking in account the effect of CNI on the *FOXP3* expression, this gene was excluded in a second analysis (316). Then, a second gene signature containing only *CXCL10* is more robust marker to determine the ACR episode evolution. We need to acknowledge that increases on the *CXCL10* expression paralleled with increases on LFTs in the same time. Furthermore the *CXCL10* gene signature misplaced as rejecting 33% of blood samples of tolerant liver recipients with normal LFTs and no clinical signs of rejection. One possible hypothesis to explain this finding could be the presence of a subclinical inflammatory phenomenon during the IS weaning protocol that is not strong enough to progress to a rejection episode. This subclinical inflammation was already described in animal models, where an intermediary lymphocyte allograft infiltration period is noted before the T cell deletion during the tolerance establishment process (273)**.** It is also worth to note that unfortunately our rejection gene signature was not sufficiently sensitive to diagnose rejection episodes in patients with chronic HCV infection. The clear impact of HCV on the gene expression profiles at the rejection time was confirmed by the increased number of differentially expressed genes at the rejection time in HCV-positive samples in comparison with HCV-negative samples. Moreover, we need to acknowledge the small group of HCV-positive liver recipients in addition to the limited number of samples available from those patients; which could be confounding factors for the employment of our rejection gene signature. Furthermore, the limitations due to the small number of patients and available samples prevented us from being able to stratify our patient population into any subgroups other than HCV-positive and HCV-negative. We were unable to stratify for the presence of hepatocellular carcinoma, age, gender or other indications of transplantation.

Future prospective studies are necessary to address the influence of HCV infection on the rejection episode in liver transplant recipients, which should also take into account the advent of the new direct-acting antiviral-based treatment for HCV infection after liver transplantation as well as other patient subgroups as mentioned above (360, 361).

The clinical utility of a rejection gene signature needs to be checked in larger IS withdrawal clinical trials, which combine gene expression kinetics in blood samples with LFTs evolution across the weaning period. We believe that gene expression profiles can improve the rejection diagnosis based exclusively on LFTs, which are neither sensitive nor specific for rejection. However, the measurement of LFT remains one of the most important parameters in decision making to indicate a liver biopsy to confirm or rule out a possible episode of rejection (362). The discovery of a more accurate ACR gene signature in the milieu of IS withdrawal could be an important tool for the immune monitoring of enrolled patients. As stated previously, such a monitoring tool could help to identify patients likely to develop a rejection episode across the weaning protocol before its biological, histological and clinical manifestations. In that case, once a future-rejecting patient has been identified, special clinical measures can be taken in order to hold the rejection episode evolution avoiding a complete reactivation of the immune system due to the IS withdrawal. This strategy could favour future attempts of IS withdrawal in patients not yet likely to be tolerant when such patients will be older and more time will have passed from the transplant procedure which are the two strongest clinical factors associated with successful complete IS withdrawal (1). The identification of molecular biomarkers associated with the ACR occurring in the early phase post liver transplantation could be an important immune monitoring tool as well. In this case, the ACR-associated gene signature could be used to tailor the IS treatment. Then in case of up regulation of ACR-associated genes this could be an indicator of insufficient IS treatment. On the contrary, down-regulation of such genes could be a signal of over immunosuppression. Unfortunately few studies have addressed this question in the early period post-liver transplantation.

Our current study discloses a comprehensive understanding for the processes driving ACR in liver transplant recipients. We demonstrated a significant overlap with the rejection episode in kidney transplant recipients regarding the T cell-mediated processes. We addressed the potential clinical use of transcriptional markers detected in peripheral blood samples as a predictor tool of ACR in liver transplant recipients. Those markers could lead to more accurate ACR diagnoses reducing the need of invasive procedures in the rejection diagnosis, however

further studies are necessary either in the context of IS withdrawal or in the early period post liver transplantation. These studies could take advantage of the use of the new RNA sequence platforms, which use high-performance RNA sequence techniques, such as New Sequence Generation, for the identification of more specific and sensitive molecular rejection signatures.

6.4 Final Conclusions and Future Work

In the current work, we analysed human biological samples employing transcriptional technologies and set up two experimental animal models to investigate tolerance and rejection biomarkers in the context of immunosuppression withdrawal post liver transplantation, which resulted in two *peer reviewed* publications (160, 363).

The analysis of biological samples collected from patients who developed a rejection episode during the weaning period allowed us to identify a distinct rejection transcriptional profile. Some of these genes were also differentially expressed in biopsies collected in cases of rejection taking place early post liver transplantation in patients treated with standard-of-care regimens. Furthermore, similarities were also encountered with rejection-associated gene-sets originating from other transplanted organs. When sequential blood samples were collected across the weaning protocol, at the time and after the rejection episode, a predictive rejection model employing up to two genes could be identified. While this gene signature could theoretically identify future rejecting liver recipients enrolled in similar IS withdrawal clinical trials, the rejection-associated gene set can be used as a biomarker for immunological monitoring purposes for long-term liver recipients not necessarily enrolled in such clinical trials. Indeed, the clinical utility of this biomarker was recently demonstrated in 2 clinical studies involving protocol liver biopsies collected from paediatric and adult liver transplantation, respectively, in which the statistical enrichment of our previously identified gene sets in the transcriptome of liver biopsies showing subclinical idiopathic inflammation suggested rejection as a plausible pathogenic explanation (364, 365). The implications of these recent studies in those patients bearing subclinical inflammatory histological abnormalities show that they might be in need of strengthened immunosuppression, which is something that will now need to be tested in randomised controlled studies. Efforts are needed to address the current limitations of biomarkers of molecular rejection, such as the low specificity and sensitivity to identify a rejection episode before its clinical, biological and histological manifestations and the time

required for sample processing and obtainment of results. Cost is another problem that must be addressed. If these points are attained, the molecular rejection profile can become an important clinical tool in the future for the diagnosis and monitoring of acute cell rejection in the field of transplantation. Our animal studies have provided information supporting a potential role of iron metabolism in the regulation of intra-hepatic inflammatory responses and tolerance. Given the significant influence of iron on bacterial growth, the participation of the gut microbiome in the effects reported in our murine model of immune-mediated liver damage, which we could only superficially explore in our studies, will need to be investigated further. Additional experimental work will also be required to better clarify the role of iron in the spontaneous development of tolerance, as originally hypothesized, the robustness of the model chosen might have overshadowed the effects of iron. To address this, our future work will include the use of more immunogenic donor-recipient strain combination. In this regard, experiments are in preparation using the Tacrolimus-induced tolerance rat strain combination, which might be more prone to be influenced by metabolic mediators such as iron.

Appendix A: Congress presentations and publications

1) Congress publications

1) **Eliano Bonaccorsi-Riani,** Adam Pennycuick, Maria C Londoño Juanjo J Lozano, Carlos Benitez, Brigit Sawitzki, Marta Martínez-Picola, Feliz Bohne, Marc Martinez-Llordella, Rosa Miquel, Antoni Rimola, and Alberto Sanchez-Fueyo. Molecular Characterization of Acute Cellular Rejection during Immunosuppression Withdrawal in Liver Transplantation. Oral presentation. British Transplant Congress, February 2016, Glasgow – United Kingdom

2) **Eliano Bonaccorsi-Riani,** Richard Danger, Elisavet Kodela, Rosa Miquel, Marc Martinez-Llordella, Maria Hernandez-Fuentes, Alberto Sanchez-Fueyo. Iron Deficiency Increases Early Inflammatory Allo-Immune Responses After Liver Transplantation in Rats, But Does Not Impair the Establishment of Spontaneous Tolerance. Poster presentation. 21st Annual Congress of ILTS, July 2015, Chicago, USA

3) **Eliano Bonaccorsi-Riani,** Juanjo J Lozano, Carlos Benitez, Maria C Londoño, Feliz Bohne, Marc Martinez-Llordella, Antoni Rimola, Alberto Sanchez-Fueyo. Molecular Characterization of Acute Cellular Rejection during Immunosuppression Withdrawal in Liver Transplantation. Oral presentation. 20th Annual Congress of ILTS, July 2014, London – United Kingdom.

4) **Eliano Bonaccorsi-Riani,** Richard Danger, Marc Martinez-Llordella, Marta Martinez, Anna Rodriguez, Miquel Bruguera, Antoni Rimola, Hellen Collins, Alberto Sanchez-Fueyo. Iron Regulates Intra-Hepatic Lymphocyte-Mediated Immune Responses. Oral presentation. 20th Annual Congress of ILTS, July 2014 - London – United Kingdom.

5) **Eliano Bonaccorsi-Riani,** Richard Danger, Marc Martinez-Llordella, Marta Martinez, Anna Rodriguez, Miquel Bruquera, Antoni Rimola, Hellen Collins, Alberto Sanchez-Fueyo. Iron regulates intra-hepatic lymphocyte-mediated immune responses. Poster presentation. ESOT and TTS joint basic science meeting. November 2013, Paris - France.

2) Peer reviewed publications

1. **Eliano Bonaccorsi-Riani**, Richard Danger, Juan José Lozano, Marta Martinez-Picola, Elisavet Kodela, Roser Mas-Malavila, Miquel Bruguera, Helen Collins, Robert Hider, Marc Martinez-Llordella, Alberto Sanchez-Fueyo. Iron deficiency impairs intra-hepatic immune responses. *PLoS One*. 2015 Aug 19: 10(8): e0136106.
2. **Bonaccorsi-Riani E**, Pennycuick A, Londoño MC, Lozano JJ, Benítez C, Sawitzki B, Martínez-Picola M, Bohne F, Martínez-Llordella M, Miquel R, Rimola A, Sánchez-Fueyo A. Molecular Characterization of Acute Cellular Rejection Occurring During Intentional Immunosuppression Withdrawal in Liver Transplantation. *Am J Transplant*. 2016 Feb; 16(2): 484-496 Oct 30.

Appendix B: Paper: Iron Deficiency Impairs Intra-Hepatic Lymphocyte Mediated Immune Response

PLOS ONE

RESEARCH ARTICLE

Iron Deficiency Impairs Intra-Hepatic Lymphocyte Mediated Immune Response

Eliano Bonaccorsi-Riani[1☯], Richard Danger[1☯], Juan José Lozano[2], Marta Martinez-Picola[2], Elisavet Kodela[1], Roser Mas-Malavila[1], Miquel Bruguera[2], Helen L. Collins[3], Robert C. Hider[4], Marc Martinez-Llordella[1], Alberto Sanchez-Fueyo[1]*

1 Department of Liver Studies, Division of Transplantation Immunology & Mucosal Biology, Medical Research Council (MRC) Centre for Transplantation, Faculty of Life Sciences & Medicine, King's College London University, King's College Hospital, Denmark Hill, London, United Kingdom, **2** Liver Unit and Bioinformatic platform, CIBEREHD, Hospital Clinic Barcelona, Villaroel 170, Barcelona, Spain, **3** Department of Immunobiology, Division of Immunology, Infection & Inflammatory Disease, Faculty of Life Sciences & Medicine, King's College London, Franklin-Wilkins Building, Stamford Street, London, United Kingdom, **4** Institute of Pharmaceutical Science, Faculty of Life Sciences & Medicine, King's College London, Franklin-Wilkins Building, Stamford Street, London, United Kingdom

☯ These authors contributed equally to this work.
* sanchez_fueyo@kcl.ac.uk

CrossMark
click for updates

OPEN ACCESS

Citation: Bonaccorsi-Riani E, Danger R, Lozano JJ, Martinez-Picola M, Kodela E, Mas-Malavila R, et al. (2015) Iron Deficiency Impairs Intra-Hepatic Lymphocyte Mediated Immune Response. PLoS ONE 10(8): e0136106. doi:10.1371/journal.pone.0136106

Editor: Bernhard Ryffel, French National Centre for Scientific Research, FRANCE

Received: May 29, 2015

Accepted: July 29, 2015

Published: August 19, 2015

Copyright: © 2015 Bonaccorsi-Riani et al. This is an open access article distributed under the terms of the Creative Commons Attribution License, which permits unrestricted use, distribution, and reproduction in any medium, provided the original author and source are credited.

Data Availability Statement: All relevant data are within the paper and its Supporting Information file.

Funding: The Institute of Liver Studies (KCL) is supported by the Medical Research Council (MRC) Centre for Transplantation, King's College London, UK (transplantation.kcl.ac.uk) – MRC grant no. MR/J006742/1 and by the National Institute for Health Research (NIHR) Biomedical Research Centre at Guy's and St Thomas' NHS Foundation Trust and King's College London. The views expressed are those of the author(s) and not necessarily those of the NHS, the NIHR or the Department of Health. The

Abstract

Hepatic expression of iron homeostasis genes and serum iron parameters predict the success of immunosuppression withdrawal following clinical liver transplantation, a phenomenon known as spontaneous operational tolerance. In experimental animal models, spontaneous liver allograft tolerance is established through a process that requires intra-hepatic lymphocyte activation and deletion. Our aim was to determine if changes in systemic iron status regulate intra-hepatic lymphocyte responses. We used a murine model of lymphocyte-mediated acute liver inflammation induced by Concanavalin A (ConA) injection employing mice fed with an iron-deficient (IrDef) or an iron-balanced diet (IrRepl). While the mild iron deficiency induced by the IrDef diet did not significantly modify the steady state immune cell repertoire and systemic cytokine levels, it significantly dampened inflammatory liver damage after ConA challenge. These findings were associated with a marked decrease in T cell and NKT cell activation following ConA injection in IrDef mice. The decreased liver injury observed in IrDef mice was independent from changes in the gut microflora, and was replicated employing an iron specific chelator that did not modify intra-hepatic hepcidin secretion. Furthermore, low-dose iron chelation markedly impaired the activation of isolated T cells *in vitro*. All together, these results suggest that small changes in iron homeostasis can have a major effect in the regulation of intra-hepatic lymphocyte mediated responses.

funders had no role in study design, data collection and analysis, decision to publish, or preparation of the manuscript.

Competing Interests: The authors have declared that no competing interests exist.

Introduction

Iron homeostasis and the immune system are closely interconnected. Inflammatory cytokines induce a rapid increase of hepcidin [1], the central mediator of iron homeostasis, which reduces iron export from enterocytes, hepatocytes and, most importantly, macrophages [2]. This results in iron accumulation within macrophages and decreased circulating iron levels, which appears to be an effective defence strategy against extracellular microorganisms that need access to iron to exert pathogenic effects [2]. On the other hand, iron loaded macrophages exhibit reduced effector functions, which can compromise their capacity to clear intra-cellular infections [3, 4]. Iron also contributes to the formation of potent reactive radicals, which promote oxidative stress and induce inflammation and tissue injury. Thus, iron restriction has been shown to ameliorate oxidative stress and inflammatory organ damage in models of murine acute hepatitis [5, 6], experimental autoimmune encephalomyelitis (EAE) [7], renal interstitial fibrosis [8] and type 2 diabetes in rats [9]. In addition to its effects on innate immune responses and inflammation, iron is also required for the function and differentiation of adaptive immune cells such as T lymphocytes. Thus, iron deficiency impairs T cell proliferation *in vitro* [10]. The impact of iron homeostasis manipulations on lymphocyte function *in vivo*, however, has not been investigated in detail.

A role for iron homeostasis in the regulation of intra-hepatic lymphocyte responses and in the development of transplantation tolerance has been recently suggested on the basis of the results of a clinical trial in which immunosuppressive drugs were intentionally withdrawn from a cohort of 98 long-term surviving liver transplant recipients [11]. As compared to tolerant liver recipients who successfully discontinued immunosuppression and age-matched healthy individuals, non-tolerant patients who rejected during the weaning process exhibited lower serum hepcidin and ferritin levels, as well as lower intra-hepatic iron content and hepcidin gene expression. An intra-hepatic iron-related gene expression signature was indeed the most accurate marker to predict the outcome of the drug withdrawal protocol. The phenomenon of spontaneous liver allograft tolerance has been extensively studied in experimental animal models, particularly in rodents, in which an essential step in the induction of tolerance is the activation and subsequent deletion of liver infiltrating lymphocytes [12, 13]. On account of these data, we hypothesized that small changes in iron homeostasis could influence intra-hepatic immune responses by interfering with intra-hepatic lymphocyte activation. To test this hypothesis, in the current study we induced mild iron deficiency in mice by administering either an iron-free diet or low-dose iron chelators, and assessed how iron deficiency influenced intra-hepatic lymphocyte activation and its downstream effects. Reduction of iron availability significantly interfered with lymphocyte activation, proliferation and cytokine production and resulted in dampened immune-mediated hepatitis. These findings highlight a previously not well-recognized phenomenon through which small changes in iron homeostasis can influence outcomes in inflammatory liver disorders.

Material and Methods

Mice

Male C57Bl/6 mice (purchased from Charles River) were bred under specific pathogen-free conditions. All procedures were conducted in accordance with national and institutional guidelines for animal care and use and have been approved by the Denmark Hill Animal Welfare and Ethical Review Body (AWERB–KCL) and the Home Office. Anesthesia was performed by isoflurane inhalation whereas euthanasia was performed in CO_2 chamber.

Four-week old mice were fed with either iron deficient (<6mg/kg iron) or iron replete (iron deficient diet supplemented with 200 mg/kg iron carbonyl) diets (SAFE, France) for a total of 3 weeks prior to the performance of experiments. In some experiments, mice also received an antibiotic cocktail consisting of ampicillin 1 g/L, vancomycin 0.5 g/L, (Laboratoiros Normon S. A., Spain), metronidazole 1 g/L (BBraun Medical S.A., Spain) and neomycin 1 g/L (Laboratorios Salvat, Spain), which was added to drinking water and changed every 3 days for the entire duration of the 3-week period as described [14].

Concanavalin A (ConA) induced hepatitis

In order to investigate a potential iron-related functional effect in immune system, we used an immune-modulated model of acute hepatitis using a sublethal injection of Concanavalin A (ConA) [15]. Immune-mediated acute hepatitis was induced by intravenous injection of 15mg/kg of type IV ConA (Sigma-Aldrich, St. Louis, MO). Following ConA injection mice were anesthetized and sacrificed at various time points to collect blood, spleen and liver tissue. Additional experiments were performed with a single previous IP injection of 100μg of mouse hepcidin (PLP-3773, Peptides International, KY, USA) or sterile PBS two hours before the ConA challenge.

Iron chelators

For some *in vivo* experiments, a 3 day-course of a hydroxypyridinone iron based chelator (HPO CP28; 20 nmoles, i.p.) [16, 17] was performed before ConA challenge. *In vitro*, cells were incubated with low doses of either HPO CP182 (5μM) or desferoxamine (DFO, 10μM, Sigma-Aldrich). At these doses iron chelators had no discernible effects on lymphocyte cell death (S1 Fig).

Serum biochemistry and cytokine analyses

Serum was obtained after 10 minutes centrifugation at 8,000g and stored at -80C. The alanine aminotransferase (ALT) plasma activities, which reflect the liver injury intensity, and the serum iron level were quantified by automated measurements using the ADVIA 2400 System kits (Siemens). Hematologic parameters were assessed by automated measurements using the ADVIA 2120 System kits (Siemens). Serum cytokine levels were measured with multiplex fluorescent bead-based Luminex technology according to manufacturer's recommendation.

Liver histology

Formalin-fixed and paraffin embedded liver tissue sections were stained with haematoxylin and eosin stained and the presence of hepatocyte necrosis, cellular infiltration and hepatocyte cohesion were assessed by a senior liver histopathologist who was blinded to the identity of the experimental groups (MB).

Isolation of non-parenchymal liver cells

After harvesting, the liver was perfused with sterile PBS through the portal vein, and digested at 37°C in the presence of collagenase II 5%,(PAA Laboratories) and 100μg/mL DNase I (Roche) for 30 minutes, as described [18]. The liver tissue was then passed through a 70μm nylon mesh. Hepatocytes were then removed following low-speed centrifugation (60 xg, 2minutes) and liver mononuclear cells were isolated using Ficoll separation (800 xg, 20 minutes).

Isolation of splenic and lymph node leukocytes

Spleens were passed through a 70um nylon mesh, and blood cells were removed using ammonium chloride potassium lysing buffer (Life Technologies) for 5 minutes.

In vitro naïve $CD4^+$ T cell stimulation

$CD4^+$ naïve T cells were isolated from spleen and lymph nodes using EasySep Mouse Naïve $CD4^+$ T Cell Isolation Kit (Stem Cell). Enriched cells were labelled with 2.5 μM CFSE (Biolegend) during 10 minutes. A total of 250.10^3 cells were incubated during 5 days in 96 well-plate coated with anti-CD3 anti-CD28 antibodies (2ug each, clone 145-2C11 and 37.51, respectively) in RPMI-1640 (Life technologies) supplemented with 5% Foetal Calf Serum (Sigma-Aldrich), 1% penicillin-streptomycin and 2 mM L-glutamine and 50μM β-mercaptoethanol (Life technologies).

Flow cytometry

Up to 1.10^6 cells were labelled in staining solution (PBS, Foetal Calf Serum 2%, 2mM EDTA). Antibodies used were: APC/Cy7 anti-CD3e, PE/Cy7 anti-CD4, APC anti-CD25, PE anti-CD44, FITC anti-CD62L (all from Biolegend). Dead cells were stained either with 7-AAD (Biolegend) or Livedead cell viability assay (Life Technologies). Cells were fixed using fixation solution 20 minutes at room temperature (Biolegend). For regulatory T cells labelling, FOXP3 Perm/Fix solution was use with PE anti-FOXP3 antibody (Biolegend) according to manufacturer's instructions. Intracellular IFNγ staining was performed using permeabilisation buffer following manufacturer's instructions and FITC anti-IFNγ antibody and APC anti-IL4 antibody (Biolegend). Data were acquired on a BD FACSCanto II flow cytometer (BD) and analyzed employing FlowJo software (Tree Star).

RNA extraction and gene expression experiments

Liver or spleen tissue samples were cryopreserved at -80C in RNAlater reagent (Ambion). For RNA extraction, samples were first homogeneized using a RNAse-free pestle in Trizol reagent (Invitrogen), and total RNA was extracted according to TRIzol manufacturer's protocol. DNA was removed from total RNA preparations using Turbo DNA-free DNAse treatment (Ambion). Quality and quantity were assessed with the Agilent 2100 Bioanalyzer (Agilent Technologies) and Nanodrop ND-1000, respectively. Total RNA was then reverse transcribed into cDNA using the High-Capacity cDNA Reverse Transcription Kit (Applied Biosystems). A pre-amplification of cDNA was performed using pooled TaqMan Assays (final concentration of 0.2X each) and the TaqMan PreAmp Master Mix using 10 cycles of amplification. qPCR was performed using the 48.48 Dynamic Array (Fluidigm Corporation, CA, USA) following manufacturer's protocol using a BioMark Instrument (Fluidigm Corporation). To quantify transcript levels, target gene Ct values were normalized using Ct values of HPRT1 as a reference gene to generate -ΔCt values. Real-time PCR gene expression experiments were performed at 12 hours post injection. This time point was selected to coincide with the peak of transaminases and after determining that it required more than 3 hours to detect significant gene expression differences (in a pilot experiment, Illumina microarrays performed at 3 hours showed minimal differential gene expression (data not shown)).

Statistical analyses

Statistical analyses were performed with GraphPrism software. Student T-test was used for comparison between two groups and ANOVA analysis with Tukey's post-hoc correction for

pairwise comparisons was used to compare more than 2 groups. Fisher test was used for categorical variables. P-values <0.05 (two-tailed) were considered statistically significant in all analyses.

Results

Induction of mild iron deficiency by dietary manipulation

As compared to mice fed with an iron replete diet (IrRepl), mice fed with an iron deficient diet (IrDef) displayed decreased serum iron (mean 73.22 ±56.49 *versus* 156.38 ±36.99 μg/dL; p <0.0001) and serum transferrin saturation (18.80 ±6.32 vs 56.20 ±4.53%; p = 0.0013) (Fig 1). In addition, liver tissue analysis revealed reduced liver iron stores and hepcidin (*Hamp*) gene expression (p = 0.017 and p<0.0001, respectively) (Fig 1). None of these iron parameters were found different between IrRepl diet and regular diet. As previously reported [19, 20], IrDef mice also developed mild anemia (hemoglogin 107.6 ±46.10 versus 147.9 ±6.50 g/L; p = 0.028), and increased platelet count (1405 ±469.2 versus 769.4 ±174.4 x10^9/L; p = 0.0004) (Fig 1). IrDef mice remained otherwise healthy and gained weight at the same rate as IrRepl mice.

Mild iron deficiency does not modify the steady state immune cell repertoire and systemic cytokine levels

To assess the impact of mild iron deficiency induced by an iron deficient diet on immune parameters, we first compared liver and spleen immune cell subsets in IrDef and IrRepl mice.

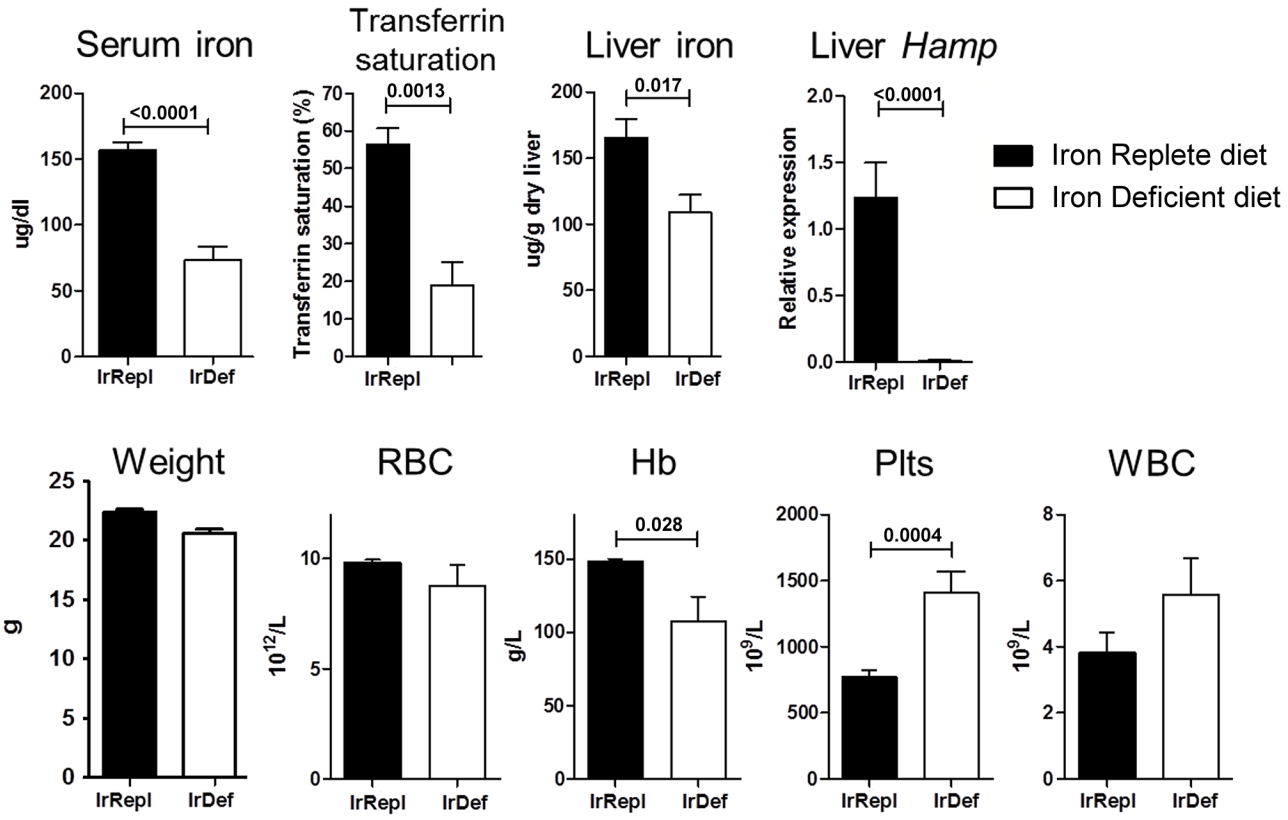

Fig 1. Iron and haematological parameters in mice fed with an iron-deficient diet. Mice were fed for 3 weeks with an iron deficient (IrDef) or iron replete (IrRepl) diet. Bar plots display mean and SEM. Abbreviations: RBC (red blood cells), Hb (Hemoglobin), Plts (platelets), WBC (white blood cells).

doi:10.1371/journal.pone.0136106.g001

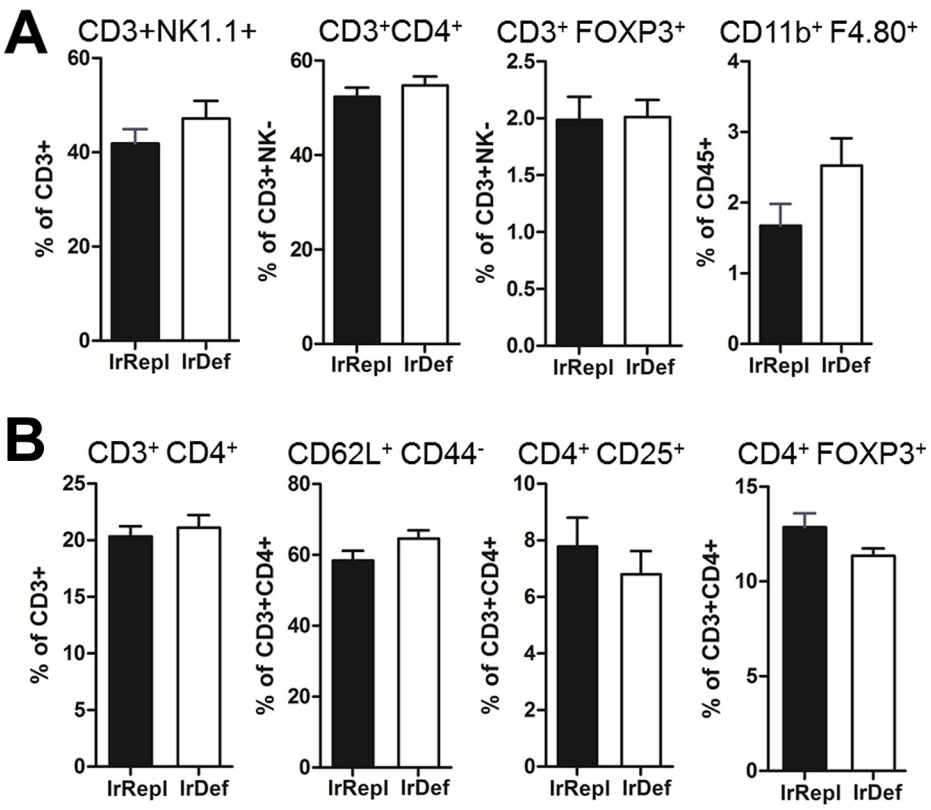

Fig 2. Influence of iron levels on the immunophenotype of intra-hepatic (A) and spleen (B) leukocytes. Mice were fed for 3 weeks with an iron deficient (IrDef) or iron replete (IrRepl) diet. Bar plots show the frequency (mean and SEM) of specific leukocyte subsets in the liver (A) and spleen (B), as assessed by flow cytometry after excluding dead cells.

doi:10.1371/journal.pone.0136106.g002

The 2 groups of mice displayed similar frequencies of intra-hepatic NK1.1$^+$CD3$^+$ NKT, CD4$^+$ and CD8$^+$ T cells, FOXP3$^+$ T cells, cells and resident CD45$^+$CD11b$^+$F4.80$^+$ Kupffer cells (Fig 2A). Similarly, no differences between IrDef and IrRepl splenic T cell subsets were noted, suggesting that in the steady state IrDef does not induce major immunological effects (Fig 2B). We next explored the effects of the iron deficient diet on pro-inflammatory and immunoregulatory genes by measuring the expression of interleukins *Il2*, *Il4*, *Il6*, *Il10*, *Il15*, tumor necrosis factor α (*Tnf*), transforming growth factor β (*Tgfb1*), interferon γ (*Ifng*), *Cd86*, forkhead box P3 (*Foxp3*), and *Cd274* in whole livers, spleens and mesenteric lymph nodes from IrDef and IrRepl mice. No significant changes were observed except for small decreases of *TNFα* (fold change (FC) = -0.36, p = 0.032) and *IFNγ* (FC = -0.72, p = 0.044) transcript levels in the liver and spleen of IrDef mice, respectively (Table 1). Serum cytokine levels were also measured using Luminex technology, and again no significant changes between IrDef and IrRepl mice were observed (Table 2).

Mild iron deficiency significantly dampens inflammatory liver damage following ConA injection

To determine the functional effect of mild iron deficiency on intra-hepatic lymphocyte responses we employed the ConA-induced immune-mediated hepatitis model. Following ConA injection, the rise of alanine aminotransferases (ALT) was significantly lower in IrDef

Table 1. Gene expression in liver, spleen and mesenteric lymph nodes (mesLN) of immune-related molecules from IrDef and IrRepl mice. FC is exhibited as Log_2 of IrDef/IrRepl values. Genes with significant differential expression are highlighted in bold.

		Liver		Spleen		mesLN	
Symbol	**Name**	**FC**	**p.value**	**FC**	**p.value**	**FC**	**p.value**
Il2	Interleukin 2	0.75	0.090	-0.49	0.20	-0.26	0.28
Il4	Interleukin 4	0.32	0.14	-0.038	0.90	0.24	0.50
Il6	Interleukin 6	-0.20	0.39	-0.094	0.70	-0.48	0.15
Il10	Interleukin 10	-0.15	0.48	-0.11	0.74	0.060	0.83
Il15	Interleukin 15	0.098	0.68	-0.38	0.18	0.36	0.13
Ifng	Interferon gamma	0.31	0.26	**-0.72**	**0.044**	0.40	0.54
Tnf	Tumor necrosis factor	**-0.36**	**0.032**	-0.29	0.38	0.024	0.94
Tgfb1	Transforming growth factor, beta 1	0.17	0.14	-0.26	0.14	-0.12	0.53
Foxp3	Forkhead box P3	-0.046	0.88	-0.32	0.34	0.052	0.85
Cd86	CD86 antigen	0.003	0.97	-0.41	0.083	-0.24	0.26
Cd274	CD274 antigen	0.10	0.38	-0.40	0.10	0.020	0.95

doi:10.1371/journal.pone.0136106.t001

mice than in IrRepl mice (p = 0.0028 and 0.0035 at 6 and 12 hours after ConA administration, respectively) (Fig 3A). This was associated with reduced serum levels of the pro-inflammatory cytokines IFNγ, IL6 and TNFα, which reached statistical significance at 6 hours after ConA injection (p = 0.0037, 0.0013 and 0.0021, respectively; Fig 3B). Similar changes were observed in the intra-hepatic expression of *Il4 and Tnfa*, whose transcript levels significantly decreased in IrDef mice 12 hours after ConA injection (p = 0.0053 and p = 0.021, respectively; Fig 3C). These data were consistent with the results of the liver histopathology analysis, which revealed decreased hepatocyte necrosis and inflammatory infiltration in IrDef as compared to IrRepl mice (p = 0.0082 and 0.0020, respectively) (Fig 3D).

Reduced iron availability impairs lymphocyte proliferation and activation

ConA administration triggers an inflammatory cascade that requires activation of T and NKT lymphocytes and eventually results in liver tissue damage [15, 21]. Following ConA activation, lymphocytes produce IFNγ, which is directly involved in the pathogenesis of ConA-induced hepatitis [21–23]. Furthermore, NKT cells down-regulate NK1.1 and CD3 surface markers,

Table 2. Serum level of cytokines measured by Luminex technology from IrDef and IrRepl mice. FC is exhibited as Log_2 of IrDef/IrRepl values.

Symbol	Name	FC	p.value
IFNy	Interferon gamma	0.85	0.59
IL-1α	Interleukin 1alpha	-0.73	0.57
IL-2	Interleukin 2	-3.35	0.20
IL-4	Interleukin 4	0.90	0.48
IL-6	Interleukin 6	-0.48	0.68
IL-10	Interleukin 10	-1.11	0.26
IL-15	Interleukin 15	1.47	0.10
IL-17	Interleukin 17	-1.69	0.15
CXCL10	chemokine (C-X-C motif) ligand 10 (IP-10)	0.008	0.96
CXCL9	chemokine (C-X-C motif) ligand 9 (MIG)	0.41	0.61
TNF α	Tumor necrosis factor alpha	-0.27	0.51

doi:10.1371/journal.pone.0136106.t002

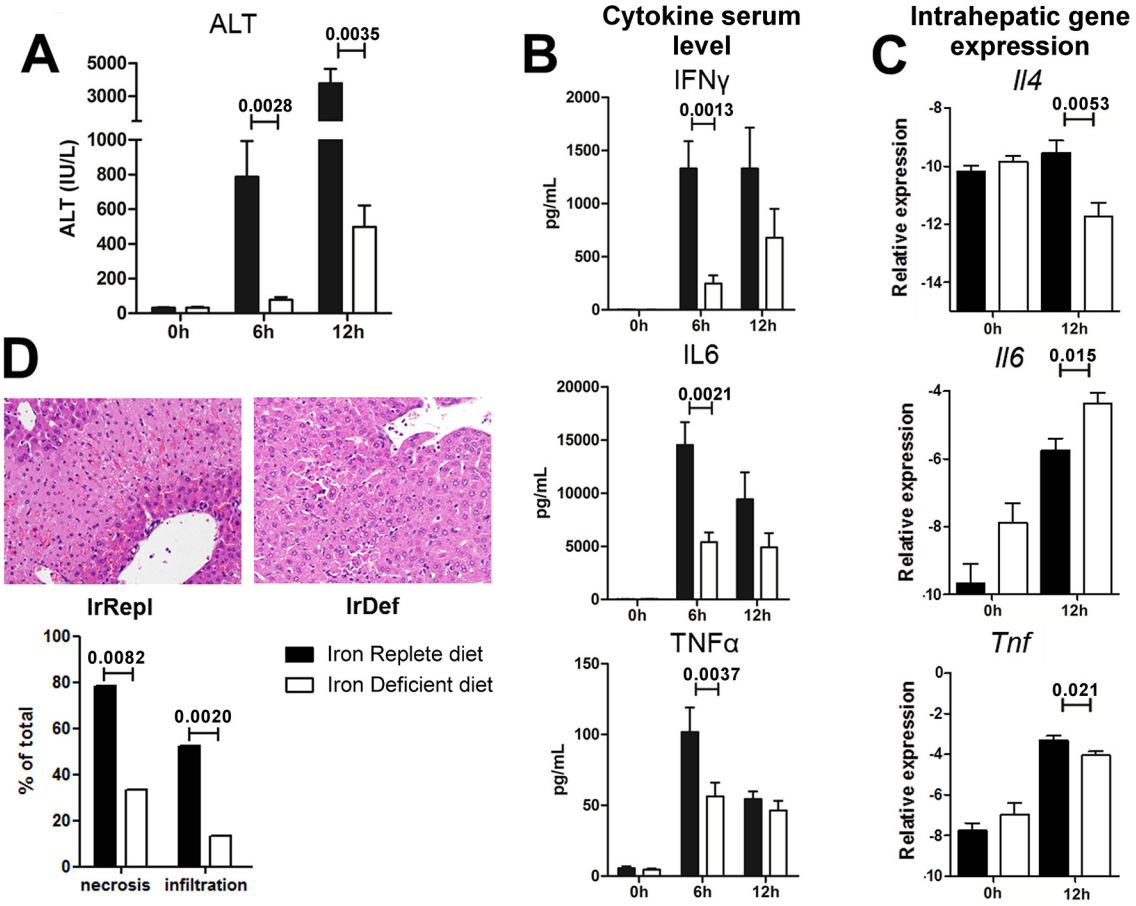

Fig 3. Iron deficiency results in attenuated immune-mediated hepatitis following ConA administration. (A) Serum levels of alanine aminotransferase (ALT; IU/mL) before, 6 hours and 12 hours after administration of ConA in mice fed for 3 weeks with an iron deficient (IrDef) or iron replete (IrRepl) diet. (B) Cytokine levels in serum samples collected before, 6 hours and 12 hours after the administration of ConA. (C) Transcript levels of *Il4*, *Il6 and TNFα* in liver tissue samples collected before and 12 hours after the administration of ConA. (D) Representative liver histology (200x) at 12 hours after the administration of ConA (upper panel) and histologic evaluation of necrosis and infiltration (lower panel).

doi:10.1371/journal.pone.0136106.g003

and the expression of these markers is inversely correlated to the degree of NKT activation [24]. To explore if the effects of iron deficiency are mediated by defective lymphocyte activation, we isolated spleen and intra-hepatic lymphocytes at different time points following ConA administration and assessed their phenotypic and functional properties. In IrDef mice, ConA induced significantly less accumulation of liver-infiltrating $CD3^+$ lymphocytes than in IrRepl mice ($p = 0.048$ at 6 hours; Fig 4A). This was associated with a less striking decrease in the expression of NK1.1 among CD3 cells (a marker of NKT cell activation) both at 3 and 6h following ConA injection ($p = 0.0056$ and 0.029, respectively; Fig 4A). In addition, as compared to IrRepl, 3h after ConA administration intra-hepatic NKT and T lymphocytes from IrDef displayed lower intra-cellular IFNγ levels ($p = 0.034$ and 0.081, respectively; Fig 4B). Interestingly, in contrast to the significant differences observed in the liver compartment, the frequence of IFNγ-producing lymphocytes in the spleen was similar in IrDef and IrRepl mice (Fig 4C).

To confirm the effects of iron deficiency on T cells, we incubated splenocytes *in vitro* with ConA (0.1mg/mL) in the presence of low doses of a specific hydroxypyridinone iron chelator [16, 17] (HPO CP182; 5μM) or desferoxamine (DFO; 10μM). Iron chelation resulted in impaired $CD3^+CD4^+$ T cell proliferation ($p<0.001$). Furthermore, iron chelators also

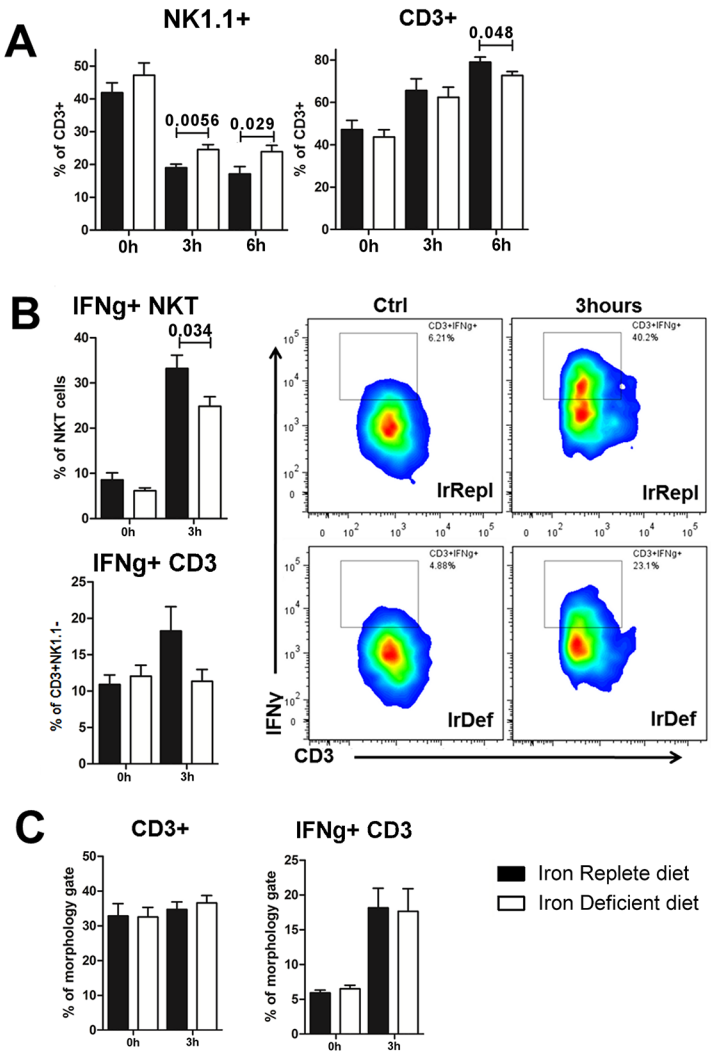

Fig 4. ConA-induced T and NKT lymphocyte activation is reduced in iron deficiency. (A) Intra-hepatic frequency of $CD3^+$ expressing NK1.1 and $CD3^+NK1.1^-$ at baseline, 3 hours and 6 hours after ConA injection. (B) Intra-hepatic frequency of IFNγ production by NKT cells and T cells, defined as $CD3^+NK1.1^+$ and $CD3^+NK1.1^-$, respectively, (left panel) and representative staining of IFNγ production by NKT cells (right panel) (C) Frequency of splenic $CD3^+$ $NK1.1^-$ T cells and the percentage of these ones producing IFNγ.

doi:10.1371/journal.pone.0136106.g004

hampered the activation of isolated $CD4^+$ naïve T cells, which, following stimulation with plate-bound anti-CD3/CD28, showed decreased CD25 expression and cell proliferation (Fig 5).

The effects of iron deficiency in intra-hepatic inflammatory responses are independent from changes in the gut microbiota

Given the influence of the gut microbiota on the liver environment [25] and the well-recognized effects of iron levels on bacterial growth and intestinal microbial composition [26], we next investigated if the reduced immune-mediated hepatitis observed in IrDef mice could be mediated by changes in the number of gut bacteria. IrDef and IrRepl mice received a 3-week course of a 4-antibiotic cocktail known to eliminate >90% of the fecal microbial populations, and ConA was injected at the end of the 3-week period. The results were similar to those

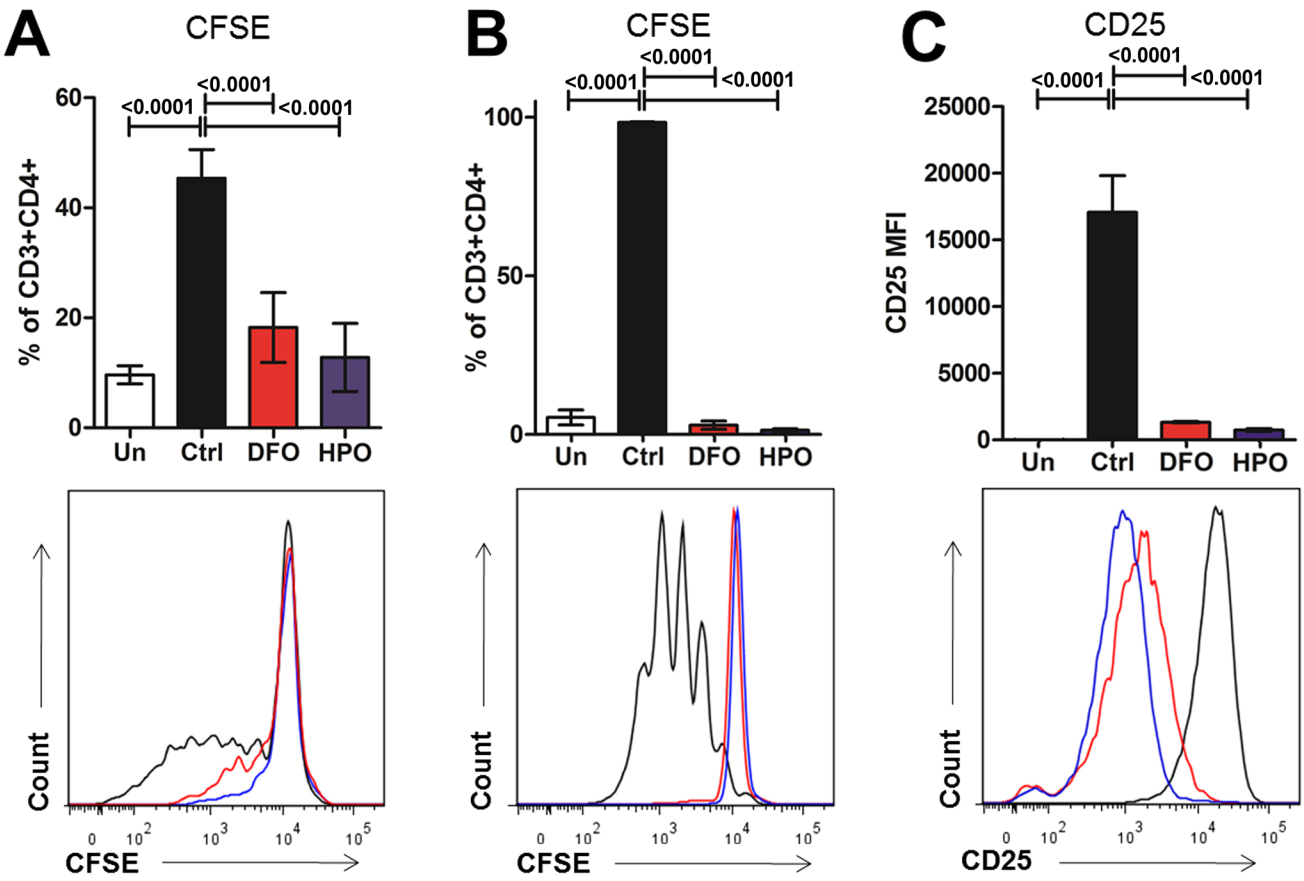

Fig 5. Iron chelation impairs CD4$^+$ T cell activation and proliferation *in vitro*. (A) Percentages of CD3$^+$CD4$^+$ cells from splenocytes undergoing in at least one division are represented with representative fluorescent histogram in the lower part. Splenocytes were incubated 96 hours in presence of ConA (0.1mg/mL) and in presence of low doses of iron chelator (HPO CP182, 5μM or DFO, 10μM). (B) Percentages of CD3$^+$CD4$^+$ cells from isolated naive CD4$^+$ cells undergoing in at least one division and (C) CD25 MFI are represented are displayed with representative fluorescent histogram in the lower part. Isolated CD4$^+$ naïve T cells incubated 5 days in presence of anti-CD3/CD28 plate-bound antibody (2μg each). *Un* means unstimulated cells.

doi:10.1371/journal.pone.0136106.g005

observed in mice receiving no antibiotics, with ALT levels being significantly reduced in IrDef as compared with IrRepl mice (Fig 6A).

Intra-hepatic inflammatory responses are influenced by iron but not by baseline hepcidin level

Iron deficiency results in reduced hepcidin expression which in some models can exert direct immune regulatory effects [19]. We sought to determine if the effects of the iron deficient diet on immune-mediated hepatitis could be due to differences in hepcidin levels rather than to changes in iron status. Mice fed with a standard diet were treated with a 3 day-course of the HPO CP28 iron chelator [16, 17] capable of specifically chelating intra-cellular iron without decreasing intra-hepatic hepcidin expression ($p = 0.48$) (Fig 6B). Similarly to what was observed employing iron deficient diet, mice treated with the iron chelator displayed a significantly reduced ConA-induced hepatitis ($p = 0.041$) (Fig 6C). In parallel, administration of exogenous hepcidin to IrDef mice 2h prior to ConA injection did not restore the blunted immune-mediated hepatitis induced by ConA ($p = 0.84$; Fig 6D). Altogether, these results suggest that iron restriction inhibits lymphocyte activation and ConA-induced hepatitis independently from its effects on hepcidin secretion.

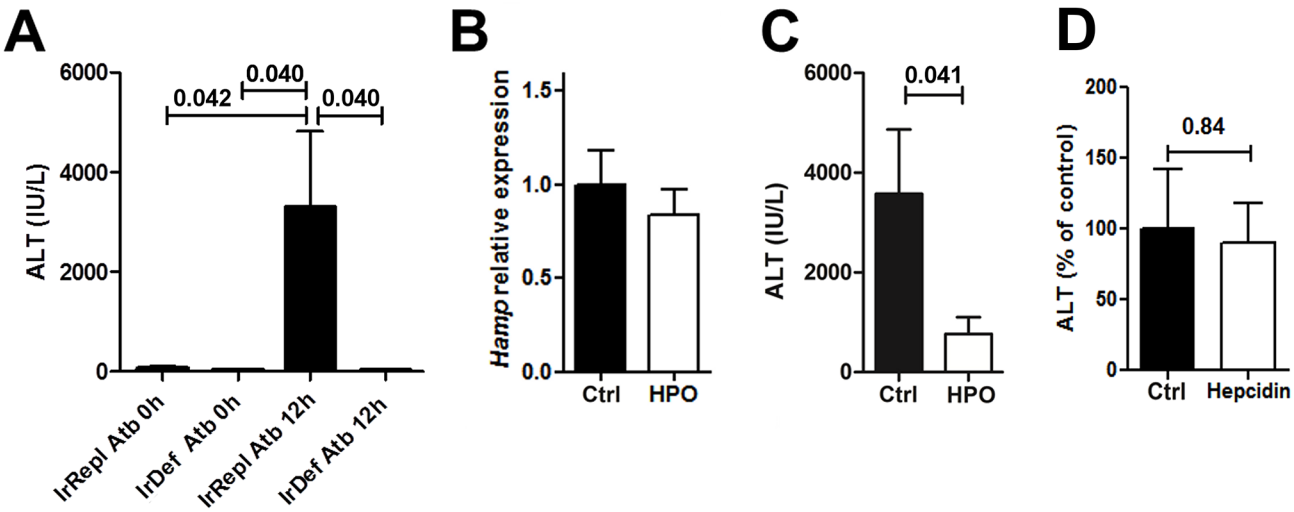

Fig 6. The inhibitory effects of iron deficiency in ConA-induced hepatitis are independent from changes in gut microbiome and hepcidin levels. (A) ALT serum levels (IU/mL) before, and 12 hours after the administration of ConA to mice fed for 3 weeks with an iron deficient (IrDef) or iron replete (IrRepl) diet, in the presence or absence of a 4-antibiotic (Atb) cocktail. (B) Relative expression of *Hamp* in liver tissue samples from mice receiving a 3 day-course of HPO CP28 (20 nmoles, daily) compared to control mice receiving PBS (p = 0.48). (C) ALT serum levels 12 hours after ConA challenge in mice treated with HPO CP28 or with PBS (p = 0.041). (D) ALT serum levels 12 hours after ConA challenge in mice pre-treated two hours before with a single intraperitoneal injection of 100μg of mouse hepcidin or sterile PBS (p = 0.84). Bar plots display mean and SEM.

doi:10.1371/journal.pone.0136106.g006

Discussion

In the current study we investigated the impact of small changes in systemic iron status on intra-hepatic lymphocyte-mediated immune responses. Our experiments were prompted by the results of a recently reported multi-centre clinical trial of immunosuppression discontinuation following liver transplantation [11, 27], in which liver recipients who developed rejection exhibited lower iron storage markers (*e.g.* serum ferritin and serum and intra-hepatic hepcidin) than recipients who successfully discontinued immunosuppression (operationally tolerant recipients). These differences were statistically significant and very reproducible, but small in magnitude and not clinically apparent. Given that spontaneous liver allograft tolerance is known to require activation of recipient alloreactive T cells prior to lymphocyte deletion [12, 13, 28], we hypothesized that the iron/hepcidin axis could play an unappreciated role in the regulation of intra-hepatic lymphocyte activation and function.

To test this hypothesis we selected a well-established model of immune-mediated hepatitis that is tightly controlled by the interplay between cytokines, lymphocytes and Kupffer cells, and in which intra-hepatic T/NKT cell activation is necessary for inflammatory liver damage to occur [15, 21, 23]. We replicated the mild iron homeostasis changes observed in the cohort of liver transplant recipients by feeding mice with an iron-deficient diet for just 3 weeks or by administering low-dose iron-specific chelators. Short-term reduction in iron intake did not have a significant impact on the hepatic steady-state immune homeostasis. On the other hand, the magnitude of liver damage upon ConA stimulation was significantly reduced in iron deficient mice, as assessed by decreased serum ALT levels, hepatic necrosis and intra-hepatic cellular infiltration. This was associated with a decrease in systemic levels of pro-inflammatory cytokines such as IL6, TNFα and IFNγ, and with reduced intra-hepatic transcript levels of *IL4* and *Tnfα*, all of them known to regulate ConA immune-mediated hepatitis.

A beneficial effect of dietary iron restriction or DFO iron chelation on liver inflammation was previously reported in experimental animal models of thioacetamide-induced toxic

hepatitis [5] and Fas-induced fulminant hepatitis [6]. The anti-inflammatory effects of iron restriction were attributed to a reduction in oxidative stress, and a decreased Kupffer and hepatic stellate cell activation. While oxidative stress and macrophage activation are certainly involved in amplifying liver damage following ConA administration, our findings that iron deficiency results in decreased intra-hepatic T/NKT lymphocyte infiltration and reduced lymphocyte activation and effector function indicates that iron deficiency can also influence the outcome of immune-mediated hepatitis by directly inhibiting intra-hepatic lymphocyte function. These results were confirmed in *in vitro* experiments in which isolated T cells were stimulated with either ConA or anti-CD3/anti-CD28. In these experiments, iron chelation resulted in impaired T cell activation and proliferation.

Our observations indicating that changes in iron status can regulate inflammatory organ damage by influencing lymphocyte activation and proliferation are consistent with results obtained in experimental autoimmune encephalomyelitis, a $CD4^+$-driven model in which iron deficiency prevents the development of immunopathology [7]. The mechanisms responsible for T lymphocyte inhibition still remain to be fully deciphered. Intracellular iron deprivation can impair the function of various enzymes involved in cell-cycle control, such as the ribonucleotide reductase [29], involved in DNA synthesis during phase S of cell cycle, cyclin A, and Cdc2 [30]. Iron restriction can also inhibit the hydrolysis of phosphatidyl inositol-4,5-biphosphate and the activity of kinase C protein, both of which are key in the cascade of intracellular signalling events elicited by T cell activation [10, 31]. In addition, at least in the central nervous system, DFO inhibits CXCL10 release following Toll-like receptor 3 (TLR3) engagement [32], which can result in decreased tissue infiltration by $CXCR3^+$ T cells.

Given that in some experimental models hepcidin has been reported to be capable of directly inhibiting systemic inflammatory responses independently from iron levels [19, 33], we explored the relative contributions of low iron versus low hepcidin levels in the regulation of ConA-induced immune hepatitis. As expected, iron deprivation resulted in decreased hepatocyte hepcidin expression, which persisted even following the induction of immune-mediated liver damage (data not shown). We investigated the role of low iron levels by administering an iron-specific chelator that does not influence hepatocyte hepcidin expression. Iron chelation replicated the results observed by feeding the animals with an iron deficient diet. We next tested the effect of injecting exogenous hepcidin prior to ConA challenge, which did not modify the inhibitory effects of iron deprivation. We concluded that low iron levels are the major determinant of the reduced liver inflammatory damage observed in iron deficient mice following ConA administration. Considering the effector role played by macrophages in ConA-induced hepatitis, our results appear to be in contrast with observations indicating that iron-deprived macrophages exhibit increased release of pro-inflammatory mediators following activation with LPS [19, 33]. While these observations still need to be clarified, as they have not been confirmed by other studies [34], they suggest that iron deficiency elicits complex immunological effects that are dependent on the specific cell being targeted and on the organ involved in the inflammatory response. Hence, we speculate that the need for effective T cell activation in order for ConA to induce immune mediated liver damage injection, in contrast to what happens when systemic inflammation is provoked by LPS administration, is what determines the different outcomes observed in the 2 models in situations of iron deficiency.

Dietary iron manipulations can modify gut microbiota composition, which may influence liver metabolism and immunogenicity [25]. To exclude this possibility we employed an antibiotic cocktail capable of eliminating >90% of the fecal microbial populations [14]. Iron deficiency was still associated with significantly reduced immune mediated liver damage even in the presence of markedly reduced intestinal bacterial populations. It is noteworthy, however, that as compared with control animals receiving no antibiotic treatment, mice treated with

antibiotics exhibited lower transaminase levels following ConA. This was particularly striking in IrDef mice, in which hepatitis was almost completely abrogated. These observations are in agreement with a previous report in which gentamycin decreased ConA-induced liver injury by impairing intestinal dendritic cells function and intra-hepatic NKT cells activation [35]. Thus, in the ConA model, iron deficiency and antibiotic treatment are likely to deliver additive effects by powerfully inhibiting T/NKT cell activation.

While serum Il6 level was decreased after ConA injection in IrDef, we observed an increase of *Il6* expression in the liver. Il6 is commonly described as a pro-inflammatory molecules but our clear read-out of transaminases in the ConA model excludes an exacerbation of liver inflammation. Conversely, Il6 and the subsequent STAT3 phosphorylation have been described to be associated with a reduction of liver injury [36, 37]. The increase *Il6* expression is consistent with a hepatoprotective effect in our setting, but whether IrDef directly participate to this increase of *Il6* expression or this expression is hampered by higher liver damages in IrRepl remains to be determined. The inverse correlation of Il6 levels between serum and liver may reflect the different immunological effects exerted by iron deficiency in the liver as compared with other compartments, or may be the result of an opposite effect exerted on different cell types (*e.g.* hepatocytes versus macrophages). Indeed, low hepcidin levels induced by IrDef could be responsible of increased IL6 production by intra-hepatic macrophages as previously described [33].

In conclusion, we report here that iron deprivation impairs intra-hepatic lymphocyte activation and proliferation and results in a beneficial effect on immune mediated hepatitis. Given the central role of the liver in the regulation of iron homeostasis, both as an iron reservoir and as the main source of circulating hepcidin, these findings have implications for a variety of inflammatory liver disorders. Further studies will be needed to ascertain whether all lymphocyte subsets are equally sensitive to iron deprivation, and to determine how iron influences lymphocyte function in situations of chronic antigenic stimulation.

Supporting Information

S1 Fig. percentages of dead cells ($7AAD^+CD4^+$) relative to control in presence of various concentrations of DFO and CP182 with splenocytes activated with CD3/CD28 antibodies during 3 days (1A) and in experiments presented in Fig 5A and 5B and 5C with activated total splenocytes or $CD4^+$ naïve T cells, respectively. Representative Annexin V stainings in activated $CD4^+$ naïve T cells are exhibited in supplementary figure 1D with no significant differences between groups.
(PPTX)

Acknowledgments

The research was funded by the Medical Research Council (MRC) grant no. MR/L008890/1. The research was supported by the MRC Centre for Transplantation (MRC grant no. MR/J006742/1) and by the National Institute for Health Research (NIHR) Biomedical Research Centre based at Guy's and St Thomas' NHS Foundation Trust and King's College London. The views expressed are those of the author(s) and not necessarily those of the NHS, the NIHR or the Department of Health.

Author Contributions

Conceived and designed the experiments: ER RD MML ASF. Performed the experiments: ER RD MMP EK RMM MB MML. Analyzed the data: ER RD JJ MB MML. Contributed reagents/materials/analysis tools: HLC RCH. Wrote the paper: RD HLC RCH MML ASF.

References

1. Nemeth E, Rivera S, Gabayan V, Keller C, Taudorf S, Pedersen BK, et al. IL-6 mediates hypoferremia of inflammation by inducing the synthesis of the iron regulatory hormone hepcidin. The Journal of clinical investigation. 2004; 113(9):1271–6. doi: 10.1172/JCI20945 PMID: 15124018; PubMed Central PMCID: PMC398432.
2. Ganz T. Systemic iron homeostasis. Physiological reviews. 2013; 93(4):1721–41. doi: 10.1152/physrev.00008.2013 PMID: 24137020.
3. Nairz M, Fritsche G, Crouch ML, Barton HC, Fang FC, Weiss G. Slc11a1 limits intracellular growth of Salmonella enterica sv. Typhimurium by promoting macrophage immune effector functions and impairing bacterial iron acquisition. Cellular microbiology. 2009; 11(9):1365–81. doi: 10.1111/j.1462-5822.2009.01337.x PMID: 19500110; PubMed Central PMCID: PMC3467104.
4. Oexle H, Kaser A, Most J, Bellmann-Weiler R, Werner ER, Werner-Felmayer G, et al. Pathways for the regulation of interferon-gamma-inducible genes by iron in human monocytic cells. Journal of leukocyte biology. 2003; 74(2):287–94. PMID: 12885946.
5. Otogawa K, Ogawa T, Shiga R, Nakatani K, Ikeda K, Nakajima Y, et al. Attenuation of acute and chronic liver injury in rats by iron-deficient diet. American journal of physiology Regulatory, integrative and comparative physiology. 2008; 294(2):R311–20. doi: 10.1152/ajpregu.00735.2007 PMID: 18032466.
6. Sato T, Kobune M, Murase K, Kado Y, Okamoto T, Tanaka S, et al. Iron chelator deferasirox rescued mice from Fas-induced fulminant hepatitis. Hepatology research: the official journal of the Japan Society of Hepatology. 2011; 41(7):660–7. doi: 10.1111/j.1872-034X.2011.00821.x PMID: 21711425.
7. Grant SM, Wiesinger JA, Beard JL, Cantorna MT. Iron-deficient mice fail to develop autoimmune encephalomyelitis. The Journal of nutrition. 2003; 133(8):2635–8. PMID: 12888650.
8. Ikeda Y, Ozono I, Tajima S, Imao M, Horinouchi Y, Izawa-Ishizawa Y, et al. Iron chelation by deferoxamine prevents renal interstitial fibrosis in mice with unilateral ureteral obstruction. PloS one. 2014; 9(2): e89355. doi: 10.1371/journal.pone.0089355 PMID: 24586712; PubMed Central PMCID: PMC3929716.
9. Minamiyama Y, Takemura S, Kodai S, Shinkawa H, Tsukioka T, Ichikawa H, et al. Iron restriction improves type 2 diabetes mellitus in Otsuka Long-Evans Tokushima fatty rats. American journal of physiology Endocrinology and metabolism. 2010; 298(6):E1140–9. doi: 10.1152/ajpendo.00620.2009 PMID: 20215574.
10. Kuvibidila S, Baliga BS, Murthy KK. Impaired protein kinase C activation as one of the possible mechanisms of reduced lymphocyte proliferation in iron deficiency in mice. The American journal of clinical nutrition. 1991; 54(5):944–50. PMID: 1951169.
11. Bohne F, Martínez-Llordella M, Lozano J-J, Miquel R, Benítez C, Londoño M-C, et al. Intra-graft expression of genes involved in iron homeostasis predicts the development of operational tolerance in human liver transplantation. J Clin Invest. 2012; 122(1):368–82. doi: 10.1172/JCI59411 PMID: 22156196
12. Benseler V, McCaughan GW, Schlitt HJ, Bishop GA, Bowen DG, Bertolino P. The liver: a special case in transplantation tolerance. Seminars in liver disease. 2007; 27(2):194–213. doi: 10.1055/s-2007-979471 PMID: 17520518.
13. Li W, Kuhr CS, Zheng XX, Carper K, Thomson AW, Reyes JD, et al. New insights into mechanisms of spontaneous liver transplant tolerance: the role of Foxp3-expressing CD25+CD4+ regulatory T cells. American journal of transplantation: official journal of the American Society of Transplantation and the American Society of Transplant Surgeons. 2008; 8(8):1639–51. doi: 10.1111/j.1600-6143.2008.02300.x PMID: 18557727.
14. Corbitt N, Kimura S, Isse K, Specht S, Chedwick L, Rosborough BR, et al. Gut bacteria drive Kupffer cell expansion via MAMP-mediated ICAM-1 induction on sinusoidal endothelium and influence preservation-reperfusion injury after orthotopic liver transplantation. The American journal of pathology. 2013; 182(1):180–91. doi: 10.1016/j.ajpath.2012.09.010 PMID: 23159949; PubMed Central PMCID: PMC3532712.
15. Tiegs G, Hentschel J, Wendel A. A T cell-dependent experimental liver injury in mice inducible by concanavalin A. The Journal of clinical investigation. 1992; 90(1):196–203. doi: 10.1172/JCI115836 PMID: 1634608; PubMed Central PMCID: PMC443081.
16. Fakih S, Podinovskaia M, Kong X, Schaible UE, Collins HL, Hider RC. Monitoring intracellular labile iron pools: A novel fluorescent iron(III) sensor as a potential non-invasive diagnosis tool. Journal of pharmaceutical sciences. 2009; 98(6):2212–26. doi: 10.1002/jps.21583 PMID: 18823046.
17. Baek JH, Reiter CE, Manalo DJ, Buehler PW, Hider RC, Alayash AI. Induction of hypoxia inducible factor (HIF-1alpha) in rat kidneys by iron chelation with the hydroxypyridinone, CP94. Biochimica et biophysica acta. 2011; 1809(4–6):262–8. doi: 10.1016/j.bbagrm.2011.04.010 PMID: 21558026.

18. Ramachandran P, Pellicoro A, Vernon MA, Boulter L, Aucott RL, Ali A, et al. Differential Ly-6C expression identifies the recruited macrophage phenotype, which orchestrates the regression of murine liver fibrosis. Proceedings of the National Academy of Sciences of the United States of America. 2012; 109 (46):E3186–95. doi: 10.1073/pnas.1119964109 PMID: 23100531; PubMed Central PMCID: PMC3503234.

19. Pagani A, Nai A, Corna G, Bosurgi L, Rovere-Querini P, Camaschella C, et al. Low hepcidin accounts for the proinflammatory status associated with iron deficiency. Blood. 2011; 118(3):736–46. doi: 10.1182/blood-2011-02-337212 PMID: 21628413.

20. Evstatiev R, Bukaty A, Jimenez K, Kulnigg-Dabsch S, Surman L, Schmid W, et al. Iron deficiency alters megakaryopoiesis and platelet phenotype independent of thrombopoietin. American journal of hematology. 2014; 89(5):524–9. doi: 10.1002/ajh.23682 PMID: 24464533; PubMed Central PMCID: PMC4114532.

21. Wang HX, Liu M, Weng SY, Li JJ, Xie C, He HL, et al. Immune mechanisms of Concanavalin A model of autoimmune hepatitis. World journal of gastroenterology: WJG. 2012; 18(2):119–25. doi: 10.3748/wjg.v18.i2.119 PMID: 22253517; PubMed Central PMCID: PMC3257438.

22. Kusters S, Gantner F, Kunstle G, Tiegs G. Interferon gamma plays a critical role in T cell-dependent liver injury in mice initiated by concanavalin A. Gastroenterology. 1996; 111(2):462–71. PMID: 8690213.

23. Sass G, Heinlein S, Agli A, Bang R, Schumann J, Tiegs G. Cytokine expression in three mouse models of experimental hepatitis. Cytokine. 2002; 19(3):115–20. PMID: 12242077.

24. Wilson MT, Johansson C, Olivares-Villagomez D, Singh AK, Stanic AK, Wang CR, et al. The response of natural killer T cells to glycolipid antigens is characterized by surface receptor down-modulation and expansion. Proceedings of the National Academy of Sciences of the United States of America. 2003; 100(19):10913–8. doi: 10.1073/pnas.1833166100 PMID: 12960397; PubMed Central PMCID: PMC196902.

25. Bjorkholm B, Bok CM, Lundin A, Rafter J, Hibberd ML, Pettersson S. Intestinal microbiota regulate xenobiotic metabolism in the liver. PloS one. 2009; 4(9):e6958. doi: 10.1371/journal.pone.0006958 PMID: 19742318; PubMed Central PMCID: PMC2734986.

26. Tompkins GR, O'Dell NL, Bryson IT, Pennington CB. The effects of dietary ferric iron and iron deprivation on the bacterial composition of the mouse intestine. Current microbiology. 2001; 43(1):38–42. doi: 10.1007/s002840010257 PMID: 11375662.

27. Benitez C, Londono MC, Miquel R, Manzia TM, Abraldes JG, Lozano JJ, et al. Prospective multicenter clinical trial of immunosuppressive drug withdrawal in stable adult liver transplant recipients. Hepatology. 2013; 58(5):1824–35. doi: 10.1002/hep.26426 PMID: 23532679.

28. Crispe IN. Hepatic T cells and liver tolerance. Nature reviews Immunology. 2003; 3(1):51–62. doi: 10.1038/nri981 PMID: 12511875.

29. Hoffbrand AV, Ganeshaguru K, Hooton JW, Tattersall MH. Effect of iron deficiency and desferrioxamine on DNA synthesis in human cells. British journal of haematology. 1976; 33(4):517–26. PMID: 1009024.

30. Lucas JJ, Szepesi A, Domenico J, Takase K, Tordai A, Terada N, et al. Effects of iron-depletion on cell cycle progression in normal human T lymphocytes: selective inhibition of the appearance of the cyclin A-associated component of the p33cdk2 kinase. Blood. 1995; 86(6):2268–80. PMID: 7662974.

31. Kuvibidila SR, Baliga BS, Warrier RP, Suskind RM. Iron deficiency reduces the hydrolysis of cell membrane phosphatidyl inositol-4,5-bisphosphate during splenic lymphocyte activation in C57BL/6 mice. The Journal of nutrition. 1998; 128(7):1077–83. PMID: 9649588.

32. Imaizumi T, Sakashita N, Mushiga Y, Yoshida H, Hayakari R, Xing F, et al. Desferrioxamine, an iron chelator, inhibits CXCL10 expression induced by polyinosinic-polycytidylic acid in U373MG human astrocytoma cells. Neuroscience research. 2015. doi: 10.1016/j.neures.2015.01.001 PMID: 25591911.

33. De Domenico I, Zhang TY, Koening CL, Branch RW, London N, Lo E, et al. Hepcidin mediates transcriptional changes that modulate acute cytokine-induced inflammatory responses in mice. J Clin Invest. 2010; 120(7):2395–405. doi: 10.1172/JCI42011 PMID: 20530874; PubMed Central PMCID: PMC2898601.

34. Wang L, Harrington L, Trebicka E, Shi HN, Kagan JC, Hong CC, et al. Selective modulation of TLR4-activated inflammatory responses by altered iron homeostasis in mice. J Clin Invest. 2009; 119 (11):3322–8. doi: 10.1172/JCI39939 PMID: 19809161; PubMed Central PMCID: PMC2769199.

35. Chen J, Wei Y, He J, Cui G, Zhu Y, Lu C, et al. Natural killer T cells play a necessary role in modulating of immune-mediated liver injury by gut microbiota. Scientific reports. 2014; 4:7259. doi: 10.1038/srep07259 PMID: 25435303; PubMed Central PMCID: PMC4248284.

36. Mizuhara H, O'Neill E, Seki N, Ogawa T, Kusunoki C, Otsuka K, et al. T cell activation-associated hepatic injury: mediation by tumor necrosis factors and protection by interleukin 6. The Journal of experimental medicine. 1994; 179(5):1529–37. PMID: 8163936; PubMed Central PMCID: PMC2191474.

37. Klein C, Wustefeld T, Assmus U, Roskams T, Rose-John S, Muller M, et al. The IL-6-gp130-STAT3 pathway in hepatocytes triggers liver protection in T cell-mediated liver injury. The Journal of clinical investigation. 2005; 115(4):860–9. doi: 10.1172/JCI23640 PMID: 15761498; PubMed Central PMCID: PMC1059450.

Figure S1

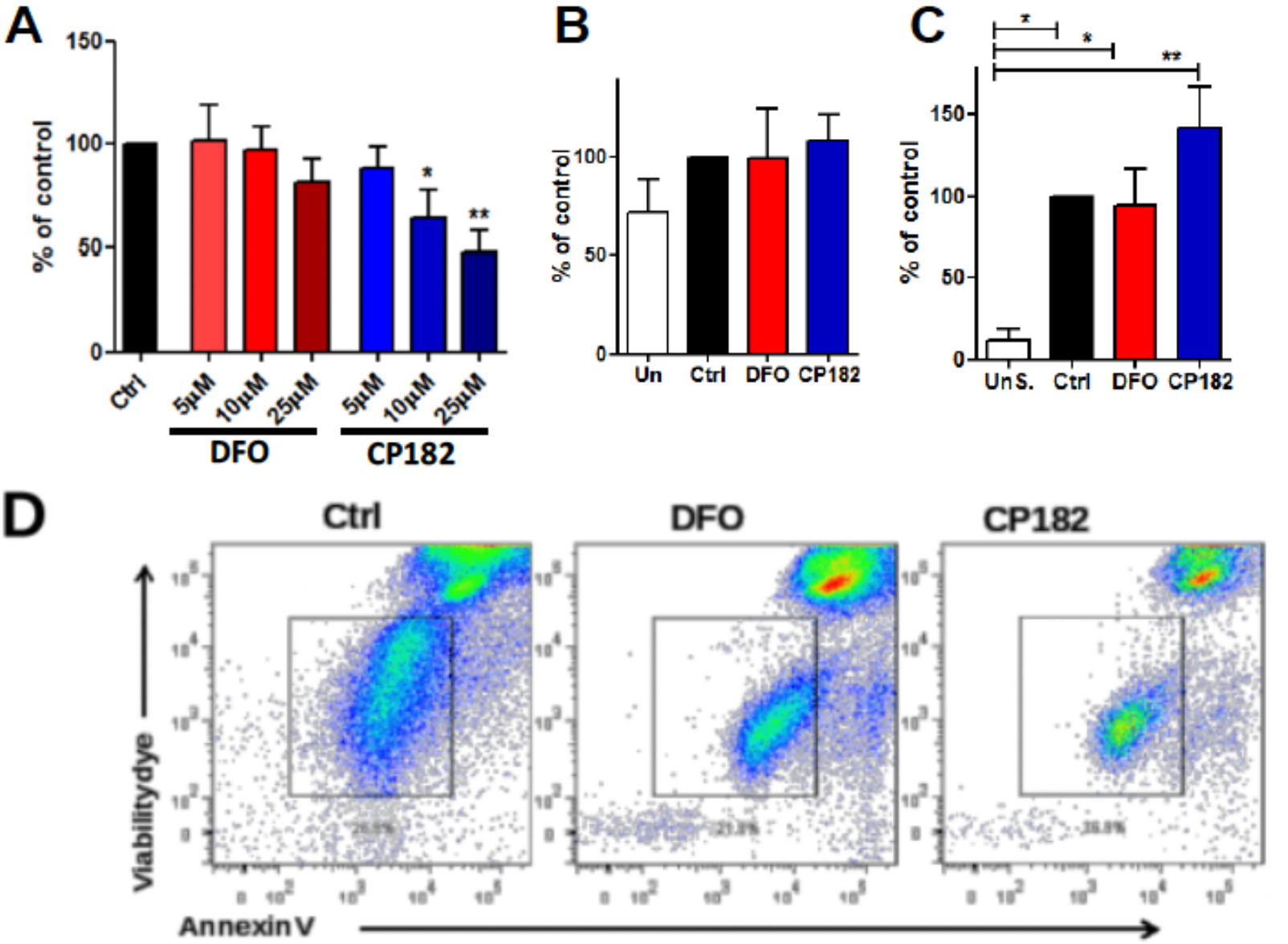
A
150
100
50
0
% of control
*
**
Ctrl
5μM
10μM
25μM
5μM
10μM
25μM
DFO
CP182
B
100
50
0
% of control
Un
Ctrl
DFO
CP182
C
*
*
**
150
100
50
0
% of control
Un S.
Ctrl
DFO
CP182
D
Ctrl
DFO
CP182
Viability dye
Annexin V

Appendix C: Paper: Molecular Characterization of Acute Cellular Rejection Occurring During Intentional Immunosuppression Withdrawal in Liver Transplantation.

American Journal of Transplantation 2015; XX: 1–13
Wiley Periodicals Inc.

© Copyright 2015 The American Society of Transplantation and the American Society of Transplant Surgeons

doi: 10.1111/ajt.13488

Molecular Characterization of Acute Cellular Rejection Occurring During Intentional Immunosuppression Withdrawal in Liver Transplantation

E. Bonaccorsi-Riani[1,†], A. Pennycuick[1,†], M.-C. Londoño[2], J.-J. Lozano[3], C. Benítez[2], B. Sawitzki[4], M. Martínez-Picola[2], F. Bohne[5], M. Martínez-Llordella[1], R. Miquel[1], A. Rimola[2] and A. Sánchez-Fueyo[1,2,*]

[1]*Department of Liver Studies, Division of Transplantation Immunology and Mucosal Biology, Medical Research Council Centre for Transplantation, Faculty of Life Sciences and Medicine, King's College London University, King's College Hospital, Denmark Hill, London, UK*
[2]*Liver Unit, Hospital Clinic Barcelona, Institut d' Investigacions Biomedicas August Pi i Sunyer (IDIBAPS), Networked Biomedical Research Centre of Hepatic and Digestive Diseases (CIBERehd), University of Barcelona, Barcelona, Spain*
[3]*Bioinformatics Platform, CIBEREHD, Barcelona, Spain*
[4]*AG Transplantationstoleranz, Charite Universitätsmedizin, Institut für Med. Immunologie, Berlin, Germany*
[5]*Institute of Virology, Technische Universität München/ Helmholtz Zentrum München, Munich, Germany*
[*]*Corresponding author: Alberto Sanchez-Fueyo, sanchez_fueyo@kcl.ac.uk*
[†]*Contributed equally.*

Acute cellular rejection occurs frequently during the first few weeks following liver transplantation. During this period, its molecular phenotype is confounded by peri- and postoperative proinflammatory events. To unambiguously define the molecular profile associated with rejection, we collected sequential biological specimens from 55 patients at least 3 years after liver transplantation who developed rejection during trials of intentional immunosuppression withdrawal. We analyzed liver tissue and blood samples obtained before initiation of drug withdrawal and at rejection, alongside blood samples collected during the weaning process. Gene expression profiling was conducted using whole-genome microarrays and real-time polymerase chain reaction. Rejection resulted in distinct blood and liver tissue transcriptional changes in patients who were either positive or negative for hepatitis C virus (HCV). Gene expression changes were mostly independent from pharmacological immunosuppression, and their magnitude correlated with severity of histological damage. Differential expression of a subset of genes overlapped across all conditions. These were used to define a blood predictive model that accurately identified rejection in HCV-negative, but not HCV-positive, patients. Changes were detectable 1–2 mo before rejection was diagnosed. Our results provide insight into the molecular processes underlying acute cellular rejection in liver transplantation and help clarify the potential utility and limitations of transcriptional biomarkers in this setting.

Abbreviations: ABMR, antibody-mediated rejection; ACR, acute cellular rejection; AKI, acute kidney injury; ALT, alanine aminotransferase; AST, aspartate aminotransferase; AUC, area under the curve; CNI, calcineurin inhibitor; CSA, cyclosporin A; DSA, donor-specific antibody; FC, fold change; FDR, false discovery rate; GGT, γ-glutamyltransferase; GSEA, gene set enrichment analysis; HBV, hepatitis B virus; HCV, hepatitis C virus; IFN-γ, interferon-γ; IS, immunosuppression; MSigDB, Molecular Signatures Database; MMF, mycophenolate mofetil; mTOR, mammalian target of rapamycin; NA, not available; NES, normalized enrichment score; PCR, polymerase chain reaction; TAC, tacrolimus; TCMR, T cell–mediated rejection; Tx, transplant

Received 26 June 2015, revised 26 July 2015 and accepted for publication 02 August 2015

Introduction

Over the past three decades, liver transplantation has become an accepted and well-standardized treatment for end-stage liver disease. Together with improvements in surgical techniques, intensive care and infection control, the development of efficient immunosuppressant drugs has been instrumental in increasing patient and graft survival rates (1). Acute cellular rejection (ACR) remains a frequent event, particularly early after liver transplantation, with recent series reporting incidence of ≈30% (2–4). Provided diagnosis is made early, ACR can be easily controlled with additional immunosuppressive medication and does not have negative prognostic implications. If unchecked, it can induce irreversible graft damage and thus remains a key consideration in the differential diagnosis of liver allograft dysfunction. This results in the need to closely monitor transplant recipients and to conduct confirmatory liver biopsies, which are cumbersome and incur substantial costs.

In kidney transplantation, molecular profiling techniques have been widely used to clarify the pathophysiology of

ACR and to develop novel diagnostic tools. In contrast, very few studies have attempted to comprehensively characterize ACR in liver transplantation; therefore, the molecular features of clinical liver allograft rejection remain only partially understood.

Molecular profiling studies in liver transplantation are complicated by the fact that ACR overwhelmingly occurs during the first 2–3 weeks after transplantation, during which time (1) allograft function is often abnormal as a consequence of inflammatory liver damage induced by reperfusion injury and surgical complications, and (2) a substantial proportion of liver recipients develop spontaneously resolving subclinical rejection episodes that are not detected unless protocol liver biopsies are conducted. Unambiguously defining rejection-associated molecular changes remains challenging in this scenario. Trials of intentional immunosuppression withdrawal in selected stable liver recipients provide a unique opportunity to thoroughly characterize the immunobiology of rejection because the medical intervention and the initiation of the rejection response can be timed, potential confounders can be adequately controlled, and sequential biological specimens including liver biopsies are typically obtained. In the current study, we analyzed sequential blood and liver tissue specimens collected from adult liver transplant recipients enrolled in two multicenter clinical trials of immunosuppression withdrawal. We were able to identify rejection-specific gene expression markers in these cohorts. Furthermore, we showed that gene expression changes preceded the clinical diagnosis of ACR and could be used as a predictive tool in this clinical scenario.

Patients and Methods

Patient population and study design

A total of 136 stable liver transplant recipients at least 3 years after liver transplantation were enrolled in two prospective multicenter clinical trials of immunosuppression withdrawal. The first trial (ClinicalTrials.gov NCT00647283) (5) enrolled 102 patients, 12 of whom had hepatitis C virus (HCV) infection with detectable HCV RNA. The second trial (ClinicalTrials.gov NCT00668369) enrolled 34 patients, all whom were HCV RNA positive (6). Identical drug withdrawal protocols were used in the two studies and have been described previously (5,6) (Figure 1). Briefly, immunosuppressive drug doses were gradually tapered by reducing approximately one-quarter to half of the doses every 3 weeks until complete discontinuation over a 6- to 9-mo period. Patients were then followed-up for at least 12 additional months. Protocol liver biopsy samples were obtained in all patients at baseline, at 12 mo after successful drug withdrawal in patients who did not reject, or at time of rejection. Blood samples were taken at enrollment, every 3 weeks during the withdrawal period, at the rejection episode, and monthly during the 12 mo after drug cessation or after resolution of the rejection episode. Patients who did not develop rejection were classified as operationally tolerant as long as immunosuppressive drug cessation was maintained for at least 12 mo and no histological evidence of acute and/or chronic rejection was observed. Rejection was diagnosed by the combination of allograft dysfunction and characteristic liver biopsy findings according to Banff criteria (7).

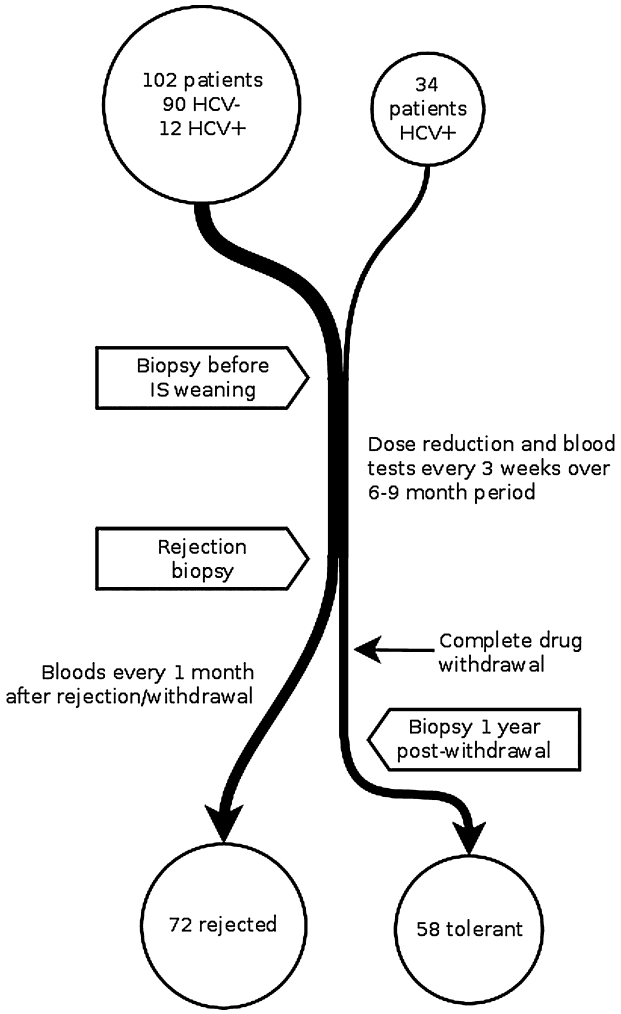

Figure 1: Flow chart showing immunosuppression withdrawal trial design. Data were included from two trials with identical withdrawal protocols (ClinicalTrials.gov NCT00647283 and NCT00668369). A subset of these patients was included in the current study. HCV, hepatitis C virus.

In the first trial, drug withdrawal was successfully achieved in 41 patients, whereas 57 rejected. In the second trial, withdrawal was successful in 17 patients and rejection occurred in 15. Rejection episodes were predominantly mild to moderate and resolved promptly following reinstitution of immunosuppression. No grafts were lost due to rejection. For the current study, we analyzed sequential samples collected from 55 rejecting recipients, 9 of whom were HCV RNA positive (Table 1). In addition, we collected blood samples from a cohort of 86 stable immunosuppressed liver recipients who were matched for age, sex and time from transplantation, with no biochemical evidence of rejection and in whom no attempts at drug withdrawal were performed. Nine early posttransplant rejection biopsies, collected from HCV-negative patients within the first 4 weeks following transplantation and outside the drug-withdrawal setting, were included as a control cohort. Finally, we reanalyzed previously generated gene expression data derived from baseline blood samples from a subset of 25 tolerant recipients.

Table 1: Demographic and clinical characteristics of enrolled patients

Characteristic	Total cohort (n = 55)
Age at transplant (years)	48.23 ± 11.73
Age at weaning start (years)	55.53 ± 11.83
Sex (% male)	54.5
White (%)	100
Transplant indication	
HCV cirrhosis	21
HCV RNA positive at enrolment	(9)
HBV cirrhosis	9
Alcoholic cirrhosis	9
Amyloidotic polyneuropathy	5
Fulminant hepatitis	3
Other causes	8
Time from transplant to weaning start (years)	6.83 ± 3.55
Time from weaning start to rejection (months)	7.82 ± 4.49
Immunosuppressive therapy at weaning start	
Tacrolimus	25
Cyclosporin A	22
Mycophenolate	11
Rapamycine	2
Cyclosporin A + mycophenolate	5
CNI-based immunosuppression at weaning start (%)	85
Immunosuppressive drug trough levels at weaning start (ng/ml)	
Tacrolimus	5.2 ± 2.3
Cyclosporin A	57.4 ± 36
Liver function tests at weaning start	
AST (U/l)	33 ± 22
ALT (U/l)	38 ± 35
GGT (U/l)	40 ± 70
Alkaline phosphatase (U/l)	172 ± 64
Total bilirubin (mg/dl)	0.75 ± 0.3
Rejection severity	
Indeterminate	19
Mild	23
Moderate	7
Severe	6
Banff score*	4 (2–9)
Liver function tests at rejection time	
AST (U/l)	150 ± 137
ALT (U/l)	207 ± 196
GGT (U/l)	188 ± 208
Alkaline phosphatase (U/l)	287 ± 173
Total bilirubin (mg/dl)	1.55 ± 4.51
Rejection treatment	
Baseline IS	23
Baseline IS + prednisone 20 mg/day (4–6 weeks)	26
Baseline IS + prednisone 40–60 mg/day (4–6 weeks)	4
Corticosteroids boluses	2

ALT, alanine aminotransferase; AST, aspartate aminotransferase; CNI, calcineurin inhibitor; GGT, gglutamyltransferase; HBV, hepatitis B virus; HCV, hepatitis C virus; IS, immunosuppression.
*Banff score is expressed as median (range).
Data are expressed as mean ± standard deviation.

Biological specimens

Liver biopsies were taken before the initiation of the immunosuppressive drug withdrawal protocol (baseline) and at the time of rejection. Histological analysis was performed including quantitative measurements obtained for lobular inflammation, central vein perivenulitis, central vein endothelitis, portal inflammation, interface hepatitis, bile duct lesions, ductular reaction, ductopenia, portal vein endothelitis, perisinusoidal fibrosis and portal fibrosis. Blood samples were collected at enrollment, at each drug dose modification (every 3 weeks), at the time rejection was diagnosed, and monthly during the year after rejection or complete drug discontinuation. For the current study, sequential blood and liver tissue specimens were made available from 77 and 33 patients, respectively. RNA was extracted from tissue and blood samples, as described in the Supplementary Methods.

Liver tissue and blood microarray gene expression experiments

Transcriptional profiling of liver tissue samples was conducted using Illumina microarrays. Forty liver tissue RNA samples (preweaning and rejection time points) from 20 patients (13 HCV-negative and 7 HCV-positive patients) were profiled, as described in the Supplementary Methods.

RNA extracted from blood samples was analyzed on a custom Agilent complementary DNA microarray containing probes for 5069 preselected immunology-related transcripts (8). Seventy-four blood samples (37 preweaning blood samples and 37 rejecting blood samples) from 37 nontolerant HCV-negative patients were analyzed. Data acquisition and normalization methods are described in the Supplemental Methods. Analysis for differential expression on a probe basis was done by *limma*, including correction for multiple testing using the false discovery rate (FDR) method.

We defined statistically significant differences in gene expression as those showing fold change (FC) >1.2 and FDR <0.05. To compare expression data across different microarray platforms (i.e. blood vs liver tissue), a lower threshold of significance was used (FC >1.2 and p-value <0.01).

Gene set enrichment analysis

To assess the functional pathways associated with ACR, we used a gene set enrichment analysis (GSEA) application (9,10). This tool compares differentially expressed genes with previously identified gene sets. Three different gene set databases were used for our analyses: (1) the Hallmark gene sets from the Molecular Signatures Database (MSigDB) at the Massachusetts Institute of Technology Broad Institute (10), with 50 gene sets mapped to known biological processes; (2) the HaemAtlas gene set database (11), which contains gene sets preferentially expressed by specific peripheral blood cell subsets (CD4, CD8, CD19, CD14, CD56, CD 66B, EB, MK); and (3) pathogenesis-based transcript gene sets, which have been associated with different subtypes of rejection in both experimental animal models and human kidney and heart allografts (http://atagc.med.ualberta.ca/Research/GeneLists/Pages/default.aspx) (12,13). The full list of gene sets used is shown in Table 3 and Table S2. All analyses were performed using the GSEAPreranked tool, based on t-statistic and a weighted scoring scheme with 1000 permutations.

Correlation between gene expression and liver histopathology

To investigate which histological compartment contributed to the rejection-associated transcriptional changes, we correlated histopathology data with complete liver tissue microarray data. We used a set of 80 biopsy samples from which full quantitative histological data could be uniquely mapped to tissue microarray data. This included 21 samples taken at the point of rejection, 57 biopsies obtained prior to weaning, and two follow-up samples from tolerant patients 1 year after cessation of immunosuppression. Quantitative measurements were available for each of 11 available histological parameters. Each parameter was graded from 0 to 3 for each sample. For each parameter, differentially expressed genes were identified using the limma bioconductor package. A linear regression model was constructed to correlate gene expression with severity of that parameter.

Influence of type of immunosuppression on gene expression patterns

We assessed the influence of immunosuppression (tacrolimus, TAC; cyclosporine A, CSA; mycophenolate mofetil, MMF) on baseline gene expression profiles by constructing linear regression models that explored the impact of each type of immunosuppression on the blood (n = 72) and liver tissue (n = 33) microarray data, using the limma bioconductor package.

Validation real-time polymerase chain reaction experiments in peripheral blood samples

Quantitative real-time polymerase chain reaction (PCR) gene expression experiments were performed using a Fluidigm Biomark HD system, fully described in the Supplementary Methods. The gene expression profiles of 45 target genes plus two housekeeping genes (Table S1) were quantified in 21 paired blood samples (collected at baseline and at the time of rejection) from 14 HCV-negative and 8 HCV-positive patients. An additional group of blood samples collected from 86 stable immunosuppressed liver recipients with no biochemical evidence of rejection was used for comparative purposes. To define a gene expression signature predictive of rejection, we performed a multivariate logistic regression analysis incorporating all Fluidigm gene expression data in the set of paired samples from the group of HCV-negative patients. The best gene model was used to compute the risk probability of rejection in the blood samples collected from the same patients but at different intervals and in all available blood samples from the remaining patients.

In addition to the Fluidigm analyses, we conducted additional real-time PCR experiments as part of the biomarker portfolio studies dictated by the Reprogramming the Immune System for the Establishment of Tolerance (RISET) European consortium. These experiments used an Applied Biosystem real-time PCR platform and quantified the expression of *CD3*, *FOXP3*, *MAN1A1*, *PRF1*, and *TOAG-1* in blood samples collected before the initiation of weaning.

Identification of predictive signatures of rejection

We used multivariate logistic regression to identify gene signatures predictive of rejection among the 45 genes analyzed by Fluidigm real-time PCR. A training set of 14 nontolerant patients from whom Fluidigm data were available both at baseline and at the point of rejection (total samples n = 28) was initially assessed. Given the small number of samples available, the analysis was restricted to signatures containing up to two genes. The regression algorithm used is defined in the varSelec method of the MMIX bioconductor package.

Following variable selection, a generalized linear model was generated using the glm method of the R statistical package (R Foundation for Statistical Computing), using the 28 paired samples to classify a given sample into a rejection or nonrejection (baseline) group. Internal cross-validation was performed using the boot R package. This model was then applied to additional samples to generate a probability of being rejection sample. When applied to samples from patients not exhibiting clinically apparent rejection, we defined the model as giving a ''correct'' result if the probability of rejection was $<50\%$ and an ''incorrect'' result if predicted rejection with $>50\%$ probability.

Results

Acute cellular rejection is associated with a common transcriptional signature regardless of the presence of underlying liver inflammation

To identify the transcriptional patterns most highly associated with ACR, we conducted a paired microarray analysis comparing baseline (preweaning) liver tissue samples with those obtained at the time of rejection in patients with or without HCV infection (7 and 13, respectively). In HCV-negative recipients, rejection was associated with statistically significant changes in 34 transcripts. The impact of rejection was more substantial in HCV-positive recipients, in whom it significantly modified the expression of 408 genes. HCV-positive and -negative recipients shared a common set of 19 genes (Figure 2, Table 2).

We explored functional pathways more highly associated with ACR using GSEA. We compared our data with Hallmark gene sets from MSigDB to identify high-level functional pathways. Differentially expressed genes were involved in a variety of pathways related to, among others, inflammatory response, interferon signaling, IL-6/JAK/STAT3 signaling and apoptosis (Table S2). We next explored the overrepresentation of pathogenesis-based transcript gene sets, which were previously validated in kidney and heart human allografts (12,14–21). Liver samples with ACR showed significant overlap with gene sets associated with T cell–mediated rejection in kidney and heart transplantation, with infiltrating macrophages and effector T lymphocytes being the principal cell subsets involved. ACR was also associated with enrichment in transcripts related to B cells and donor-specific antibodies (DSAs), although the signal was weaker than for T cell–associated transcripts (Table 3).

To confirm the specificity of our results for ACR, we compared our 13 HCV-negative patients with 9 early posttransplant rejection biopsies all taken from HCV-negative patients within the first 4 weeks after transplantation. Although the two cohorts of rejecting patients (i.e. those enrolled in the weaning study and those developing ACR shortly after transplantation) differed in the expression of 213 genes, no differences were noted in the expression of the 19 genes associated with rejection across all conditions (Figure 2C). Furthermore, GSEA revealed enrichment in similar functional pathways (Table S3).

Histological features of rejection correlate with specific gene expression changes

Liver ACR is characterized by portal and, sometimes, lobular inflammation, portal tract nonsuppurative cholangiolitis and portal and/or central vein subendothelial inflammation. To identify the main histological drivers of transcriptional patterns associated with ACR, we correlated gene expression profiles with quantified histological data (Table 4, Table S4). Table 4 shows the distribution of histological damage in our cohort and the number of genes for which expression was significantly correlated with severity of damage (FC >1.2, FDR <0.05).

We observed a correlation between the magnitude of histological damage in each histological compartment and expression of a set of 423 genes mostly associated with

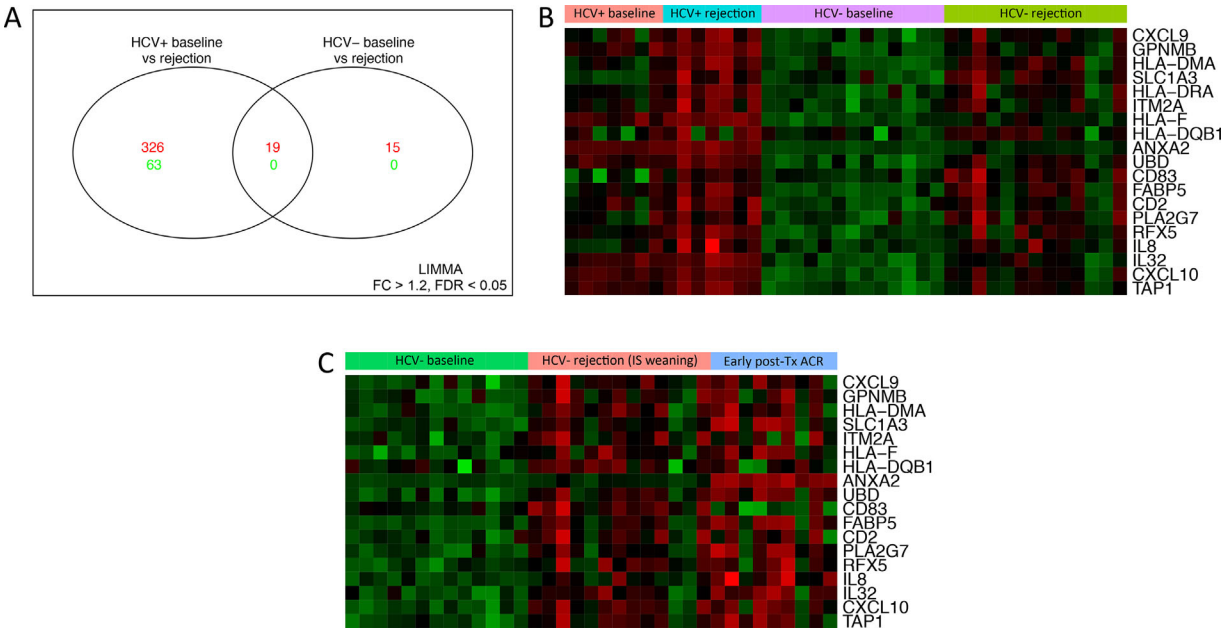

Figure 2: Transcriptional changes associated with rejection in HCV-negative and -positive patients. (A) Venn displaying the number of upregulated (red) or downregulated (green) genes at FDR <5% and FC >1.2 following limma analysis comparing liver tissue samples obtained from HCV-negative and -positive patients at baseline (before IS weaning) and at the time of rejection. (B) Heat map displaying the common set of 19 significantly expressed genes (FC >1.2 and FDR <0.05) comparing baseline (preweaning) liver tissue samples with those collected at time of rejection in HCV-negative and -positive patients. (C) Heat map showing the 19-gene set in HCV-negative patients undergoing weaning and in HCV-negative patients developing rejection shortly after transplantation. *HLA-DRA* is excluded due to poor data quality in the control group. ACR, acute cellular rejection; FC, fold change; FDR, false discovery rate; HCV, hepatitis C virus; IS, immunosuppression; Tx, transplant.

inflammation and rejection. The genes expressed were relatively homogeneous across histological compartments; however, the signal was much stronger in acute inflammatory processes such as lobular inflammation, portal inflammation and interface hepatitis (Figure 3, Table S4).

We used GSEA to investigate the functional pathways driving these histological processes (Table S5). Again, this demonstrated homogeneity across histological compartments, with inflammatory and rejection-associated pathways upregulated across all compartments (with the exception of ductopenia, which was a very infrequent finding and thus could not be adequately explored).

Within the group of rejection biopsies, the overall severity of rejection as defined by the Banff Rejection Activity Index (7) was not associated with significant differential gene expression (based on 20 biopsies with complete rejection activity index data) (data not shown).

Acute cellular rejection results in distinct transcriptional changes in blood that only partially overlap with those observed in the liver allograft

We used the same exploratory approach described above to identify ACR-associated transcriptional patterns in whole blood. This was conducted in paired baseline/rejection samples from 37 HCV-negative patients, with a custom Agilent microarray. Overall, 293 differentially expressed genes were identified with FDR <0.05 and FC >1.2 (Figure 4). Functional analysis using GSEA with the MSigDB Hallmark gene sets showed similar pathways to be upregulated in blood and liver tissue, although the signal was weaker in blood than in tissue (Table 3). Additional analyses using HaemAtlas gene sets (11) revealed that ACR was significantly associated with transcripts preferentially expressed by CD14-positive cells (monocytes). In contrast, transcripts associated with CD8 (cytotoxic T cells) and CD66B (granulocytes) cells were significantly downregulated at the time of rejection. No other blood cell types significantly contributed to the rejection-associated transcriptional pattern. A small group of 22 genes, mostly related to immune response and cell cycle control (e.g. *CXCL9*, *CXCL10*, *CNPM*, *CDC20*, *CCNB2*, and *CD74*), were significantly associated with ACR in both blood and liver tissue samples (Figure 5).

The expression of ACR-associated markers at baseline does not predict the outcome of immunosuppression discontinuation

To determine whether ACR-specific genes were differentially expressed between tolerant and nontolerant liver recipients

Table 2: Liver tissue gene expression markers associated with acute cellular rejection

Gene symbol	Gene name	FC, rejection vs prewean time, HCV−	FDR, HCV−	FC, rejection vs prewean time, HCV+	FDR, HCV+
CXCL9	Chemokine (C-X-C motif) ligand 9	3.214	0.002	3.241	1.42×10^{-6}
GPNMB	Glycoprotein (transmembrane) nmb	1.779	0.006	1.832	0.001
HLA-DMA	Major histocompatibility complex, class II, DM alpha	1.573	0.027	1.764	0.001
SLC1A3	Solute carrier family 1 (glial high affinity glutamate transporter), member 3	1.572	0.027	1.854	0.001
HLA-DRA	Major histocompatibility complex, class II, DR alpha	1.529	0.027	1.734	0.001
ITM2A	Integral membrane protein 2A	1.554	0.027	1.615	0.003
HLA-F	Major histocompatibility complex, class I, F	1.520	0.041	1.605	0.004
HLA-DQB1	Major histocompatibility complex, class II, DQ beta 1	1.615	0.008	1.607	0.005
ANXA2	Annexin A2	1.556	0.032	1.743	0.006
UBD	Ubiquitin D	3.370	0.002	1.678	0.009
CD83	CD83 molecule	1.615	0.008	1.667	0.009
FABP5	Fatty acid binding protein 5 (psoriasis-associated)	2.105	0.002	1.625	0.011
CD2	CD2 molecule	1.480	0.034	1.503	0.013
PLA2G7	Phospholipase A2, group VII	1.631	0.013	1.454	0.022
RFX5	Regulatory factor X, 5 (influences HLA class II expression)	1.419	0.029	1.403	0.026
IL8	Interleukin 8	1.549	0.021	2.194	0.029
IL32	Interleukin 32	1.848	0.006	1.537	0.031
CXCL10	Chemokine (C-X-C motif) ligand 10	3.738	0.002	1.485	0.039
TAP1	Transporter 1, ATP-binding cassette, sub-family B (MDR/TAP)	1.651	0.027	1.363	0.047

Table 2 shows the 19 common differentially expressed genes in HCV-negative and -positive recipients when comparing liver samples at rejection time with liver samples collected before the start the IS withdrawal. FC >1.2, FDR <5%, $p < 0.001$. FC, fold change; FDR, false discovery rate; HCV, hepatitis C virus.

before immunosuppression weaning was initiated, we reinterrogated a previously described Affymetrix microarray gene expression database generated with blood samples collected at baseline (before the initiation of weaning) from 43 nontolerant and 25 tolerant liver recipients (22). At baseline, none of the ACR-associated gene expression markers differed between patients who eventually rejected and those who successfully discontinued immunosuppression (data not shown). In addition to the microarray data, we quantified the expression of *CD3*, *FOXP3*, *MAN1A1*, *PRF1*, and *TOAG-1*, which were part of the RISET consortium biomarker portfolio and had been previously assessed in the setting of kidney transplantation (8,23). Foxp3 expression, which was upregulated in tolerant recipients, was the only marker differentially expressed between the tolerant and nontolerant recipients at baseline (Figure 6).

Pharmacological immunosuppression has a minimal impact on rejection-associated gene expression changes in both blood and liver tissue

We explored the transcriptional impact of specific immunosuppressive drugs to investigate the extent to which pharmacological immunosuppression could act as a confounder in the analyses. The type of immunosuppressive agent did not influence liver tissue gene expression. Analyses of blood gene expression patterns revealed no differences between patients on tacrolimus monotherapy versus cyclosporin A monotherapy. In contrast, a set of 17 genes was differentially expressed between patients on calcineurin inhibitor monotherapy and patients on mycophenolate mofetil monotherapy (Table 5), but only eight were included in the set of 293 genes associated with ACR (LOC652494, ENST00000359488, LOC100132941, ENST00000377226, C13ORF33, A_24_P110487, ENST00000322032, SPTA1).

Sequential gene expression profiling in blood samples during the immunosuppression withdrawal process predicts the development of rejection

To investigate whether changes in rejection-associated transcriptional markers precede the clinical diagnosis of ACR and could be used as a predictive tool, we quantified the expression of a set of 45 target genes in sequential blood samples collected from 14 HCV RNA–negative and 8 HCV RNA–positive recipients. A mean of six sequential blood samples collected before the diagnosis of rejection were available per patient. Univariate analysis of blood samples collected at baseline and at time of rejection revealed that eight and two genes were significantly upregulated at the time of rejection in HCV-negative and -positive patients, respectively (Table 6). Using stepwise multivariate logistic regression, we identified *CXCL10* plus *FOXP3* as the best combination of markers discriminating between rejection and baseline blood samples in

Table 3: Pathogenesis-based transcript sets significantly enriched in liver allograft rejection–associated transcriptional patterns (GSEA)

Symbol	Description	Reference	Size[1]	NES[2] HCV−	FDR HCV−	NES HCV+	FDR HCV+
GRIT1	Human orthologs of IFN-γ dependent, rejection associated transcripts defined in mice; expressed in TCMR, especially in association with AMAT1	(17)	19	2.64	0.00*	2.42	0.00*
QCMAT	Macrophage associated transcripts defined in purified cell lines, associated with TCMR in kidney patients	(16)	45	2.54	0.00*	2.34	0.00*
QCAT	Transcripts associated with cytotoxic T lymphocytes, defined in purified cell lines; associated with TCMR in renal transplants, with expression levels correlating with T cell infiltration	(15)	21	2.48	0.00*	2.44	0.00*
IRITD3	Injury and rejection induced transcripts upregulated day 3 after isograft transplant (humanized results from mouse model)	(39)	173	2.30	0.00*	2.60	0.00*
IRITD5	As for IRITD3, measured on day 5.	(39)	133	2.25	0.00*	2.68	0.00*
CIRIT	Cardiac injury- and repair-induced transcripts, expressed following heart isograft transplant; mouse data extrapolated to humans	(40)	174	2.20	0.00*	2.22	0.00*
IRRAT	Injury-repair response associated transcripts, defined in early renal transplants with no rejection, derived as a model for AKI	(39)	22	2.05	0.00*	1.67	0.00*
BAT	B cell–associated transcripts, derived from purified B cells; upregulated in both ABMR and TCMR	(19)	55	1.97	0.00*	2.15	0.00*
DSAST	DSA-positive–specific transcripts derived from comparative analysis of DSA with and without renal biopsies; observed in both ABMR and TCMR with much higher levels in ABMR	(18)	15	1.64	0.01*	1.18	0.29
HTS	Heart-selective transcripts derived from control mice without inflammation present	(40)	385	1.54	0.03*	1.59	0.01*
TCB	T cell–specific transcripts based on purified cell lines	(21)	4	1.47	0.04*	1.66	0.00*
ENDAT	Endothelial cell associated transcripts derived from purified cell lines; increased in ABMR and TCMR with higher levels in ABMR	(20,41)	81	1.46	0.04*	2.23	0.00*
NKB	Natural killer cell–specific transcripts derived from purified cell lines; identified in early TCMR and late ABMR in renal patients	(21)	3	1.43	0.05	1.04	0.43
IGT	Immunoglobulin associated transcripts, observed in both ABMR and TCMR	(19)	4	1.36	0.08	1.57	0.01*
AMAT1	Alternative Macrophage Associated Transcript 1; human orthologs of mouse data; high GRIT1 plus AMAT1 scores correlate with TCMR	(16)	6	1.31	0.12	1.73	0.00*
MCAT	Mast cell associated transcripts, associated with scarring and poor survival in renal transplants	(22)	3	−0.80	0.78	1.13	0.32

ABMR, antibody-mediated rejection; AKI, acute kidney injury; DSA, donor-specific antibody; FDR, false discovery rate; GSEA, gene set enrichment analysis; IFN-γ, interferon-γ; NES, normalized enrichment score; TCMR, T cell–mediated rejection.

*Significance threshold based on FDR <0.05

[1]Size is the number of transcripts in the gene set.

[2]NES as calculated by GSEA software (http://www.broadinstitute.org/gsea/doc/GSEAUserGuideTEXT.htm#_Interpreting_GSEA_Results).

Table 4: Differential gene expression by histological compartment

	No. of patients by severity level				
Histological compartment	0	1	2	3	Gene count
Lobular inflammation	29	34	15	0	354
Portal inflammation	17	33	21	2	223
Interface hepatitis	44	23	10	0	284
Central vein perivenulitis	53	12	4	0	10
Endothelitis central vein	0	3	0	0	1
Endothelitis portal veins	54	16	3	1	4
Bile duct lesions	51	19	3	1	16
Ductular reaction	50	20	0	0	0
Ductopenia	76	3	0	0	4
Perisinusoildal fibrosis	52	8	5	0	0
Portal fibrosis	29	24	21	2	31

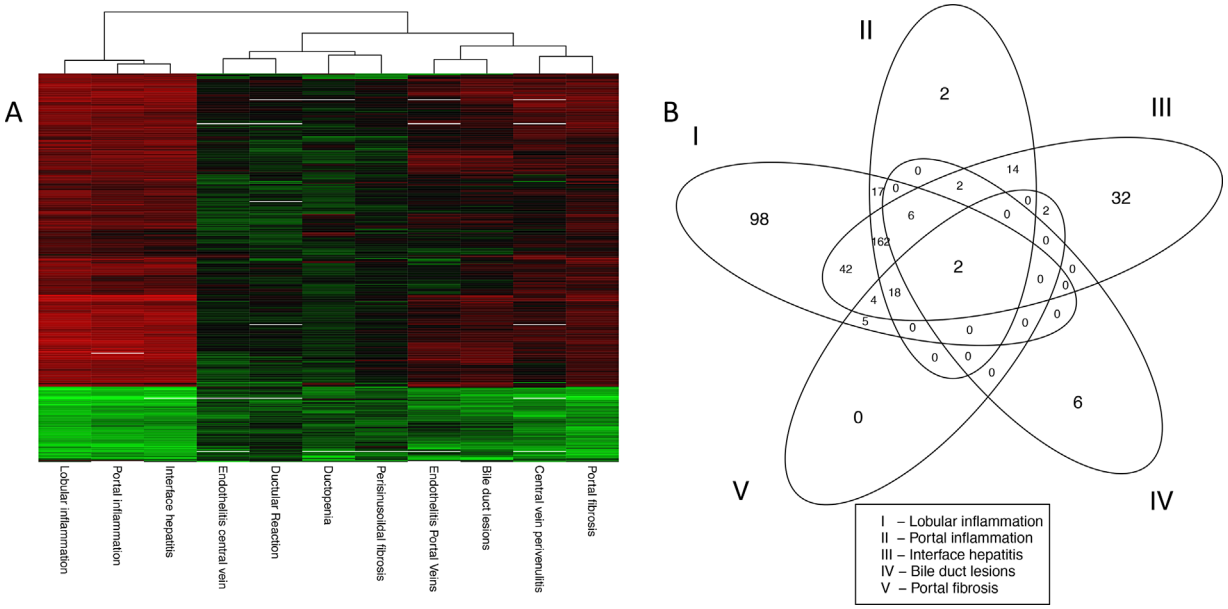

Figure 3: Differentially expressed genes across histological compartments. (A) Clustered heat map demonstrating all genes significantly differentially expressed across histological compartments (fold change >1.2 and false discovery rate <0.05 in at least one compartment). Analysis performed in limma comparing gene expression against quantified severity score for each histological parameter. Red indicates upregulation, green indicates downregulation. (B) Venn diagram showing the number of genes differentially expressed in each histological compartment and demonstrating overlap between compartments.

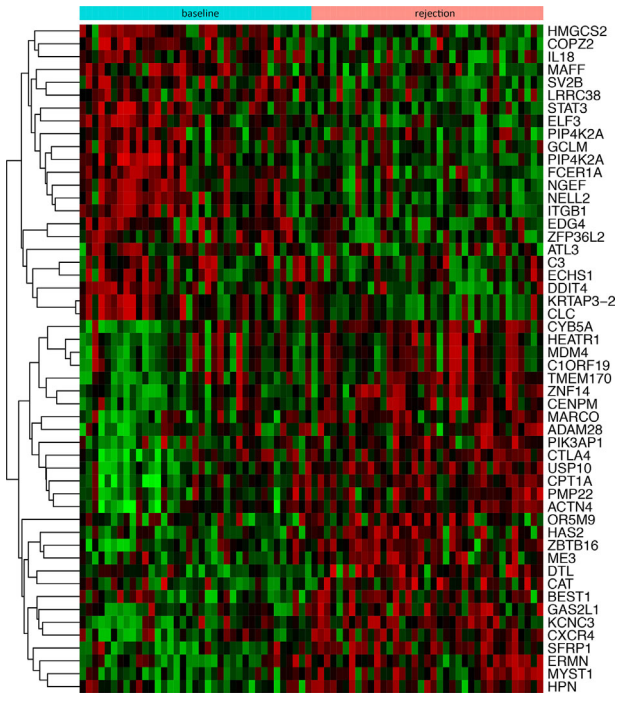

Figure 4: Differentially expressed genes in whole blood. Heat map of the top 50 genes differentially expressed in whole blood based on t-statistic comparing paired baseline (preweaning) and rejection samples. All patients were negative for hepatitis C virus.

HCV-negative patients (cross-validated area under the curve [AUC] 0.82). When using this signature in all sequentially collected blood samples, we observed that the probability of ACR progressively increased with time, with a peak that coincided with the time of the diagnosis of biopsy-proven ACR and a rapid decline following reinstitution of robust immunosuppression (Figure 7A). *CXCL10* plus *FOXP3* expression correctly predicted the absence of rejection in 81% of 86 liver recipients with stable graft function under immunosuppression 3–10 years after transplantation. In contrast, this model failed to correctly classify 70% of 57 blood samples sequentially collected from seven tolerant liver recipients who were successfully weaned from immunosuppression. Given the well-known influence of calcineurin inhibitors on *FOXP3* expression (24), we repeated the logistic regression analysis excluding *FOXP3*. This resulted in *CXCL10* alone being selected as the most robust predictor. *CXCL10* accurately classified rejecting samples with a cross-validated AUC of 0.76 and correctly predicted absence of rejection in 79% of stable patients and 67% of samples from tolerant patients (Figure 7C). The probability of rejection as predicted by *CXCL10* expression increased 1–2 mo prior to rejection being clinically apparent and a liver biopsy considered indicated. A detailed analysis of the kinetics of liver function tests, however, revealed that the changes in *CXCL10* expression mirrored mild but gradually increasing changes in γ-glutamyltransferase, aspartate aminotransferase and alanine aminotransferase occurring over the same time period (Figure 7D). In contrast to these results observed in

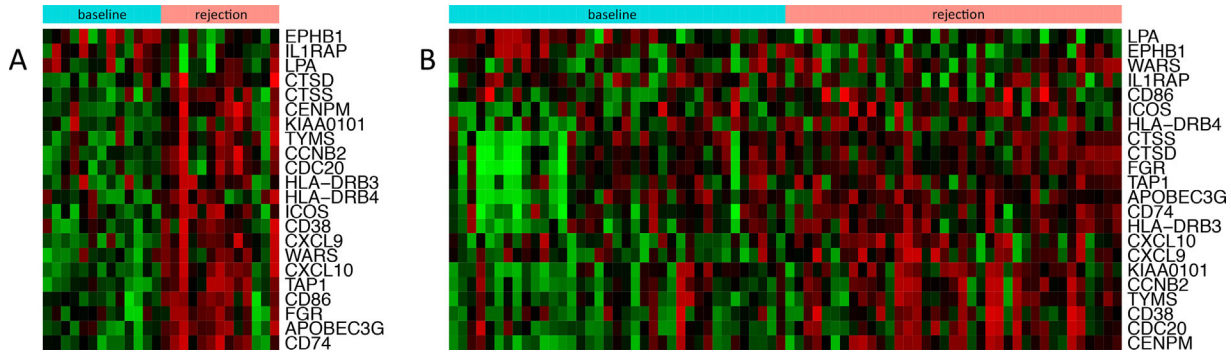

Figure 5: Significantly expressed genes in liver tissues and in PBMC of HCV-negative patients. Heat maps displaying the common set of 22 significantly expressed genes (fold change >1.2 and false discovery rate <0.05) when comparing baseline (preweaning) liver tissue samples (A) with those collected at the time of rejection in HCV-negative patients and in PBMC samples (B) at the same time points for the same patient groups. HCV, hepatitis C virus; PBMC, peripheral blood mononuclear cells.

HCV-negative recipients, a gene expression model with adequate diagnostic performance could not be generated from the 45-gene PCR expression data set in the cohort of seven recipients with active HCV infection (data not shown).

Discussion

The identification of reproducible noninvasive biomarkers of graft rejection remains an important area of research in organ transplantation. In kidney transplantation, the molecular profiles associated with allograft rejection have been comprehensively defined, and results from single- and multicenter studies have shown that specific biomarkers, in particular, mRNAs, can be useful diagnostic tools. In contrast, in liver transplantation, the field is much less developed, and our understanding of the predictive accuracy and specificity of molecular biomarkers in different biological specimens is incomplete.

Similar to other organ transplantation settings, our microarray experiments revealed that there are transcriptional differences between rejecting and nonrejecting liver allografts. Many genes identified in our study are well studied in the context of transplant rejection and correspond to functional networks known to be associated with rejection, such as nuclear factor-κB, STAT1/interferon-γ, tumor necrosis factor-α, chemokine receptor networks and immune effector networks (25). In particular, the set of 19 genes that we identified in tissue samples in both HCV-positive and -negative patients includes genes previously associated with rejection in kidney (*CXCL9, HLA-DMA, IL32, CXCL10, HLA-F, CD2*) (26,27), in lung (*ITM2A, IL8, IL32*) (28), and in heart transplantation (*CXCL9, HLA-F, CXCL10*) (29). A meta-analysis by Spivey *et al* (25) identified 330 genes known to be differentially expressed in rejection tissue samples across a variety of transplanted organs, including liver, kidney, heart and lung. From our set of 19 genes, 12 were previously identified (*CXCL9, HLA-DMA, HLA-DRA, ITM2A, HLA-F, HLA-DQB1, UBD, CD2, IL8,*

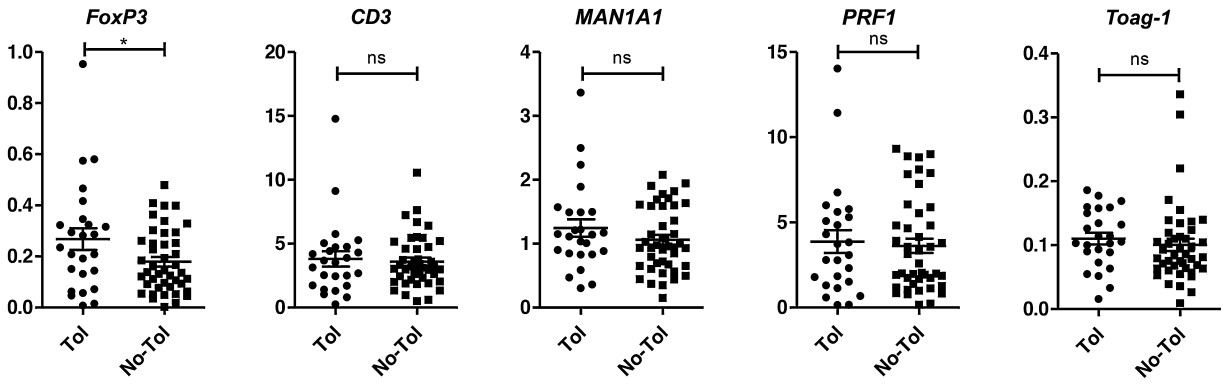

Figure 6: Baseline acute cellular rejection–associated gene expression in nontolerant and tolerant patients. Graphics showing the quantitative gene expression of five genes included in the Reprogramming the Immune System for the Establishment of Tolerance (RISET) consortium biomarker portfolio performed at baseline (preweaning) in 43 nontolerant and 25 tolerant patients. No-Tol, nontolerant; Tol, tolerant. *$p < 0.05$.

Table 5: Differential gene expression by baseline immunosuppression

	Tissue		Blood (microarray)		Blood (Fluidigm)	
Immunosuppression	n	Genes expressed	n	Genes expressed	n	Genes expressed
TAC	18	0	29	0	12	0
CSA	14		23		11	
CNI monotherapy	32	0	52	17[1]	23	NA
MMF monotherapy	6		12		0	
CNI monotherapy	32	0	52	1[2]	23	3[3]
CNI + MMF	6		8		6	
mTOR inhibitor	2	13[4]	0	NA	2	3[5]
Other therapies	44		72		29	

CNI, calcineurin inhibitor; CSA, cyclosporin A; MMF, mycophenolate mofetil; mTOR, mammalian target of rapamycin; NA, not available; TAC, tacrolimus.
[1]*FA2H, SPTA1, TFPI, ENST00000322032, C13ORF33, LOC653513;LOC727893; LOC727927;LOC727942;LOC728802;PDE4DIP;XXYAC-YX155B6.2, CCNF, POGK, SLFN12, LOC652494, ENST00000359488, LOC100132941, ENST00000377226, IGJ, A_24_P110487, LOC644538, PTPRF.*
[2]*IFNA2.*
[3]*CENPM, EZH2, PARVG.*
[4]*TIMD4, GDF15, FOS, IL8, CXCR7, MELK, CETP, JUN, EZH2, CIDEC, STAB2, FOLR2, ZGPAT.*
[5]*CD74, TOP2A, HLA-DMA.*

IL32, CXCL10, TAP1), whereas seven were unique to our study (*GPNMB, SLC1A3, ANXA2, CD83, FABP5, PLA2G7, RFX5*).

Specific to the liver, Sreekumar et al identified a gene signature associated with ACR in HCV-positive patients (30). This study highlighted the difficulties of differentiating ACR from HCV histopathologically. Our HCV-positive results implicate many of the same pathways (e.g. MHC, ubiquitin), if not exactly the same genes. The large number of differentially expressed genes in HCV-positive patients relative to HCV-negative patients in our study supports previous data showing a significant interaction between HCV infection and alloimmune responses at a molecular level (6). The identification of ACR-specific genes independent of HCV infection, however, supports the conclusion of Sreekumar et al that molecular profiling could be useful to aid in this difficult histopathological diagnosis.

T cell–related transcripts were more highly differentially expressed in the liver at the time of ACR. These findings indicate that at the transcriptional level, liver allografts respond to T cell–mediated rejection (TCMR) similarly to what has been described for other organs, particularly kidneys. A significant association, however, was also found with genes known to be overexpressed in kidney allografts exhibiting antibody-mediated rejection (ABMR; i.e. B cells and natural killer cells). This is not entirely surprising, given that the transcriptional differences between TCMR and ABMR in kidney transplantation are more quantitative than qualitative (i.e. pathways described as being specific for ABMR are also observed, albeit with a weaker signal, in the setting of TCMR). This observation will need to be considered if transcriptional profiling is ever used to provide pathogenic guidance in the analyses of liver allograft biopsies exhibiting mixed or unclear histological phenotypes. In contrast to the liver tissue transcriptome results, T cell–related transcripts were decreased in blood at the time of ACR. We hypothesize that this is due to the well-known homing of T cells, particularly $CD8^+$ T cells, to the transplanted organ at the time of allograft rejection (31).

Table 6: Significantly differentially expressed genes at baseline vs rejection based on univariate analysis of Fluidigm data

Gene	p-value (HCV+)	p-value (HCV−)
ABCB1	0.441	0.048*
APOL3	0.383	0.942
CCL19	0.570	0.369
CCN2B	0.053	0.799
CD52	0.083	0.144
CD74	0.567	0.742
CD8A	0.587	0.011*
CDC20	0.777	0.559
CECR1	0.141	0.911
CENPM	0.634	0.505
CXCL10	0.019*	0.794
CXCL9	0.010*	0.809
DHRS9	0.046*	0.933
DOCK11	0.412	0.511
EMILIN2	0.096	0.604
EZH2	0.329	0.263
FOXP3	0.002*	0.321
GBP1	0.689	0.078
GBP2	0.680	0.610
GPNMB	0.856	0.233
GZMB	0.149	0.234
GZMK	0.518	0.053
HLA.DMA	0.718	0.927
HLA.DMB	0.935	0.624
HMMR	0.935	0.254
IL15	0.335	0.436
IL18BP	0.592	0.761
IL32	0.586	0.136
IRF1	0.084	0.532
LYZ	0.062	0.952
ME2	0.327	0.554
MMP9	0.836	0.366
PARVG	0.353	0.354
PLEKHG1	0.788	0.873
PRF1	0.670	0.068
RFX5	0.604	0.731
STAT1	0.024*	0.839
TAP1	0.154	0.937
TGFb1	0.166	0.098
TK1	0.019*	0.608
TLR8	0.978	0.748
TOP2A	0.203	0.572
TYMS	0.013*	0.720
UBD	0.002*	0.209
ZWINT	0.144	0.368

HCV, hepatitis C virus.
*Significant difference between baseline and rejection ($p < 0.05$).

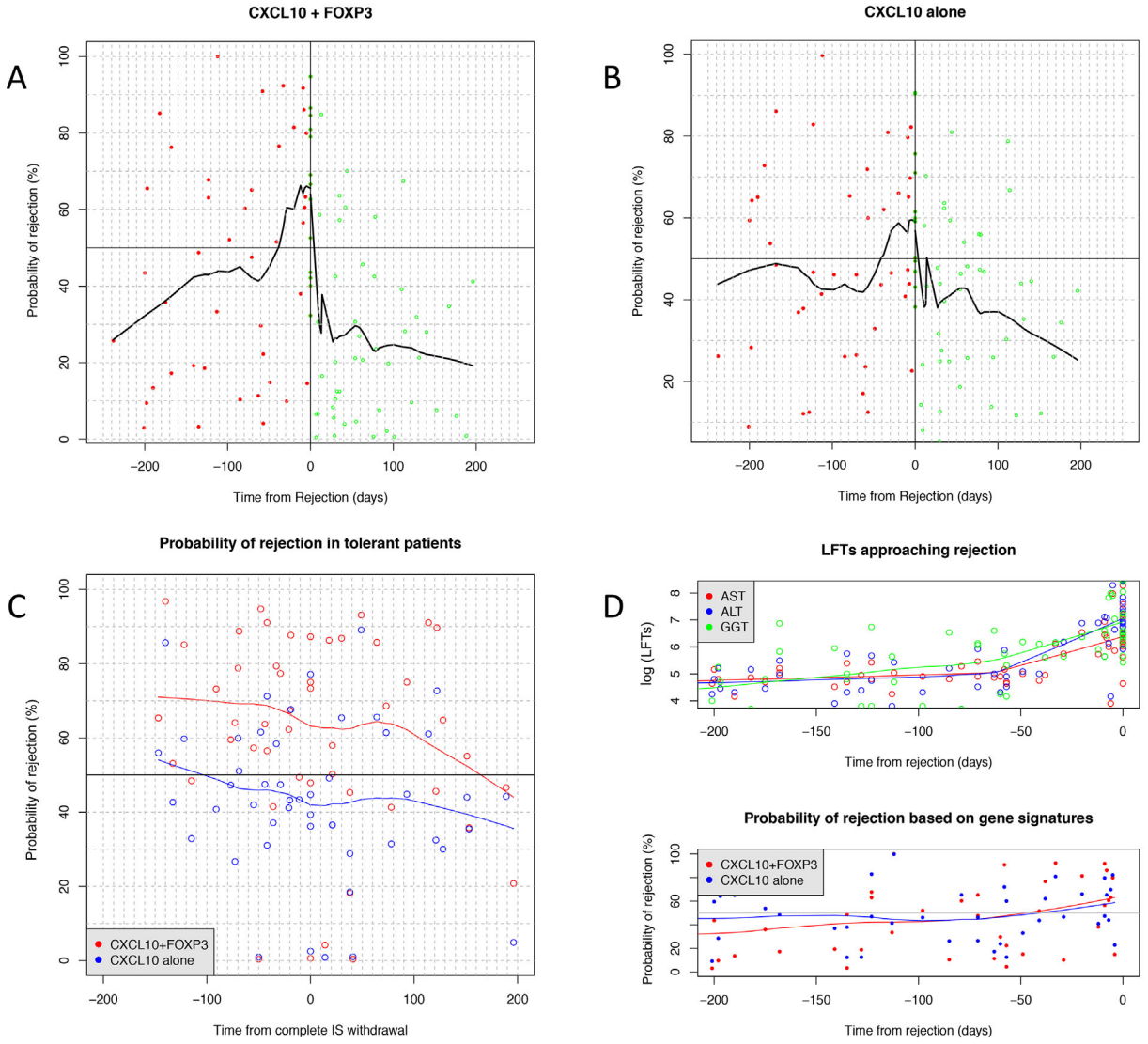

Figure 7: Prediction of rejection by sequential gene expression in blood samples. (A, B) Time evolution of risk probabilities based on gene signatures for *CXCL10* plus *FOXP3* and *CXCL10* alone, respectively. Both models show a peak coinciding with acute cellular rejection biopsy-proven diagnosis (time 0), with a rapid reduction following reinstitution or reinforcement of IS. (C) Evolution of risk probabilities in operationally tolerant patients up to and after complete withdrawal of immunosuppression (time 0), showing that *CXCL10* plus *FOXP3*, but not *CXCL10* alone, misclassifies as rejecting 70% of blood samples. (D) Sequential risk probabilities based on gene signature models alongside conventional LFTs (logarithmic scale). Risk increases gradually from ≈1–2 mo prior to rejection, mirroring a rise in LFTs. IS, immunosuppression; LFT, liver function test.

In comparing ACR signatures in tissue and blood, we acknowledge that the use of different microarray platforms presents challenges in drawing firm conclusions. A relatively low significance threshold was required for between-platform analyses to extract meaningful data. We note, however, that functional analyses were similar between tissue and blood, supporting our findings of overlapping transcriptional profiles.

Our histological analysis demonstrates a clear correlation between severity of inflammatory histological damage and expression of genes associated with inflammatory and rejection processes. This is a homogeneous finding across the different histological compartments, but the signal is particularly striking in lobular and portal inflammation and in interface hepatitis. Similar results have been reported in renal patients, in whom expression of inflammatory response genes correlates with the Banff scoring system for histological rejection (32). It should be acknowledged that the number of patients exhibiting severe central vein endothelitis or ductopenia was small (Table 4). This is because patients were very closely followed, and rejection

was diagnosed as soon as allograft dysfunction occurred. Consequently, our ability to detect transcriptional signatures for the most severe forms of rejection was limited.

CXCL10 and *FOXP3* whole-blood expression warrants further investigation as a potential biomarker for rejection, although its utility in the setting of immunosuppression withdrawal is questionable, given the influence of CNI on *FOXP3* expression. In this setting, *CXCL10* alone is a more robust marker, although it is noteworthy that this model misclassified as rejecting 33% of blood samples collected from tolerant liver recipients exhibiting no clinical signs of rejection. We hypothesize that some of these misclassifications may reflect subclinical inflammation caused by the withdrawal process that was not sufficiently severe to lead to a diagnosis of rejection.

The clinical applicability of transcriptional biomarkers of rejection in blood will need to be established in larger clinical trials in which gene expression data are combined with sequential liver function test measurements. We hope to improve on diagnosis based on liver function tests alone, which are neither sensitive nor specific for rejection (33). A note of caution is warranted, however, considering that blood gene expression was not sensitive enough to detect rejection in patients with chronic HCV infection. Further work is required to identify other potential confounding factors.

Our study provides insight into the processes underlying ACR in liver transplant patients. We observed significant overlap with T cell–mediated rejection processes that are well characterized in renal patients and identified characteristic tissue and blood signatures specific to the liver. Clinically, we demonstrated the potential utility of transcriptional markers in peripheral blood as a predictor for rejection. Although further work is required, these markers could lead to more accurate diagnosis and reduce the need for invasive biopsies.

Acknowledgments

The research was funded by Roche Organ Transplantation Research Foundation (ROTRF) and Instituto de Salud Carlos III Spain (FISS 1881/2011). In addition, the investigator team was supported by the Medical Research Council (MRC) Centre for Transplantation (MRC grant no. MR/J006742/1) and by the National Institute for Health Research (NIHR) Biomedical Research Centre based at Guy's and St Thomas' National Health Service (NHS) Foundation Trust and King's College London. The views expressed are those of the authors and not necessarily those of the NHS, the NIHR or the Department of Health. F.B. was supported by a research fellowship of the Deutsche Forschungsgemeinschaft (DfG reference BO 3370/1-1). CIBEREHD is funded by the Instituto de Salud Carlos III Spain.

Disclosure

The authors of this manuscript have no conflicts of interest to disclose as described by the *American Journal of Transplantation*.

References

1. Scientific Registry of Transplant Recipients. OPTN/SRTR 2010 annual data report. Rockville, MD: Department of Health, Human Services, Healthcare Systems Bureau, Division of Transplantation; 2011.
2. Asrani SK, Wiesner RH, Trotter JF, et al. *De novo* sirolimus and reduced-dose tacrolimus versus standard-dose tacrolimus after liver transplantation: The 2000-2003 phase II prospective randomized trial. Am J Transplant 2014; 14: 356–366.
3. Knechtle SJ, Kwun J. Unique aspects of rejection and tolerance in liver transplantation. Semin Liver Dis 2009; 29: 91–101.
4. Musat AI, Pigott CM, Ellis TM, et al. Pretransplant donor-specific anti-HLA antibodies as predictors of early allograft rejection in ABO-compatible liver transplantation. Liver Transpl 2013; 19: 1132–1141.
5. Benitez C, Londono MC, Miquel R, et al. Prospective multicenter clinical trial of immunosuppressive drug withdrawal in stable adult liver transplant recipients. Hepatology 2013; 58: 1824–1835.
6. Bohne F, Londono MC, Benitez C, et al. HCV-induced immune responses influence the development of operational tolerance after liver transplantation in humans. Sci Transl Med 2014; 6: 242ra81.
7. Banff schema for grading liver allograft rejection: An international consensus document. Hepatology 1997; 25: 658–663.
8. Sagoo P, Perucha E, Sawitzki B, et al. Development of a cross-platform biomarker signature to detect renal transplant tolerance in humans. J Clin Invest 2010; 120: 1848–1861.
9. Mootha VK, Lindgren CM, Eriksson KF, et al. PGC-1alpha-responsive genes involved in oxidative phosphorylation are coordinately downregulated in human diabetes. Nat Genet 2003; 34: 267–273.
10. Subramanian A, Tamayo P, Mootha VK, et al. Gene set enrichment analysis: A knowledge-based approach for interpreting genome-wide expression profiles. Proc Natl Acad Sci U S A 2005; 102: 15545–15550.
11. Watkins NA, Gusnanto A, de Bono B, et al. A HaemAtlas: Characterizing gene expression in differentiated human blood cells. Blood 2009; 113: e1–e9.
12. Alberta Transplant Applied Genomics Centre. Gene lists. [cited 2015 May 11]. Available from: http://atagc.med.ualberta.ca/Research/GeneLists/Pages/default.aspx.
13. Halloran PF, de Freitas DG, Einecke G, et al. The molecular phenotype of kidney transplants. Am J Transplant 2010; 10: 2215–2222.
14. Hidalgo LG, Einecke G, Allanach K, et al. The transcriptome of human cytotoxic T cells: Measuring the burden of CTL-associated transcripts in human kidney transplants. Am J Transplant 2008; 8: 637–646.
15. Famulski KS, Einecke G, Sis B, et al. Defining the canonical form of T-cell-mediated rejection in human kidney transplants. Am J Transplant 2010; 10: 810–820.
16. Famulski KS, Einecke G, Reeve J, et al. Changes in the transcriptome in allograft rejection: IFN-gamma-induced transcripts in mouse kidney allografts. Am J Transplant 2006; 6: 1342–1354.
17. Hidalgo LG, Sis B, Sellares J, et al. NK cell transcripts and NK cells in kidney biopsies from patients with donor-specific antibodies: Evidence for NK cell involvement in antibody-mediated rejection. Am J Transplant 2010; 10: 1812–1822.
18. Einecke G, Reeve J, Mengel M, et al. Expression of B cell and immunoglobulin transcripts is a feature of inflammation in late allografts. Am J Transplant 2008; 8: 1434–1443.

19. Einecke G, Sis B, Reeve J, et al. Antibody-mediated microcirculation injury is the major cause of late kidney transplant failure. Am J Transplant 2009; 9: 2520–2531.
20. Hidalgo LG, Sellares J, Sis B, Mengel M, Chang J, Halloran PF. Interpreting NK cell transcripts versus T cell transcripts in renal transplant biopsies. Am J Transplant 2012; 12: 1180–1191.
21. Mengel M, Reeve J, Bunnag S, et al. Molecular correlates of scarring in kidney transplants: The emergence of mast cell transcripts. Am J Transplant 2009; 9: 169–178.
22. Bohne F, Martinez-Llordella M, Lozano JJ, et al. Intra-graft expression of genes involved in iron homeostasis predicts the development of operational tolerance in human liver transplantation. J Clin Invest 2012; 122: 368–382.
23. Hutchinson JA, Riquelme P, Sawitzki B, et al. Cutting edge: Immunological consequences and trafficking of human regulatory macrophages administered to renal transplant recipients. J Immunol 2011; 187: 2072–2078.
24. Wang Z, Shi B, Jin H, Xiao L, Chen Y, Qian Y. Low-dose of tacrolimus favors the induction of functional CD4(+)CD25(+) FoxP3(+) regulatory T cells in solid-organ transplantation. Int Immunopharmacol 2009; 9: 564–569.
25. Spivey TL, Uccellini L, Ascierto ML, et al. Gene expression profiling in acute allograft rejection: Challenging the immunologic constant of rejection hypothesis. J Transl Med 2011; 9: 174.
26. Sarwal M, Chua MS, Kambham N, et al. Molecular heterogeneity in acute renal allograft rejection identified by DNA microarray profiling. N Engl J Med 2003; 349: 125–138.
27. Flechner SM, Kurian SM, Head SR, et al. Kidney transplant rejection and tissue injury by gene profiling of biopsies and peripheral blood lymphocytes. Am J Transplant 2004; 4: 1475–1489.
28. Patil J, Lande JD, Li N, Berryman TR, King RA, Hertz MI. Bronchoalveolar lavage cell gene expression in acute lung rejection: Development of a diagnostic classifier. Transplantation 2008; 85: 224–231.
29. Karason K, Jernas M, Hagg DA, Svensson PA. Evaluation of CXCL9 and CXCL10 as circulating biomarkers of human cardiac allograft rejection. BMC Cardiovasc Disord 2006; 6: 29.
30. Sreekumar R, Rasmussen DL, Wiesner RH, Charlton MR. Differential allograft gene expression in acute cellular rejection and recurrence of hepatitis C after liver transplantation. Liver Transpl 2002; 8: 814–821.
31. Walch JM, Lakkis FG. T-cell migration to vascularized organ allografts. Curr Opin Organ Transplant 2014; 19: 28–32.
32. Reeve J, Einecke G, Mengel M, et al. Diagnosing rejection in renal transplants: A comparison of molecular- and histopathology-based approaches. Am J Transplant 2009; 9: 1802–1810.
33. Abraham SC, Furth EE. Receiver operating characteristic analysis of serum chemical parameters as tests of liver transplant rejection and correlation with histology. Transplantation 1995; 59: 740–746.

Supporting Information

Additional Supporting Information may be found in the online version of this article.

Supplementary Methods

Table S1: List of gene expression markers assessed using Fluidigm quantitative polymerase chain reaction experiments.

Table S2: Functional pathways significantly overrepresented in liver allograft rejection–associated transcriptional patterns (Hallmark pathways, Molecular Signatures Database; gene set enrichment analysis).

Table S3: Comparison of functional pathways associated with rejection in patients enrolled in withdrawal trials against early posttransplant rejection outside of the trial setting.

Table S4: Full list of genes differentially expressed in different histological compartments, showing t-statistic.

Table S5: Functional pathways associated with severity of different histological parameters. Analysis performed using gene set enrichment analysis software against Hallmark gene sets from the Molecular Signatures Database and pathogenesis-based transcript sets from the University of Alberta. Normalized enrichment score and false discovery rate (FDR) are shown for each parameter. Significantly enriched pathways (FDR <0.05) are highlighted.

Supplementary table 1. List of gene expression markers assessed employing Fluidigm qPCR experiments.

Gene Symbol	Name
ABCB1	ATP-binding cassette, sub-family B member 1
APOL3	Apolipoprotein L, 3 (APOL3), transcript variant beta/a,
CCL19	Chemokine (C-C motif) ligand 19
CCN2B	Cyclin B2
CD52	CD52 molecule
CD74	CD74 molecule, major histocompatibility complex, class II invariant chain
CD8A	CD8a molecule (CD8A), transcript variant 2, mRNA.
CDC20	Cell division cycle 20
CECR1	Cat eye syndrome chromosome region, candidate 1
CENPM	Centromere protein M
CXCL10	Chemokine (C-X-C motif) ligand 10
CXCL9	Homo sapiens chemokine (C-X-C motif) ligand 9
DHRS9	Dehydrogenase/reductase (SDR family) member 9
DOCK11	Dedicator of cytokinesis 11
EMILIN2	Elastin microfibril interfacer 2
EZH2	Enhancer of zeste homolog 2
FOXP3	Forkhead box P3
GBP1	Guanylate binding protein 1, interferon-inducible
GBP2	Guanylate binding protein 2, interferon-inducible
GPNMB	Glycoprotein (transmembrane) nmb
GZMB	Granzyme B
GZMK	Granzyme K (granzyme 3; tryptase II)
HLA-DMA	Major histocompatibility complex, class II, DM alpha
HLA-DMB	Major histocompatibility complex, class II, DM beta
HMMR	Hyaluronan-mediated motility receptor
IL15	Interleukin 15
IL18BP	Interleukin 18 binding protein
IL32	Interleukin 32
IRF1	Interferon regulatory factor 1
LYZ	Lysozyme
ME2	Malic enzyme 2, NAD(+)-dependent, mitochondrial
MMP9	Matrix metallopeptidase 9 (gelatinase B, 92kDa gelatinase, 92kDa type IV collagenase)
PARVG	Gamma-parvin
PLEKHG1	Pleckstrin homology domain containing, family G (with RhoGef domain) member 1
PRF1	Perforin 1 (pore forming protein)
RFX5	Regulatory factor X, 5 (influences HLA class II expression)
STAT1	Signal transducer and activator of transcription 1
TAP1	Transporter 1, ATP-binding cassette, sub-family B (MDR/TAP)
TGFb1	Transforming growth factor, beta 1
TK1	Thymidine kinase 1, soluble
TLR8	Toll-like receptor 8
TOP2A	Topoisomerase (DNA) II alpha 170kDa
TYMS	Thymidylate synthetase
UBD	Ubiquitin D
ZWINT	ZW10 interacting kinetochore protein

Supplementary Table 2. Functional pathaways significantly over-represented in liver allograft rejection-associated transcriptional patterns (*Hallmark* pathways, MSigDB, GSEA analysis).

Gene Set	NES[1] HCV-	FDR[2] HCV-	NES HCV+	FDR HCV+	NES Blood	FDR Blood
ALLOGRAFT_REJECTION	2.93	0.00*	2.97	0.00*	1.84	0.02*
INTERFERON_GAMMA_RESPONSE	3.00	0.00*	2.38	0.00*	2.11	0.00*
E2F_TARGETS	2.51	0.00*	2.56	0.00*	1.79	0.02*
INTERFERON_ALPHA_RESPONSE	2.77	0.00*	1.78	0.00*	2.14	0.00*
G2M_CHECKPOINT	2.31	0.00*	2.55	0.00*	1.69	0.03*
IL6_JAK_STAT3_SIGNALING	2.25	0.00*	2.22	0.00*	1.86	0.02*
INFLAMMATORY_RESPONSE	2.49	0.00*	2.24	0.00*	1.56	0.07
TNFA_SIGNALING_VIA_NFKB	2.66	0.00*	2.25	0.00*	1.13	0.39
APOPTOSIS	2.28	0.00*	2.33	0.00*	1.37	0.17
IL2_STAT5_SIGNALING	2.19	0.00*	2.25	0.00*	1.31	0.22
COMPLEMENT	2.08	0.00*	2.09	0.00*	1.26	0.23
EPITHELIAL_MESENCHYMAL_TRANSITION	1.79	0.00*	2.60	0.00*	0.97	0.66
P53_PATHWAY	1.91	0.00*	2.07	0.00*	1.29	0.20
MYC_TARGETS_V1	1.36	0.07	1.62	0.01*	1.75	0.02*
ESTROGEN_RESPONSE_LATE	1.75	0.00*	1.91	0.00*	1.05	0.48
UV_RESPONSE_UP	1.66	0.00*	1.48	0.03*	1.52	0.08
PI3K_AKT_MTOR_SIGNALING	1.60	0.01*	1.66	0.01*	1.30	0.21
APICAL_JUNCTION	1.64	0.01*	1.86	0.00*	0.89	0.73
MTORC1_SIGNALING	1.72	0.00*	1.65	0.01*	0.96	0.66
KRAS_SIGNALING_UP	2.28	0.00*	2.48	0.00*	-0.80	1.00
ADIPOGENESIS	1.21	0.21	1.16	0.23	1.38	0.17
PEROXISOME	1.30	0.11	1.27	0.13	1.08	0.46
DNA_REPAIR	1.12	0.34	1.54	0.02*	0.73	0.91
SPERMATOGENESIS	0.91	0.66	1.31	0.10	1.07	0.48
NOTCH_SIGNALING	0.95	0.62	1.46	0.03*	0.81	0.84
MITOTIC_SPINDLE	1.87	0.00*	2.00	0.00*	-0.83	1.00
TGF_BETA_SIGNALING	0.92	0.66	1.18	0.21	0.93	0.67
MYC_TARGETS_V2	0.88	0.71	1.19	0.21	0.94	0.67
ANGIOGENESIS	1.83	0.00*	2.23	0.00*	-1.26	1.00
HYPOXIA	1.56	0.01*	1.71	0.00*	-0.73	1.00
GLYCOLYSIS	1.60	0.01*	1.80	0.00*	-0.86	1.00
MYOGENESIS	1.69	0.00*	1.41	0.04*	-0.60	0.98
ESTROGEN_RESPONSE_EARLY	1.55	0.01*	1.80	0.00*	-0.88	1.00
HEDGEHOG_SIGNALING	1.50	0.02*	1.45	0.04*	-0.73	1.00
PROTEIN_SECRETION	1.39	0.06	1.64	0.01*	-0.88	1.00
UNFOLDED_PROTEIN_RESPONSE	1.42	0.04*	1.49	0.03*	-0.78	1.00
COAGULATION	1.45	0.03*	1.59	0.01*	-0.98	1.00
ANDROGEN_RESPONSE	1.10	0.36	1.50	0.03*	-0.64	1.00
UV_RESPONSE_DN	1.47	0.03*	1.60	0.01*	-1.12	1.00
REACTIVE_OXIGEN_SPECIES_PATHWAY	1.64	0.01*	0.99	0.50	-0.84	1.00
HEME_METABOLISM	1.48	0.03*	1.19	0.21	-1.19	0.95
WNT_BETA_CATENIN_SIGNALING	1.09	0.37	1.42	0.04*	-1.05	1.00
APICAL_SURFACE	0.97	0.59	1.61	0.01*	-1.23	1.00
PANCREAS_BETA_CELLS	-1.13	0.43	0.83	0.77	1.36	0.17
KRAS_SIGNALING_DN	1.10	0.35	0.90	0.66	-1.33	1.00
CHOLESTEROL_HOMEOSTASIS	1.30	0.11	-1.61	0.04*	0.82	0.84
XENOBIOTIC_METABOLISM	0.81	0.82	-1.55	0.03*	1.22	0.26
OXIDATIVE_PHOSPHORYLATION	-1.04	0.50	-1.25	0.10	1.50	0.08
FATTY_ACID_METABOLISM	-0.83	0.84	-1.41	0.04*	1.25	0.22
BILE_ACID_METABOLISM	-1.31	0.25	-1.50	0.03*	-0.92	1.00

[1] Normalised Enrichment Score, as generated by GSEA software
[2] False Discovery Rate

Supplementary Table S3

We performed a comparative analysis of the 13 HCV negative patients with rejection enrolled in withdrawal trials against 9 biopsies from HCV negative patients with early post-transplant rejection (within 4 weeks of transplantation).

Comparing pre-weaning samples from trial-enrolled patients to early post-transplant rejection samples showed 1193 differentially expressed genes, which included 14 of the 19 ACR-related genes described in this study (Figure 2C). Comparing rejection samples from trial-enrolled patients against early post-transplant rejection samples showed 213 genes differentially expressed, which showed no overlap with the 19 ACR-related genes above.

Functional analysis using GSEA did not identify any significant differences between early post-transplant rejection and rejection in the withdrawal-trial setting. Full GSEA data is shown below.

Analysis performed using Gene Set Enrichment Analysis (GSEA) software against Hallmark gene sets from MSigDB and Pathogenesis Based Transcript (PBT) sets from the University of Alberta. Normalised Enrichment Score (NES) and False Discovery Rate (FDR) are shown for each parameter. NES is a quantified measure of strength of enrichment determined by the GSEA software and defined on the MIT Broad Institue website (http://www.broadinstitute.org/gsea/doc/GSEAUserGuideTEXT.htm#_Normalized_Enrichment_Score). Significantly enriched pathways (FDR < 0.05) are highlighted

	Early-transplant rejection samples vs HCV-neg patients at baseline (unpaired analysis)		Rejection samples from HCV-neg withdrawal trial patients vs baseline samples from same patients (paired analysis)	
Gene set name	**NES**	**FDR q-val**	**NES**	**FDR q-val**
HALLMARK_INTERFERON_GAMMA_RESPONSE	2.84	0.00	2.97	0.00
HALLMARK_E2F_TARGETS	2.81	0.00	2.52	0.00
HALLMARK_G2M_CHECKPOINT	2.79	0.00	2.30	0.00
HALLMARK_INTERFERON_ALPHA_RESPONSE	2.59	0.00	2.79	0.00
HALLMARK_TNFA_SIGNALING_VIA_NFKB	2.52	0.00	2.65	0.00
HALLMARK_IL6_JAK_STAT3_SIGNALING	2.47	0.00	2.27	0.00
HALLMARK_INFLAMMATORY_RESPONSE	2.30	0.00	2.50	0.00
HALLMARK_ALLOGRAFT_REJECTION	2.29	0.00	2.89	0.00
HALLMARK_UNFOLDED_PROTEIN_RESPONSE	2.21	0.00	1.43	0.05
HALLMARK_MTORC1_SIGNALING	2.18	0.00	1.71	0.00
HALLMARK_EPITHELIAL_MESENCHYMAL_TRANSITION	2.17	0.00	1.81	0.00
HALLMARK_UV_RESPONSE_UP	2.17	0.00	1.66	0.01
HALLMARK_COMPLEMENT	2.14	0.00	2.07	0.00
HALLMARK_APOPTOSIS	2.12	0.00	2.28	0.00
HALLMARK_P53_PATHWAY	2.11	0.00	1.94	0.00
HALLMARK_BILE_ACID_METABOLISM	-2.09	0.00	-1.31	0.63

HALLMARK_MITOTIC_SPINDLE	2.05	0.00	1.89	0.00
HALLMARK_MYC_TARGETS_V1	1.97	0.00	1.39	0.06
HALLMARK_IL2_STAT5_SIGNALING	1.94	0.00	2.20	0.00
HALLMARK_ANGIOGENESIS	1.94	0.00	1.79	0.00
HALLMARK_KRAS_SIGNALING_UP	1.84	0.00	2.28	0.00
HALLMARK_CHOLESTEROL_HOMEOSTASIS	1.81	0.00	1.30	0.12
HALLMARK_APICAL_JUNCTION	1.79	0.00	1.64	0.01
HALLMARK_HYPOXIA	1.75	0.00	1.55	0.02
HALLMARK_ESTROGEN_RESPONSE_LATE	1.75	0.00	1.75	0.00
HALLMARK_DNA_REPAIR	1.70	0.00	1.13	0.33
HALLMARK_PI3K_AKT_MTOR_SIGNALING	1.70	0.00	1.61	0.01
HALLMARK_GLYCOLYSIS	1.70	0.00	1.62	0.01
HALLMARK_MYC_TARGETS_V2	1.69	0.00	0.89	0.69
HALLMARK_REACTIVE_OXIGEN_SPECIES_PATHWAY	1.68	0.00	1.66	0.01
HALLMARK_COAGULATION	1.55	0.01	1.48	0.03
HALLMARK_MYOGENESIS	1.50	0.02	1.68	0.01
HALLMARK_ESTROGEN_RESPONSE_EARLY	1.49	0.02	1.56	0.02
HALLMARK_OXIDATIVE_PHOSPHORYLATION	-1.41	0.06	-1.04	0.79
HALLMARK_UV_RESPONSE_DN	1.35	0.08	1.46	0.04
HALLMARK_HEDGEHOG_SIGNALING	1.31	0.10	1.48	0.03
HALLMARK_HEME_METABOLISM	1.26	0.14	1.45	0.04
HALLMARK_FATTY_ACID_METABOLISM	-1.26	0.15	-0.83	0.92
HALLMARK_ADIPOGENESIS	1.20	0.19	1.21	0.21
HALLMARK_ANDROGEN_RESPONSE	1.20	0.19	1.10	0.37
HALLMARK_PROTEIN_SECRETION	1.20	0.19	1.37	0.07
HALLMARK_PANCREAS_BETA_CELLS	-1.17	0.20	-1.12	0.70
HALLMARK_XENOBIOTIC_METABOLISM	1.17	0.22	0.78	0.84
HALLMARK_SPERMATOGENESIS	1.16	0.23	0.93	0.64
HALLMARK_NOTCH_SIGNALING	1.11	0.30	0.94	0.61
HALLMARK_TGF_BETA_SIGNALING	1.09	0.32	0.95	0.62
HALLMARK_PEROXISOME	1.05	0.38	1.29	0.12
HALLMARK_WNT_BETA_CATENIN_SIGNALING	-1.01	0.46	1.07	0.42
HALLMARK_APICAL_SURFACE	-0.97	0.53	0.96	0.59
HALLMARK_KRAS_SIGNALING_DN	0.97	0.53	1.10	0.37
PBT_QCMAT	2.72	0.00	2.53	0.00
PBT_CIRIT	2.66	0.00	2.18	0.00
PBT_IRITD3	2.62	0.00	2.30	0.00
PBT_IRITD5	2.53	0.00	2.22	0.00
PBT_GRIT1	2.26	0.00	2.63	0.00
PBT_IRRAT	2.18	0.00	2.05	0.00
PBT_QCAT	2.06	0.00	2.52	0.00
PBT_DSAST	-1.55	0.02	1.61	0.01
PBT_HTS	1.25	0.15	1.53	0.02
PBT_BAT	1.21	0.18	1.97	0.00

PBT_ENDAT	1.11	0.30	1.49	0.03

Supplementary Table S4. Full list of genes differentially expressed in different histological compartments, showing t-statistic. Genes shown satisfy a significance threshold of FC > 1.2 and FDR < 0.05 in at least one histological compartment. Red indicates increased expression with increasing severity of a histological parameter; green indicates decreased expression.

	Lobular inflammation	Portal inflammation	Interface hepatitis	Central vein perivenulitis	Endothelitis central vein	Endothelitis portal veins	Bile duct lesions	Ductular reaction	Ductopenia	Perisinusoildal fibrosis	Portal fibrosis
CXCL9	9.44	6.71	7.21	2.46	0.00	3.17	3.69	1.14	0.23	1.56	3.98
HLA-DMA	6.70	6.03	7.19	3.85	1.24	3.73	4.16	0.88	1.06	1.57	4.50
CD2	7.10	6.44	5.55	2.00	0.38	2.88	3.52	1.09	-0.28	1.26	3.74
CCL4L2	7.05	4.77	4.67	3.73	0.59	2.18	3.62	1.84	0.52	2.32	3.74
TAP1	7.03	5.73	5.12	3.50	1.13	2.31	2.81	0.66	-0.06	0.91	3.34
GBP5	7.00	5.13	5.32	2.42	0.14	2.59	2.53	0.54	0.49	0.94	2.91
GBP2	6.98	5.02	5.16	3.62	0.74	2.37	3.05	0.41	-0.36	1.80	3.32
TLR8	5.91	6.95	6.59	2.35	1.58	4.23	4.89	1.71	-0.77	1.64	4.56
CD8A	6.74	6.09	6.37	3.07	1.86	3.24	3.36	1.52	-0.42	1.53	3.56
SLAMF6	6.65	5.24	5.60	2.12	0.67	2.42	3.36	1.03	1.02	1.10	3.31
WARS	6.65	5.23	4.09	3.06	0.76	2.78	3.11	0.56	0.45	0.89	2.44
HLA-DRA	6.57	5.23	5.25	2.67	0.86	3.13	3.22	0.64	0.13	1.41	3.63
RFX5	6.57	6.28	5.40	2.92	-1.83	3.41	3.27	-0.88	0.65	1.10	3.92
CD83	6.57	5.85	4.82	2.03	-0.12	3.33	3.89	0.58	0.13	1.61	2.87
GBP1	6.54	5.19	4.24	2.91	0.82	2.89	2.84	0.94	1.02	1.29	2.83
ITGB2	6.53	5.36	5.36	2.92	1.55	3.16	3.59	1.52	-0.49	1.02	2.87
RARRES1	4.54	6.52	5.42	1.82	1.31	3.77	4.05	1.29	0.48	1.04	2.64
CD3D	6.04	6.00	6.50	3.62	1.35	1.93	3.32	1.70	0.21	1.40	4.19
FABP5	5.57	6.43	5.81	3.54	-1.74	3.68	3.55	1.01	0.05	1.24	3.00
CXCL10	6.39	6.17	4.99	2.86	0.77	2.13	2.49	0.85	0.42	1.41	3.75
FCGR1B	6.38	5.59	5.39	3.64	0.93	3.54	3.58	1.61	0.76	1.88	4.78
CCL19	5.34	4.97	6.34	2.96	0.39	2.75	2.63	-0.01	0.32	0.40	2.91
HLA-H	6.33	5.24	4.57	2.49	1.25	1.15	2.23	0.85	-0.32	0.73	3.01
TYMS	4.51	6.33	5.48	2.58	0.29	2.43	2.60	1.43	0.39	1.16	3.93
PLEK	6.33	4.94	4.33	3.13	1.34	2.50	2.41	0.12	-0.11	1.26	2.41
BTG2	4.30	6.33	5.07	1.99	0.35	2.02	3.15	1.65	0.51	0.71	2.96
CTLA4	4.47	5.63	6.30	4.11	0.71	3.17	4.43	1.50	-1.19	1.78	3.93
MCOLN2	6.28	5.26	5.45	2.04	-0.27	2.62	2.53	0.22	0.61	1.53	3.47
FYB	6.26	4.78	4.92	2.23	0.65	1.39	2.51	1.88	-0.33	0.69	2.89
CECR1	6.24	4.72	4.51	2.36	-1.16	2.41	2.78	0.82	0.39	0.88	2.73
LAPTM5	5.87	6.19	4.77	2.07	1.36	3.88	3.74	1.16	0.38	0.64	3.61
CD48	5.45	5.39	6.17	3.48	1.12	2.40	2.68	1.07	0.34	0.94	3.02
CD72	5.18	5.53	6.16	2.65	0.22	2.56	3.87	1.21	-0.33	0.69	3.63
APOL3	6.15	5.64	4.23	3.32	1.31	-1.75	1.88	-1.81	0.96	1.25	4.06
TBC1D10C	5.77	5.31	6.10	2.51	0.64	2.03	2.80	0.22	-0.05	1.60	3.24
PARVG	6.08	4.39	4.75	3.31	1.12	1.35	2.76	0.73	-0.70	0.53	2.48
ITK	6.07	4.84	5.22	2.44	0.05	1.56	2.75	-0.17	0.31	1.23	3.43
ICOS	4.96	5.61	6.07	1.96	-0.64	3.18	3.79	-0.81	1.47	1.11	3.08
HLA-F	6.06	4.73	4.44	4.06	2.05	0.44	2.35	1.27	0.43	0.68	3.53
CD74	5.81	6.03	6.05	2.10	0.44	2.92	4.67	1.84	0.95	1.75	4.37
GPNMB	6.05	5.99	5.45	2.51	-0.44	4.08	4.01	0.45	1.15	1.48	2.96
GBP4	6.04	4.80	4.61	1.45	-0.80	2.26	3.01	1.16	0.43	1.16	3.40
CD37	5.06	6.03	5.59	2.38	-0.21	2.81	4.18	1.83	0.30	0.48	2.91
ANXA2	6.02	5.47	5.30	2.42	0.81	3.90	2.93	0.24	1.17	0.50	3.88

BIRC3	6.02	4.74	3.73	1.52	-1.08	0.90	1.01	0.40	-0.75	1.34	2.64
GZMK	6.00	4.99	5.75	2.22	0.43	1.65	2.13	0.73	0.01	1.95	3.59
PRKCD	5.96	3.25	4.19	3.42	1.37	-1.56	1.31	0.70	-1.72	-1.91	2.42
HLA-DMB	5.36	5.28	5.95	3.15	1.04	2.29	2.73	1.32	0.41	1.59	3.83
MTHFD2	5.95	4.72	3.98	1.93	-0.74	2.56	2.37	1.47	1.13	-1.18	2.29
UBD	5.90	5.93	5.51	2.75	0.73	2.43	2.50	0.74	-0.23	0.87	4.04
CTSC	5.91	4.91	4.92	-2.45	-2.19	3.82	3.50	-2.60	0.43	0.60	2.57
LCP1	5.91	4.83	4.28	1.95	0.80	1.10	2.36	1.03	-0.50	0.89	2.27
MMP9	4.02	4.68	5.91	1.51	0.84	3.15	2.93	0.00	-0.18	0.55	2.31
HLA-DOB	5.89	4.85	5.20	2.68	0.93	2.37	2.85	0.21	0.30	0.47	3.60
ADA	5.13	5.89	5.02	2.92	1.88	2.06	3.05	2.09	0.05	0.88	3.42
RUNX3	5.88	4.51	5.40	2.28	0.60	1.88	2.85	0.53	-0.96	1.03	2.99
EOMES	5.87	5.08	5.41	2.91	0.15	1.49	3.44	0.97	0.34	1.45	3.59
HMMR	5.22	5.87	5.03	1.87	-0.43	4.95	4.23	-0.17	0.46	1.04	2.80
SRGN	5.86	4.43	4.90	4.16	2.03	2.57	3.58	2.38	0.72	1.83	3.60
IL32	5.85	5.75	4.85	3.65	1.80	1.79	2.79	1.51	1.81	2.06	4.99
OBFC2A	5.85	4.79	4.37	3.12	0.85	2.60	3.57	1.13	0.95	1.71	2.96
CD53	5.82	5.27	4.44	2.07	0.43	2.30	2.88	1.31	0.64	0.92	3.49
STAT1	5.82	5.59	4.52	3.35	0.90	1.56	2.52	0.66	0.39	1.13	3.23
RAC2	5.81	5.50	5.46	3.30	1.21	1.86	3.22	1.61	0.34	1.05	2.88
HLA-DQA1	5.79	4.86	4.86	1.10	0.86	2.58	2.87	1.17	0.40	0.42	2.43
PILRA	5.78	3.10	3.88	3.23	1.69	2.31	2.99	1.53	1.37	2.25	3.20
C16orf75	3.65	5.76	4.50	3.02	0.44	2.37	1.76	0.15	0.68	0.12	3.11
CD69	5.75	4.41	4.04	1.11	-0.27	1.86	1.38	0.37	0.87	1.29	2.56
STAMBPL1	5.74	4.53	4.61	1.66	-0.65	3.24	2.95	0.45	-0.05	0.76	2.89
PPP1R1A	-5.73	-4.19	-3.74	-2.04	-0.23	-1.42	-1.94	-0.40	-0.83	-0.74	-3.25
MMP7	3.54	3.86	5.72	3.07	-0.32	1.70	2.99	0.57	0.17	1.65	4.50
FERMT3	5.72	4.94	5.23	3.53	1.57	2.71	3.08	2.05	1.37	0.96	3.62
TAP2	5.72	3.93	3.32	1.30	-0.54	1.28	1.42	-1.55	-1.21	1.12	1.74
IRF1	5.70	3.32	3.61	3.12	0.83	1.76	1.00	-0.21	0.14	1.73	2.37
LYVE1	-5.52	-5.53	-5.70	-3.57	-0.26	-1.39	-2.25	-0.56	-1.42	-0.84	-5.15
MCM6	4.11	5.69	3.85	1.58	-0.29	1.79	1.37	0.39	-0.36	0.72	2.84
CTSS	5.69	4.48	4.36	0.88	-0.17	2.52	2.11	1.15	0.21	1.19	2.94
ASNS	5.68	3.39	4.29	2.47	-1.10	0.84	1.87	1.27	0.38	0.85	1.91
CDC45L	4.59	5.68	5.20	2.72	0.18	2.67	2.11	0.72	-0.40	0.98	3.80
WASPIP	5.67	4.70	4.53	0.54	-0.32	1.97	2.37	1.07	-0.88	-0.01	1.35
HLA-DRB6	5.66	4.28	4.77	3.03	1.64	1.60	1.93	0.53	1.52	0.47	2.85
IL18BP	5.66	4.50	4.74	3.15	1.00	2.21	2.11	-0.69	1.13	-1.56	2.27
LPXN	4.39	4.84	5.66	1.59	-0.47	1.90	2.93	0.54	-0.53	1.21	3.37
DGKA	3.63	4.52	5.65	2.83	2.01	1.99	2.97	-1.59	1.07	1.23	1.83
ARHGAP9	5.64	4.82	5.37	2.80	1.53	1.99	3.04	1.77	-0.44	1.89	3.04
CD79A	4.39	4.51	5.64	2.47	-0.55	1.66	3.30	-0.35	-0.43	0.66	2.63
HLA-DOA	5.44	5.28	5.62	3.02	0.86	2.76	3.95	2.12	0.23	1.14	4.28
LTB	4.57	4.72	5.61	2.51	1.22	0.99	2.30	0.84	-1.31	1.43	3.03
MELK	5.50	5.60	5.24	2.44	0.47	3.71	3.49	0.93	-0.73	0.80	2.50
AIM2	5.59	4.10	3.45	2.47	1.22	1.74	2.24	1.19	1.58	1.21	2.11
IL7R	5.59	4.81	4.52	1.34	-1.64	2.00	2.14	-0.50	-0.84	1.06	2.23
C15orf48	5.59	4.25	4.08	2.03	-1.41	4.67	3.53	-1.15	1.63	1.05	3.79
SLFN11	5.59	4.94	4.19	0.66	-2.16	2.89	2.39	-0.51	1.32	1.72	2.60
UHRF1	4.77	5.59	4.95	2.65	0.98	2.95	2.51	1.65	-0.38	1.96	3.18
CCND2	5.58	4.58	4.77	1.95	0.96	1.21	2.49	-0.67	-0.92	0.42	2.05
EMILIN2	5.57	4.91	5.54	2.66	0.19	1.91	2.89	0.43	0.71	1.35	3.58
ARHGEF3	4.92	5.56	4.24	1.51	0.93	1.46	3.35	1.09	-0.10	-0.03	1.68
FCN1	4.67	3.88	5.56	3.11	0.83	2.61	3.86	1.43	0.88	2.11	3.69
SAMD9L	5.54	3.83	2.59	1.86	0.08	0.91	2.05	0.97	0.18	1.30	2.72

IFI30	5.04	5.53	5.13	5.05	2.60	3.38	3.37	1.72	0.87	0.29	3.86
HIST1H3F	-0.99	-2.62	-3.33	-0.84	-0.11	-4.19	-5.52	-0.03	-0.64	-0.17	-0.72
SPOCK2	5.33	5.29	5.52	2.19	0.00	2.10	3.13	0.46	-0.40	0.77	3.28
PIM2	4.56	4.97	5.52	3.64	1.13	1.01	2.68	1.15	0.59	1.32	2.89
ACADSB	-4.13	-4.60	-4.49	-3.99	-1.49	-2.54	-2.56	-1.12	-0.30	-0.74	-5.52
GPR98	-5.50	-3.81	-5.07	-2.57	0.55	-2.03	-2.51	1.04	-1.87	-0.53	-3.01
CDH23	-4.82	-5.48	-4.71	-3.37	1.10	-2.45	-2.62	-0.88	2.04	1.36	-4.80
ADAMDEC1	3.69	4.46	5.47	1.19	0.38	4.25	3.41	-0.09	-0.32	-0.16	2.07
STX11	5.46	3.37	3.18	1.36	0.68	1.35	1.34	0.49	-0.45	0.64	2.55
ANKRD29	4.68	3.87	5.45	1.52	-0.74	1.11	1.07	1.47	0.44	0.88	3.64
SAMD4A	-5.45	-3.08	-3.28	-0.93	1.10	-0.48	-0.44	0.82	-1.14	-1.49	-3.17
HCG4	5.44	4.71	4.40	2.33	1.26	-1.75	2.94	1.62	-0.66	1.11	2.72
SERPINB8	5.41	4.31	4.17	2.04	0.39	3.65	2.37	0.79	1.40	1.40	4.44
SAMSN1	5.41	4.31	3.78	2.17	0.74	2.34	2.85	1.35	0.61	0.86	2.29
NIN	5.41	4.02	3.53	2.64	-1.42	2.20	2.34	0.89	-1.74	-1.60	1.96
GPR18	4.62	4.44	5.40	1.16	-1.00	3.35	3.80	0.94	0.48	3.44	3.14
ITM2A	4.67	5.25	5.40	1.53	-0.20	2.27	2.56	-0.68	-0.22	0.85	3.04
PKM2	5.39	4.45	4.76	2.23	-1.15	2.78	3.85	2.05	-0.88	1.71	2.45
CD38	5.38	4.65	4.09	3.69	0.76	2.98	2.93	1.16	0.51	2.12	3.47
TNFSF13B	5.38	5.37	4.80	2.97	0.98	2.46	3.68	1.95	0.90	1.28	3.66
APOBEC3G	4.61	5.37	4.60	2.62	1.22	1.87	2.11	0.56	1.24	2.10	3.34
EHD4	5.37	4.07	3.89	3.35	0.95	2.58	2.30	-0.29	2.19	0.65	3.01
AMICA1	4.33	5.36	4.46	1.56	0.61	1.60	2.54	1.63	-0.41	0.50	3.36
HLA-B	5.35	4.53	4.20	2.76	1.34	0.49	1.76	0.81	-0.29	0.72	3.17
CD96	5.03	4.64	5.34	2.75	1.09	2.72	3.19	0.64	1.11	1.83	2.96
CCDC109B	5.00	5.34	5.20	1.58	-0.28	2.50	3.21	0.61	0.31	1.35	3.21
TNRC6B	-0.98	-0.92	-0.24	-0.10	1.06	-3.54	-4.21	0.88	-5.34	0.64	-0.16
SEMA4D	5.32	4.30	3.96	1.93	0.00	0.98	2.21	0.88	-0.60	1.07	2.67
GPR56	5.31	3.66	4.70	2.20	0.53	-1.17	1.24	-1.13	1.00	1.70	3.75
UBE2C	4.41	5.31	4.71	3.50	1.16	4.05	4.43	1.59	-0.73	1.26	2.97
DUOXA1	-2.46	-2.31	-2.06	-2.98	-1.80	-2.86	-1.92	-0.68	-5.30	-1.98	-2.72
ABCB1	5.29	4.57	4.97	0.58	-1.16	2.01	3.72	-0.20	1.08	0.77	2.80
PTTG1	4.57	5.15	5.29	3.62	1.79	4.13	4.40	1.56	-0.75	0.96	3.76
HPR	-4.60	-3.77	-4.53	-3.75	0.13	-1.49	-2.04	0.49	-2.15	-1.18	-5.29
FCRLA	3.30	4.06	5.28	1.43	0.55	2.23	2.96	-0.20	0.12	0.23	1.88
FAIM3	5.10	5.15	5.27	1.45	0.13	2.00	2.93	0.53	-0.15	0.57	2.92
GK	5.27	3.98	3.62	1.24	-0.72	2.21	3.10	-1.01	1.32	0.19	2.74
IL1B	5.27	2.76	2.17	2.46	0.78	1.21	1.69	0.93	-0.11	1.38	2.37
ANKRD22	5.26	3.52	3.23	1.70	-1.86	2.70	2.05	1.64	-0.84	1.49	3.21
ABCB4	5.26	4.29	4.25	1.47	-1.11	4.23	3.63	-1.01	2.18	0.76	2.93
IER3	5.25	2.91	3.29	3.25	0.69	2.93	2.38	-0.71	1.68	-0.69	2.51
HCST	4.93	4.46	5.25	4.16	2.09	1.71	3.64	1.81	1.08	1.36	4.59
CD86	5.25	4.71	4.92	4.69	1.58	1.98	3.25	1.93	0.75	2.75	3.97
TNFRSF12A	5.24	3.56	3.53	2.02	0.25	2.17	2.58	0.40	1.44	2.72	3.56
SLA	4.80	5.24	4.22	4.48	1.75	1.59	2.07	1.40	0.69	1.85	3.39
MGC4677	4.70	4.04	5.24	4.32	1.47	-0.37	1.55	-1.10	0.63	-1.21	5.03
HAVCR2	5.23	3.88	4.43	3.33	0.96	1.45	2.28	1.15	-0.40	1.49	3.27
PLCB2	5.23	3.45	3.88	2.37	0.95	1.52	2.48	1.01	-0.02	1.28	1.76
CD52	4.75	5.07	5.23	2.79	1.50	3.44	4.88	1.95	0.14	1.73	3.88
GZMA	5.23	4.06	4.96	3.32	0.99	0.70	1.74	1.45	0.47	1.75	3.33
RASAL3	5.23	4.38	4.69	2.16	0.26	1.41	2.10	-0.97	-0.02	1.28	2.08
RGS10	4.39	4.21	5.22	3.79	1.69	3.49	3.48	1.06	2.06	1.91	3.49
CXCL11	5.22	3.84	3.10	1.19	-0.96	1.77	2.18	0.45	0.42	1.22	2.47
SORL1	-2.61	-2.88	-2.88	-5.21	-2.31	-1.81	-2.28	-0.78	-0.46	0.56	-2.50
IGSF6	5.20	5.01	4.93	3.32	1.52	3.68	3.62	1.46	0.48	0.81	3.28

UPP2	5.19	2.88	3.53	1.72	-1.10	0.79	1.66	0.60	3.14	1.53	3.62
FCER1G	5.18	4.31	4.52	3.70	1.75	2.72	3.65	2.57	0.48	0.83	2.85
TOP2A	4.88	5.18	5.12	2.57	1.06	3.95	3.38	0.06	0.09	0.76	2.57
BTN3A3	5.18	4.02	3.41	2.62	1.67	-0.06	1.01	0.56	-0.50	0.63	2.76
DOCK10	5.18	3.61	4.27	2.29	0.83	1.67	2.77	0.21	-0.93	1.51	1.86
FAM99A	-5.18	-4.42	-4.81	-2.18	-0.52	-2.26	-2.83	0.26	-1.97	-1.92	-3.07
SLC16A3	3.83	3.70	5.18	4.77	1.46	1.21	2.60	1.45	0.35	1.97	3.95
TNFAIP8	5.17	4.57	4.73	1.60	0.80	2.00	1.76	0.37	-0.60	2.48	2.92
EVI2B	5.16	4.80	4.82	2.40	1.23	2.07	2.70	0.46	-0.34	0.75	2.30
DOCK11	5.16	4.42	4.82	0.93	-1.52	1.80	2.40	0.12	0.01	1.50	3.31
ITGAX	5.16	3.60	4.41	1.89	-1.37	2.20	1.63	0.46	1.11	1.95	3.03
PKLR	-5.16	-3.78	-3.43	-2.05	1.01	-1.44	-2.18	-2.48	-1.65	-2.30	-2.82
E2F2	5.15	5.14	4.59	2.88	1.20	2.47	3.21	1.20	-0.62	0.70	2.79
LOC606724	5.15	5.12	4.95	2.13	-0.87	1.38	2.04	1.30	-2.80	-1.97	2.38
NUSAP1	4.97	5.12	5.14	2.41	1.16	4.15	3.23	1.04	-0.90	1.56	3.21
CXCR4	5.13	4.78	5.14	1.96	0.73	3.84	3.36	0.52	0.65	2.24	2.71
CCL3L3	5.13	3.77	3.16	3.15	0.63	2.00	2.99	1.42	0.56	1.55	3.33
CKS2	4.99	5.13	4.85	3.90	2.44	2.08	2.63	1.46	-1.42	0.88	3.68
GPER	-5.13	-2.81	-2.93	-1.56	1.08	-3.19	-3.00	-1.26	-4.79	-0.30	-4.11
IFI16	5.12	4.02	4.06	1.08	-0.03	-0.19	0.78	0.28	-0.08	0.59	3.07
PSMB9	5.11	4.83	4.18	4.34	1.85	1.02	2.09	1.37	0.47	1.42	3.68
LXN	3.65	4.42	5.09	1.52	-0.61	2.29	2.58	0.01	-0.43	1.86	3.07
CD6	5.09	4.90	4.69	2.01	0.85	1.95	2.58	0.38	-0.75	0.78	3.19
PLA2G7	3.80	5.08	4.87	2.82	0.56	4.47	3.73	0.30	-0.10	-0.18	3.01
SLC1A3	4.33	4.19	5.08	3.25	-0.43	3.46	3.19	0.04	1.65	1.66	3.69
PTPRCAP	3.25	5.08	4.81	3.88	2.55	2.92	4.35	1.06	1.07	1.20	3.39
HLA-A	5.06	4.59	4.11	3.03	1.90	1.22	2.26	1.01	-0.61	0.65	2.59
CASP1	5.06	4.21	4.12	2.52	0.61	1.31	2.35	1.68	2.08	1.19	3.41
CCL8	5.05	2.69	1.94	3.71	0.78	1.00	1.30	2.03	1.03	1.43	2.51
CD44	5.04	4.31	4.12	1.60	0.90	2.31	4.48	1.64	0.45	0.54	2.84
FAT1	5.02	4.19	4.48	1.97	-0.47	1.85	1.88	-0.60	2.09	1.20	3.44
SCPEP1	4.76	4.59	5.01	3.30	1.30	2.20	1.77	0.56	-0.79	1.02	2.52
IGFALS	-5.01	-3.22	-3.87	-2.34	-0.02	-2.20	-2.52	1.28	-2.11	-0.62	-3.33
CXCR6	4.56	4.08	5.01	1.62	0.24	3.01	2.97	0.51	0.44	2.00	2.83
CCNB2	4.27	4.73	5.01	2.53	0.39	4.39	4.88	0.58	-0.30	0.75	2.65
LOC652493	5.00	4.23	4.21	3.67	0.89	1.15	1.86	0.36	0.87	0.80	3.36
VIM	5.00	4.96	4.45	0.81	0.34	2.18	2.22	-0.59	0.69	0.97	2.75
GINS2	4.07	4.99	4.05	3.12	1.06	2.17	1.66	1.71	-0.32	0.95	3.37
CCL5	4.83	4.99	4.75	2.73	0.88	1.70	3.18	1.68	0.02	1.75	4.35
FGL2	4.98	3.88	3.71	1.97	0.60	2.87	2.93	1.37	0.42	1.69	2.86
GZMB	4.11	4.64	4.97	2.44	0.41	1.07	2.55	2.25	-0.13	1.07	2.31
MUC13	4.96	2.97	4.04	2.08	-0.32	1.20	2.30	0.81	0.20	1.30	3.26
PRAMEF10	2.74	2.60	1.68	1.08	-0.84	3.56	4.96	-0.81	3.32	-1.11	2.83
C13orf15	4.10	4.25	4.94	1.41	0.55	1.33	1.29	-0.68	1.80	1.48	3.03
ADRA1B	-4.59	-4.94	-3.48	-1.58	0.46	-2.70	-1.53	0.46	-0.31	-0.41	-2.77
CCL3L1	4.05	4.16	4.68	3.74	1.02	4.93	3.75	0.99	1.79	0.70	3.06
DLEU1	-4.92	-3.44	-2.47	-0.69	0.79	-1.31	-1.36	0.68	-0.78	-0.47	-1.76
GSTA3	-4.92	-2.47	-2.61	-1.90	-0.38	-0.75	-2.34	-1.34	-1.39	-1.18	-2.46
ECGF1	4.91	3.92	3.86	3.14	1.48	1.91	2.27	1.23	0.43	1.04	3.28
AKR1B15	2.40	1.75	0.96	1.56	0.02	1.84	2.12	0.00	4.91	-0.52	1.58
KBTBD9	4.90	1.97	2.82	2.38	0.28	1.25	1.46	0.57	1.32	0.91	3.76
MAP4K1	4.48	4.57	4.89	2.41	-1.22	2.74	4.48	0.38	-0.39	1.54	2.52
GSN	3.60	3.92	4.52	1.99	0.51	-1.49	0.64	0.57	2.70	2.71	4.86
RPS6KA1	4.86	3.75	3.01	2.12	1.05	-0.65	1.29	0.85	0.20	-0.77	2.36
ZWINT	4.85	4.85	4.33	3.26	1.24	2.25	2.54	-1.13	-1.87	-3.05	2.61

RENBP	4.36	3.97	4.85	4.21	1.57	3.24	3.03	-0.11	0.45	1.03	2.83
RCAN1	4.85	3.19	2.70	0.70	-1.13	0.68	1.06	0.44	1.64	-1.61	2.77
NELL2	4.71	4.75	4.84	0.97	-1.22	1.75	2.12	-0.10	0.23	1.46	2.90
FCGR1A	4.67	4.84	3.89	2.36	0.14	2.52	2.48	0.67	0.09	1.84	3.70
TRIM22	4.83	4.71	3.85	1.84	0.85	0.97	1.79	1.40	0.35	0.52	2.34
UBE2L6	4.83	4.05	3.17	3.36	1.88	1.22	1.54	1.28	1.34	0.77	3.01
RGS1	4.61	3.95	4.82	3.05	0.38	3.82	3.17	0.48	0.23	0.96	3.12
CYP2C19	-3.87	-3.01	-3.27	-3.20	-2.91	-0.91	-1.71	-0.62	-2.11	-0.47	-4.82
SLC2A3	4.61	3.76	4.82	1.89	-0.17	1.72	2.40	0.30	0.17	0.62	1.59
MAD2L1	4.39	4.81	4.60	1.89	0.64	3.48	3.44	-1.43	-0.90	0.81	2.46
DRAM1	4.79	4.53	3.85	2.88	1.37	1.09	2.34	2.53	-0.29	0.79	4.44
LGALS3BP	4.79	3.28	3.41	1.85	0.67	0.68	0.70	0.19	1.43	1.19	2.64
HAAO	-4.79	-3.37	-2.94	-2.10	-0.58	0.24	-0.80	-1.38	0.75	-1.04	-2.73
C12orf43	-3.18	-3.42	-2.67	-4.79	-1.56	-0.96	-1.26	1.38	-0.55	0.52	-2.46
SGK	4.78	3.57	3.06	2.61	0.84	1.30	1.99	0.77	1.16	1.74	3.16
ZGPAT	-4.78	-3.40	-3.61	-1.90	1.02	-1.93	-2.18	-1.52	1.07	-0.79	-2.15
VAMP5	3.96	4.25	4.26	3.91	1.34	2.18	3.22	0.99	1.83	1.35	4.77
MS4A7	4.77	4.31	4.48	2.35	1.80	3.12	3.63	-0.23	0.33	0.85	3.11
FYN	4.77	4.04	4.25	0.76	-1.38	1.57	2.92	1.18	0.33	0.75	2.18
KIF20A	4.05	4.76	4.33	2.23	1.41	4.49	4.60	0.77	-0.54	0.37	2.26
STMN1	3.47	4.37	4.76	3.40	1.85	2.53	2.58	1.56	-1.35	-1.21	2.73
LILRB3	4.76	3.25	3.35	1.74	0.19	2.00	2.06	0.35	-0.40	1.24	2.50
CD27	4.75	4.17	4.72	3.10	0.34	3.25	2.67	-1.24	1.24	1.20	3.50
SLAMF8	4.75	3.86	4.73	3.85	0.73	2.75	3.37	0.65	1.16	1.08	3.73
MAP3K8	4.75	2.95	2.71	1.13	-0.12	1.33	1.65	0.76	-0.20	1.39	1.46
TSPAN17	4.36	3.79	4.22	4.74	2.13	1.63	1.43	0.21	0.96	1.30	3.97
OVGP1	-4.72	-3.43	-3.47	-2.38	0.01	-0.37	-1.29	0.99	-0.64	-0.90	-1.53
SUSD1	4.71	3.41	3.60	1.64	1.13	1.23	1.82	1.48	-0.59	0.43	2.25
TK1	3.05	4.71	3.98	3.19	1.98	1.94	2.36	0.62	-1.45	0.11	2.07
PTPRE	4.70	3.80	3.33	1.58	-0.67	1.83	2.94	-0.80	1.21	1.17	1.85
RNASE6	3.01	3.74	3.79	4.70	2.82	3.34	2.31	0.73	1.71	0.88	3.16
OIP5	3.25	4.67	4.09	2.20	1.01	2.95	3.00	1.00	-1.79	1.50	2.87
MCM2	3.45	4.67	3.52	1.25	-0.52	1.68	1.50	1.01	-0.84	0.20	2.69
LOC647450	4.67	3.99	3.98	3.44	0.58	1.00	1.55	0.12	0.94	0.77	3.09
C3orf14	3.61	4.67	4.64	4.27	1.69	1.86	2.81	0.48	0.92	1.19	3.59
CDCA5	4.37	4.66	4.56	2.89	0.63	3.20	3.11	0.38	-1.02	0.88	3.01
GPBAR1	3.60	2.01	2.25	4.66	2.64	2.58	2.82	1.06	1.44	1.20	2.29
FGR	4.65	4.39	3.98	3.57	1.02	3.34	3.49	2.45	1.20	2.17	3.81
TMPRSS3	4.64	3.35	4.20	2.48	-1.62	-3.55	-2.18	-1.17	2.77	-2.24	4.25
VMO1	3.16	3.47	3.04	4.64	2.91	0.37	3.17	0.97	0.43	0.50	2.82
DOCK8	4.64	3.31	3.99	0.78	-0.01	0.39	0.74	-0.18	-0.46	0.45	1.51
MTHFD2L	-2.13	-2.60	-3.06	-3.13	-0.28	-4.64	-2.70	0.66	-0.02	0.63	-2.31
C18orf56	3.16	4.64	4.43	3.02	1.34	1.46	1.40	1.59	0.36	1.26	3.17
UCP2	4.40	4.62	4.16	2.94	1.43	1.37	2.82	2.45	-0.25	0.60	2.00
DNAJC12	-4.61	-4.08	-3.91	-1.93	1.28	-3.42	-2.96	1.16	-0.96	-0.49	-3.92
HLA-DRB3	3.67	3.82	4.60	1.29	0.77	2.01	1.85	-0.58	0.89	0.15	1.20
EPSTI1	4.60	3.41	2.79	2.22	1.18	0.02	0.85	0.40	-0.15	1.14	2.65
PSMB8	4.60	4.39	3.86	4.01	2.07	1.50	2.95	1.35	0.77	-1.13	3.61
NKG7	3.98	4.59	4.33	3.07	1.25	1.76	4.13	2.56	0.45	1.30	3.22
MBL1P1	-3.34	-4.22	-4.59	-1.91	-0.64	-1.90	-1.25	-1.07	0.63	-0.02	-3.41
ENPP2	4.58	2.75	3.00	1.28	-1.05	0.77	0.30	0.67	1.21	1.76	4.45
CD247	3.66	3.27	4.57	4.13	1.68	-0.13	2.18	0.86	-0.77	1.48	3.12
OSTbeta	4.38	4.07	3.00	2.37	-0.38	4.56	3.91	-0.28	3.66	0.66	3.34
CPVL	4.19	4.55	4.04	2.37	1.46	3.73	2.87	0.53	-1.00	-0.50	3.14
ARPC5	4.54	3.26	3.42	1.53	0.37	1.15	0.24	0.35	-0.55	-0.34	2.33

SARDH	-4.53	-2.74	-2.98	-2.08	-0.89	-0.63	-0.54	-0.80	1.10	-1.32	-2.56
GPSM3	4.53	4.46	4.00	2.73	1.48	3.16	2.77	-0.26	0.98	0.59	2.17
HCP5	4.52	4.32	3.65	2.65	1.61	0.74	2.02	0.62	-0.90	0.77	2.22
COL3A1	4.52	3.66	3.36	0.96	-1.15	1.18	1.23	-0.21	0.82	3.39	2.22
IGLL1	4.51	3.76	4.32	2.70	0.69	1.12	1.06	-0.56	0.27	0.79	2.48
SH3PXD2A	-2.69	-2.79	-3.28	-2.76	-1.70	-1.09	-0.30	-0.36	-1.50	-1.65	-4.50
CCL21	3.94	3.99	4.50	3.19	1.18	1.40	1.87	0.01	0.62	0.82	2.97
FPR3	4.48	4.40	3.39	2.78	1.18	1.22	1.50	1.34	0.69	2.20	3.41
LPAL2	-4.48	-3.37	-3.20	-2.49	0.21	-2.31	-1.89	0.52	-1.68	-0.75	-2.95
RAD51AP1	4.47	4.13	4.03	1.64	0.04	3.46	3.15	0.26	-0.30	0.41	3.62
GPR125	-2.96	-4.46	-4.45	-2.92	-1.63	-2.75	-2.60	1.58	-1.03	2.94	-3.31
KCNN2	-4.15	-2.54	-2.80	-2.31	-0.10	-0.27	-0.42	-0.22	-1.27	-1.84	-4.44
LOC642113	4.31	4.04	4.43	3.14	0.57	1.97	1.82	0.65	0.68	0.69	3.13
ALOX5AP	3.41	3.66	4.43	2.61	1.63	0.17	1.39	1.11	-0.60	0.96	3.14
DHRS9	4.41	3.70	4.18	2.66	0.86	3.79	4.10	-0.65	1.42	1.79	1.80
TIMP1	3.93	3.77	4.40	3.47	1.29	1.63	2.21	-0.41	1.14	0.93	3.93
PCOLCE2	-4.39	-3.89	-3.84	-3.39	-1.14	-1.21	-1.64	-0.71	-0.54	-0.66	-2.54
ZDHHC23	2.54	2.75	4.37	1.60	0.88	1.25	0.97	-1.30	0.04	0.06	0.85
KIAA0101	3.87	4.36	4.09	3.69	1.81	2.26	2.37	-1.68	-0.58	1.61	3.37
AURKA	4.08	3.70	4.34	2.36	1.09	2.83	3.32	0.47	0.03	0.52	3.29
GSTA5	-4.33	-2.11	-2.25	-2.08	0.17	-1.08	-2.83	0.10	-1.21	-0.66	-1.89
CACNA1H	-4.33	-3.94	-3.39	-3.43	-1.40	-0.17	-1.19	1.21	-2.72	-0.66	-3.77
PIGR	4.29	4.32	3.76	2.63	1.43	1.25	1.13	1.21	-0.90	0.69	3.15
SELL	4.32	3.84	3.76	0.80	-0.46	1.47	2.79	0.64	-0.39	0.68	1.63
LOC652694	4.00	4.32	3.71	3.42	0.58	1.20	2.18	0.55	0.98	0.97	2.81
DNMT3L	-4.31	-2.24	-2.29	-1.64	0.53	0.28	-0.82	0.70	-1.79	-1.25	-1.87
TRIM55	-2.58	-1.66	-3.24	-1.77	1.24	1.06	0.68	0.72	-1.16	-0.78	-4.30
ATP1B3	4.19	4.30	4.07	1.87	-0.64	1.58	2.42	1.47	-1.89	-2.70	2.19
PLGLB1	-3.62	-3.59	-4.30	-3.21	-0.31	-3.89	-2.78	1.06	-1.38	0.43	-1.66
RNF144B	-3.12	-4.03	-4.07	-2.37	0.26	-3.16	-4.29	0.33	-2.84	-0.23	-2.35
LYZ	3.04	3.59	4.28	2.77	1.72	2.30	2.42	0.93	0.38	1.32	2.53
BCHE	-3.34	-3.12	-4.28	-4.02	-1.24	-1.23	-3.25	0.04	-1.70	-0.72	-3.71
BLVRA	3.43	3.62	4.13	4.27	2.34	1.53	1.93	1.58	0.01	0.83	2.93
ANKRD35	-3.76	-2.86	-3.07	-2.13	0.13	1.10	0.36	1.07	-0.53	1.60	-4.27
MATN2	-4.27	-2.98	-2.89	-3.33	-0.74	-1.27	-2.51	0.42	-2.65	-0.18	-2.44
PRKCB1	4.13	3.23	4.25	2.62	1.14	1.00	1.93	1.97	-1.02	1.05	1.57
PLA2G4C	4.24	3.69	3.50	3.30	0.66	0.64	0.67	-0.44	0.97	1.17	2.63
PCOLCE	-3.14	-2.89	-3.24	-2.24	0.28	-0.24	-1.42	0.25	-0.56	-0.43	-4.24
DIRAS3	-4.17	-4.24	-3.40	-3.47	-1.61	-0.91	-2.46	-0.23	0.14	0.40	-1.95
MOXD1	3.97	4.22	3.75	1.31	-0.62	2.78	3.12	-1.91	0.50	0.74	2.44
NCOR1	-4.22	-3.45	-2.79	-1.18	0.51	-0.47	-0.51	0.48	0.37	-1.32	-3.48
LGALS9	2.47	3.71	2.85	2.58	0.69	2.60	4.22	2.01	0.62	0.94	2.55
SLC15A3	4.19	3.39	2.56	2.26	1.33	1.22	1.20	-0.06	-0.28	0.89	1.71
SLC38A1	3.88	4.19	3.62	-0.81	-1.67	1.20	1.68	1.06	-0.67	-0.49	2.19
CDC20	3.16	3.97	4.01	2.94	0.92	3.65	4.16	1.10	-1.01	0.10	2.64
CXCL6	4.16	3.66	3.85	2.27	-0.43	1.61	2.04	-0.82	0.88	1.91	3.49
HSD17B14	-4.16	-3.71	-3.18	-1.97	-0.72	1.03	-0.26	-1.15	-0.56	-1.20	-3.25
LOC644322	-4.13	-1.87	-2.66	-1.09	0.23	-1.41	-1.02	-0.01	-0.39	-0.98	-2.05
IL8	4.13	4.03	3.86	2.65	-0.33	2.70	2.55	0.49	0.16	1.30	4.11
ASPM	3.45	4.13	3.62	1.33	0.05	3.12	2.92	-0.12	-1.16	-0.07	2.09
LOC401115	3.48	3.26	4.13	2.93	1.39	0.60	1.31	0.62	-0.14	0.67	3.80
KDELR3	4.12	3.58	4.13	1.89	-0.83	1.61	0.93	0.90	0.56	0.92	3.69
XLKD1	-4.13	-3.69	-3.70	-2.40	-0.11	-1.91	-2.79	-1.28	-0.21	-0.10	-3.95
PNMA6A	-4.12	-2.88	-2.10	-1.83	-2.13	-1.12	-0.76	-0.40	-0.49	-0.92	-0.55
FAM129A	4.12	3.62	3.42	1.26	-0.28	0.98	1.40	0.79	-0.37	1.37	2.21

ISG20	4.12	3.69	3.00	2.96	1.15	0.49	1.14	0.33	0.72	0.96	3.14
MNS1	3.94	3.61	3.50	2.38	0.32	3.08	2.78	-1.57	3.41	1.51	4.11
NCAPG	4.02	3.96	4.11	1.85	-0.67	2.82	2.62	0.18	-0.70	0.96	2.54
FAM134B	-3.57	-4.11	-3.65	-2.60	-1.81	1.61	-2.51	-0.55	1.94	0.78	-3.68
CD24	4.10	2.98	2.91	2.10	-0.80	0.86	1.71	0.57	0.96	0.94	3.18
CCL15	-4.10	-3.07	-3.48	1.82	2.09	1.70	2.05	1.60	-1.54	-2.73	-2.20
LOC644743	3.26	3.00	3.20	2.48	-0.07	4.09	2.44	0.24	2.31	0.29	2.91
GSTA2	-4.09	-2.50	-3.05	-2.85	-0.85	-0.20	-1.29	0.63	-1.40	-0.06	-3.05
LAMP2	4.07	3.59	3.42	1.22	-0.90	1.99	1.41	-1.13	1.20	0.87	2.24
KRT8	3.24	3.50	3.49	3.37	0.85	3.59	3.05	0.62	2.43	-0.07	4.07
ADCY1	-3.57	-3.01	-2.10	-2.56	-0.21	0.85	-1.25	-0.16	0.06	-0.78	-4.06
HPS5	4.06	2.23	1.97	0.42	-0.39	0.43	0.90	1.08	1.16	1.09	3.01
UGT2A3	4.05	2.70	2.67	1.03	-0.27	1.16	0.82	-0.49	-1.01	1.19	2.28
HLA-DPB1	4.05	3.05	3.41	1.00	-0.03	1.00	1.06	-1.24	0.25	1.47	2.31
CHST9	3.56	2.18	3.31	2.78	1.05	0.68	0.65	-0.25	0.87	0.82	4.04
NEDD4L	3.78	4.04	3.31	2.89	0.80	1.64	1.41	0.05	2.12	-0.35	3.24
FIS	-3.79	-2.71	-4.03	-3.56	0.14	-0.53	-1.48	0.45	-1.31	-2.20	-3.98
HSD17B13	-4.02	-3.63	-3.74	-3.69	0.69	-2.72	-3.96	-0.84	-1.47	-1.10	-3.24
CCL20	3.78	3.00	3.03	2.56	0.99	1.05	1.69	0.26	0.19	0.99	4.01
PRC1	3.99	4.00	4.00	2.64	0.93	3.13	2.97	0.06	-1.15	0.32	2.33
CXCL13	2.68	3.05	3.98	0.35	-0.64	2.31	2.66	0.86	-0.96	0.76	1.36
LIPC	-3.96	-3.98	-3.58	-2.34	0.38	-2.43	-2.61	0.15	-0.44	0.51	-2.08
C1orf54	3.79	2.39	3.97	3.70	1.19	0.90	2.19	1.87	-0.91	0.79	2.81
KBTBD11	-2.81	-3.41	-3.96	-2.06	-0.35	-2.05	-3.16	-1.81	-1.74	-0.99	-3.17
ACSL4	3.16	2.80	-2.86	-1.68	-0.51	1.46	1.10	1.18	-2.57	-3.96	-2.31
SLC43A1	3.96	2.35	2.88	2.18	1.10	0.13	0.30	0.39	1.12	0.33	2.82
GDF15	2.86	3.44	3.96	1.48	0.00	3.22	2.73	-0.18	2.27	0.68	2.20
SERPINE2	3.32	3.53	3.93	1.02	-0.76	1.05	1.17	-0.58	0.36	-0.03	3.03
H2AFZ	2.60	3.15	3.91	2.69	1.83	1.70	1.83	0.93	-0.83	0.19	2.01
LOC654201	-3.91	-3.33	-2.86	-2.51	-1.19	0.63	-0.19	-0.62	-0.54	-0.39	-3.14
LPA	-3.90	-3.48	-3.01	-2.57	-0.85	-2.85	-1.73	0.61	-1.29	-0.73	-2.81
TMEM45B	3.90	1.91	1.74	1.15	-0.01	0.16	-0.36	-0.23	1.21	0.62	2.67
MAP2K1	-3.60	-3.56	-3.89	-1.97	0.05	-2.12	-2.53	-0.83	-2.23	0.18	-2.89
S100A4	3.79	3.54	3.88	2.72	2.45	1.30	1.89	1.96	-0.51	0.92	2.33
SLCO2A1	3.86	2.01	2.70	1.50	-0.23	0.15	0.63	-1.49	3.28	1.63	2.06
USH2A	-3.84	-2.84	-3.79	-2.42	0.28	-2.34	-2.48	1.20	-0.86	1.07	-3.35
LUM	3.83	3.01	3.73	-1.29	-0.36	1.88	0.71	-1.70	0.74	1.59	1.72
BTN3A2	3.22	3.83	3.36	1.64	-0.71	1.63	2.25	-0.31	-0.44	1.16	2.24
ANXA1	3.82	2.98	2.88	0.51	0.34	0.93	0.41	-0.16	-0.36	1.78	1.07
RNASE1	3.31	3.53	3.80	3.65	1.82	1.51	1.90	0.50	1.95	0.68	2.26
KRT222	3.43	3.78	3.02	2.69	0.73	2.49	2.35	-0.50	0.39	-0.41	2.23
FLJ40504	2.67	2.73	3.78	2.54	1.78	3.43	1.78	-1.08	1.85	0.98	2.69
LOXL4	3.75	2.78	3.09	2.28	-0.45	2.62	2.22	-0.05	2.57	1.24	3.78
HLA-DRB4	3.59	3.57	3.77	0.81	-2.16	2.31	2.14	0.78	1.49	1.98	3.18
FXYD1	-3.75	-2.19	-1.52	-0.63	0.50	0.47	-0.54	-0.33	0.95	-1.24	-1.78
ZNFX1	3.74	3.28	2.16	2.69	1.33	0.81	1.12	0.74	0.58	0.37	2.35
RARRES3	3.71	3.28	3.04	3.21	2.25	-0.25	1.18	1.23	-0.73	0.99	2.32
DTNA	3.17	3.69	3.32	1.27	-1.05	1.47	1.54	-1.23	2.25	1.99	3.67
GCDH	-3.69	-1.93	-1.94	-1.18	-0.60	-1.26	-0.58	-0.13	1.42	-0.52	-2.30
IL2RB	3.22	2.38	3.66	2.37	0.55	1.24	2.02	-1.30	-0.88	0.52	0.84
EMP1	3.54	1.90	1.12	0.82	-0.42	1.31	1.13	0.21	3.64	0.55	2.45
CAP2	3.64	3.37	2.95	1.43	-1.11	2.64	1.86	-0.81	1.43	1.08	2.45
OSTalpha	3.01	2.81	3.42	1.77	-1.14	1.96	3.00	0.20	2.00	0.42	3.64
HLA-G	3.37	3.57	3.64	1.66	1.04	0.82	1.21	-0.17	-0.53	0.11	1.95
OAS2	3.64	2.56	1.52	1.69	1.50	0.88	-0.62	0.31	-0.48	0.91	1.79

NEU4	-3.64	-3.25	-3.02	-1.80	0.75	-0.64	-2.47	0.38	-0.54	0.28	-2.91
TACSTD2	3.64	2.47	2.76	1.83	0.07	0.89	1.29	-0.78	-0.01	1.32	2.68
IFIH1	3.62	2.32	1.76	0.88	0.01	-0.07	-0.24	-0.55	0.05	0.41	1.08
LOC649923	3.08	3.61	3.24	2.07	-0.26	1.57	1.31	0.07	0.77	0.45	1.78
CES7	-3.60	-1.36	-2.14	-1.53	-0.25	-0.18	-0.62	1.71	-1.36	-0.74	-1.76
VIL1	-3.25	-3.59	-3.05	-2.30	-0.70	-0.21	-0.93	1.02	0.06	0.06	-1.89
CHAD	-3.55	-3.04	-2.46	-2.43	-1.78	-1.19	-1.43	-0.05	0.20	-0.60	-1.73
GZMH	3.54	2.82	3.43	2.77	1.31	0.25	1.59	2.19	-0.54	1.53	3.05
SLITRK3	-3.07	-3.44	-3.42	-1.32	0.09	-1.34	-0.70	0.13	-0.85	-0.82	-3.52
CCND1	3.52	2.85	2.74	1.68	0.04	0.83	1.27	-1.29	1.07	1.48	3.09
PPT1	3.51	2.63	2.90	1.05	0.81	-0.03	0.38	0.82	-1.06	0.27	1.78
PTGDS	3.00	2.66	3.51	1.66	-0.59	0.93	1.68	-0.12	0.60	1.56	2.58
IFIT3	3.50	3.00	1.67	1.89	1.05	1.27	1.40	0.77	1.07	0.80	2.01
THOP1	-3.50	-1.84	-3.41	-1.62	-0.23	0.61	-0.92	0.98	-2.07	-2.25	-3.31
HOPX	2.64	2.99	3.50	1.34	0.87	2.64	2.59	1.15	0.21	1.92	1.59
LOC339766	-3.48	-2.27	-2.67	-2.18	0.09	-1.06	-1.52	0.62	-0.88	-0.23	-2.57
GNMT	-3.48	-2.90	-3.07	-1.27	-0.59	-2.01	-1.58	-0.75	-0.06	0.12	-1.94
MDK	2.86	3.34	3.47	3.26	2.35	2.18	1.61	1.11	-1.66	-0.76	2.56
JUN	3.46	1.79	2.93	1.97	-0.16	1.84	1.54	-0.44	2.84	1.53	2.49
LY96	3.39	2.97	3.35	3.23	1.96	0.07	0.73	1.38	-0.03	0.54	2.14
ARHGAP10	-2.51	-2.45	-3.39	-1.86	0.67	-1.64	-1.01	-0.16	-0.61	-0.54	-2.29
CDKN1A	3.36	3.18	2.25	1.24	0.27	0.34	0.29	0.08	1.70	1.17	3.11
SAMD9	3.36	2.28	1.84	1.82	1.00	-0.56	-0.29	0.66	-0.49	0.66	1.43
ASB9	-3.36	-1.76	-2.17	-1.14	-0.76	-1.78	-1.11	0.53	-0.44	-1.89	-1.92
CCL2	3.35	2.86	2.33	2.24	0.26	1.41	0.96	-0.39	0.75	2.00	1.99
BBOX1	-3.15	-2.31	-2.38	-1.18	-0.05	-3.03	-3.34	0.11	-1.33	0.05	-2.00
CRIP1	3.16	3.25	3.34	2.64	1.41	1.06	1.81	-0.17	0.50	0.74	2.12
GPX2	0.82	3.31	2.40	3.02	2.49	0.76	1.61	0.27	-0.16	0.18	1.89
RND2	-3.21	-3.31	-2.41	-1.76	-1.06	-2.48	-2.15	-1.11	-0.26	-0.10	-3.00
DDX60	3.28	2.45	1.77	0.82	0.29	-0.21	0.61	0.28	-0.10	0.82	1.68
PACSIN3	-3.28	-3.02	-3.28	-1.04	-0.21	-1.10	-0.60	-0.06	-0.49	-1.09	-2.86
SP110	3.27	2.70	2.35	2.16	1.29	1.22	0.88	-1.94	1.77	0.96	1.38
EFHD1	-3.17	-2.56	-1.67	-1.77	-1.30	0.98	0.20	1.09	-0.67	-1.67	-3.26
LOC651751	3.25	2.96	2.88	2.28	-0.46	1.92	1.20	-0.17	1.08	1.72	2.06
IFI27	3.24	2.66	2.14	2.93	1.56	-1.43	-0.13	0.72	-0.40	1.15	3.01
LOC651894	-3.22	-1.74	-1.89	-0.88	0.75	-0.26	-0.77	0.59	-0.38	-1.73	-1.35
TMEM20	2.87	3.21	3.09	1.81	0.22	1.27	0.67	-0.23	0.30	0.06	2.64
FCAMR	3.19	2.85	2.01	2.10	1.22	0.21	-0.35	1.00	-1.66	1.54	2.52
IL1RAP	-3.14	-2.17	-1.20	-1.54	-1.36	-2.90	-2.08	-1.11	-0.40	-0.35	-1.68
IFIT2	3.13	2.09	1.10	1.50	0.77	0.52	0.39	-0.93	1.19	0.84	1.57
IGJ	3.09	1.91	2.02	2.10	0.93	0.89	0.23	-0.32	0.19	1.51	1.27
ALDH1L1	-4.87	-4.21	-3.85				-1.14	0.60			-4.27
B3GNT9	-0.05		0.81	-3.13	-5.42		0.18	-1.64	-0.64	-0.25	-0.56
DOCK2	5.47		5.13	2.33	0.34	2.63	3.73	1.12	-0.22	1.45	2.86
HLA-DPA1	6.04	5.35	5.13		1.19	2.84	2.81		0.17	1.09	3.70
LIPA	4.69	3.97	3.26	0.83	0.30	2.02	2.14		-0.95	0.70	1.83
TYROBP	4.71	4.80	5.47		1.67		3.78			1.09	4.37
ZBTB33	5.35	4.38	4.35				2.30		0.54	1.54	4.41
ZNF511	-5.94	-5.19				-0.24	-2.14		-0.84	-0.75	-4.11

Supplementary Table S5. Functional pathways associated with severity of different histological parameters. Analysis performed using Gene Set Enrichment Analysis (GSEA) software against Hallmark gene sets from MSigDB and Pathogenesis Based Transcript (PBT) sets from the University of Alberta. Normalised Enrichment Score (NES) and False Discovery Rate (FDR) are shown for each parameter. NES is a quantified measure of strength of enrichment determined by the GSEA software and defined on the MIT Broad Institue website (http://www.broadinstitute.org/gsea/doc/GSEAUserGuideTEXT.htm#_Normalized_Enrichment_Score). Significantly enriched pathways (FDR < 0.05) are highlighted.

	lobular inflammation		portal inflammation		interface hepatitis		ductopenia		perisinusoidal fibrosis		endothelitis central vein		ductular reaction		endothelitis portal veins		bile duct lesions		central vein perivenulitis		portal fibrosis	
Gene Set	**NES**	**FDR**	**NES**	**FDR**	**NES**	**FDR**	**NES**	**FDR**	**NES**	**FDR**	**NES**	**FDR**	**NES**	**FDR**	**NES**	**FDR**	**NES**	**FDR**	**NES**	**FDR**	**NES**	**FDR**
PBT_QCMAT	2.65	0.00	2.61	0.00	2.63	0.00	0.90	0.89	1.84	0.00	1.94	0.00	2.32	0.00	2.47	0.00	2.44	0.00	2.45	0.00	2.59	0.00
PBT_QCAT	2.54	0.00	2.54	0.00	2.60	0.00	0.50	1.00	1.95	0.00	1.76	0.01	1.87	0.00	2.31	0.00	2.61	0.00	2.44	0.00	2.48	0.00
PBT_CIRIT	2.40	0.00	2.39	0.00	2.40	0.00	0.93	0.89	1.32	0.12	1.27	0.26	1.49	0.07	2.29	0.00	2.01	0.00	1.72	0.01	1.92	0.00
PBT_GRIT1	2.38	0.00	2.51	0.00	2.43	0.00	0.87	0.92	1.47	0.04	2.03	0.00	1.69	0.01	2.04	0.00	2.51	0.00	2.44	0.00	2.37	0.00
PBT_IRITD5	2.32	0.00	2.19	0.00	2.41	0.00	-0.98	1.00	1.81	0.00	0.98	0.69	1.09	0.50	1.89	0.00	1.88	0.00	1.30	0.14	1.88	0.00
PBT_IRITD3	2.20	0.00	2.11	0.00	2.15	0.00	1.68	0.07	1.86	0.00	1.24	0.28	1.34	0.19	2.04	0.00	1.96	0.00	1.88	0.00	2.22	0.00
PBT_BAT	2.09	0.00	2.31	0.00	2.26	0.00	0.64	1.00	0.85	0.77	1.13	0.45	0.93	0.69	2.06	0.00	2.13	0.00	1.59	0.02	1.66	0.01
PBT_ENDAT	1.95	0.00	1.79	0.00	1.90	0.00	1.27	0.41	1.60	0.01	0.79	0.97	1.05	0.56	1.11	0.34	1.15	0.32	1.35	0.10	1.52	0.02
PBT_TCB	1.72	0.00	1.74	0.00	1.77	0.00	-0.82	1.00	1.17	0.31	0.72	0.99	1.14	0.45	1.52	0.03	1.62	0.01	1.33	0.12	1.56	0.02
PBT_IRRAT	1.59	0.01	1.65	0.01	1.70	0.00	0.84	0.94	1.46	0.05	1.14	0.44	1.14	0.43	1.53	0.03	1.58	0.02	1.25	0.18	1.58	0.01
PBT_AMAT1	1.56	0.01	1.04	0.46	1.70	0.00	0.67	1.00	0.74	0.92	0.54	0.99	1.14	0.44	1.59	0.02	1.56	0.02	0.95	0.66	1.06	0.42
PBT_IGT	1.49	0.03	1.38	0.06	1.49	0.03	0.84	0.96	1.13	0.35	0.64	1.00	-1.09	1.00	1.18	0.26	1.11	0.37	1.48	0.04	1.34	0.09
PBT_HTS	1.40	0.05	1.40	0.05	1.33	0.09	1.17	0.50	1.24	0.20	-1.05	1.00	1.05	0.54	1.31	0.12	1.15	0.32	0.86	0.79	1.05	0.42
PBT_NKB	1.25	0.15	1.21	0.19	1.48	0.03	1.40	0.26	1.35	0.11	1.37	0.18	1.18	0.40	1.17	0.27	1.39	0.07	1.33	0.12	1.10	0.34
PBT_DSAST	1.18	0.23	1.38	0.06	1.52	0.02	1.09	0.61	1.63	0.01	1.31	0.22	0.91	0.71	1.38	0.07	1.40	0.07	1.17	0.28	0.52	1.00
PBT_MCAT	-1.10	0.50	-0.55	0.99	-0.52	0.99	1.23	0.42	-1.10	0.52	1.16	0.44	0.96	0.66	0.71	0.93	-0.53	1.00	-1.17	0.43	-1.16	0.34
HALLMARK_INTERFERON_GAMMA_RESPONSE	2.97	0.00	2.93	0.00	2.68	0.00	1.28	0.43	1.91	0.00	2.20	0.00	1.84	0.00	2.10	0.00	2.22	0.00	2.80	0.00	2.69	0.00
HALLMARK_ALLOGRAFT_REJECTION	2.92	0.00	2.92	0.00	2.94	0.00	0.54	1.00	2.06	0.00	1.80	0.01	1.91	0.00	2.45	0.00	2.75	0.00	2.70	0.00	2.63	0.00
HALLMARK_INTERFERON_ALPHA_RESPONSE	2.76	0.00	2.81	0.00	2.53	0.00	0.90	0.88	1.75	0.01	2.21	0.00	1.85	0.00	1.62	0.01	1.78	0.00	2.63	0.00	2.40	0.00
HALLMARK_TNFA_SIGNALING_VIA_NFKB	2.63	0.00	2.39	0.00	2.38	0.00	1.58	0.08	2.12	0.00	1.09	0.52	1.15	0.45	2.03	0.00	2.32	0.00	2.31	0.00	2.40	0.00
HALLMARK_E2F_TARGETS	2.57	0.00	2.65	0.00	2.64	0.00	0.78	1.00	1.90	0.00	1.40	0.16	1.79	0.01	2.62	0.00	2.48	0.00	2.37	0.00	2.37	0.00
HALLMARK_G2M_CHECKPOINT	2.56	0.00	2.56	0.00	2.64	0.00	-1.08	1.00	1.96	0.00	1.33	0.21	1.75	0.01	2.46	0.00	2.40	0.00	2.07	0.00	2.16	0.00
HALLMARK_INFLAMMATORY_RESPONSE	2.56	0.00	2.47	0.00	2.36	0.00	-0.69	0.95	2.04	0.00	1.40	0.17	1.56	0.04	1.92	0.00	2.11	0.00	2.03	0.00	2.21	0.00
HALLMARK_IL6_JAK_STAT3_SIGNALING	2.48	0.00	2.40	0.00	2.45	0.00	0.52	1.00	1.61	0.01	1.61	0.04	0.98	0.65	1.76	0.00	1.95	0.00	2.17	0.00	2.19	0.00
HALLMARK_KRAS_SIGNALING_UP	2.45	0.00	2.41	0.00	2.41	0.00	1.16	0.48	1.72	0.01	1.15	0.44	1.40	0.14	2.09	0.00	1.92	0.00	1.97	0.00	2.33	0.00
HALLMARK_APOPTOSIS	2.36	0.00	2.41	0.00	2.35	0.00	1.28	0.45	1.71	0.01	1.36	0.19	1.80	0.00	2.08	0.00	2.13	0.00	1.94	0.00	2.18	0.00
HALLMARK_COMPLEMENT	2.33	0.00	2.24	0.00	2.32	0.00	1.15	0.49	1.52	0.03	0.85	0.93	1.37	0.16	1.94	0.00	2.04	0.00	1.75	0.00	2.11	0.00
HALLMARK_MITOTIC_SPINDLE	2.23	0.00	2.13	0.00	2.21	0.00	1.35	0.32	1.68	0.01	-1.01	1.00	0.90	0.72	2.26	0.00	2.02	0.00	1.25	0.18	1.83	0.00
HALLMARK_IL2_STAT5_SIGNALING	2.20	0.00	2.24	0.00	2.18	0.00	0.93	0.87	1.37	0.09	1.21	0.34	1.36	0.17	2.03	0.00	2.16	0.00	1.73	0.01	1.88	0.00
HALLMARK_MTORC1_SIGNALING	2.12	0.00	2.21	0.00	2.18	0.00	1.03	0.69	1.44	0.05	1.31	0.22	1.80	0.01	1.61	0.02	1.63	0.01	1.95	0.00	1.80	0.00
HALLMARK_P53_PATHWAY	2.12	0.00	2.22	0.00	2.15	0.00	1.48	0.17	1.70	0.01	1.82	0.01	1.37	0.16	1.68	0.01	1.80	0.00	2.17	0.00	1.97	0.00
HALLMARK_ANGIOGENESIS	2.05	0.00	1.93	0.00	2.07	0.00	1.61	0.10	1.70	0.01	0.58	1.00	0.89	0.72	1.85	0.00	2.01	0.00	1.60	0.02	2.08	0.00
HALLMARK_UV_RESPONSE_UP	1.93	0.00	1.73	0.00	1.80	0.00	1.14	0.50	0.99	0.59	1.40	0.20	1.20	0.40	1.40	0.06	1.41	0.07	1.41	0.07	1.80	0.00

HALLMARK_HYPOXIA	1.93	0.00	1.70	0.00	1.85	0.00	1.25	0.40	1.69	0.01	0.84	0.93	-1.06	0.96	1.41	0.06	1.34	0.11	1.62	0.01	1.62	0.01
HALLMARK_ESTROGEN_RESPONSE_LATE	1.89	0.00	1.84	0.00	1.77	0.00	-1.01	1.00	0.98	0.62	0.98	0.70	1.12	0.44	1.63	0.01	1.76	0.00	1.63	0.01	1.44	0.04
HALLMARK_MYC_TARGETS_V1	1.85	0.00	1.83	0.00	1.85	0.00	1.21	0.44	0.90	0.73	1.09	0.51	1.31	0.21	1.48	0.04	1.16	0.31	1.88	0.00	1.73	0.00
HALLMARK_UNFOLDED_PROTEIN_RESPONSE	1.78	0.00	1.76	0.00	1.75	0.00	0.82	0.95	1.16	0.31	1.24	0.29	1.30	0.21	1.17	0.27	1.07	0.45	1.58	0.02	1.60	0.01
HALLMARK_EPITHELIAL_MESENCHYMAL_TRANSITI	1.77	0.00	1.66	0.01	1.78	0.00	1.03	0.71	1.72	0.01	-1.31	1.00	1.05	0.55	1.36	0.08	1.38	0.08	0.98	0.60	1.57	0.02
HALLMARK_PI3K_AKT_MTOR_SIGNALING	1.76	0.00	1.77	0.00	1.98	0.00	1.21	0.43	1.64	0.01	1.03	0.59	1.08	0.53	1.47	0.04	1.50	0.03	1.60	0.02	1.54	0.02
HALLMARK_ANDROGEN_RESPONSE	1.75	0.00	1.53	0.02	1.52	0.02	-0.94	1.00	0.86	0.77	1.14	0.44	0.83	0.81	1.34	0.10	0.89	0.75	0.92	0.70	1.24	0.18
HALLMARK_COAGULATION	1.73	0.00	1.62	0.01	1.76	0.00	1.55	0.10	1.10	0.38	-0.86	0.92	-1.21	0.88	1.54	0.03	1.25	0.19	1.16	0.28	1.47	0.03
HALLMARK_ESTROGEN_RESPONSE_EARLY	1.68	0.00	1.46	0.03	1.54	0.02	1.10	0.61	1.08	0.42	0.77	0.97	0.99	0.65	1.42	0.06	1.48	0.04	1.26	0.18	1.31	0.11
HALLMARK_UV_RESPONSE_DN	1.62	0.01	1.39	0.06	1.37	0.07	1.17	0.49	1.52	0.03	0.88	0.91	-1.11	1.00	1.48	0.04	1.04	0.50	1.04	0.49	1.22	0.20
HALLMARK_DNA_REPAIR	1.60	0.01	1.85	0.00	1.51	0.02	0.83	0.94	1.14	0.34	1.70	0.02	1.88	0.00	1.62	0.01	1.49	0.04	1.81	0.00	1.71	0.00
HALLMARK_PROTEIN_SECRETION	1.60	0.01	1.88	0.00	1.74	0.00	1.00	0.75	1.17	0.31	0.98	0.68	1.20	0.39	1.53	0.03	1.47	0.04	1.22	0.21	1.57	0.02
HALLMARK_GLYCOLYSIS	1.58	0.01	1.51	0.02	1.74	0.00	1.27	0.42	1.25	0.20	1.04	0.62	0.99	0.64	1.59	0.02	1.51	0.03	1.44	0.06	1.56	0.02
HALLMARK_APICAL_SURFACE	1.57	0.01	1.23	0.17	1.62	0.01	-0.87	1.00	1.16	0.31	0.99	0.70	-1.03	0.86	1.18	0.26	1.23	0.22	1.17	0.27	1.20	0.21
HALLMARK_WNT_BETA_CATENIN_SIGNALING	1.48	0.03	1.30	0.11	1.45	0.04	0.75	1.00	0.93	0.67	-0.99	0.93	0.64	0.98	1.09	0.37	1.22	0.23	1.36	0.10	1.45	0.04
HALLMARK_ADIPOGENESIS	1.41	0.05	1.31	0.10	1.17	0.25	1.19	0.46	1.24	0.21	-0.96	0.94	-0.88	1.00	1.42	0.06	1.15	0.31	0.79	0.89	1.19	0.22
HALLMARK_HEME_METABOLISM	1.37	0.07	1.56	0.01	1.58	0.01	0.93	0.85	0.94	0.67	1.32	0.23	0.94	0.70	1.36	0.08	1.18	0.29	1.47	0.04	1.28	0.14
HALLMARK_PEROXISOME	1.37	0.07	1.61	0.01	1.60	0.01	1.42	0.24	-1.35	0.80	1.26	0.27	1.24	0.32	1.53	0.03	1.50	0.03	1.23	0.19	1.46	0.04
HALLMARK_TGF_BETA_SIGNALING	1.32	0.10	0.70	0.95	0.79	0.87	0.73	1.00	0.89	0.73	1.51	0.09	1.18	0.41	0.78	0.87	-0.60	1.00	0.91	0.71	1.18	0.23
HALLMARK_APICAL_JUNCTION	1.30	0.11	1.47	0.03	1.63	0.01	1.25	0.42	1.20	0.27	0.83	0.91	0.80	0.86	1.69	0.01	1.52	0.03	1.36	0.10	1.41	0.05
HALLMARK_HEDGEHOG_SIGNALING	1.28	0.13	1.30	0.11	1.38	0.06	1.38	0.27	1.25	0.20	-0.68	0.96	1.31	0.22	1.07	0.41	1.34	0.11	0.76	0.91	1.47	0.03
HALLMARK_SPERMATOGENESIS	1.28	0.13	1.48	0.03	1.38	0.06	-1.23	0.88	0.92	0.69	0.98	0.67	0.93	0.69	1.23	0.20	1.26	0.18	0.92	0.70	1.40	0.06
HALLMARK_CHOLESTEROL_HOMEOSTASIS	1.25	0.16	1.35	0.08	1.28	0.13	-1.51	0.25	1.68	0.01	0.87	0.92	1.78	0.00	0.96	0.59	1.03	0.49	1.57	0.02	1.56	0.02
HALLMARK_OXIDATIVE_PHOSPHORYLATION	1.24	0.15	1.55	0.02	1.40	0.05	1.08	0.60	-0.97	0.73	-0.85	0.87	-0.81	0.89	1.27	0.16	1.05	0.48	1.09	0.39	1.21	0.21
HALLMARK_REACTIVE_OXIGEN_SPECIES_PATHWA	1.21	0.19	1.27	0.14	1.31	0.10	1.59	0.09	1.42	0.07	0.84	0.91	-1.00	0.88	0.94	0.62	1.03	0.50	1.13	0.32	1.38	0.07
HALLMARK_MYC_TARGETS_V2	1.14	0.29	1.28	0.12	1.18	0.25	0.70	1.00	1.74	0.01	1.40	0.19	1.15	0.44	1.10	0.36	1.00	0.53	1.67	0.01	1.03	0.46
HALLMARK_KRAS_SIGNALING_DN	1.10	0.35	1.08	0.39	0.92	0.68	-0.84	1.00	0.97	0.61	-0.95	0.88	1.00	0.63	1.02	0.49	1.18	0.29	-1.04	0.49	0.80	0.85
HALLMARK_FATTY_ACID_METABOLISM	0.98	0.56	0.93	0.67	1.01	0.52	-0.97	1.00	0.63	0.98	1.05	0.61	0.90	0.71	1.04	0.46	0.74	0.93	0.77	0.90	0.81	0.84
HALLMARK_NOTCH_SIGNALING	0.91	0.68	0.77	0.90	0.94	0.65	-0.74	1.00	1.13	0.35	0.86	0.93	-1.21	1.00	-0.83	1.00	-0.81	1.00	0.95	0.65	1.37	0.07
HALLMARK_MYOGENESIS	0.75	0.93	1.21	0.20	0.72	0.93	0.89	0.90	1.34	0.11	-1.08	1.00	1.05	0.57	1.14	0.30	0.69	0.96	-1.12	0.37	-1.30	0.36
HALLMARK_BILE_ACID_METABOLISM	0.69	0.97	0.68	0.95	0.89	0.73	1.09	0.62	-1.08	0.51	0.73	1.00	-0.90	1.00	1.19	0.26	0.77	0.90	-0.90	0.67	-1.12	0.35
HALLMARK_PANCREAS_BETA_CELLS	0.40	1.00	-0.76	1.00	1.06	0.42	-0.71	1.00	-1.21	0.67	-0.88	0.94	1.03	0.58	1.49	0.04	0.83	0.85	0.61	0.99	-0.61	0.98
HALLMARK_XENOBIOTIC_METABOLISM	-1.27	0.39	-0.97	1.00	-0.98	0.67	0.93	0.89	-0.84	0.92	1.29	0.24	0.96	0.67	0.88	0.73	-1.05	1.00	-1.27	0.31	-1.25	0.33

Supplementary Methods

Biological specimen collection

For liver biopsies, a 2- to 3-mm portion of the biopsy cylinder was immediately preserved in RNAlater reagent (Ambion) following percutaneous liver biopsy, kept at 4ºC for 24hours, and then cryopreserved in liquid nitrogen after removal of the RNAlater reagent. Blood samples were immediately stabilised in Paxgene tubes and cryopreserved at -80ºC.

Total RNA extraction from liver tissue and whole blood samples

Cryopreserved liver tissue samples were homogenized in TRIzol reagent (Invitrogen) using a pestle and nuclease-free 1.5-ml reaction tubes (Ambion). Total RNA was then extracted following the manufacturers guidelines, and quality was assessed with the Agilent2100 Bioanalyzer (Agilent Technologies). To extract RNA from the cryopreserved whole blood samples, the PAXgene Blood RNA kit (PreAnalytikX) was used following the manufacturers guidelines.

Liver tissue data acquisition and normalisation

Samples were processed into cRNA and hybridized onto IlluminaHT-12 Expression BeadChips containing 48,771 probes corresponding to 25,000 annotated genes and analysed using a BeadArray Reader (Illumina). Microarray expression data was computed using BeadStudio data analysis software (Illumina) and subsequently processed employing quantiles normalisation using the Lumi bioconductor package. Next we conducted a conservative probe-filtering step excluding those probes with a coefficient of variation <4%, which resulted in a list of 20,965 evaluable from the from the original set of 48,771 probes.

Blood sample data acquisition and normalisation

Samples were hybridized on the custom Agilent cDNA microarrays according to the manufacturer's instructions. Array images were acquired with Agilent's microarray scanner G2505C and signal data were collected with dedicated Agilent Feature Extraction software (v9.5.1). Probes with gIsPosAndSignif value of zero in at least 10 samples were disregarded and labeled as "null". Background adjustment and normalization were done using normexp and quantile normalization. Median values were calculated for multiple probes with the same Agilent Probe ID.

Gene expression data processing from Fluidigm Biomark HD samples

DNA was removed from total RNA preparations using Turbo DNA-free DNAse treatment (Ambion), and RNA was then reverse transcribed into cDNA using the HighCapacity cDNA Reverse Transcription Kit (Applied Biosystems). A pre-amplification step was performed as per Fluidigm Biomark HD protocol. To quantify transcript levels target gene Ct values were normalized to the housekeeping genes HPRT1 and GAPDH to generate ΔCt values. The results were then computed as relative expression between cDNA of the target samples and a calibrated sample according to the ΔΔCt method.

References

1. Benitez C, Londono MC, Miquel R, Manzia TM, Abraldes JG, Lozano JJ, et al. Prospective multicenter clinical trial of immunosuppressive drug withdrawal in stable adult liver transplant recipients. Hepatology. 2013;58(5):1824-35.
2. Bohne F, Martinez-Llordella M, Lozano JJ, Miquel R, Benitez C, Londono MC, et al. Intra-graft expression of genes involved in iron homeostasis predicts the development of operational tolerance in human liver transplantation. J Clin Invest. 2012;122(1):368-82.
3. Starzl TE, Marchioro TL, Vonkaulla KN, Hermann G, Brittain RS, Waddell WR. Homotransplantation of the Liver in Humans. Surg Gynecol Obstet. 1963;117:659-76.
4. Song AT, Avelino-Silva VI, Pecora RA, Pugliese V, D'Albuquerque LA, Abdala E. Liver transplantation: fifty years of experience. World J Gastroenterol. 2014;20(18):5363-74.
5. Adam R, Karam V, Delvart V, O'Grady J, Mirza D, Klempnauer J, et al. Evolution of indications and results of liver transplantation in Europe. A report from the European Liver Transplant Registry (ELTR). J Hepatol. 2012;57(3):675-88.
6. Charlton MR. Roadmap for improving patient and graft survival in the next 10 years. Liver Transpl. 2016;22(S1):71-8.
7. Ng S, Tan KA, Anil G. The role of interventional radiology in complications associated with liver transplantation. Clin Radiol. 2015;70(12):1323-35.
8. Adams DH, Sanchez-Fueyo A, Samuel D. From immunosuppression to tolerance. J Hepatol. 2015;62(1 Suppl):S170-85.
9. O'Grady JG, Burroughs A, Hardy P, Elbourne D, Truesdale A, Uk, et al. Tacrolimus versus microemulsified ciclosporin in liver transplantation: the TMC randomised controlled trial. Lancet. 2002;360(9340):1119-25.
10. Shaked A, Ghobrial RM, Merion RM, Shearon TH, Emond JC, Fair JH, et al. Incidence and severity of acute cellular rejection in recipients undergoing adult living donor or deceased donor liver transplantation. Am J Transplant. 2009;9(2):301-8.
11. Musat AI, Pigott CM, Ellis TM, Agni RM, Leverson GE, Powell AJ, et al. Pretransplant donor-specific anti-HLA antibodies as predictors of early allograft rejection in ABO-compatible liver transplantation. Liver Transpl. 2013;19(10):1132-41.
12. Hubscher SG. Recurrent autoimmune hepatitis after liver transplantation: diagnostic criteria, risk factors, and outcome. Liver Transpl. 2001;7(4):285-91.
13. Faisal N, Renner EL. Recurrence of autoimmune liver diseases after liver transplantation. World J Hepatol. 2015;7(29):2896-905.
14. Kerkar N, Yanni G. 'De novo' and 'recurrent' autoimmune hepatitis after liver transplantation: A comprehensive review. J Autoimmun. 2016;66:17-24.
15. Jain A, Demetris AJ, Kashyap R, Blakomer K, Ruppert K, Khan A, et al. Does tacrolimus offer virtual freedom from chronic rejection after primary liver transplantation? Risk and prognostic factors in 1,048 liver transplantations with a mean follow-up of 6 years. Liver Transpl. 2001;7(7):623-30.
16. Ojo AO, Held PJ, Port FK, Wolfe RA, Leichtman AB, Young EW, et al. Chronic renal failure after transplantation of a nonrenal organ. N Engl J Med. 2003;349(10):931-40.
17. Desai S, Hong JC, Saab S. Cardiovascular risk factors following orthotopic liver transplantation: predisposing factors, incidence and management. Liver Int. 2010;30(7):948-57.
18. Watt KD. Metabolic syndrome: is immunosuppression to blame? Liver Transpl. 2011;17 Suppl 3:S38-42.
19. Rodriguez-Peralvarez M, De la Mata M, Burroughs AK. Liver transplantation: immunosuppression and oncology. Curr Opin Organ Transplant. 2014;19(3):253-60.
20. Lerut J, Sanchez-Fueyo A. An appraisal of tolerance in liver transplantation. Am J Transplant. 2006;6(8):1774-80.
21. Sanchez-Fueyo A. Strategies for minimizing immunosuppression: State of the Art. Liver Transpl. 2016;22(S1):68-70.
22. Heidt S, Wood KJ. Biomarkers of Operational Tolerance in Solid Organ Transplantation. Expert Opin Med Diagn. 2012;6(4):281-93.
23. Pruthi J, Medkiff KA, Esrason KT, Donovan JA, Yoshida EM, Erb SR, et al. Analysis of causes of death in liver transplant recipients who survived more than 3 years. Liver Transpl. 2001;7(9):811-5.
24. Watt KD, Pedersen RA, Kremers WK, Heimbach JK, Charlton MR. Evolution of causes and risk factors for mortality post-liver transplant: results of the NIDDK long-term follow-up study. Am J Transplant. 2010;10(6):1420-7.
25. Gelson W, Hoare M, Dawwas MF, Vowler S, Gibbs P, Alexander G. The pattern of late mortality in liver transplant recipients in the United Kingdom. Transplantation. 2011;91(11):1240-4.

26. Daniel KE, Eickhoff J, Lucey MR. Why do patients die after a liver transplantation? Clin Transplant. 2017;31(3).
27. Geissler EK, Schlitt HJ. Immunosuppression for liver transplantation. Gut. 2009;58(3):452-63.
28. Gonwa TA, Mai ML, Melton LB, Hays SR, Goldstein RM, Levy MF, et al. End-stage renal disease (ESRD) after orthotopic liver transplantation (OLTX) using calcineurin-based immunotherapy: risk of development and treatment. Transplantation. 2001;72(12):1934-9.
29. Duvoux C, Pageaux GP. Immunosuppression in liver transplant recipients with renal impairment. J Hepatol. 2011;54(5):1041-54.
30. Creput C, Blandin F, Deroure B, Roche B, Saliba F, Charpentier B, et al. Long-term effects of calcineurin inhibitor conversion to mycophenolate mofetil on renal function after liver transplantation. Liver Transpl. 2007;13(7):1004-10.
31. Boudjema K, Camus C, Saliba F, Calmus Y, Salame E, Pageaux G, et al. Reduced-dose tacrolimus with mycophenolate mofetil vs. standard-dose tacrolimus in liver transplantation: a randomized study. Am J Transplant. 2011;11(5):965-76.
32. Naesens M, Kuypers DR, Sarwal M. Calcineurin inhibitor nephrotoxicity. Clin J Am Soc Nephrol. 2009;4(2):481-508.
33. Pallet N, Djamali A, Legendre C. Challenges in diagnosing acute calcineurin-inhibitor induced nephrotoxicity: from toxicogenomics to emerging biomarkers. Pharmacol Res. 2011;64(1):25-30.
34. Thoefner LB, Rostved AA, Pommergaard HC, Rasmussen A. Risk factors for metabolic syndrome after liver transplantation: A systematic review and meta-analysis. Transplant Rev (Orlando). 2017.
35. Segev DL, Sozio SM, Shin EJ, Nazarian SM, Nathan H, Thuluvath PJ, et al. Steroid avoidance in liver transplantation: meta-analysis and meta-regression of randomized trials. Liver Transpl. 2008;14(4):512-25.
36. Weiler N, Thrun I, Hoppe-Lotichius M, Zimmermann T, Kraemer I, Otto G. Early steroid-free immunosuppression with FK506 after liver transplantation: long-term results of a prospectively randomized double-blinded trial. Transplantation. 2010;90(12):1562-6.
37. Saliba F, Rostaing L, Gugenheim J, Durand F, Radenne S, Leroy V, et al. Corticosteroid-Sparing and Optimization of Mycophenolic Acid Exposure in Liver Transplant Recipients Receiving Mycophenolate Mofetil and Tacrolimus: A Randomized, Multicenter Study. Transplantation. 2016;100(8):1705-13.
38. Bianchi G, Marchesini G, Marzocchi R, Pinna AD, Zoli M. Metabolic syndrome in liver transplantation: relation to etiology and immunosuppression. Liver Transpl. 2008;14(11):1648-54.
39. Kuo HT, Sampaio MS, Ye X, Reddy P, Martin P, Bunnapradist S. Risk factors for new-onset diabetes mellitus in adult liver transplant recipients, an analysis of the Organ Procurement and Transplant Network/United Network for Organ Sharing database. Transplantation. 2010;89(9):1134-40.
40. Holdaas H, Potena L, Saliba F. mTOR inhibitors and dyslipidemia in transplant recipients: a cause for concern? Transplant Rev (Orlando). 2015;29(2):93-102.
41. D'Avola D, Cuervas-Mons V, Marti J, Ortiz de Urbina J, Llado L, Jimenez C, et al. Cardiovascular morbidity and mortality after liver transplantation: The protective role of mycophenolate mofetil. Liver Transpl. 2017;23(4):498-509.
42. Johnston SD, Morris JK, Cramb R, Gunson BK, Neuberger J. Cardiovascular morbidity and mortality after orthotopic liver transplantation. Transplantation. 2002;73(6):901-6.
43. Guckelberger O. Long-term medical comorbidities and their management: hypertension/cardiovascular disease. Liver Transpl. 2009;15 Suppl 2:S75-8.
44. Maluccio M, Sharma V, Lagman M, Vyas S, Yang H, Li B, et al. Tacrolimus enhances transforming growth factor-beta1 expression and promotes tumor progression. Transplantation. 2003;76(3):597-602.
45. Datta D, Contreras AG, Basu A, Dormond O, Flynn E, Briscoe DM, et al. Calcineurin inhibitors activate the proto-oncogene Ras and promote protumorigenic signals in renal cancer cells. Cancer Res. 2009;69(23):8902-9.
46. Vivarelli M, Cucchetti A, La Barba G, Ravaioli M, Del Gaudio M, Lauro A, et al. Liver transplantation for hepatocellular carcinoma under calcineurin inhibitors: reassessment of risk factors for tumor recurrence. Ann Surg. 2008;248(5):857-62.
47. Pons JA, Ramirez P, Revilla-Nuin B, Pascual D, Baroja-Mazo A, Robles R, et al. Immunosuppression withdrawal improves long-term metabolic parameters, cardiovascular risk factors and renal function in liver transplant patients. Clin Transplant. 2009;23(3):329-36.

48. Orlando G, Manzia T, Baiocchi L, Sanchez-Fueyo A, Angelico M, Tisone G. The Tor Vergata weaning off immunosuppression protocol in stable HCV liver transplant patients: the updated follow up at 78 months. Transpl Immunol. 2008;20(1-2):43-7.
49. Sanchez-Fueyo A, Strom TB. Immunologic basis of graft rejection and tolerance following transplantation of liver or other solid organs. Gastroenterology. 2011;140(1):51-64.
50. Wood KJ, Goto R. Mechanisms of rejection: current perspectives. Transplantation. 2012;93(1):1-10.
51. Afzali B, Lechler RI, Hernandez-Fuentes MP. Allorecognition and the alloresponse: clinical implications. Tissue Antigens. 2007;69(6):545-56.
52. Afzali B, Lombardi G, Lechler RI. Pathways of major histocompatibility complex allorecognition. Curr Opin Organ Transplant. 2008;13(4):438-44.
53. Li XC, Rothstein DM, Sayegh MH. Costimulatory pathways in transplantation: challenges and new developments. Immunol Rev. 2009;229(1):271-93.
54. Le Moine A, Goldman M, Abramowicz D. Multiple pathways to allograft rejection. Transplantation. 2002;73(9):1373-81.
55. Banff schema for grading liver allograft rejection: an international consensus document. Hepatology. 1997;25(3):658-63.
56. Verhelst XP, Troisi RI, Colle I, Geerts A, van Vlierberghe H. Biomarkers for the diagnosis of acute cellular rejection in liver transplant recipients: A review. Hepatol Res. 2013;43(2):165-78.
57. Shetty S, Adams DH, Hubscher SG. Post-transplant liver biopsy and the immune response: lessons for the clinician. Expert Rev Clin Immunol. 2012;8(7):645-61.
58. Tippner C, Nashan B, Hoshino K, Schmidt-Sandte E, Akimaru K, Boker KH, et al. Clinical and subclinical acute rejection early after liver transplantation: contributing factors and relevance for the long-term course. Transplantation. 2001;72(6):1122-8.
59. Jenne CN, Kubes P. Immune surveillance by the liver. Nat Immunol. 2013;14(10):996-1006.
60. Crispe IN. Hepatic T cells and liver tolerance. Nat Rev Immunol. 2003;3(1):51-62.
61. Crispe IN. Immune tolerance in liver disease. Hepatology. 2014;60(6):2109-17.
62. Calne RY, Sells RA, Pena JR, Davis DR, Millard PR, Herbertson BM, et al. Induction of immunological tolerance by porcine liver allografts. Nature. 1969;223(5205):472-6.
63. Kamada N, Davies HS, Roser B. Reversal of transplantation immunity by liver grafting. Nature. 1981;292(5826):840-2.
64. Pu LY, Wang XH, Zhang F, Li XC, Yao AH, Yu Y, et al. Adoptive transfusion of ex vivo donor alloantigen-stimulated CD4(+)CD25(+) regulatory T cells ameliorates rejection of DA-to-Lewis rat liver transplantation. Surgery. 2007;142(1):67-73.
65. Rodriguez-Peralvarez M, Tsochatzis E, Naveas MC, Pieri G, Garcia-Caparros C, O'Beirne J, et al. Reduced exposure to calcineurin inhibitors early after liver transplantation prevents recurrence of hepatocellular carcinoma. J Hepatol. 2013;59(6):1193-9.
66. Neuberger J, Adams DH. What is the significance of acute liver allograft rejection? J Hepatol. 1998;29(1):143-50.
67. Wiesner RH, Demetris AJ, Belle SH, Seaberg EC, Lake JR, Zetterman RK, et al. Acute hepatic allograft rejection: incidence, risk factors, and impact on outcome. Hepatology. 1998;28(3):638-45.
68. Markus BH, Duquesnoy RJ, Gordon RD, Fung JJ, Vanek M, Klintmalm G, et al. Histocompatibility and liver transplant outcome. Does HLA exert a dualistic effect? Transplantation. 1988;46(3):372-7.
69. Muro M, Lopez-Alvarez MR, Campillo JA, Marin L, Moya-Quiles MR, Bolarin JM, et al. Influence of human leukocyte antigen mismatching on rejection development and allograft survival in liver transplantation: is the relevance of HLA-A locus matching being underestimated? Transpl Immunol. 2012;26(2-3):88-93.
70. Sugawara Y, Makuuchi M, Kaneko J, Kishi Y, Hata S, Kokudo N. Positive T lymphocytotoxic cross-match in living donor liver transplantation. Liver Transpl. 2003;9(10):1062-6.
71. Starzl TE, Demetris AJ, Trucco M, Murase N, Ricordi C, Ildstad S, et al. Cell migration and chimerism after whole-organ transplantation: the basis of graft acceptance. Hepatology. 1993;17(6):1127-52.
72. Knolle P, Schlaak J, Uhrig A, Kempf P, Meyer zum Buschenfelde KH, Gerken G. Human Kupffer cells secrete IL-10 in response to lipopolysaccharide (LPS) challenge. J Hepatol. 1995;22(2):226-9.
73. John B, Crispe IN. TLR-4 regulates CD8+ T cell trapping in the liver. J Immunol. 2005;175(3):1643-50.

74. Perez CP, Patel N, Mardis CR, Meadows HB, Taber DJ, Pilch NA. Belatacept in Solid Organ Transplant: Review of Current Literature Across Transplant Types. Transplantation. 2018;102(9):1440-52.
75. Klintmalm GB, Feng S, Lake JR, Vargas HE, Wekerle T, Agnes S, et al. Belatacept-based immunosuppression in de novo liver transplant recipients: 1-year experience from a phase II randomized study. Am J Transplant. 2014;14(8):1817-27.
76. Knechtle SJ, Adams AB. Belatacept: is there BENEFIT for liver transplantation too? Am J Transplant. 2014;14(8):1717-8.
77. Riella LV, Paterson AM, Sharpe AH, Chandraker A. Role of the PD-1 pathway in the immune response. Am J Transplant. 2012;12(10):2575-87.
78. Levitsky J. Immunosuppression withdrawal following liver transplantation: the older, the wiser... but maybe too late. Hepatology. 2013;58(5):1529-32.
79. Londono MC, Rimola A, O'Grady J, Sanchez-Fueyo A. Immunosuppression minimization vs. complete drug withdrawal in liver transplantation. J Hepatol. 2013;59(4):872-9.
80. Starzl TE, Murase N, Abu-Elmagd K, Gray EA, Shapiro R, Eghtesad B, et al. Tolerogenic immunosuppression for organ transplantation. Lancet. 2003;361(9368):1502-10.
81. Marcos A, Eghtesad B, Fung JJ, Fontes P, Patel K, Devera M, et al. Use of alemtuzumab and tacrolimus monotherapy for cadaveric liver transplantation: with particular reference to hepatitis C virus. Transplantation. 2004;78(7):966-71.
82. Donckier V, Troisi R, Le Moine A, Toungouz M, Ricciardi S, Colle I, et al. Early immunosuppression withdrawal after living donor liver transplantation and donor stem cell infusion. Liver Transpl. 2006;12(10):1523-8.
83. Donckier V, Craciun L, Miqueu P, Troisi RI, Lucidi V, Rogiers X, et al. Expansion of memory-type CD8+ T cells correlates with the failure of early immunosuppression withdrawal after cadaver liver transplantation using high-dose ATG induction and rapamycin. Transplantation. 2013;96(3):306-15.
84. Safinia N, Leech J, Hernandez-Fuentes M, Lechler R, Lombardi G. Promoting transplantation tolerance; adoptive regulatory T cell therapy. Clin Exp Immunol. 2013;172(2):158-68.
85. Safinia N, Scotta C, Vaikunthanathan T, Lechler RI, Lombardi G. Regulatory T Cells: Serious Contenders in the Promise for Immunological Tolerance in Transplantation. Front Immunol. 2015;6:438.
86. Todo S, Yamashita K, Goto R, Zaitsu M, Nagatsu A, Oura T, et al. A pilot study of operational tolerance with a regulatory T-cell-based cell therapy in living donor liver transplantation. Hepatology. 2016;64(2):632-43.
87. Adams AB, Newell KA. Transplantation tolerance: Coming of age. Hepatology. 2016;64(2):347-9.
88. Sanchez-Fueyo A. Hot-topic debate on tolerance: immunosuppression withdrawal. Liver Transpl. 2011;17 Suppl 3:S69-73.
89. Mazariegos GV, Reyes J, Marino IR, Demetris AJ, Flynn B, Irish W, et al. Weaning of immunosuppression in liver transplant recipients. Transplantation. 1997;63(2):243-9.
90. Devlin J, Doherty D, Thomson L, Wong T, Donaldson P, Portmann B, et al. Defining the outcome of immunosuppression withdrawal after liver transplantation. Hepatology. 1998;27(4):926-33.
91. Takatsuki M, Uemoto S, Inomata Y, Sakamoto S, Hayashi M, Ueda M, et al. Analysis of alloreactivity and intragraft cytokine profiles in living donor liver transplant recipients with graft acceptance. Transpl Immunol. 2001;8(4):279-86.
92. Pons JA, Yelamos J, Ramirez P, Oliver-Bonet M, Sanchez A, Rodriguez-Gago M, et al. Endothelial cell chimerism does not influence allograft tolerance in liver transplant patients after withdrawal of immunosuppression. Transplantation. 2003;75(7):1045-7.
93. Eason JD, Cohen AJ, Nair S, Alcantera T, Loss GE. Tolerance: is it worth the risk? Transplantation. 2005;79(9):1157-9.
94. Tryphonopoulos P, Tzakis AG, Weppler D, Garcia-Morales R, Kato T, Madariaga JR, et al. The role of donor bone marrow infusions in withdrawal of immunosuppression in adult liver allotransplantation. Am J Transplant. 2005;5(3):608-13.
95. Tisone G, Orlando G, Cardillo A, Palmieri G, Manzia TM, Baiocchi L, et al. Complete weaning off immunosuppression in HCV liver transplant recipients is feasible and favourably impacts on the progression of disease recurrence. J Hepatol. 2006;44(4):702-9.
96. Assy N, Adams PC, Myers P, Simon V, Minuk GY, Wall W, et al. Randomized controlled trial of total immunosuppression withdrawal in liver transplant recipients: role of ursodeoxycholic acid. Transplantation. 2007;83(12):1571-6.
97. Pons JA, Revilla-Nuin B, Baroja-Mazo A, Ramirez P, Martinez-Alarcon L, Sanchez-Bueno F, et al. FoxP3 in peripheral blood is associated with operational tolerance in liver

transplant patients during immunosuppression withdrawal. Transplantation. 2008;86(10):1370-8.
98. Feng S, Ekong UD, Lobritto SJ, Demetris AJ, Roberts JP, Rosenthal P, et al. Complete immunosuppression withdrawal and subsequent allograft function among pediatric recipients of parental living donor liver transplants. JAMA. 2012;307(3):283-93.
99. de la Garza RG, Sarobe P, Merino J, Lasarte JJ, D'Avola D, Belsue V, et al. Trial of complete weaning from immunosuppression for liver transplant recipients: factors predictive of tolerance. Liver Transpl. 2013;19(9):937-44.
100. Bohne F, Londono MC, Benitez C, Miquel R, Martinez-Llordella M, Russo C, et al. HCV-induced immune responses influence the development of operational tolerance after liver transplantation in humans. Sci Transl Med. 2014;6(242):242ra81.
101. Londono MC, Danger R, Giral M, Soulillou JP, Sanchez-Fueyo A, Brouard S. A need for biomarkers of operational tolerance in liver and kidney transplantation. Am J Transplant. 2012;12(6):1370-7.
102. Behnam Sani K, Sawitzki B. Immune monitoring as prerequisite for transplantation tolerance trials. Clin Exp Immunol. 2017;189(2):158-70.
103. Biomarkers Definitions Working G. Biomarkers and surrogate endpoints: preferred definitions and conceptual framework. Clin Pharmacol Ther. 2001;69(3):89-95.
104. Mazariegos GV, Zahorchak AF, Reyes J, Ostrowski L, Flynn B, Zeevi A, et al. Dendritic cell subset ratio in peripheral blood correlates with successful withdrawal of immunosuppression in liver transplant patients. Am J Transplant. 2003;3(6):689-96.
105. Mazariegos GV, Zahorchak AF, Reyes J, Chapman H, Zeevi A, Thomson AW. Dendritic cell subset ratio in tolerant, weaning and non-tolerant liver recipients is not affected by extent of immunosuppression. Am J Transplant. 2005;5(2):314-22.
106. Li Y, Koshiba T, Yoshizawa A, Yonekawa Y, Masuda K, Ito A, et al. Analyses of peripheral blood mononuclear cells in operational tolerance after pediatric living donor liver transplantation. Am J Transplant. 2004;4(12):2118-25.
107. Martinez-Llordella M, Puig-Pey I, Orlando G, Ramoni M, Tisone G, Rimola A, et al. Multiparameter immune profiling of operational tolerance in liver transplantation. Am J Transplant. 2007;7(2):309-19.
108. Li Y, Zhao X, Cheng D, Haga H, Tsuruyama T, Wood K, et al. The presence of Foxp3 expressing T cells within grafts of tolerant human liver transplant recipients. Transplantation. 2008;86(12):1837-43.
109. Martinez-Llordella M, Lozano JJ, Puig-Pey I, Orlando G, Tisone G, Lerut J, et al. Using transcriptional profiling to develop a diagnostic test of operational tolerance in liver transplant recipients. J Clin Invest. 2008;118(8):2845-57.
110. Khatri P, Sarwal MM. Using gene arrays in diagnosis of rejection. Curr Opin Organ Transplant. 2009;14(1):34-9.
111. Naesens M, Sarwal MM. Molecular diagnostics in transplantation. Nat Rev Nephrol. 2010;6(10):614-28.
112. Cahan P, Rovegno F, Mooney D, Newman JC, St Laurent G, 3rd, McCaffrey TA. Meta-analysis of microarray results: challenges, opportunities, and recommendations for standardization. Gene. 2007;401(1-2):12-8.
113. Duggan DJ, Bittner M, Chen Y, Meltzer P, Trent JM. Expression profiling using cDNA microarrays. Nat Genet. 1999;21(1 Suppl):10-4.
114. Miller MB, Tang YW. Basic concepts of microarrays and potential applications in clinical microbiology. Clin Microbiol Rev. 2009;22(4):611-33.
115. Weintraub LA, Sarwal MM. Microarrays: a monitoring tool for transplant patients? Transpl Int. 2006;19(10):775-88.
116. Wang A, Sarwal MM. Computational Models for Transplant Biomarker Discovery. Front Immunol. 2015;6:458.
117. Butte A. The use and analysis of microarray data. Nat Rev Drug Discov. 2002;1(12):951-60.
118. Mueller TF, Reeve J, Jhangri GS, Mengel M, Jacaj Z, Cairo L, et al. The transcriptome of the implant biopsy identifies donor kidneys at increased risk of delayed graft function. Am J Transplant. 2008;8(1):78-85.
119. Simon RM, Dobbin K. Experimental design of DNA microarray experiments. Biotechniques. 2003;Suppl:16-21.
120. Somorjai RL, Dolenko B, Baumgartner R. Class prediction and discovery using gene microarray and proteomics mass spectroscopy data: curses, caveats, cautions. Bioinformatics. 2003;19(12):1484-91.
121. Simon R, Radmacher MD, Dobbin K, McShane LM. Pitfalls in the use of DNA microarray data for diagnostic and prognostic classification. J Natl Cancer Inst. 2003;95(1):14-8.

122. Brouard S, Mansfield E, Braud C, Li L, Giral M, Hsieh SC, et al. Identification of a peripheral blood transcriptional biomarker panel associated with operational renal allograft tolerance. Proc Natl Acad Sci U S A. 2007;104(39):15448-53.
123. Sagoo P, Perucha E, Sawitzki B, Tomiuk S, Stephens DA, Miqueu P, et al. Development of a cross-platform biomarker signature to detect renal transplant tolerance in humans. J Clin Invest. 2010;120(6):1848-61.
124. Newell KA, Asare A, Kirk AD, Gisler TD, Bourcier K, Suthanthiran M, et al. Identification of a B cell signature associated with renal transplant tolerance in humans. J Clin Invest. 2010;120(6):1836-47.
125. Radmacher MD, McShane LM, Simon R. A paradigm for class prediction using gene expression profiles. J Comput Biol. 2002;9(3):505-11.
126. Morgun A, Shulzhenko N, Perez-Diez A, Diniz RV, Sanson GF, Almeida DR, et al. Molecular profiling improves diagnoses of rejection and infection in transplanted organs. Circ Res. 2006;98(12):e74-83.
127. Khatri P, Roedder S, Kimura N, De Vusser K, Morgan AA, Gong Y, et al. A common rejection module (CRM) for acute rejection across multiple organs identifies novel therapeutics for organ transplantation. J Exp Med. 2013;210(11):2205-21.
128. Hogeweg P. The roots of bioinformatics in theoretical biology. PLoS Comput Biol. 2011;7(3):e1002021.
129. Armstrong NJ, van de Wiel MA. Microarray data analysis: from hypotheses to conclusions using gene expression data. Cell Oncol. 2004;26(5-6):279-90.
130. Yang YH, Dudoit S, Luu P, Lin DM, Peng V, Ngai J, et al. Normalization for cDNA microarray data: a robust composite method addressing single and multiple slide systematic variation. Nucleic Acids Res. 2002;30(4):e15.
131. Dudoit S, Yang YH, Callow MJ, Speed TP. Statistical methods for identifying differentially expressed genes in replicated cDNA microarray experiments. Statistica Sinica. 2002;12:111-39.
132. Yang YH, Dudoit S, Luu P, Speed TP, editors. Normalization for cDNA microarray data. Microarrays: Optical Technologies and Informatics 2001 4 June 2001; BiOs 2001 The international Symposium on Biomedical Optics, San Jose, CA, United States.
133. Nadon R, Shoemaker J. Statistical issues with microarrays: processing and analysis. Trends Genet. 2002;18(5):265-71.
134. Sebastiani P, Gussoni E, Kohane IS, Ramoni M. Statistical challenges in functional genomics. Statistical Science. 2003;18(1):33-70.
135. Benjamini Y, Hochberg Y. Controlling the false discovery rate: a practical and powerful approach to multiple testing. Journal of the Royal Statistical Society Series B (Methodological). 1995;57(1):289-300.
136. Storey JD, Tibshirani R. Statistical significance for genomewide studies. Proc Natl Acad Sci U S A. 2003;100(16):9440-5.
137. Calza S, Raffelsberger W, Ploner A, Sahel J, Leveillard T, Pawitan Y. Filtering genes to improve sensitivity in oligonucleotide microarray data analysis. Nucleic Acids Res. 2007;35(16):e102.
138. Pounds S, Cheng C. Statistical development and evaluation of microarray gene expression data filters. J Comput Biol. 2005;12(4):482-95.
139. Dudoit S, Shaffer JP, Boldrick JC. Multiple hypothesis testing in microarray experiments. Statistical Science. 2003;18(1):71-103.
140. Breitling R. Biological microarray interpretation: the rules of engagement. Biochim Biophys Acta. 2006;1759(7):319-27.
141. Pawitan Y, Michiels S, Koscielny S, Gusnanto A, Ploner A. False discovery rate, sensitivity and sample size for microarray studies. Bioinformatics. 2005;21(13):3017-24.
142. Sarwal M, Chua MS, Kambham N, Hsieh SC, Satterwhite T, Masek M, et al. Molecular heterogeneity in acute renal allograft rejection identified by DNA microarray profiling. N Engl J Med. 2003;349(2):125-38.
143. Flechner SM, Kurian SM, Head SR, Sharp SM, Whisenant TC, Zhang J, et al. Kidney transplant rejection and tissue injury by gene profiling of biopsies and peripheral blood lymphocytes. Am J Transplant. 2004;4(9):1475-89.
144. Naesens M, Khatri P, Li L, Sigdel TK, Vitalone MJ, Chen R, et al. Progressive histological damage in renal allografts is associated with expression of innate and adaptive immunity genes. Kidney Int. 2011;80(12):1364-76.
145. Li L, Khatri P, Sigdel TK, Tran T, Ying L, Vitalone MJ, et al. A peripheral blood diagnostic test for acute rejection in renal transplantation. Am J Transplant. 2012;12(10):2710-8.
146. Tusher VG, Tibshirani R, Chu G. Significance analysis of microarrays applied to the ionizing radiation response. Proc Natl Acad Sci U S A. 2001;98(9):5116-21.

147. Reeve J, Einecke G, Mengel M, Sis B, Kayser N, Kaplan B, et al. Diagnosing rejection in renal transplants: a comparison of molecular- and histopathology-based approaches. Am J Transplant. 2009;9(8):1802-10.
148. Tibshirani R, Hastie T, Narasimhan B, Chu G. Diagnosis of multiple cancer types by shrunken centroids of gene expression. Proc Natl Acad Sci U S A. 2002;99(10):6567-72.
149. Subramanian A, Tamayo P, Mootha VK, Mukherjee S, Ebert BL, Gillette MA, et al. Gene set enrichment analysis: a knowledge-based approach for interpreting genome-wide expression profiles. Proc Natl Acad Sci U S A. 2005;102(43):15545-50.
150. Mootha VK, Lindgren CM, Eriksson KF, Subramanian A, Sihag S, Lehar J, et al. PGC-1alpha-responsive genes involved in oxidative phosphorylation are coordinately downregulated in human diabetes. Nat Genet. 2003;34(3):267-73.
151. Liberzon A, Subramanian A, Pinchback R, Thorvaldsdottir H, Tamayo P, Mesirov JP. Molecular signatures database (MSigDB) 3.0. Bioinformatics. 2011;27(12):1739-40.
152. Dudoit S, Gentleman RC, Quackenbush J. Open source software for the analysis of microarray data. Biotechniques. 2003;Suppl:45-51.
153. Gentleman RC, Carey VJ, Bates DM, Bolstad B, Dettling M, Dudoit S, et al. Bioconductor: open software development for computational biology and bioinformatics. Genome Biol. 2004;5(10):R80.
154. Ball CA, Brazma A, Causton H, Chervitz S, Edgar R, Hingamp P, et al. Submission of microarray data to public repositories. PLoS Biol. 2004;2(9):E317.
155. Simon R. Lost in translation: problems and pitfalls in translating laboratory observations to clinical utility. Eur J Cancer. 2008;44(18):2707-13.
156. Canales RD, Luo Y, Willey JC, Austermiller B, Barbacioru CC, Boysen C, et al. Evaluation of DNA microarray results with quantitative gene expression platforms. Nat Biotechnol. 2006;24(9):1115-22.
157. Chen JJ, Hsueh HM, Delongchamp RR, Lin CJ, Tsai CA. Reproducibility of microarray data: a further analysis of microarray quality control (MAQC) data. BMC Bioinformatics. 2007;8:412.
158. Halloran PF, de Freitas DG, Einecke G, Famulski KS, Hidalgo LG, Mengel M, et al. The molecular phenotype of kidney transplants. Am J Transplant. 2010;10(10):2215-22.
159. Halloran PF, Venner JM, Madill-Thomsen KS, Einecke G, Parkes MD, Hidalgo LG, et al. Review: The transcripts associated with organ allograft rejection. Am J Transplant. 2018;18(4):785-95.
160. Bonaccorsi-Riani E, Pennycuick A, Londono MC, Lozano JJ, Benitez C, Sawitzki B, et al. Molecular Characterization of Acute Cellular Rejection Occurring During Intentional Immunosuppression Withdrawal in Liver Transplantation. Am J Transplant. 2016;16(2):484-96.
161. Kothapalli R, Yoder SJ, Mane S, Loughran TP, Jr. Microarray results: how accurate are they? BMC Bioinformatics. 2002;3:22.
162. Wang Z, Gerstein M, Snyder M. RNA-Seq: a revolutionary tool for transcriptomics. Nat Rev Genet. 2009;10(1):57-63.
163. Hrdlickova R, Toloue M, Tian B. RNA-Seq methods for transcriptome analysis. Wiley Interdiscip Rev RNA. 2017;8(1).
164. Hurd PJ, Nelson CJ. Advantages of next-generation sequencing versus the microarray in epigenetic research. Brief Funct Genomic Proteomic. 2009;8(3):174-83.
165. Git A, Dvinge H, Salmon-Divon M, Osborne M, Kutter C, Hadfield J, et al. Systematic comparison of microarray profiling, real-time PCR, and next-generation sequencing technologies for measuring differential microRNA expression. RNA. 2010;16(5):991-1006.
166. Winterbourn CC. Toxicity of iron and hydrogen peroxide: the Fenton reaction. Toxicol Lett. 1995;82-83:969-74.
167. Ganz T. Systemic iron homeostasis. Physiol Rev. 2013;93(4):1721-41.
168. Hentze MW, Muckenthaler MU, Galy B, Camaschella C. Two to tango: regulation of Mammalian iron metabolism. Cell. 2010;142(1):24-38.
169. Porto G, De Sousa M. Iron overload and immunity. World J Gastroenterol. 2007;13(35):4707-15.
170. Green R, Charlton R, Seftel H, Bothwell T, Mayet F, Adams B, et al. Body iron excretion in man: a collaborative study. Am J Med. 1968;45(3):336-53.
171. Coffey R, Ganz T. Iron homeostasis: An anthropocentric perspective. J Biol Chem. 2017;292(31):12727-34.
172. Gunshin H, Mackenzie B, Berger UV, Gunshin Y, Romero MF, Boron WF, et al. Cloning and characterization of a mammalian proton-coupled metal-ion transporter. Nature. 1997;388(6641):482-8.

173. Shawki A, Engevik MA, Kim RS, Knight PB, Baik RA, Anthony SR, et al. Intestinal brush-border Na+/H+ exchanger-3 drives H+-coupled iron absorption in the mouse. Am J Physiol Gastrointest Liver Physiol. 2016;311(3):G423-30.
174. Raffin SB, Woo CH, Roost KT, Price DC, Schmid R. Intestinal absorption of hemoglobin iron-heme cleavage by mucosal heme oxygenase. J Clin Invest. 1974;54(6):1344-52.
175. Shayeghi M, Latunde-Dada GO, Oakhill JS, Laftah AH, Takeuchi K, Halliday N, et al. Identification of an intestinal heme transporter. Cell. 2005;122(5):789-801.
176. Qiu A, Jansen M, Sakaris A, Min SH, Chattopadhyay S, Tsai E, et al. Identification of an intestinal folate transporter and the molecular basis for hereditary folate malabsorption. Cell. 2006;127(5):917-28.
177. Gottlieb Y, Truman M, Cohen LA, Leichtmann-Bardoogo Y, Meyron-Holtz EG. Endoplasmic reticulum anchored heme-oxygenase 1 faces the cytosol. Haematologica. 2012;97(10):1489-93.
178. White C, Yuan X, Schmidt PJ, Bresciani E, Samuel TK, Campagna D, et al. HRG1 is essential for heme transport from the phagolysosome of macrophages during erythrophagocytosis. Cell Metab. 2013;17(2):261-70.
179. Kovtunovych G, Eckhaus MA, Ghosh MC, Ollivierre-Wilson H, Rouault TA. Dysfunction of the heme recycling system in heme oxygenase 1-deficient mice: effects on macrophage viability and tissue iron distribution. Blood. 2010;116(26):6054-62.
180. Balla G, Jacob HS, Eaton JW, Belcher JD, Vercellotti GM. Hemin: a possible physiological mediator of low density lipoprotein oxidation and endothelial injury. Arterioscler Thromb. 1991;11(6):1700-11.
181. Dennery PA. Signaling function of heme oxygenase proteins. Antioxid Redox Signal. 2014;20(11):1743-53.
182. Riquelme SA, Carreno LJ, Espinoza JA, Mackern-Oberti JP, Alvarez-Lobos MM, Riedel CA, et al. Modulation of antigen processing by haem-oxygenase 1. Implications on inflammation and tolerance. Immunology. 2016;149(1):1-12.
183. Balla G, Jacob HS, Balla J, Rosenberg M, Nath K, Apple F, et al. Ferritin: a cytoprotective antioxidant strategem of endothelium. J Biol Chem. 1992;267(25):18148-53.
184. Herrada AA, Llanos C, Mackern-Oberti JP, Carreno LJ, Henriquez C, Gomez RS, et al. Haem oxygenase 1 expression is altered in monocytes from patients with systemic lupus erythematosus. Immunology. 2012;136(4):414-24.
185. Fagone P, Patti F, Mangano K, Mammana S, Coco M, Touil-Boukoffa C, et al. Heme oxygenase-1 expression in peripheral blood mononuclear cells correlates with disease activity in multiple sclerosis. J Neuroimmunol. 2013;261(1-2):82-6.
186. Gueron G, De Siervi A, Ferrando M, Salierno M, De Luca P, Elguero B, et al. Critical role of endogenous heme oxygenase 1 as a tuner of the invasive potential of prostate cancer cells. Mol Cancer Res. 2009;7(11):1745-55.
187. Gandini NA, Fermento ME, Salomon DG, Blasco J, Patel V, Gutkind JS, et al. Nuclear localization of heme oxygenase-1 is associated with tumor progression of head and neck squamous cell carcinomas. Exp Mol Pathol. 2012;93(2):237-45.
188. Gandini NA, Alonso EN, Fermento ME, Mascaro M, Abba MC, Colo GP, et al. Heme Oxygenase-1 Has an Antitumor Role in Breast Cancer. Antioxid Redox Signal. 2019;30(18):2030-49.
189. Ollinger R, Pratschke J. Role of heme oxygenase-1 in transplantation. Transpl Int. 2010;23(11):1071-81.
190. Kadono K, Dery KJ, Hirao H, Ito T, Kageyama S, Nakamura K, et al. Heme Oxygenase-1 dictates innate - adaptive immune phenotype in human liver transplantation. Arch Biochem Biophys. 2019;671:162-6.
191. Abboud S, Haile DJ. A novel mammalian iron-regulated protein involved in intracellular iron metabolism. J Biol Chem. 2000;275(26):19906-12.
192. Donovan A, Brownlie A, Zhou Y, Shepard J, Pratt SJ, Moynihan J, et al. Positional cloning of zebrafish ferroportin1 identifies a conserved vertebrate iron exporter. Nature. 2000;403(6771):776-81.
193. McKie AT, Marciani P, Rolfs A, Brennan K, Wehr K, Barrow D, et al. A novel duodenal iron-regulated transporter, IREG1, implicated in the basolateral transfer of iron to the circulation. Mol Cell. 2000;5(2):299-309.
194. Delaby C, Pilard N, Puy H, Canonne-Hergaux F. Sequential regulation of ferroportin expression after erythrophagocytosis in murine macrophages: early mRNA induction by haem, followed by iron-dependent protein expression. Biochem J. 2008;411(1):123-31.
195. Knutson MD, Vafa MR, Haile DJ, Wessling-Resnick M. Iron loading and erythrophagocytosis increase ferroportin 1 (FPN1) expression in J774 macrophages. Blood. 2003;102(12):4191-7.

196. Ohgami RS, Campagna DR, Greer EL, Antiochos B, McDonald A, Chen J, et al. Identification of a ferrireductase required for efficient transferrin-dependent iron uptake in erythroid cells. Nat Genet. 2005;37(11):1264-9.
197. Andrews NC. Forging a field: the golden age of iron biology. Blood. 2008;112(2):219-30.
198. Andrews NC, Schmidt PJ. Iron homeostasis. Annu Rev Physiol. 2007;69:69-85.
199. Park CH, Valore EV, Waring AJ, Ganz T. Hepcidin, a urinary antimicrobial peptide synthesized in the liver. J Biol Chem. 2001;276(11):7806-10.
200. Nicolas G, Bennoun M, Devaux I, Beaumont C, Grandchamp B, Kahn A, et al. Lack of hepcidin gene expression and severe tissue iron overload in upstream stimulatory factor 2 (USF2) knockout mice. Proc Natl Acad Sci U S A. 2001;98(15):8780-5.
201. Pigeon C, Ilyin G, Courselaud B, Leroyer P, Turlin B, Brissot P, et al. A new mouse liver-specific gene, encoding a protein homologous to human antimicrobial peptide hepcidin, is overexpressed during iron overload. J Biol Chem. 2001;276(11):7811-9.
202. Nemeth E, Tuttle MS, Powelson J, Vaughn MB, Donovan A, Ward DM, et al. Hepcidin regulates cellular iron efflux by binding to ferroportin and inducing its internalization. Science. 2004;306(5704):2090-3.
203. Babitt JL, Huang FW, Wrighting DM, Xia Y, Sidis Y, Samad TA, et al. Bone morphogenetic protein signaling by hemojuvelin regulates hepcidin expression. Nat Genet. 2006;38(5):531-9.
204. Wang RH, Li C, Xu X, Zheng Y, Xiao C, Zerfas P, et al. A role of SMAD4 in iron metabolism through the positive regulation of hepcidin expression. Cell Metab. 2005;2(6):399-409.
205. Shi Y, Massague J. Mechanisms of TGF-beta signaling from cell membrane to the nucleus. Cell. 2003;113(6):685-700.
206. Kaelin WG, Jr., Ratcliffe PJ. Oxygen sensing by metazoans: the central role of the HIF hydroxylase pathway. Mol Cell. 2008;30(4):393-402.
207. Ju C, Colgan SP, Eltzschig HK. Hypoxia-inducible factors as molecular targets for liver diseases. J Mol Med (Berl). 2016;94(6):613-27.
208. Lee PJ, Jiang BH, Chin BY, Iyer NV, Alam J, Semenza GL, et al. Hypoxia-inducible factor-1 mediates transcriptional activation of the heme oxygenase-1 gene in response to hypoxia. J Biol Chem. 1997;272(9):5375-81.
209. Sonnweber T, Nachbaur D, Schroll A, Nairz M, Seifert M, Demetz E, et al. Hypoxia induced downregulation of hepcidin is mediated by platelet derived growth factor BB. Gut. 2014;63(12):1951-9.
210. Haase VH. Hypoxic regulation of erythropoiesis and iron metabolism. Am J Physiol Renal Physiol. 2010;299(1):F1-13.
211. Liu Q, Davidoff O, Niss K, Haase VH. Hypoxia-inducible factor regulates hepcidin via erythropoietin-induced erythropoiesis. J Clin Invest. 2012;122(12):4635-44.
212. Dao MC, Meydani SN. Iron biology, immunology, aging, and obesity: four fields connected by the small peptide hormone hepcidin. Adv Nutr. 2013;4(6):602-17.
213. O'Shea JJ, Murray PJ. Cytokine signaling modules in inflammatory responses. Immunity. 2008;28(4):477-87.
214. Peyssonnaux C, Zinkernagel AS, Datta V, Lauth X, Johnson RS, Nizet V. TLR4-dependent hepcidin expression by myeloid cells in response to bacterial pathogens. Blood. 2006;107(9):3727-32.
215. Nemeth E, Rivera S, Gabayan V, Keller C, Taudorf S, Pedersen BK, et al. IL-6 mediates hypoferremia of inflammation by inducing the synthesis of the iron regulatory hormone hepcidin. J Clin Invest. 2004;113(9):1271-6.
216. Otogawa K, Ogawa T, Shiga R, Nakatani K, Ikeda K, Nakajima Y, et al. Attenuation of acute and chronic liver injury in rats by iron-deficient diet. Am J Physiol Regul Integr Comp Physiol. 2008;294(2):R311-20.
217. Sato T, Kobune M, Murase K, Kado Y, Okamoto T, Tanaka S, et al. Iron chelator deferasirox rescued mice from Fas-induced fulminant hepatitis. Hepatol Res. 2011;41(7):660-7.
218. Ikeda Y, Ozono I, Tajima S, Imao M, Horinouchi Y, Izawa-Ishizawa Y, et al. Iron chelation by deferoxamine prevents renal interstitial fibrosis in mice with unilateral ureteral obstruction. PLoS One. 2014;9(2):e89355.
219. Grant SM, Wiesinger JA, Beard JL, Cantorna MT. Iron-deficient mice fail to develop autoimmune encephalomyelitis. J Nutr. 2003;133(8):2635-8.
220. Minamiyama Y, Takemura S, Kodai S, Shinkawa H, Tsukioka T, Ichikawa H, et al. Iron restriction improves type 2 diabetes mellitus in Otsuka Long-Evans Tokushima fatty rats. Am J Physiol Endocrinol Metab. 2010;298(6):E1140-9.

221. Pietrangelo A, Dierssen U, Valli L, Garuti C, Rump A, Corradini E, et al. STAT3 is required for IL-6-gp130-dependent activation of hepcidin in vivo. Gastroenterology. 2007;132(1):294-300.
222. Wrighting DM, Andrews NC. Interleukin-6 induces hepcidin expression through STAT3. Blood. 2006;108(9):3204-9.
223. Nicolas G, Chauvet C, Viatte L, Danan JL, Bigard X, Devaux I, et al. The gene encoding the iron regulatory peptide hepcidin is regulated by anemia, hypoxia, and inflammation. J Clin Invest. 2002;110(7):1037-44.
224. Arezes J, Jung G, Gabayan V, Valore E, Ruchala P, Gulig PA, et al. Hepcidin-induced hypoferremia is a critical host defense mechanism against the siderophilic bacterium Vibrio vulnificus. Cell Host Microbe. 2015;17(1):47-57.
225. Khan FA, Fisher MA, Khakoo RA. Association of hemochromatosis with infectious diseases: expanding spectrum. Int J Infect Dis. 2007;11(6):482-7.
226. Portugal S, Carret C, Recker M, Armitage AE, Goncalves LA, Epiphanio S, et al. Host-mediated regulation of superinfection in malaria. Nat Med. 2011;17(6):732-7.
227. Sazawal S, Black RE, Ramsan M, Chwaya HM, Stoltzfus RJ, Dutta A, et al. Effects of routine prophylactic supplementation with iron and folic acid on admission to hospital and mortality in preschool children in a high malaria transmission setting: community-based, randomised, placebo-controlled trial. Lancet. 2006;367(9505):133-43.
228. Nairz M, Fritsche G, Crouch ML, Barton HC, Fang FC, Weiss G. Slc11a1 limits intracellular growth of Salmonella enterica sv. Typhimurium by promoting macrophage immune effector functions and impairing bacterial iron acquisition. Cell Microbiol. 2009;11(9):1365-81.
229. Oexle H, Kaser A, Most J, Bellmann-Weiler R, Werner ER, Werner-Felmayer G, et al. Pathways for the regulation of interferon-gamma-inducible genes by iron in human monocytic cells. J Leukoc Biol. 2003;74(2):287-94.
230. Dallman PR. Iron deficiency and the immune response. Am J Clin Nutr. 1987;46(2):329-34.
231. Sanvisens N, Bano MC, Huang M, Puig S. Regulation of ribonucleotide reductase in response to iron deficiency. Mol Cell. 2011;44(5):759-69.
232. Kuvibidila S, Baliga BS, Murthy KK. Impaired protein kinase C activation as one of the possible mechanisms of reduced lymphocyte proliferation in iron deficiency in mice. Am J Clin Nutr. 1991;54(5):944-50.
233. Kuvibidila SR, Baliga BS, Warrier RP, Suskind RM. Iron deficiency reduces the hydrolysis of cell membrane phosphatidyl inositol-4,5-bisphosphate during splenic lymphocyte activation in C57BL/6 mice. J Nutr. 1998;128(7):1077-83.
234. Pagani A, Nai A, Corna G, Bosurgi L, Rovere-Querini P, Camaschella C, et al. Low hepcidin accounts for the proinflammatory status associated with iron deficiency. Blood. 2011;118(3):736-46.
235. De Domenico I, Zhang TY, Koening CL, Branch RW, London N, Lo E, et al. Hepcidin mediates transcriptional changes that modulate acute cytokine-induced inflammatory responses in mice. J Clin Invest. 2010;120(7):2395-405.
236. Pinto JP, Dias V, Zoller H, Porto G, Carmo H, Carvalho F, et al. Hepcidin messenger RNA expression in human lymphocytes. Immunology. 2010;130(2):217-30.
237. Wang L, Harrington L, Trebicka E, Shi HN, Kagan JC, Hong CC, et al. Selective modulation of TLR4-activated inflammatory responses by altered iron homeostasis in mice. J Clin Invest. 2009;119(11):3322-8.
238. Schaefer B, Effenberger M, Zoller H. Iron metabolism in transplantation. Transpl Int. 2014;27(11):1109-17.
239. Halloran PF. Immunosuppressive drugs for kidney transplantation. N Engl J Med. 2004;351(26):2715-29.
240. Zheng Y, Collins SL, Lutz MA, Allen AN, Kole TP, Zarek PE, et al. A role for mammalian target of rapamycin in regulating T cell activation versus anergy. J Immunol. 2007;178(4):2163-70.
241. Brekelmans P, van Soest P, Leenen PJ, van Ewijk W. Inhibition of proliferation and differentiation during early T cell development by anti-transferrin receptor antibody. Eur J Immunol. 1994;24(11):2896-902.
242. Bayer AL, Baliga P, Woodward JE. Transferrin receptor in T cell activation and transplantation. J Leukoc Biol. 1998;64(1):19-24.
243. Woodward JE, Bayer AL, Chavin KD, Boleza KA, Baliga P. Anti-transferrin receptor monoclonal antibody: a novel immunosuppressant. Transplantation. 1998;65(1):6-9.
244. Kuvibidila SR, Porretta C. Differential effects of iron deficiency on the expression of CD80 and CD86 co-stimulatory receptors in mitogen-treated and untreated murine spleen cells. J Cell Biochem. 2002;86(3):571-82.

245. Kuvibidila SR, Velez M, Yu L, Warrier RP, Surendra Baliga B. Differences in iron requirements by concanavalin A-treated and anti-CD3-treated murine splenic lymphocytes. Br J Nutr. 2002;88(1):67-72.
246. Ghosh MC, Wang X, Li S, Klee C. Regulation of calcineurin by oxidative stress. Methods Enzymol. 2003;366:289-304.
247. Chen L, Xiong S, She H, Lin SW, Wang J, Tsukamoto H. Iron causes interactions of TAK1, p21ras, and phosphatidylinositol 3-kinase in caveolae to activate IkappaB kinase in hepatic macrophages. J Biol Chem. 2007;282(8):5582-8.
248. Kiessling MK, Klemke CD, Kaminski MM, Galani IE, Krammer PH, Gulow K. Inhibition of constitutively activated nuclear factor-kappaB induces reactive oxygen species- and iron-dependent cell death in cutaneous T-cell lymphoma. Cancer Res. 2009;69(6):2365-74.
249. Bauckman KA, Haller E, Flores I, Nanjundan M. Iron modulates cell survival in a Ras- and MAPK-dependent manner in ovarian cells. Cell Death Dis. 2013;4:e592.
250. Ohyashiki JH, Kobayashi C, Hamamura R, Okabe S, Tauchi T, Ohyashiki K. The oral iron chelator deferasirox represses signaling through the mTOR in myeloid leukemia cells by enhancing expression of REDD1. Cancer Sci. 2009;100(5):970-7.
251. Benseler V, McCaughan GW, Schlitt HJ, Bishop GA, Bowen DG, Bertolino P. The liver: a special case in transplantation tolerance. Semin Liver Dis. 2007;27(2):194-213.
252. Li W, Kuhr CS, Zheng XX, Carper K, Thomson AW, Reyes JD, et al. New insights into mechanisms of spontaneous liver transplant tolerance: the role of Foxp3-expressing CD25+CD4+ regulatory T cells. Am J Transplant. 2008;8(8):1639-51.
253. Zoller H, Knisely AS. Control of iron metabolism--lessons from neonatal hemochromatosis. J Hepatol. 2012;56(6):1226-9.
254. Schranz M, Talasz H, Graziadei I, Winder T, Sergi C, Bogner K, et al. Diagnosis of hepatic iron overload: a family study illustrating pitfalls in diagnosing hemochromatosis. Diagn Mol Pathol. 2009;18(1):53-60.
255. Ludwig J, Hashimoto E, Porayko MK, Moyer TP, Baldus WP. Hemosiderosis in cirrhosis: a study of 447 native livers. Gastroenterology. 1997;112(3):882-8.
256. Brandhagen DJ. Liver transplantation for hereditary hemochromatosis. Liver Transpl. 2001;7(8):663-72.
257. Crawford DH, Fletcher LM, Hubscher SG, Stuart KA, Gane E, Angus PW, et al. Patient and graft survival after liver transplantation for hereditary hemochromatosis: Implications for pathogenesis. Hepatology. 2004;39(6):1655-62.
258. Fenton H, Torbenson M, Vivekanandan P, Yeh MM, Hart J, Ferrell L. Marked iron in liver explants in the absence of major hereditary hemochromatosis gene defects: a risk factor for cardiac failure. Transplantation. 2009;87(8):1256-60.
259. Kerkweg U, Li T, de Groot H, Rauen U. Cold-induced apoptosis of rat liver cells in University of Wisconsin solution: the central role of chelatable iron. Hepatology. 2002;35(3):560-7.
260. Niu X, Huang WH, De Boer B, Delriviere L, Mou LJ, Jeffrey GP. Iron-induced oxidative rat liver injury after non-heart-beating warm ischemia is mediated by tumor necrosis factor alpha and prevented by deferoxamine. Liver Transpl. 2014;20(8):904-11.
261. Tiegs G, Hentschel J, Wendel A. A T cell-dependent experimental liver injury in mice inducible by concanavalin A. J Clin Invest. 1992;90(1):196-203.
262. Wang HX, Liu M, Weng SY, Li JJ, Xie C, He HL, et al. Immune mechanisms of Concanavalin A model of autoimmune hepatitis. World J Gastroenterol. 2012;18(2):119-25.
263. Fakih S, Podinovskaia M, Kong X, Schaible UE, Collins HL, Hider RC. Monitoring intracellular labile iron pools: A novel fluorescent iron(III) sensor as a potential non-invasive diagnosis tool. J Pharm Sci. 2009;98(6):2212-26.
264. Baek JH, Reiter CE, Manalo DJ, Buehler PW, Hider RC, Alayash AI. Induction of hypoxia inducible factor (HIF-1alpha) in rat kidneys by iron chelation with the hydroxypyridinone, CP94. Biochim Biophys Acta. 2011;1809(4-6):262-8.
265. Corbitt N, Kimura S, Isse K, Specht S, Chedwick L, Rosborough BR, et al. Gut bacteria drive Kupffer cell expansion via MAMP-mediated ICAM-1 induction on sinusoidal endothelium and influence preservation-reperfusion injury after orthotopic liver transplantation. Am J Pathol. 2013;182(1):180-91.
266. Ramachandran P, Pellicoro A, Vernon MA, Boulter L, Aucott RL, Ali A, et al. Differential Ly-6C expression identifies the recruited macrophage phenotype, which orchestrates the regression of murine liver fibrosis. Proc Natl Acad Sci U S A. 2012;109(46):E3186-95.
267. Evstatiev R, Bukaty A, Jimenez K, Kulnigg-Dabsch S, Surman L, Schmid W, et al. Iron deficiency alters megakaryopoiesis and platelet phenotype independent of thrombopoietin. Am J Hematol. 2014;89(5):524-9.

268. Kusters S, Gantner F, Kunstle G, Tiegs G. Interferon gamma plays a critical role in T cell-dependent liver injury in mice initiated by concanavalin A. Gastroenterology. 1996;111(2):462-71.
269. Sass G, Heinlein S, Agli A, Bang R, Schumann J, Tiegs G. Cytokine expression in three mouse models of experimental hepatitis. Cytokine. 2002;19(3):115-20.
270. Wilson MT, Johansson C, Olivares-Villagomez D, Singh AK, Stanic AK, Wang CR, et al. The response of natural killer T cells to glycolipid antigens is characterized by surface receptor down-modulation and expansion. Proc Natl Acad Sci U S A. 2003;100(19):10913-8.
271. Bjorkholm B, Bok CM, Lundin A, Rafter J, Hibberd ML, Pettersson S. Intestinal microbiota regulate xenobiotic metabolism in the liver. PLoS One. 2009;4(9):e6958.
272. Tompkins GR, O'Dell NL, Bryson IT, Pennington CB. The effects of dietary ferric iron and iron deprivation on the bacterial composition of the mouse intestine. Curr Microbiol. 2001;43(1):38-42.
273. Kamada N, Davies HS, Wight D, Culank L, Roser B. Liver transplantation in the rat. Biochemical and histological evidence of complete tolerance induction in non-rejector strains. Transplantation. 1983;35(4):304-11.
274. Taubert R, Danger R, Londono MC, Christakoudi S, Martinez-Picola M, Rimola A, et al. Hepatic Infiltrates in Operational Tolerant Patients After Liver Transplantation Show Enrichment of Regulatory T Cells Before Proinflammatory Genes Are Downregulated. Am J Transplant. 2016;16(4):1285-93.
275. Ishii E, Shimizu A, Kuwahara N, Kanzaki G, Higo S, Kajimoto Y, et al. Hepatic artery reconstruction prevents ischemic graft injury, inhibits graft rejection, and mediates long-term graft acceptance in rat liver transplantation. Transplant Proc. 2013;45(5):1748-53.
276. Tu Y, Arima T, Flye MW. Rejection of spontaneously accepted rat liver allografts with recipientinterleukin-2 treatment or donor irradiation. Transplantation. 1997;63(2):177-81.
277. Delriviere L, Havaux X, Latinne D, Bazin H, Kamada N, Nordlinger B, et al. Administration of exogenous interleukin-2 abrogates spontaneous rat liver allograft acceptance but does not affect long-term established graft survival. Transplantation. 1997;63(11):1698-701.
278. Kamada N, Calne RY. Orthotopic liver transplantation in the rat. Technique using cuff for portal vein anastomosis and biliary drainage. Transplantation. 1979;28(1):47-50.
279. Kamada N, Calne RY. A surgical experience with five hundred thirty liver transplants in the rat. Surgery. 1983;93(1 Pt 1):64-9.
280. Kuznetsova LV, Zhao D, Wheatley AM. Effect of orthotopic transplantation of liver on systemic and splanchnic hemodynamics in conscious rat. Am J Physiol. 1995;269(1 Pt 1):G153-9.
281. Imamura H, Rocheleau B, Cote J, Huet PM. Long-term consequence of rat orthotopic liver transplantation with and without hepatic arterial reconstruction: a clinical, pathological, and hemodynamic study. Hepatology. 1997;26(1):198-205.
282. Lee S, Charters AC, Chandler JG, Orloff MJ. A technique for orthotopic liver transplantation in the rat. Transplantation. 1973;16(6):664-9.
283. Ariyakhagorn V, Schmitz V, Olschewski P, Polenz D, Boas-Knoop S, Neumann U, et al. Improvement of microsurgical techniques in orthotopic rat liver transplantation. J Surg Res. 2009;153(2):332-9.
284. Burhoe SO. Blood Groups of the Rat (Rattus Norvegicus) and Their Inheritance. Proc Natl Acad Sci U S A. 1947;33(5):102-9.
285. Gunther E, Walter L. The major histocompatibility complex of the rat (Rattus norvegicus). Immunogenetics. 2001;53(7):520-42.
286. Fujino M, Kitazawa Y, Kawasaki M, Funeshima N, Kimura H, Nakajima T, et al. Differences in lymphocyte gene expression between tolerant and syngeneic liver grafted rats. Liver Transpl. 2004;10(3):379-91.
287. Zimmermann FA, Davies HS, Knoll PP, Gokel JM, Schmidt T. Orthotopic liver allografts in the rat. The influence of strain combination on the fate of the graft. Transplantation. 1984;37(4):406-10.
288. Fentener van Vlissingen JM, Borrens M, Girod A, Lelovas P, Morrison F, Torres YS. The reporting of clinical signs in laboratory animals: FELASA Working Group Report. Laboratory animals. 2015;49(4):267-83.
289. Watkins NA, Gusnanto A, de Bono B, De S, Miranda-Saavedra D, Hardie DL, et al. A HaemAtlas: characterizing gene expression in differentiated human blood cells. Blood. 2009;113(19):e1-9.
290. Alberta Transplant Aplied Genomics Centre. Gene lists http://atagc.med.ualberta.ca/Reseaerch/GeneLists/Pages/default.aspx [updated 2015 May 11.

291. Tokunaga R, Zhang W, Naseem M, Puccini A, Berger MD, Soni S, et al. CXCL9, CXCL10, CXCL11/CXCR3 axis for immune activation - A target for novel cancer therapy. Cancer Treat Rev. 2018;63:40-7.
292. Gimino VJ, Lande JD, Berryman TR, King RA, Hertz MI. Gene expression profiling of bronchoalveolar lavage cells in acute lung rejection. Am J Respir Crit Care Med. 2003;168(10):1237-42.
293. Kim SH, Han SY, Azam T, Yoon DY, Dinarello CA. Interleukin-32: a cytokine and inducer of TNFalpha. Immunity. 2005;22(1):131-42.
294. Netea MG, Lewis EC, Azam T, Joosten LA, Jaekal J, Bae SY, et al. Interleukin-32 induces the differentiation of monocytes into macrophage-like cells. Proc Natl Acad Sci U S A. 2008;105(9):3515-20.
295. Meinl E, Lengenfelder D, Blank N, Pirzer R, Barata L, Hivroz C. Differential requirement of ZAP-70 for CD2-mediated activation pathways of mature human T cells. J Immunol. 2000;165(7):3578-83.
296. Kalland ME, Oberprieler NG, Vang T, Tasken K, Torgersen KM. T cell-signaling network analysis reveals distinct differences between CD28 and CD2 costimulation responses in various subsets and in the MAPK pathway between resting and activated regulatory T cells. J Immunol. 2011;187(10):5233-45.
297. Leitner J, Herndler-Brandstetter D, Zlabinger GJ, Grubeck-Loebenstein B, Steinberger P. CD58/CD2 Is the Primary Costimulatory Pathway in Human CD28-CD8+ T Cells. J Immunol. 2015;195(2):477-87.
298. Li Z, Ju X, Silveira PA, Abadir E, Hsu WH, Hart DNJ, et al. CD83: Activation Marker for Antigen Presenting Cells and Its Therapeutic Potential. Front Immunol. 2019;10:1312.
299. Eggensperger S, Tampe R. The transporter associated with antigen processing: a key player in adaptive immunity. Biol Chem. 2015;396(9-10):1059-72.
300. Lin A, Yan WH. The Emerging Roles of Human Leukocyte Antigen-F in Immune Modulation and Viral Infection. Front Immunol. 2019;10:964.
301. Koehn B, Gangappa S, Miller JD, Ahmed R, Larsen CP. Patients, pathogens, and protective immunity: the relevance of virus-induced alloreactivity in transplantation. J Immunol. 2006;176(5):2691-6.
302. Goldstein DR. Inflammation and transplantation tolerance. Semin Immunopathol. 2011;33(2):111-5.
303. Demetris AJ. Evolution of hepatitis C virus in liver allografts. Liver Transpl. 2009;15 Suppl 2:S35-41.
304. Hidalgo LG, Einecke G, Allanach K, Mengel M, Sis B, Mueller TF, et al. The transcriptome of human cytotoxic T cells: measuring the burden of CTL-associated transcripts in human kidney transplants. Am J Transplant. 2008;8(3):637-46.
305. Mengel M, Reeve J, Bunnag S, Einecke G, Sis B, Mueller T, et al. Molecular correlates of scarring in kidney transplants: the emergence of mast cell transcripts. Am J Transplant. 2009;9(1):169-78.
306. Famulski KS, Einecke G, Reeve J, Ramassar V, Allanach K, Mueller T, et al. Changes in the transcriptome in allograft rejection: IFN-gamma-induced transcripts in mouse kidney allografts. Am J Transplant. 2006;6(6):1342-54.
307. Famulski KS, Einecke G, Sis B, Mengel M, Hidalgo LG, Kaplan B, et al. Defining the canonical form of T-cell-mediated rejection in human kidney transplants. Am J Transplant. 2010;10(4):810-20.
308. Famulski KS, de Freitas DG, Kreepala C, Chang J, Sellares J, Sis B, et al. Molecular phenotypes of acute kidney injury in kidney transplants. J Am Soc Nephrol. 2012;23(5):948-58.
309. Mengel M, Sis B, Kim D, Chang J, Famulski KS, Hidalgo LG, et al. The molecular phenotype of heart transplant biopsies: relationship to histopathological and clinical variables. Am J Transplant. 2010;10(9):2105-15.
310. Einecke G, Reeve J, Mengel M, Sis B, Bunnag S, Mueller TF, et al. Expression of B cell and immunoglobulin transcripts is a feature of inflammation in late allografts. Am J Transplant. 2008;8(7):1434-43.
311. Hidalgo LG, Sis B, Sellares J, Campbell PM, Mengel M, Einecke G, et al. NK cell transcripts and NK cells in kidney biopsies from patients with donor-specific antibodies: evidence for NK cell involvement in antibody-mediated rejection. Am J Transplant. 2010;10(8):1812-22.
312. Hidalgo LG, Sellares J, Sis B, Mengel M, Chang J, Halloran PF. Interpreting NK cell transcripts versus T cell transcripts in renal transplant biopsies. Am J Transplant. 2012;12(5):1180-91.

313. Einecke G, Sis B, Reeve J, Mengel M, Campbell PM, Hidalgo LG, et al. Antibody-mediated microcirculation injury is the major cause of late kidney transplant failure. Am J Transplant. 2009;9(11):2520-31.
314. Sis B, Jhangri GS, Bunnag S, Allanach K, Kaplan B, Halloran PF. Endothelial gene expression in kidney transplants with alloantibody indicates antibody-mediated damage despite lack of C4d staining. Am J Transplant. 2009;9(10):2312-23.
315. Hutchinson JA, Riquelme P, Sawitzki B, Tomiuk S, Miqueu P, Zuhayra M, et al. Cutting Edge: Immunological consequences and trafficking of human regulatory macrophages administered to renal transplant recipients. J Immunol. 2011;187(5):2072-8.
316. Wang Z, Shi B, Jin H, Xiao L, Chen Y, Qian Y. Low-dose of tacrolimus favors the induction of functional CD4(+)CD25(+)FoxP3(+) regulatory T cells in solid-organ transplantation. Int Immunopharmacol. 2009;9(5):564-9.
317. Hoffbrand AV, Ganeshaguru K, Hooton JW, Tattersall MH. Effect of iron deficiency and desferrioxamine on DNA synthesis in human cells. Br J Haematol. 1976;33(4):517-26.
318. Lucas JJ, Szepesi A, Domenico J, Takase K, Tordai A, Terada N, et al. Effects of iron-depletion on cell cycle progression in normal human T lymphocytes: selective inhibition of the appearance of the cyclin A-associated component of the p33cdk2 kinase. Blood. 1995;86(6):2268-80.
319. Imaizumi T, Sakashita N, Mushiga Y, Yoshida H, Hayakari R, Xing F, et al. Desferrioxamine, an iron chelator, inhibits CXCL10 expression induced by polyinosinic-polycytidylic acid in U373MG human astrocytoma cells. Neurosci Res. 2015;94:10-6.
320. Chen J, Wei Y, He J, Cui G, Zhu Y, Lu C, et al. Natural killer T cells play a necessary role in modulating of immune-mediated liver injury by gut microbiota. Sci Rep. 2014;4:7259.
321. Marinelli L, Tenore GC, Novellino E. Probiotic species in the modulation of the anticancer immune response. Semin Cancer Biol. 2017;46:182-90.
322. Elkrief A, Derosa L, Zitvogel L, Kroemer G, Routy B. The intimate relationship between gut microbiota and cancer immunotherapy. Gut Microbes. 2019;10(3):424-8.
323. Gopalakrishnan V, Spencer CN, Nezi L, Reuben A, Andrews MC, Karpinets TV, et al. Gut microbiome modulates response to anti-PD-1 immunotherapy in melanoma patients. Science. 2018;359(6371):97-103.
324. Zheng Y, Wang T, Tu X, Huang Y, Zhang H, Tan D, et al. Gut microbiome affects the response to anti-PD-1 immunotherapy in patients with hepatocellular carcinoma. J Immunother Cancer. 2019;7(1):193.
325. Routy B, Le Chatelier E, Derosa L, Duong CPM, Alou MT, Daillere R, et al. Gut microbiome influences efficacy of PD-1-based immunotherapy against epithelial tumors. Science. 2018;359(6371):91-7.
326. Tanaka T, Narazaki M, Kishimoto T. IL-6 in inflammation, immunity, and disease. Cold Spring Harb Perspect Biol. 2014;6(10):a016295.
327. Mizuhara H, O'Neill E, Seki N, Ogawa T, Kusunoki C, Otsuka K, et al. T cell activation-associated hepatic injury: mediation by tumor necrosis factors and protection by interleukin 6. J Exp Med. 1994;179(5):1529-37.
328. Sun R, Tian Z, Kulkarni S, Gao B. IL-6 prevents T cell-mediated hepatitis via inhibition of NKT cells in CD4+ T cell- and STAT3-dependent manners. J Immunol. 2004;172(9):5648-55.
329. Klein C, Wustefeld T, Assmus U, Roskams T, Rose-John S, Muller M, et al. The IL-6-gp130-STAT3 pathway in hepatocytes triggers liver protection in T cell-mediated liver injury. J Clin Invest. 2005;115(4):860-9.
330. Taub R. Liver regeneration: from myth to mechanism. Nat Rev Mol Cell Biol. 2004;5(10):836-47.
331. Schmidt-Arras D, Rose-John S. IL-6 pathway in the liver: From physiopathology to therapy. J Hepatol. 2016;64(6):1403-15.
332. Hori T, Nguyen JH, Zhao X, Ogura Y, Hata T, Yagi S, et al. Comprehensive and innovative techniques for liver transplantation in rats: a surgical guide. World J Gastroenterol. 2010;16(25):3120-32.
333. Prasnicka A, Cermanova J, Hroch M, Dolezelova E, Rozkydalova L, Smutny T, et al. Iron depletion induces hepatic secretion of biliary lipids and glutathione in rats. Biochim Biophys Acta Mol Cell Biol Lipids. 2017;1862(12):1469-80.
334. Kamei A, Watanabe Y, Ishijima T, Uehara M, Arai S, Kato H, et al. Dietary iron-deficient anemia induces a variety of metabolic changes and even apoptosis in rat liver: a DNA microarray study. Physiol Genomics. 2010;42(2):149-56.
335. Toyokawa H, Nakao A, Bailey RJ, Nalesnik MA, Kaizu T, Lemoine JL, et al. Relative contribution of direct and indirect allorecognition in developing tolerance after liver transplantation. Liver Transpl. 2008;14(3):346-57.

336. Fujiki M, Esquivel CO, Martinez OM, Strober S, Uemoto S, Krams SM. Induced tolerance to rat liver allografts involves the apoptosis of intragraft T cells and the generation of CD4(+)CD25(+)FoxP3(+) T regulatory cells. Liver Transpl. 2010;16(2):147-54.
337. Engemann R, Ulrichs K, Thiede A, Muller-Ruchholtz W, Hamelmann H. Value of a physiological liver transplant model in rats. Induction of specific graft tolerance in a fully allogeneic strain combination. Transplantation. 1982;33(5):566-8.
338. Post S, Menger MD, Rentsch M, Gonzalez AP, Herfarth C, Messmer K. The impact of arterialization on hepatic microcirculation and leukocyte accumulation after liver transplantation in the rat. Transplantation. 1992;54(5):789-94.
339. Zhao D, Zimmermann A, Kuznetsova LV, Wheatley AM. Regression of bile duct damage and bile duct proliferation in the non-rearterialized transplanted rat liver is associated with spontaneous graft rearterialization. Hepatology. 1995;21(5):1353-60.
340. Regev A, Molina E, Moura R, Bejarano PA, Khaled A, Ruiz P, et al. Reliability of histopathologic assessment for the differentiation of recurrent hepatitis C from acute rejection after liver transplantation. Liver Transpl. 2004;10(10):1233-9.
341. Burton JR, Jr., Rosen HR. Acute rejection in HCV-infected liver transplant recipients: The great conundrum. Liver Transpl. 2006;12(11 Suppl 2):S38-47.
342. Spivey TL, Uccellini L, Ascierto ML, Zoppoli G, De Giorgi V, Delogu LG, et al. Gene expression profiling in acute allograft rejection: challenging the immunologic constant of rejection hypothesis. J Transl Med. 2011;9:174.
343. Akalin E, Hendrix RC, Polavarapu RG, Pearson TC, Neylan JF, Larsen CP, et al. Gene expression analysis in human renal allograft biopsy samples using high-density oligoarray technology. Transplantation. 2001;72(5):948-53.
344. Saint-Mezard P, Berthier CC, Zhang H, Hertig A, Kaiser S, Schumacher M, et al. Analysis of independent microarray datasets of renal biopsies identifies a robust transcript signature of acute allograft rejection. Transpl Int. 2009;22(3):293-302.
345. Karason K, Jernas M, Hagg DA, Svensson PA. Evaluation of CXCL9 and CXCL10 as circulating biomarkers of human cardiac allograft rejection. BMC Cardiovasc Disord. 2006;6:29.
346. Patil J, Lande JD, Li N, Berryman TR, King RA, Hertz MI. Bronchoalveolar lavage cell gene expression in acute lung rejection: development of a diagnostic classifier. Transplantation. 2008;85(2):224-31.
347. Sreekumar R, Rasmussen DL, Wiesner RH, Charlton MR. Differential allograft gene expression in acute cellular rejection and recurrence of hepatitis C after liver transplantation. Liver Transpl. 2002;8(9):814-21.
348. Asaoka T, Kato T, Marubashi S, Dono K, Hama N, Takahashi H, et al. Differential transcriptome patterns for acute cellular rejection in recipients with recurrent hepatitis C after liver transplantation. Liver Transpl. 2009;15(12):1738-49.
349. Asaoka T, Marubashi S, Kobayashi S, Hama N, Eguchi H, Takeda Y, et al. Intragraft transcriptome level of CXCL9 as biomarker of acute cellular rejection after liver transplantation. J Surg Res. 2012;178(2):1003-14.
350. Kramer K, Thye T, Treszl A, Peine S, Koch M, Sterneck M, et al. Polymorphism in NFKBIA gene is associated with recurrent acute rejections in liver transplant recipients. Tissue Antigens. 2014;84(4):370-7.
351. Bathgate AJ, Pravica V, Perrey C, Therapondos G, Plevris JN, Hayes PC, et al. The effect of polymorphisms in tumor necrosis factor-alpha, interleukin-10, and transforming growth factor-beta1 genes in acute hepatic allograft rejection. Transplantation. 2000;69(7):1514-7.
352. Walch JM, Lakkis FG. T-cell migration to vascularized organ allografts. Curr Opin Organ Transplant. 2014;19(1):28-32.
353. Taubert R, Pischke S, Schlue J, Wedemeyer H, Noyan F, Heim A, et al. Enrichment of regulatory T cells in acutely rejected human liver allografts. Am J Transplant. 2012;12(12):3425-36.
354. He Q, Fan H, Li JQ, Qi HZ. Decreased circulating CD4+CD25highFoxp3+ T cells during acute rejection in liver transplant patients. Transplant Proc. 2011;43(5):1696-700.
355. Haas M, Sis B, Racusen LC, Solez K, Glotz D, Colvin RB, et al. Banff 2013 meeting report: inclusion of c4d-negative antibody-mediated rejection and antibody-associated arterial lesions. Am J Transplant. 2014;14(2):272-83.
356. Demetris AJ, Bellamy C, Hubscher SG, O'Leary J, Randhawa PS, Feng S, et al. 2016 Comprehensive Update of the Banff Working Group on Liver Allograft Pathology: Introduction of Antibody-Mediated Rejection. Am J Transplant. 2016;16(10):2816-35.
357. Reeve J, Sellares J, Mengel M, Sis B, Skene A, Hidalgo L, et al. Molecular diagnosis of T cell-mediated rejection in human kidney transplant biopsies. Am J Transplant. 2013;13(3):645-55.

358. Sellares J, Reeve J, Loupy A, Mengel M, Sis B, Skene A, et al. Molecular diagnosis of antibody-mediated rejection in human kidney transplants. Am J Transplant. 2013;13(4):971-83.
359. Rebollo-Mesa I, Nova-Lamperti E, Mobillo P, Runglall M, Christakoudi S, Norris S, et al. Biomarkers of Tolerance in Kidney Transplantation: Are We Predicting Tolerance or Response to Immunosuppressive Treatment? Am J Transplant. 2016;16(12):3443-57.
360. Kasarala G, Choi S, Lopez K, Britt RB, Boatright C, Tillmann HL. Curing hepatitis C virus (HCV) after organ transplantation: Increased risk of rejection following HCV elimination. Transpl Infect Dis. 2018;20(1).
361. Chan C, Schiano T, Agudelo E, Paul Haydek J, Hoteit M, Laurito MP, et al. Immune-mediated graft dysfunction in liver transplant recipients with hepatitis C virus treated with direct-acting antiviral therapy. Am J Transplant. 2018;18(10):2506-12.
362. Abraham SC, Furth EE. Receiver operating characteristic analysis of serum chemical parameters as tests of liver transplant rejection and correlation with histology. Transplantation. 1995;59(5):740-6.
363. Bonaccorsi-Riani E, Danger R, Lozano JJ, Martinez-Picola M, Kodela E, Mas-Malavila R, et al. Iron Deficiency Impairs Intra-Hepatic Lymphocyte Mediated Immune Response. PLoS One. 2015;10(8):e0136106.
364. Feng S, Bucuvalas JC, Demetris AJ, Burrell BE, Spain KM, Kanaparthi S, et al. Evidence of Chronic Allograft Injury in Liver Biopsies From Long-term Pediatric Recipients of Liver Transplants. Gastroenterology. 2018;155(6):1838-51 e7.
365. Londono MC, Souza LN, Lozano JJ, Miquel R, Abraldes JG, Llovet LP, et al. Molecular profiling of subclinical inflammatory lesions in long-term surviving adult liver transplant recipients. J Hepatol. 2018;69(3):626-34.